CENTRO INTERNACIONAL DE ESTUDOS
DE DOUTORAMENTO E AVANZADOS
DA USC (CIEDUS)

DOCTORAL THESIS

Design and evaluation of sphingomyelin nanosystems for the development of anticancer targeted therapies

Belén López Bouzo

INTERNATIONAL DOCTORAL SCHOOL

DOCTORAL PROGRAM IN DRUG RESEARCH AND DEVELOPMENT

SANTIAGO DE COMPOSTELA

2019

USC
UNIVERSIDADE
DE SANTIAGO
DE COMPOSTELA

CENTRO INTERNACIONAL DE ESTUDOS
DE DOUTORAMENTO E AVANZADOS
DA USC (CIEDUS)

TESIS DE DOCTORADO

Diseño y evaluación de nanosistemas de esfingomielina para el desarrollo de terapias dirigidas frente al cáncer

Belén López Bouzo

ESCUELA DE DOCTORADO INTERNACIONAL

PROGRAMA DE DOCTORADO EN I+D DE MEDICAMENTOS

SANTIAGO DE COMPOSTELA

2019

USC
UNIVERSIDADE
DE SANTIAGO
DE COMPOSTELA

AUTHORIZATION OF THE THESIS SUPERVISORS

Design and evaluation of sphingomyelin nanosystems for the development of anticancer targeted therapies

Dr. María de la Fuente Freire, Full time Researcher (Miguel Servet program). Head of the Nano-Oncology Unit, Health Research Institute of Santiago de Compostela (IDIS).

Prof. María José Alonso Fernández, Full Professor of the Department of Pharmacology, Pharmacy and Pharmaceutical Technology at the University of Santiago de Compostela

Prof. Rafael López López, Associate Professor, Department of Medicine, University of Santiago de Compostela, Spain.

REPORT:

That the present thesis, corresponds to the work carried out by Miss **Belén López Bouzo**, under our supervision, and that we authorize its presentation considering it gathers the necessary requirements of article 34 of the USC Doctoral Studies regulation, and that as supervisors of this thesis, it does not incur in the abstention causes established by the law 40/2015.

At Santiago de Compostela, on _____ 2019

Sgd.: Dr. María de la Fuente Sgd.: Prof. María José Alonso Sgd.: Prof. Rafael López

USC
UNIVERSIDADE
DE SANTIAGO
DE COMPOSTELA

AUTORIZACIÓN DEL DIRECTOR / TUTOR DE LA TESIS

Diseño y evaluación de nanosistemas de esfingomielina para el desarrollo de terapias dirigidas frente al cáncer

Dra María de la Fuente Freire, Investigadora Principal (programa Miguel Servet). Directora de la Unidad de Nano-Oncología del Instituto de Investigación Sanitaria de Santiago de Compostela (IDIS)

Prof. María José Alonso Fernández, Catedrática del Departamento de Farmacología, Farmacia y Tecnología Farmacéutica de la Universidad de Santiago de Compostela.

Prof. Rafael López López, Profesor asociado del Departamento de Medicina de la Universidad de Santiago de Compostela

INFORMAN:

Que la presente tesis, se corresponde con el trabajo realizado por Dña. **Belén López Bouzo**, bajo mi dirección, y autorizo su presentación, considerando que reúne los requisitos exigidos en la Regulación de Estudios de Doctorado de la USC, y que como director de esta no incurre en las causas de abstención establecidas en la Ley 40/2015.

En Santiago de Compostela, a _____ de 2019

Fdo.: Dra. María de la Fuente Fdo.: Prof. María José Alonso Fdo.: Prof. Rafael López

USC
UNIVERSIDADE
DE SANTIAGO
DE COMPOSTELA

PhD CANDIDATE STATEMENT

Design and evaluation of sphingomyelin nanosystems for the development of anticancer targeted therapies

Miss Belén Lopez Bouzo

I submit my Doctoral thesis, following the procedure according to the Regulation, stating that:

1) This thesis gathers the results corresponding to my work.

2) When applicable, explicit mention is given to the collaborations the work may have had.

3) The present document is the final version submitted for its defense and coincide with the document sent in electronic format.

4) I confirm that this thesis does not incur in any plagiarism of any other authors or documents submitted by me for obtaining other degrees.

At Santiago de Compostela, _____ 2019

Sgd.: Belén López Bouzo

USC
UNIVERSIDADE
DE SANTIAGO
DE COMPOSTELA

DECLARACIÓN DEL AUTOR/A DE LA TESIS

Diseño y evaluación de nanosistemas de esfingomielina para el desarrollo de terapias dirigidas frente al cáncer

Dña. Belén López Bouzo

Presento mi tesis, siguiendo el procedimiento adecuado a la Regulación y declaro que:

1) La tesis abarca los resultados de la elaboración de mi trabajo.

2) De ser el caso, en la tesis se hace referencia a las colaboraciones que tuvo este trabajo.

3) La tesis es la versión definitiva presentada para su defensa y coincide con la versión enviada en formato electrónico.

4) Confirmo que la tesis no incurre en ningún tipo de plagio de otros autores ni de trabajos presentados por mí para la obtención de otros títulos.

En Santiago de Compostela a _____ *de 2019*

Fdo.: Belén López Bouzo

USC
UNIVERSIDADE
DE SANTIAGO
DE COMPOSTELA

Ó meu pai

USC
UNIVERSIDADE
DE SANTIAGO
DE COMPOSTELA

"The difference in winning and losing is most often not quitting"

"La diferencia entre ganar y perder a menudo consiste en no rendirse"

Walt Disney

USC
UNIVERSIDADE
DE SANTIAGO
DE COMPOSTELA

ACKNOWLEDGMENTS

USC
UNIVERSIDADE
DE SANTIAGO
DE COMPOSTELA

Chegados a este momento, que difícil se fai afrontar esta páxina en branco pensando como agradecer a todos os que formaron parte desta tese indirecta ou directamente. Como non, non podía deixar pasar a oportunidade de referirme á sabedoría galega neste momento (que os que me coñecen saben que tanto me gusta) asique, como di o refrán *¨Non hai mal que cen anos dure, nin corpo que o aguante*¨ podo dicir que ¡Por fin chegou o final!

En primeiro lugar gustaríame dar as gracias ós meus tres directores, María de la Fuente, María José Alonso e Rafael López, por permitírenme formar parte deste apaixonante mundo da investigación e acollerme nos seus grupos.

Gracias María José por haberme inspirado, por haber encendido la bombilla de mi curiosidad en la primera charla en la que te escuché durante mi etapa de máster. Gracias por inspirarme a tomar el interesante sendero de la nanotecnología, que tantas alegrías me ha dado, además de mi segunda familia.

Gracias María. A ti me gustaría agradecerte especialmente que no solo hayas sido mi directora sino tantas veces una buena amiga o incluso se podría decir que una madre. Gracias por tu apoyo, tu comprensión, por tu paciencia, por tus ganas y por hacerme ver siempre el lado positivo que a veces pierdo. ¡Ya sabes que esta tesis es tanto tuya como mía!

Gracias a todos los grupos que han permitido que esta tesis sea el reflejo de una investigación multidisciplinar y con la que haya ampliado tanto mi campo de formación. Gracias a Rebeca Fandiño y a Martín Calvelo (CIQUS, USC) por ayudarme con toda la parte de simulación computacional. Gracias a Manuel Martín (RIAIDT, USC) por su ayuda y dedicación en la interpretación de los resultados de RMN. Gracias al grupo de Laura Sánchez Piñón y en especial a Carlha Gutierrez por dejarme meter mi nariz en el mundo del pez cebra. Gracias al grupo de Ramón Eritja del Instituto de Biología Molecular de Barcelona (IBMB, CSIC) y dentro de él a Anna Aviñó y a Santiago Grijalvo por vuestra inmensa amabilidad conmigo tanto en persona como en la distancia y por supuesto, gracias por la contribución con la síntesis de los ácidos nucleicos modificados. Gracias a Rocio Arranz (CNB, CSIC, UAM) por tu amabilidad y disponibilidad en toda la parte de Criomicroscopía.

Gracias también a todos los profesores del departamento de Farmacología, Farmacia y Tecnología Farmacéutica, en especial a Loli, Marcos, Noemi y Begoña Seijo por su disposición a ayudar, por compartir su experiencia y sus consejos. Gracias también a Puri, Rafa, Balby, Vanessa, Desi y Cris por ayudarme en todo siempre que he necesitado una mano. Y gracias Sagrario porque en el último aliento tu ayuda es imprescindible.

En este momento me gustaría expresar un sincero agradecimiento a todos mis familiares, compañer@s y amig@s por estar conmigo durante todo este tiempo. ¡Cada granito de arena aportado ha sido la mejor ayuda posible!

GRACIAS en especial….

A Sara Cordeiro, por ser mi mentora, la iniciadora en el mundo de la nanotecnología a una foránea del campo que se inmiscuía en el mundo de los farmacéuticos. ¡Gracias por tener siempre el abrazo que lo cura todo!

A Josiño, buf que decirche... é imposible poñer con palabras todo o que agradezo terte atopado na miña vida. Dende a primeira clase que nos sentamos o lado xa o camiño foi xuntos. Creo completamente que esta tese non estaría acá sen a túa axuda, o teu apoio e os teus consellos. Sabes que es como o irmán maior que non teño, de corazón, mil gracias por todo Jose.

A Irene, o no sé si debería decir mamá Irene!! Eres inigualable Ire, es imposible encontrar en el mundo otra persona con tu espíritu, tu capacidad de trabajo, tu cariño y preocupación. Podría confiarte mi vida que sé que la tendrías intacta al volver!! 15 días en Turín me permitieron conocer a la persona más auténtica del laboratorio. Gracias por compartir todo el camino conmigo churri!

A Tamara, por tu dulzura, por tu alegría y por tu gran corazón, porque sabes que desde el primer momento hemos tenido esa conexión especial que no sabemos de dónde viene pero que pase lo que pase está ahí. Muchas gracias pequeña.

A Belén Cuesta, gracias, gracias y gracias por ser mi madre adoptiva. Porque aunque me llames ladilla se que en el fondo me quieres. Siempre recordaré esas risas que nos echamos y las conversaciones que solo pueden tener dos belenes!! Eres genial!!

To Lu, thanks for letting me take care of you when you needed it the most. My living room has been the starting point for long multicultural talks, impossible manicures, singing concerts at any times and of course for a beautiful friendship. Ngiyakutsandza nana!!

A Inma, porque es imposible agradecer el simple hecho de conocerte. Ha sido ya en si una gran aventura. Porque me has permitido crear un mundo paralelo contigo y porque ya sabemos que como en pingüilandia no se vive en ningún sitio. Gracias por estar a mi lado todos estos años aguantando mis crisis y dándome tu apoyo.

A Raquel, integrante del grupo de las zumbadas jajaja. Ha sido tan extraña la forma en la que hemos congeniado la una con la otra, desde mi aportación musical para tu boda hasta todos los cafés compartidos en la 5ª planta parece que hemos sido dos personas diferentes. Gracias por tu paciencia, preocupación y tus consejos. Espero que aunque la vida nos lleve por caminos distintos siempre que nos veamos sea como si no hubiese pasado más que un día.

A Adri, ¡porque quien sino entendería y se reiría de vídeos rarunos conmigo… y quien se pondría en el lab en plan ingenieras a fabricar nuevos equipos! Gracias por esos SEÑOOOOR que tanto me hacen reír

y por enseñarme a relativizar muchas cosas, pero también por ayudarme a sacar esa mala ostia que tenemos escondida en el momento apropiado.

A Sonia. La que has liaooo pollito!! La sexta no habría sido mi nueva casa si no te hubiese tenido al lado. Gracias por las fotos locas, por tus consejos y por compartir siempre tu experiencia conmigo y evitarme muchos accidentes. Gracias pollo!

To Bhanu, thanks a lot for your patience, kindness and your permanent smile!! And of course for your superspicy meals!! You know you are an inspiration for me. Thanks also for having me always present in your thoughts and also for the long hours we spend talking. I wish you the best with your new life!!

To Raneem, although you have been the last addition in this thesis pathway, by living together we have shared so many unforgettable moments that will accompany us for our lifetime. I will miss you a lot!!

Ad Anna, per il tuo amore infinito e la tua amicizia, per tutti i problemi che mi hai aiutato ad affrontare nell'ultima fase della tesi, per avermi fatto parte della tua vita a Santiago e per avermi fatto sentire che sarò sempre a casa quando saremo insieme.

A toda la familia de *Nanochachos* que he conocido en estos seis años en el laboratorio, junto a todos los doctorandos NanoFar y Marie Curie. Gracias por todos vuestros consejos, momentos de celebración compartidos, actividades diversas, quedadas para una caña después del lab y despedidas varias.

A todos los que habéis coincidido conmigo en este lago viaje que ha sido la tesis: a Jorge Pinto, Ana González, José Vicente, Adam, Miguel, Sonita, Khair, Mariajo, Niu, Paulina, Tania, Ana Cadete, Ana Olivera, Elena, Raquel II, María Piñón, Belén Álvarez, Ivana, Maruthi, Nataliya, Howl, Lena, Mati, Sofía, Andrea, Edi, Mireia, Vanessa Oliveira, Ovidio, Francesco, Paul, Blanca, Noelia, Esther, Carla, Chema, Diego, Iago, German, Carmen III, Ana Canaria, Mireya, Sergio, Rosana, Sheila, Fernando, Cecilia, Catarina, Ricardo, Shubaash, Sakthi y Federico… GRACIAS!!!

A mis compañeros del grupo de Oncología Médica Traslacional del IDIS desde nuestra etapa en el laboratorio 13 con Abi, Marta Alonso, Juan, Carmen, Surasa y Farimah hasta la actualidad en el laboratorio 18 con las incorporaciones de Sandra Díez, Sandra Alijas, Rebeca, María, Marce y Miguel.

También me gustaría dar las gracias a todas las personas que he tenido la oportunidad de enseñar durante todos los años de la tesis, Diego, Bea, Sandra, Carmen, Marta, Nicol y Alejandra.

Por último, y con especial cariño, me gustaría dar las gracias a mi alumna y pinche, Sainza. Tu has sido mis manos, mis ojos y mis piernas cuando yo no podía utilizar los míos. Sabes que no hay palabras para agradecerte todo lo que me has ayudado. He confiado en ti casi desde el minuto uno y creo que serás una científica excelente. Mil gracias Sai, por todo.

Porque hai mais vida despois do laboratorio.... moitas gracias a todos os amig@s que fun atopando o largo da miña carreira tanto universitaria (Vero, Vane, Saúl, Sara, Xadre, Ale, Lili, Eva, Juancho, Dani, Alex, Flori …) como na carreira musical (Sariña, Álvaro, David, Sara, Erea, Javi, Juan, Dani, Ivan, Vane, Martin, Nico, Arturo, Gabri, Leti... e todos os compañeir@s da Banda a Lira de Ribadavia), gracias polos vosos grans de area ben en forma de ceas, días de praia, conversas por teléfono; bodas, bautizos e comunións; días de concertos e certames...

Gracias Diego, por estar o meu lado durante todo este camiño a veces ben frustrante para ambos. Gracias polo teu amor e apoio incondicional. Gracias por facerme rir sempre pase o que pase.

Gracias a miña familia, sen o seu apoio esta tese non tería sentido. Gracias o meu pai que sei que houbera estado moi orgulloso de min se houbera podido estar comigo celebrando esto. Gracias a Laura por animarme a cada segundo a non renderme e a levantarme cando as pernas non podían. E por último a miña nai, Mercedes, sabes que eres e que serás sempre o meu pilar e un exemplo de persoa incansable e loitadora.

STATEMENTS

CONFLICT OF INTERESTS AND IMAGE USE

USC
UNIVERSIDADE
DE SANTIAGO
DE COMPOSTELA

Conflict of interests

I declare that there is no competing interests with the subject matter or materials discussed in this thesis.

Images use

All the images presented in this work were made by the author of the thesis. In case of images adapted from other manuscripts, permission has been asked to the publishers and has been indicated at the bottom of the correspondent figure.

Sgd.: Belén López Bouzo

USC
UNIVERSIDADE
DE SANTIAGO
DE COMPOSTELA

TABLE OF CONTENTS

USC
UNIVERSIDADE
DE SANTIAGO
DE COMPOSTELA

USC
UNIVERSIDADE
DE SANTIAGO
DE COMPOSTELA

ABSTRACT / RESUMEN

USC
UNIVERSIDADE
DE SANTIAGO
DE COMPOSTELA

Abstract

The development of new nanotechnological platforms to be used as drug delivery carriers has increased dramatically in the last decades. Cancer, being the second cause of death worldwide, is the therapeutic area that is expected to benefit the most from these advances. In this context, the main goal of this thesis has been the rational design and development of nanosystems intended to treat metastatic colorectal cancer. For this purpose, we have developed a new nanosystem platform, sphingomyelin nanosystems (SNs) constituted solely by two components, an oil in the core stabilized by sphingomyelin (SM) , which is the most extensively present sphingolipid in the cellular membranes.

The first chapter describes the novelty of this nanosystem platform with an extensive physicochemical characterization in terms of size, homogeneity, surface charge, morphology and colloidal stability. Furthermore, *in silico* methods were used to characterize them based on molecular dynamic (MD) simulations. Using coarse-grained methodology (CG), we were able to reach relevant time scales to observe the formation of two SNs ratios (10% and 50% SM). Subsequently, using more precise simulations by means of all-atoms methodology (AT), we could study several *drug-nanocarrier* interactions in a detailed manner.

Second chapter is based on the application of this SNs platform to act as a gene delivery nanocarrier. To achieve this goal, a strategy based on hydrophobically modified oligonucleotides was used to bind a negatively charged biomolecule to a neutral charged nanocarrier. The resulting nanosystems were found to be stable in relevant biological media. Toxicity studies showed a very low toxicity profile both, *in vitro* (cell culture and blood compatibility) and *in vivo* (zebrafish embryo and healthy mice). Finally, results obtained with SW480 colorectal cancer cells showed the good capacity of this approach to transport oligonucleotides into cells.

In chapter 3, we developed a potential combinatorial therapy which consisted of SNs decorated with the paracrine hormone Uroguanylin (UroG) and loaded with the cytostatic drug etoposide (Etp). UroG is a natural agonist of the Guanylyl Cyclase C receptor (GCC), membrane receptor expressed on the surface of primary and metastatic colorectal cancer cells. For this purpose, UroG was modified with an amphiphilic molecule (PEG_{12}-C_{18}) whose hydrophobic part enabled the association with the oily core of the nanosystem. *In vitro* and *in vivo* experiments aimed to confirm the effectiveness of the drugs against metastatic colorectal cancer were carried showing an effective tumor reduction.

Overall, the results obtained in this thesis show the rational development of a versatile nanosystem platform with adequate physicochemical, biopharmaceutical and functional properties to become an interesting drug delivery carrier for anticancer drugs.

Resumen

El desarrollo de nuevas plataformas nanotecnológicas destinadas a su uso como nanotransportadores de fármacos ha aumentado considerablemente en las últimas décadas. El cáncer, situándose como la segunda causa de muerte a nivel mundial, es el área terapéutica que obtendría un mayor beneficio de los avances nanotecnológicos. En este contexto, el principal objetivo de esta tesis ha sido el diseño y desarrollo racional de nanosistemas destinados a tratar el cáncer colorrectal metastásico. Para ello, se ha desarrollado una nueva plataforma nanotecnológica, nanosistemas de esfingomielina (SNs) constituidos únicamente por dos componentes, un único aceite en el núcleo estabilizado por esfingomielina (SM), el esfingolípido con mayor presencia en las membranas celulares.

En el primer capítulo se describe la novedad de esta plataforma en base a una extensa caracterización fisicoquímica en términos de tamaño, homogeneidad de población, carga superficial, morfología y estabilidad coloidal. Además, la utilización de métodos *in silico* ha permitido su caracterización complementaria en base a simulaciones de dinámica molecular (MD). Usando la metodología coarse-grained (CG) se alcanzaron escalas de tiempo relevantes para observar la formación de dos ratios de SNs (con 10% y 50% SM). Posteriormente, utilizando simulaciones más precisas mediante la metodología all-atoms (AT) ha sido posible estudiar diversas interacciones *fármaco-nanotransportador* de manera detallada.

El segundo capítulo se basa en la aplicación de estos nanosistemas (SNs) para su uso en terapia génica. Para lograr este objetivo, se empleó una estrategia basada en oligonucleótidos modificados hidrófobamente que favorezcan la unión de una biomolécula cargada negativamente a un nanotransportador con carga neutra. Los nanosistemas resultantes manifestaron una buena estabilidad coloidal en medios biológicos relevantes. Además, estudios toxicológicos mostraron un perfil de toxicidad muy bajo tanto *in vitro* (cultivos celulares y

hemocompatibilidad) como *in vivo* (estudios en embrión de pez cebra y ratones sanos). Finalmente, los resultados obtenidos con células de cáncer colorrectal, SW480, mostraron la buena capacidad de este nanosistema para transportar oligonucleótidos al citoplasma celular.

En el capítulo 3, se desarrolló una potencial terapia combinatoria consistente en SNs decorados con la hormona paracrina Uroguanilina (UroG) y cargados con el fármaco citostático etopósido (Etp). La UroG se corresponde con un agonista natural del receptor de guanilato ciclasa C (GCC), receptor de membrana expresado en la superficie de células de cáncer colorrectal primarias y metastásicas. Para este propósito, se modificó la UroG con una molécula anfifílica (PEG_{12}-C_{18}) cuya parte hidrófoba permitiría la asociación con el nanosistema. Se llevaron a cabo experimentos *in vitro* e *in vivo* dirigidos a confirmar la efectividad del tratamiento contra el cáncer colorrectal metastásico mostrando una buena eficacia y una reducción efectiva del tumor.

En conclusión, los resultados obtenidos en esta tesis muestran el desarrollo racional de una nanoplataforma versátil con propiedades fisicoquímicas, biofarmacéuticas y funcionales adecuadas para convertirse en un interesante nanotransportador de fármacos para terapias oncológicas.

RESUMEN *IN EXTENSO*

USC
UNIVERSIDADE
DE SANTIAGO
DE COMPOSTELA

La comercialización de productos nanofarmacéuticos representa hoy en día una tarea costosa, larga y arriesgada, con una serie de pasos que van desde el desarrollo en el laboratorio, pasando por diversas fases preclínicas y clínicas, hasta llegar al mercado[1,2]. El desarrollo de la nanotecnología en el campo de la biomedicina ha conducido a avances significativos en las últimas décadas, con varios nanosistemas presentes ya en la práctica clínica y muchos otros actualmente en ensayos clínicos[3–5]. Aunque la nanotecnología ha supuesto un impacto significativo en la investigación biomédica, medida por el incremento exponencial de artículos publicados por año desde 1990, el número de productos comercializados es todavía limitado[6–10]. Para tratar de solventar esta realidad, es de vital importancia el diseño racional de los nanosistemas desde las fases iniciales de su desarrollo[11,12]. La selección adecuada de los componentes del nanosistema, seguida de una fase de screening para determinar la mejor combinación entre ellos[13,14] es necesaria desde una perspectiva traslacional[5,15]. La aplicación de la nanotecnología en la terapia del cáncer, aprovechando su capacidad para modular el perfil de biodistribución y disminuir la toxicidad asociada con los fármacos quimioterapéuticos, es actualmente una realidad, con más del 30% de los nanoproductos comercializados indicados para esta condición[5]. Sin embargo, la alta incidencia y mortalidad de esta enfermedad hace que los tratamientos actuales sean insuficientes, lo que subraya la necesidad de hallar tratamientos nuevos, más eficaces y más potentes.

En este marco, el objetivo del trabajo realizado en esta tesis doctoral ha consistido en el desarrollo de una plataforma versátil de nanosistemas biodegradable con capacidad de asociar y administrar diferentes tipos de fármacos (quimioterapia clásica y biomoléculas) y en última instancia, mejorar su actividad farmacológica.

El flujo de trabajo experimental comenzó por la investigación de los parámetros clave que afectan a la formación del nanosistema desde un punto de vista de formulación (es decir, la

composición molecular, la concentración y la proporción de los componentes que integran el sistema). Complementariamente, se aplicaron técnicas *in silico* de modelado molecular para simular la formación de los nanosistemas seleccionados experimentalmente. Además se utilizaron los recursos computacionales para predecir la interacción de seis fármacos seleccionados con este modelo de nanosistema y determinar si la interacción *fármaco-nanosistema* resulta o no favorable. Al mismo tiempo, se realizaron pruebas *in vitro* e *in vivo* para demostrar la seguridad, estabilidad y biocompatibilidad de los nanosistemas desarrollados (Capítulo 1). Posteriormente, investigamos el potencial de los nanosistemas para el desarrollo de terapias oncológicas. En primer lugar, hemos explorado la capacidad de las nanoemulsiones neutras y no tóxicas para asociar y administrar eficazmente oligonucleótidos modificados hidrofóbicamente (Rlas-CH) (Capítulo 2). En segundo lugar, evaluamos la decoración de la nanoemulsión con una hormona paracrina de doble acción (ligando y compuesto terapéutico), Uroguanilina (UroG). Para ello, modificamos químicamente la secuencia proteica de la Uroguanilina con una cadena carbonada pegilada (UroG-PEG_6-C_{18}, UroGm) para favorecer su anclaje a la superficie del nanosistema. Posteriormente, hemos co-encapsulado el fármaco citostático, etopósido (Etp), con el propósito final de lograr un efecto sinérgico de ambas moléculas. Estudios *in vitro* e *in vivo* se realizaron para determinar el potencial de esta estrategia (Capítulo 3).

1. Diseño racional de nanosistemas.

La posibilidad de diseñar diferentes plataformas nanotecnológicas con una gran variedad de nanomateriales ha llevado a un desarrollo masivo en las últimas décadas[16]. Sin embargo, todavía existen desafíos relacionados con el llamado "proceso de diseño" para lograr productos nanofarmacéuticos confiables y consistentes clínicamente[17]. Esta idea concuerda con el principio de "Quality by Design" adoptado por el ICH (Consejo Internacional para la Armonización) y sucesivamente por la FDA para el descubrimiento, desarrollo y fabricación de nanomedicamentos[18]. Siguiendo estas corrientes, uno de los objetivos principales de esta tesis ha sido el diseño de un nanosistema biocompatible y biodegradable, con propiedades fisicoquímicas adecuadas y un buen perfil de seguridad mediante el control del diseño experimental desde el momento inicial.

Teniendo esto en cuenta hemos seleccionado como componente principal la vitamina E (V), vitamina liposoluble incluida en la lista GRAS (Generally Recognized As Safe) que se transporta naturalmente de la dieta incluida en las lipoproteínas[19]. Además, hemos optado por estabilizar este núcleo con uno de los lípidos presentes en la monocapa de lipoproteínas, coincidiendo también con el tercer lípido en representación de la membrana externa de la célula, la esfingomielina (SM)[20–25].

Las nanoemulsiones se prepararon utilizando una técnica muy sencilla y no agresiva denominada método de inyección de etanol. Esta técnica de fabricación de baja energía, usada tradicionalmente para la preparación de liposomas[26–29], ha sido optimizada para la preparación de este tipo de formulación. En primer lugar, se realizó un cribado utilizando los dos compuestos anteriormente mencionados para identificar la combinación adecuada de componentes para obtener las mejores propiedades fisicoquímicas (**Tabla 1**). Los resultados obtenidos a partir de este estudio sistemático pusieron de manifiesto la importancia de la

cuidadosa selección de los componentes que integran un nanosistema para obtener las características adecuadas. La caracterización fisicoquímica de las formulaciones desarrolladas se evaluó inicialmente mediante Dispersión Dinámica de Luz (DLS) y Anemometría de Láser Doppler (LDA) para la caracterización del barrido preliminar (**Tabla 1**), métodos de referencia en la caracterización de nanosistemas[30–32]. A continuación, se realizó una caracterización complementaria de las nanoemulsiones seleccionadas mediante Nanoparticle Tracking Analysis (NTA), una técnica innovadora que permite la visualización directa y la grabación de nanosistemas en solución[33].

Tabla 1: Barrido inicial de condiciones para el desarrollo de nanosistemas consistentes en un núcleo de vitamina E (V) y esfingomielina (SM) como agente estabilizante. Caracterización fisicoquímica realizada mediante Dispersión Dinámica de Luz (DLS) y Anemometría de Láser Doppler (LDA).

	Contenido total de Vitamina E (mg)								
	2			**5**			**10**		
Ratio en masa (V:SM)	**Tamaño (nm)**	**PdI**	**ZP (mV)**	**Tamaño (nm)**	**PdI**	**ZP (mV)**	**Tamaño (nm)**	**PdI**	**ZP (mV)**
1:1	119 ± 20	0,3	0 ± 1	187 ± 16	0,2	-2 ± 3	Agregación		
1:0.5	72 ±12	0,3	-1 ± 2	101 ± 10	0,2	-3 ± 2	254 ± 33	0,3	-9 ± 0
1:0.2	58 ± 18	0,2	-2 ± 0	123 ± 14	0,2	-4 ± 4	239 ± 18	0,2	-4 ± 0
1:0.1	63 ± 7	0,1	-5 ± 2	85 ± 7	0,1	-3 ± 1	169 ± 5	0,2	-1 ± 0
1:0.05	64 ± 7	0,2	-4 ± 1	97 ± 6	0,2	-2 ± 0	162 ± 2	0,2	-3 ± 2

V: Vitamina E; SM: esfingomielina; nm: nanómetro; PdI: índice de polidispersión; ZP: carga superficial; mV: milivoltios. Volumen total de la suspensión: 1 mL. Ratio etanol/agua: 1/10 v/v . Resultados presentados en media ± DE, n=3.

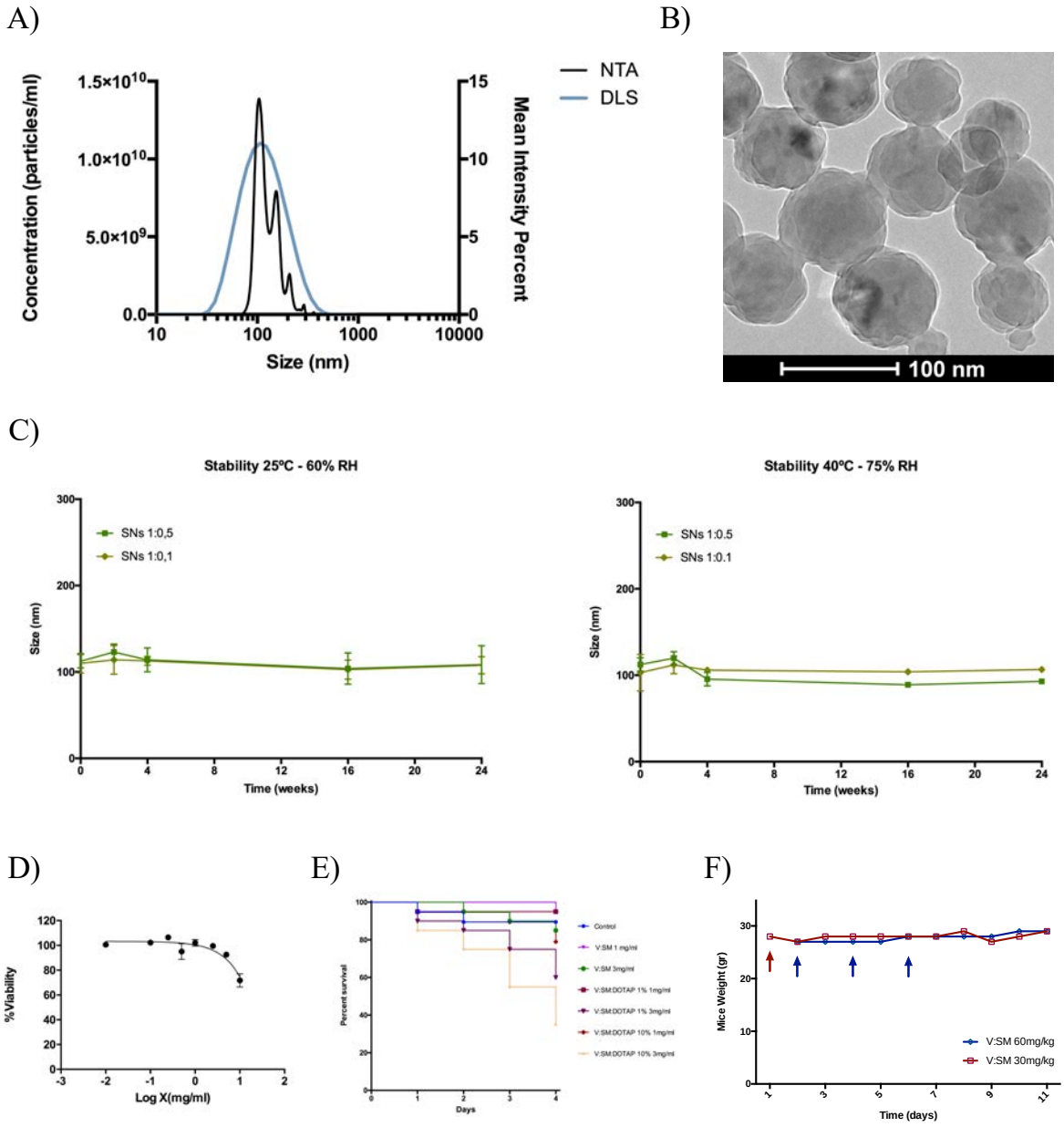

Figure 1: Ejemplos de caracterización de diferentes nanosistemas desarrollados (SNs). **(A)** Caracterización fisicoquímica complementaria mediante DLS y NTA **(B)** Examen morfológico mediante crio-microscopía **(C)** Estabilidad acelerada siguiendo las guías de la ICH (International Council for Harmonization)[34] a temperatura ambiente controlada (panel derecho, 40ºC 75%RH) y en condiciones de almacenamiento (panel izquierdo, 25ºC 60%RH). **(D)** Citotoxicidad celular después de 24h de incubación evaluada en células de cáncer colorrectal SW480 **(E)** Estudio de toxicidad en embrión de pez cebra comparando formulaciones catiónicas (V:SM:DOTAP) y neutras (V:SM). **(F)** Evaluación de la toxicidad de SNs testadas en ratones sanos en función de su peso corporal. *Las figuras A, B, D y F corresponden a SNs con un ratio V:SM 1:0.1.*

En la **Figura 1A** se muestra la comparación entre los espectros de medición obtenidos mediante DLS y NTA de la formulación compuesta por un núcleo de V y SM como surfactante en una relación V:SM 1:0.1. Adicionalmente, se realizó un examen morfológico de las formulaciones mediante varias técnicas de microscopía electrónica de transmisión, TEM, STEM y/o Cryo-TEM (**Figura 1B**) que confirmaron la forma esferoidal y la distribución de tamaño obtenida en las técnicas anteriores.

Las pruebas de estabilidad proporcionan evidencia sobre cómo la calidad de los medicamentos o productos farmacéuticos puede variar en el tiempo bajo la influencia de diversos factores como la temperatura, la humedad y la luz[35]. La estabilidad de los nanosistemas sigue siendo un problema difícil de solventar durante el desarrollo del producto, que condiciona directamente la forma de dosificación, la vía de administración e incluso la naturaleza del posible fármaco asociado[36,37]. Con el fin de explorar la estabilidad de nuestros nanosistemas, se han realizado estudios acelerados de estabilidad coloidal siguiendo la guía "Pruebas de estabilidad de nuevos medicamentos y productos Q1A (R2)" de la Conferencia Internacional de Armonización (ICH)[38]. La estabilidad acelerada se ha evaluado en dos condiciones, sustancias farmacológicas o productos destinados al almacenamiento en nevera (25ºC ± 2ºC; 60% HR ± 5% HR) y a temperatura ambiente controlada (40ºC ± 2ºC; 75% HR ± 5% HR) con una frecuencia de 5 puntos de medida en un período de 6 meses (**Figura 1C**). Se evaluó la estabilidad de dos nanosistemas, es decir, la relación V:SM 1:0.5 y 1:0.1. Los resultados mostraron un excelente perfil de estabilidad en ambas condiciones, obteniéndose una estabilidad equivalente a dos años en solución coloidal.

Una importante tarea de la nanotecnología es explotar las ventajas de la escala nanométrica para lograr el máximo beneficio clínico con los menores efectos secundarios[1]. La toxicología de los nanomateriales se está convirtiendo en un tema muy relevante en la actualidad,

especialmente con respecto a los nanomateriales destinados a uso médico[39]. Por lo tanto, una mejor comprensión de los factores de riesgo asociados a los nanomateriales ayudarán al desarrollo futuro de los nanofármacos[40]. La nanotoxicología, por lo tanto, se ha propuesto como una nueva rama de la toxicología para abordar las lagunas en el conocimiento de los efectos adversos causados por los nanomateriales[41,42]. En línea con esto, se realizaron varios estudios de referencia para evaluar y comparar la toxicidad de dos formulaciones con carga opuesta. Los SNs neutros (V:SM) y los SNs catiónicos (V:SM:DOTAP) se probaron posteriormente. Inicialmente se realizaron estudios de toxicidad colorimétricos basados en sales de tetrazolio (MTT)[39,44] a períodos de contacto de 4 y 24 horas en células de cáncer colorrectal (SW480). Los SNs neutros revelaron una ligera toxicidad dosis dependiente, pero no lo suficiente como para calcular el valor de IC50 que se situaría por encima de la dosis máxima testada (10 mg / mL) (**Figura 1D**). Este hecho representa al menos de 5 a 100 veces menos concentración tóxica en comparación con la obtenida por SNs catiónicos (0.1 mg/mL a 2 mg/mL rango). Estos resultados concuerdan con la literatura actual donde se sabe que los compuestos catiónicos exhiben *per se* un comportamiento más tóxico[43].

Posteriormente, se plantearon experimentos para evaluar la actividad hemolítica *in vitro* y con ello evaluar la biocompatibilidad de los nanosistemas *in vivo* y el impacto de sus características fisicoquímicas en los glóbulos rojos[40,45]. Los resultados mostraron una actividad hemolítica menor del 20% hasta una concentración de 5mg/mL de SNs neutros, mientras que los SNs catiónicos obtuvieron un 20% de actividad hemolítica desde la primera concentración testada (0.1 mg/mL). Con el objetivo de evaluar una condición supersaturada, se probaron concentraciones de hasta 10 mg/mL de SNs, condición en la que se obtuvo una capacidad hemolítica inferior al 40% para las SNs neutras, mientras que las SNs catiónicas presentaron más del 60% del efecto hemolítico (Capítulo 2).

Sin embargo, es bien sabido que los modelos *in vitro* no experimentan el mismo rango de efectos tóxicos que es probable que se observen *in vivo*. Por lo tanto, con objetivo de completar la caracterización nanotoxicológica se ha realizado una evaluación de los nanosistemas anteriores tanto en el modelo de embrión de pez cebra como en ratones sanos.

El embrión de pez cebra (*Danio rerio*) se ha convertido en un modelo animal prominente en una variedad de disciplinas debido a varias ventajas inherentes al propio animal, como pueden ser el pequeño tamaño, su manutención económica y su cría en grandes cantidades[46,47]. Teniendo en cuenta que los embriones de pez cebra son capaces de absorber pequeñas moléculas presentes en el agua circundante a través de la piel y las branquias, este animal se ha utilizado cada vez más como modelo predictivo de toxicidad inducida por fármacos[48]. El uso del pez cebra como modelo toxicológico se puede lograr principalmente por cuatro factores, la posibilidad de que los embriones vivan en una placa de 96 o 384 pocillos durante una semana, la administración simple en un volumen reducido (menos de 200 μL), la transparencia del cuerpo del embrión y las posibilidad de hacer estudios con suficiente tamaño poblacional pero a pequeña escala[46,48]. Además, existen guías específicamente desarrolladas para el uso de embriones de pez cebra como modelo toxicológico[47,49].

La evaluación de los nanosistemas neutros y catiónicos testados anteriormente se realizó en embriones de pez cebra, valorando las posibles alteraciones que se producen en el embrión durante un período de 96 h. Como se muestra en la **Figura 1E**, no se encontró toxicidad aparente para los SNs neutros superior a los parámetros establecidos como no tóxicos en el rango de concentración analizado (1 mg/mL a 3 mg/mL). Sin embargo, en el caso de los SNs catiónicos se registró de un 40 a 60% de muerte en el mismo rango de concentraciones.

Con el fin de confirmar el aparente comportamiento no tóxico mostrado por nuestros nanosistemas tanto *in vitro* como en el modelo de embrión de pez cebra, se realizaron estudios

complementarios *in vivo* en ratones hembra Swiss. Siguiendo el principio de un estudio de dosis máxima tolerada (MTD por sus siglas en inglés), a los ratones se les inyectó bien una dosis (30 mg/kg) o bien dosis repetidas (tres dosis consecutivas de 60 mg/kg) (**Figura 1F**). Se habría considerado el sacrificio de los animales que perdiesen más del 20% de su peso corporal o si presentaran otros signos de toxicidad significativa[50]. Sin embargo, después de una dosis acumulada de 180 mg/kg, no se encontró ninguna toxicidad aparente que afectara el comportamiento de los ratones (consumo de alimentos y agua) o el peso corporal.

Comprender cómo se comportan los nanosistemas a nivel molecular es de gran importancia para una posibles aplicación biomédica[51–53]. Aprovechando los grandes avances de la tecnología informática y en particular, de los métodos de simulación computacional, decidimos utilizar este conocimiento para obtener una mayor información de nuestros nanosistemas a escalas dimensionales y temporales que de otro modo serían técnicamente inalcanzables[54]. La combinación de estudios experimentales y computacionales ha dado como resultado una información sinérgica que nos permite llegar a una comprensión más profunda de la estructura interna de los nanosistemas desarrollados, solos o en combinación con fármacos específicos.

En esta tesis doctoral, uno de los objetivos planteados ha sido la exploración de las Simulaciones de Dinámica Molecular (MD) como herramienta para predecir la formación de nanosistemas. Reemplazando el nivel de detalle atomístico por esferas, el método de simulación de Coarse-Grained (CG) ha conseguido abrir un nuevo horizonte para simular procesos biomoleculares complejos y en escalas de tiempo inaccesibles para los modelos de All-Atom (AT)[55–57]. Usando como referencia los nanosistemas desarrollados en este trabajo y previamente caracterizados experimentalmente, intentamos investigar más en detalle su formación valiéndonos de un método *in silico*. Como primer paso, se simularon tres ratios V:SM previamente descritos en la fase de selección (**Tabla 1**), a saber, 1:0.1, 1:0.5 y 1:1 (**Figura 2A**). Curiosamente, solo mediante la aplicación de simulaciones de CG fuimos capaces de ubicar lo que denominamos un "bolsillo" de agua en el interior de todos los nanosistemas simulados, que también ha sido confirmado experimentalmente mediante Resonancia Magnética Nuclear (RMN). Basándonos en los datos obtenidos experimentalmente y los resultados de las simulaciones CG, se seleccionó el ratio V:SM 1:0.1 para su posterior modelizado con seis fármacos con características fisicoquímicas diferentes. En la **Figura 2B** se presenta representaciones esquemática (AT y GC) de cada componente implicado en las

simulaciones, desde los componentes de la formulación (en la región punteada) hasta cada fármaco testado. Los resultados obtenidos se presentan recopilados en la **Figura 2C** mostrando las características estructurales y dinámicas de los nanosistemas asociando las seis moléculas de interés. Las simulaciones de MD nos permitieron obtener información muy relevante para el desarrollo de una formulación. Por un lado fuimos capaces estudiar la capacidad de carga de los nanosistemas para cada molécula, dentro de esto su distribución/localización y las interacciones dominantes entre medicamento-nanosistema.

Nuestros resultados sugieren que estas mediciones cuantitativas a nivel molecular podrían aplicarse para diseñar, optimizar y realizar un barrido virtual de nanoplataformas. Las simulaciones de MD han avanzado a tal nivel que hoy en día sería posible hablar de "microscopía computacional" como una herramienta adicional a los métodos experimentales[55]. Numerosos estudios de simulación computacional se pueden encontrar en la literatura sobre interacciones *célula-nanosistema*, especialmente enfocados a dilucidar el papel de las propiedades fisicoquímicas de la superficie de los nanosistemas (y/o sus modificaciones químicas) para generar el contacto y la inserción con la membrana celular[52,54,58]. No obstante, la posibilidad de aplicar la simulación de GC como una herramienta de screening para el desarrollo de productos nanofarmacéuticos ha sido poco explorada hasta el momento[12]. Si bien es posible que exista una brecha entre los resultados computacionales y experimentales, estas simulaciones representan una herramienta muy prometedora que permitirá probar un amplio rango de condiciones durante el desarrollo del nanosistema, que de otra manera sería poco factible o incluso imposible de obtener experimentalmente. En general, la rápida expansión de la nanotecnología ha dado lugar a una ingente colección de nanosistemas que varían en una gran cantidad de propiedades como tamaño, forma, carga, composición química, recubrimiento y solubilidad, entre otras[40,44].

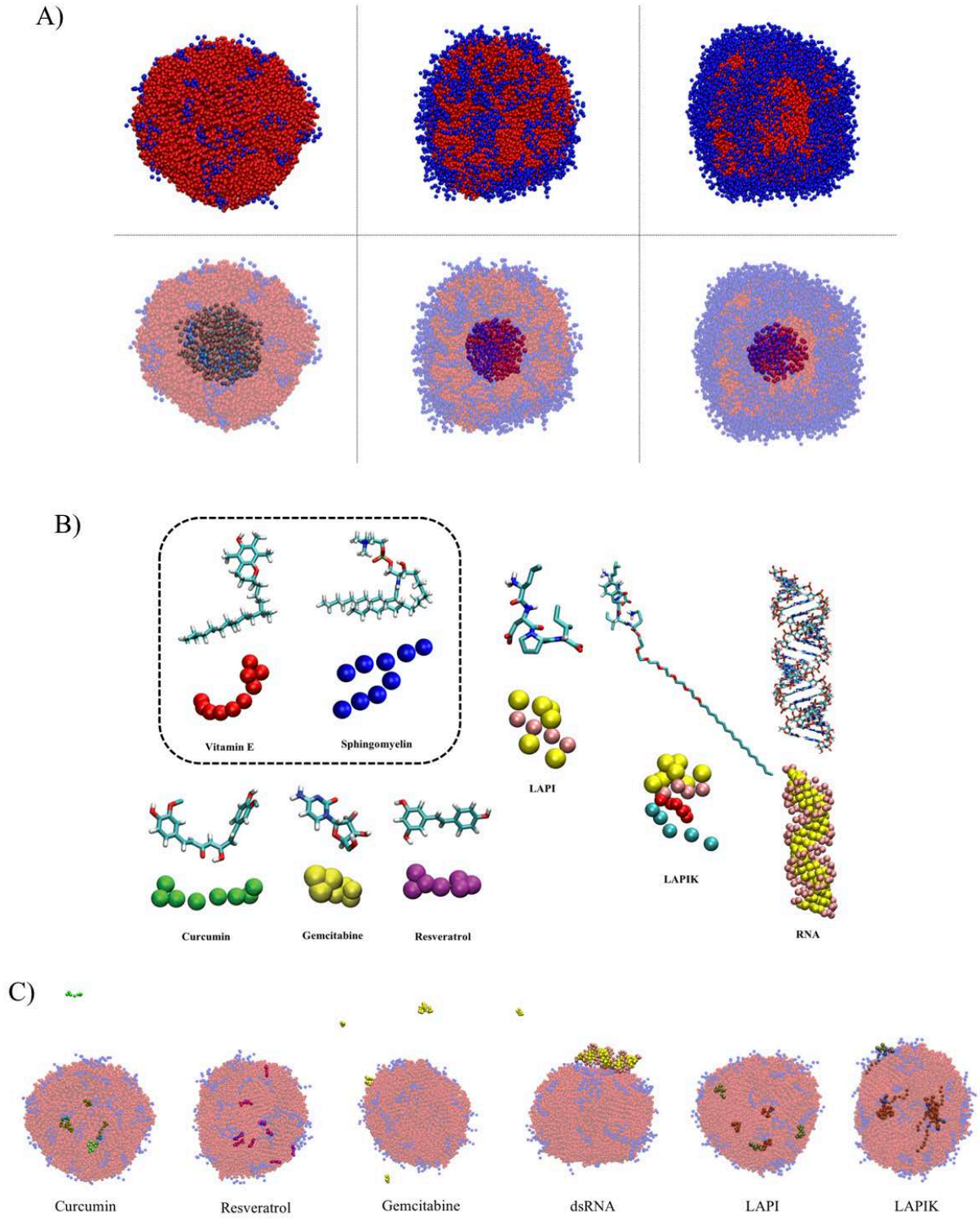

Figura 2: (A) Simulación de Dinámica Molecular Coarse-Grained (CG) de nanosistemas de vitamina E (V, esferas rojas) y esfingomielina (SM, esferas azules) en diferentes proporciones aceite/surfactante (de izquierda a derecha 1:0.1, 1:0.5 y 1:1). **(B)** Representación atomística (AT) y GC de los componentes formadores de nanoemulsión y las moléculas evaluadas. **(C)** Simulación de nanosistemas con ratio V:SM 1:0.1 con las seis moléculas seleccionadas (de izquierda a derecha: curcumina, resveratrol, gemcitabina, dsRNA, LAPI y LAPIK).

Teniendo en cuenta la primera parte del trabajo realizado en esta tesis doctoral, proponemos una estrategia a seguir desde las primeras fases de desarrollo de un nanosistemas hasta su evaluación fisicoquímica y caracterización como potencial nanomedicamento. Estrategia que podría beneficiar a una amplia gama de nanosistemas que se desarrollan actualmente o en un futuro[32]. Por lo tanto, en nuestra opinión, el diseño racional de un nanosistema debería incluir dos partes principales bien diferenciadas: primero, una caracterización fisicoquímica completa mediante diversas técnicas (las aquí señaladas y/o ampliadas) y segundo, un extenso análisis de la estructura química y biomolecular del nanosistema como unidad mediante la combinación de técnicas *in silico*, *in vitro* e *in vivo* para garantizar que la calidad y el perfil de seguridad del producto en investigación lo largo de los periodos preclínicos y clínicos de desarrollo.

2. Aplicaciones en el tratamiento del cáncer colorrectal.

El cáncer colorrectal es la tercera neoplasia maligna diagnosticada con mayor frecuencia y la cuarta causa de muerte relacionada con el cáncer en el mundo[59,60]. Incluso después de la resección quirúrgica y la quimioterapia agresiva, el 50% de los pacientes con carcinoma colorrectal desarrollan una enfermedad recurrente[61]. Este hecho resalta la necesidad de desarrollar nuevos enfoques terapéuticos para mejorar el tratamiento quimioterapéutico actual[62]. En esta tesis, hemos propuesto el desarrollo y la caracterización de nanosistemas de esfingomielina (SNs), formulación basada en únicamente dos componentes, un núcleo oleoso y una capa estabilizadora de surfactantes. Una vez caracterizada y optimizada la formulación, se exploraron dos potenciales aplicaciones, es decir, SNs en terapia génica frente al cáncer colorrectal y SNs como vehículos para una terapia combinada en cáncer colorrectal metastásico.

2.1. SNs en terapia génica frente al cáncer colorrectal

La terapia génica ha surgido como una estrategia prometedora para la modificación del material genético de células vivas con fines terapéuticos. Esta nueva terapia implica la introducción de un ácido nucleico funcional que reemplaza, amplifica, suprime o corrige un gen defectuoso[63]. En este sentido, las nanoemulsiones han demostrado ser un vehículo atractivo no solo para la administración de fármacos poco solubles sino también para biomoléculas como ácidos nucleicos oncoterapéuticos (por ejemplo, ADN plasmídico (pDNA) o ARN interferente (siRNA y miRNA))[64–66]. La administración sistémica de este tipo de biomoléculas se ha convirtido en un proceso complejo que necesita un transportador eficiente que sobrepase cada obstáculo presente. A pesar de la intensa investigación llevada a cabo en este campo, aún es necesario superar ciertas limitaciones como son la dificultad de conseguir un alto grado de especificidad celular, el aumento de su biodisponibilidad y el alargamiento de su vida media en

la circulación sanguínea para garantizar la traducción efectiva. Por lo tanto, una formulación exitosa será aquella que pueda encontrar el equilibrio entre una toxicidad aceptable, una buena eficiencia de transfección y una estabilidad adecuada[63,65,67,68].

El diseño de nanosistemas con características fisicoquímicas y biológicas apropiadas representa un parámetro crítico para asegurar su correcta interacción con los sistemas biológicos[69]. Para superar la degradación enzimática del material genético y promover su capacidad para cruzar membranas biológicas, la complejación del ADN con compuestos catiónicos ha sido la estrategia más explorada[63]. Para lograr esto, comúnmente se han incorporado a los nanotransportadores lípidos con marcada carga catiónica como DOTAP (1,2-diolyoxy-3-(trimethylammonium)propane), DOTMA (N-[1-(2,3-Dioleoyloxy)propyl]-N,N,N-trimethyl-ammonium methyl sulphate), ST (estearilamina), DC-CH (3β-[N-(N',N'-dimethylaminoethane)-carbamoyl] cholesterol) y CTAB (bromuro de cetiltrimetilamonio)[65,68]. Los nanosistemas catiónicos, aunque incorporan eficientemente los ácidos nucleicos terapéuticos, han tenido un éxito limitado en la administración *in vivo* principalmente debido a su toxicidad. Además, se sabe que los componentes catiónicos por su naturaleza química tienen predisposición a interactuar con las proteínas séricas, las lipoproteínas y la matriz extracelular, lo que lleva a la agregación del sistema o a la liberación de los oligonucleótidos antes de alcanzar las células diana[70]. Por otro lado, los nanosistemas cargados negativamente (generalmente absorbidos por las células fagocíticas) no representan una alternativa tan atractiva, ya que no resultarían en una eficiencia óptima debido a la repulsión de carga entre la nanoestructura y los oligonucleótidos cargados a su vez negativamente. Por lo tanto, los nanosistemas neutrales podrían representar una buena alternativa para evitar la toxicidad que se debe a las cargas positivas y la repulsión generada por las cargas negativas (**Tabla 2**).

Modificaciones químicas de oligonucleótidos desnudos se han utilizado para generar ácidos nucleicos resistentes a las nucleasas para evitar la degradación, mejorar su estabilidad y mejorar el tiempo de circulación[70]. La sustitución del grupo fosfodiéster por el grupo fosforotioato ha sido la primera modificación química aplicada a oligonucleótidos antisentido[71,72]. Aunque mejora la estabilidad del oligonucleótido, el fosforotioato por si solo no protege completamente, por lo que la modificación posterior con moléculas hidrofóbicas (como el colesterol) se ha explorado en este trabajo.

Tabla 2: Caracterización fisicoquímica y eficiencia de asociación de nanosistemas compuestos por Vitamina E (V) y esfingomielina (SM). Formulados con cantidades decrecientes de surfactante y un 0,5% de carga constante del oligonucleótido modificado (Rlas-CH).

Componentes del nanosistema		**Caracterización fisicoquímica**			
Ratio V:SM	**Rlas tipo**	**Tamaño (nm)**	**PdI**	**ZP (mV)**	**EA%**
1:0.1	-	125 ± 15	0.1	-6 ± 3	-
1:0.1	**Rlas-CH**	100 ± 8	0.2	-16 ± 2	19 ± 3
1:0.05		88 ± 2	0.2	-23 ± 1	17 ± 2
1:0.01		88 ± 1	0.2	-23 ± 1	19 ± 0
1:0		102 ± 12	0.2	-34 ± 3	21 ± 3

Como se muestra en la **tabla 2**, las formulaciones previamente desarrolladas y caracterizadas que poseen una carga cercana a la neutralidad (-6 ± 3 mV) se usaron para asociar los oligonucleótidos modificados con colesterol (Rlas-CH). La inclusión de un nuevo componente hidrofóbico implica la adición de un nuevo surfactante al nanosistema desarrollado. Este nuevo surfactante realiza una doble función, inicialmente hace posible que los Rlas se anclen a la nanoestructura y, por otro lado, aumenta la compactación de la nanoestructura. Dado que una de las hipótesis era que el residuo de colesterol (CH) podría favorecer la disposición de los

oligonucleótidos en la interfaz debido a su capacidad para actuar como surfactante y una posible interacción con la esfingomielina (SM)[73]. Los siguientes experimentos tuvieron como objetivo determinar si la disminución de la cantidad de SM manteniendo la misma concentración de Rlas-CH podría tener un efecto positivo. Curiosamente, observamos que los oligonucleótidos modificados con colesterol (Rlas-CH) eran capaces de estabilizar los nanosistemas en ausencia de SM, actuando de esa forma como el único surfactante de la formulación. Esta estrategia nos permitiría por lo tanto el desarrollo de nanosistemas que contengan una mínima presencia de surfactante o incluso nanosistemas libres de surfactante (**Tabla 2**). Sin embargo, serían necesarios estudios de estabilidad a largo plazo con esta formulación para probar su potencial. Por otro lado, para confirmar la encapsulación efectiva y la administración de los oligonucleótidos utilizando estos sistemas como transportadores, el oligonucleótido fue doblemente modificado con una cianina fluorescente (Cy3). Como se observa en la **Figura 3**, se logró una internalización efectiva en la línea celular SW480 de cáncer colorrectal.

En resumen, incluso siendo una formulación con carga neutra, este nanosistema ha demostrado poseer una buena capacidad para asociar oligonucleótidos modificados hidrofóbicamente (Rlas-CH) y administrarlos de manera efectiva a células cancerosas, lo que la convierte en una alternativa prometedora como terapia génica en el tratamiento del cáncer.

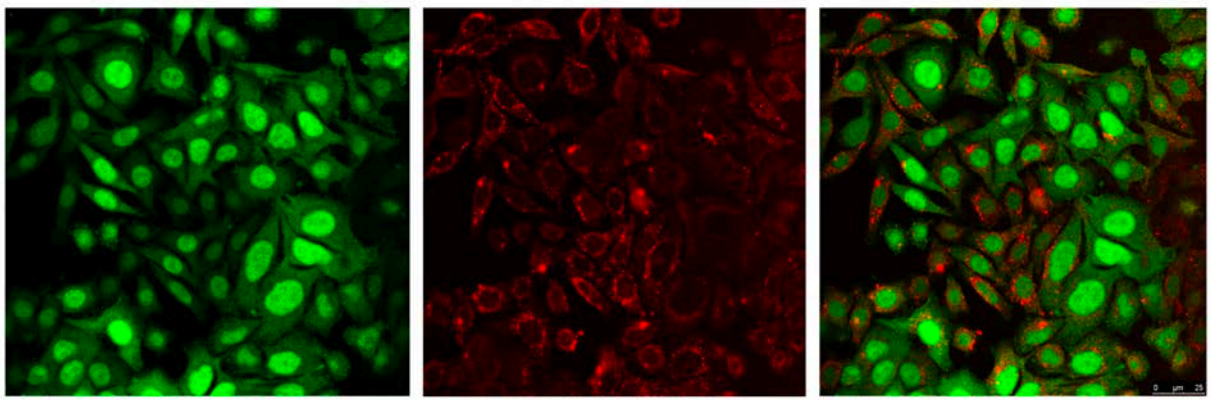

Figura 3: Estudios celulares que muestran la internalización eficiente de nanosistemas asociando Cy3-Rlas-CH (señal roja) en células de cáncer colorrectal SW480 que expresan GFP (señal verde).

2.2. SNs como vehículos para terapia combinada en cáncer colorrectal metastásico

Los nanosistemas destinados al tratamiento del cáncer se han diseñado principalmente basándose en la capacidad de las partículas nanométricas para mejorar los tiempos de circulación y, eventualmente, experimentar una acumulación pasiva en los tejidos tumorales debido al incremento de permeabilidad y retención (efecto EPR)[74]. Sin embargo, estudios recientes destacaron la necesidad de mejorar la acumulación de nanosistemas en el tumor desligando al efecto EPR de la ecuación[75,76]. Por medio de direccionalidad activa, los nanosistemas serían capaces de alcanzar niveles más altos de concentración de fármaco en los tejidos tumorales a través de la endocitosis mediada por receptores[77–79]. De hecho, el uso de ligandos de direccionamiento ha demostrado mejorar la eficacia, reducir los efectos secundarios y aumentar el rendimiento terapéutico al reconocer y unirse a receptores específicos y/o únicos de las células tumorales[80–82]. Típicamente, receptores involucrados en la progresión tumoral, tales como HER2, receptor de folato, CD44 y EGFR, han sido explotados para ese propósito[83]. Sin embargo, uno de los principales problemas relacionados con esta estrategia es que la mayoría de estos receptores no son específicos para las células cancerosas sino que se expresan de manera ubicua en el cuerpo y, en muchas ocasiones, la competencia con ligandos endógenos dificulta el potencial de este enfoque. Por lo tanto, es fundamental la búsqueda de marcadores únicos o altamente expresados en las células tumorales y no en las células normales para permitir la selectividad del tejido tumoral sobre tejido sano[61].

El receptor guanilato ciclasa C (CCG) se expresa mayoritariamente en la membrana apical de los enterocitos. Sin embargo, mantiene su expresión constitutiva en las células de cáncer colorrectal primarias y metastásicas, pero no en tejido extraintestinal sano donde las células de cáncer colorrectal generalmente metastatizan[84–88]. El receptor GCC es activado al unirse a las hormonas paracrinas Guanilina (Gn) y Uroguanilina (UroG), así como a la enterotoxina estable

al calor (ST) producida por *Escherichia coli* enterotoxigénica[89]. En base a este conocimiento previo, varias publicaciones han explotado la capacidad de dirigirse al receptor GCC para el diagnóstico molecular mediante PET y SPECT, basándose en la modificación química de los agonistas endógenos (UroG, Gn y ST)[90–93]. Recientemente, ha quedado claro que la activación del receptor GCC también desempeña un papel protector contra el cáncer colorrectal, principalmente porque las hormonas endógenas agonistas del receptor GCC desaparecen en un estado temprano en la carcinogénesis del cáncer colorrectal[94,95]. De esta forma, una estrategia basada en la quimioprevención mediante reemplazo de las hormonas endógenas ha llegado a la escena. En este trabajo, hemos propuesto la síntesis de un derivado de la hormona paracrina Uroguanilina (UroG) con una cadena de carbono pegilada (UroGm, **Figura 4**) para maximizar su interacción con los nanosistemas y explotar tanto la capacidad de targeting como terapéutica exhibida por esta hormona natural.

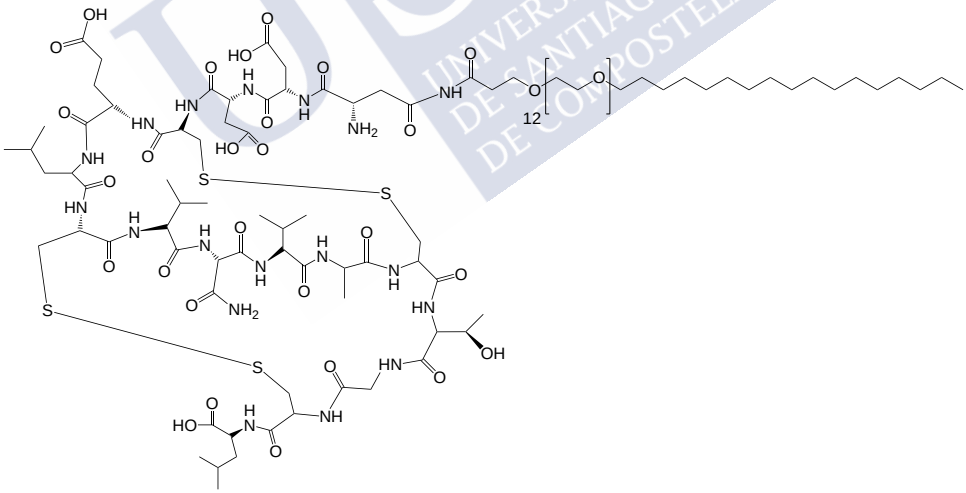

Figura 4. Uroguanilina modificada hidrofóbicamente (UroG-PEG_{12}-C_{18}, UroGm).

Está comprobado que el uso de un solo fármaco en el tratamiento del cáncer no suele producir remisiones completas o un mejor efecto terapéutico. Por lo tanto, una terapia combinada con varios agentes anticancerígenos unidos en un nanosistema podrían proporcionar una alternativa

más efectiva y superar resistencias, ya que diferentes medicamentos podrían atacar a las células cancerosas en diferentes etapas de sus ciclos de crecimiento[96]. Argumentos convincentes sobre la encapsulación de múltiples fármacos en un solo nanosistema se han propuesto anteriormente para el desarrollo de aplicaciones anti-cáncer colorrectal[61]. Uno de los parámetros clave a controlar es la unificación de la farmacocinética y la captación celular de los agentes terapéuticos, lo que permitirá el control preciso de la dosificación de los múltiples fármacos[96]. Teniendo en cuenta estos factores, la nanomedicina combinatoria debe diseñarse de tal manera que se dirija a múltiples vías de señalización manteniendo una toxicidad limitada[61]. En este trabajo se ha evaluado la decoración de nanosistemas con el derivado hidrofóbico de Uroguanilina (UroGm) combinado con la encapsulación de un fármaco anticancerígeno poco soluble en medio acuoso (etopósido, Etp).

Se realizaron experimentos *in vitro* dirigidos a confirmar la efectividad de las dos moléculas propuestas aisladamente contra células de cáncer colorrectal metastásico SW620 (ATCC® CCL-227 ™) (Capítulo 3). Adicionalmente, el ensayo de formación de colonias se empleó para evaluar el rango de concentración exacto en el que se obtiene un efecto sinérgico de ambos fármacos. Como se muestra en la **Figura 5A**, una concentración de 50nM tanto de UroGm como de Etp produce una reducción significativa de la formación de colonias comparado con sus controles. Este hecho propició que se realizase un estudio de eficacia *in vivo* en ratones con xenoinjerto de células SW620 para evaluar el potencial de esta terapia dual (UroGm + Etp). Como se muestra en la **Figura 5B**, se observó una reducción significativa del volumen del tumor para los ratones tratados con la formulación combinatoria (UroGm-Etp-SNs) mientras que el peso corporal de los ratones se mantuvo inalterado.

En conclusión, los resultados obtenidos en esta parte del trabajo exponen el gran potencial de esta alternativa terapéutica y de targeting para el tratamiento del cáncer colorrectal metastásico.

A)

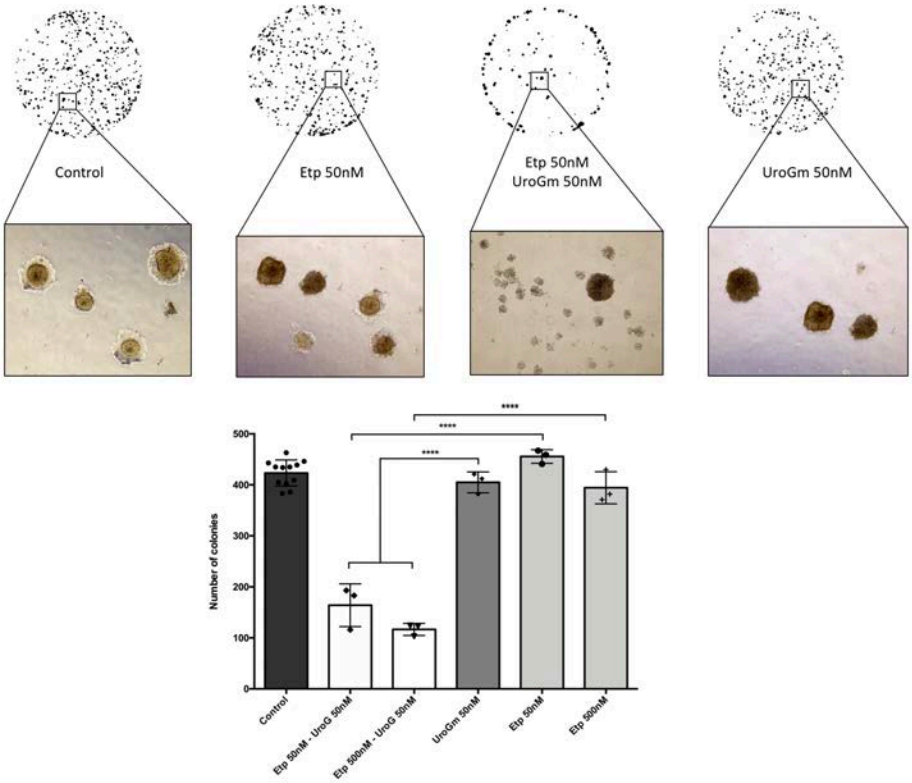

B)

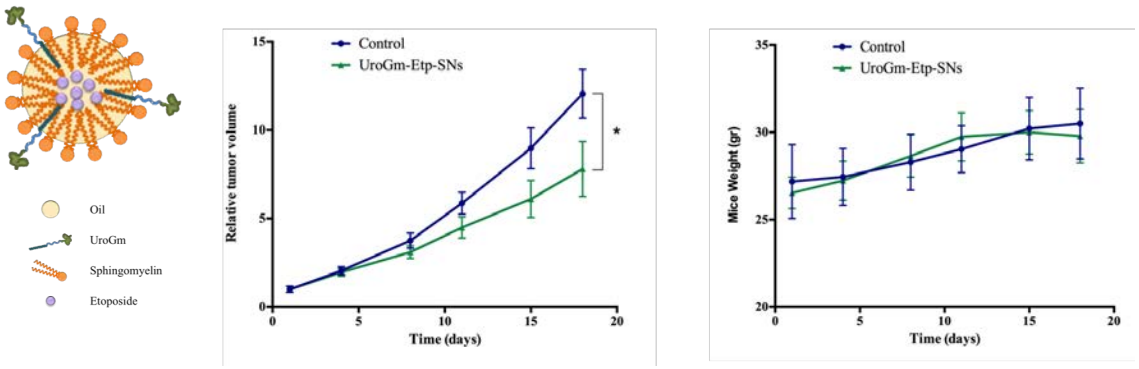

Figura 5: (A) Ensayo de formación de colonias que determina el rango de concentración en el que se observa un efecto sinérgico entre ambas moléculas terapéuticas, UroGm y Etp. **(B)** Representación esquemática de las formulaciones desarrolladas. Eficacia antitumoral en términos de volumen tumoral relativo y peso corporal de los ratones.

Conclusiones

El trabajo descrito en esta tesis tenía como objetivo el diseño racional de un nuevo tipo de plataforma, nanosistemas de esfingomielina (SNs), para la administración de fármacos oncológicos. Los datos obtenidos del trabajo experimental nos llevaron a plantear las siguientes conclusiones:

1. Se han desarrollado nanosistemas conteniendo esfingomielina como único surfactante estabilizante y un aceite en el núcleo (SNs). Para su formulación se ha utilizado una metodología simple y no agresiva, el método de inyección de etanol. Los nanosistemas mostraron una excelente estabilidad coloidal durante el almacenamiento y también tras la incubación en medios biológicamente relevantes.
2. Haciendo uso de estrategias computacionales *in silico* (simulaciones de dinámica molecular, MD), ha sido posible estudiar las interacciones fundamentales que rigen el ensamblaje, las características estructurales y dinámicas de los SNs. Además, se ha evaluado su capacidad de carga con diferentes fármacos recopilando información sobre la distribución/localización de las moléculas de fármaco dentro del nanosistema y además de la naturaleza de las interacciones *fármaco-nanosistema-medio circundante*.
3. Los SNs, aún mostrando una capacidad moderada para cargar oligonucleótidos, obtuvieron una citotoxicidad muy baja mientras que conservan la capacidad de promover la administración intracelular de las biomoléculas asociadas.
4. Los SNs demostraron a su vez su utilidad para el desarrollo de terapias dirigidas contra el cáncer. La hormona endógena (Uroguanilina, UroG), capaz de dirigirse al receptor de guanilato ciclasa C (GCC) y actuar de forma agonista hacia ella, se asoció

eficazmente a los SNs después de su modificación química generando un derivado hidrofobizado (UroGm). La combinación de esta formulación dirigida con el fármaco citostático etopósido (Etp) resultó en un efecto sinérgico *in vitro* y una respuesta moderada pero significativa en un modelo de xenoinjerto de cáncer colorrectal metastásico.

En general, este trabajo destaca la importancia del diseño racional para obtener nanosistemas con características fisicoquímicas y morfológicas adecuadas, perfiles coloidales y toxicológicos para maximizar las perspectivas de la traducción clínica. Además, proporciona las bases para el desarrollo de múltiples aplicaciones.

REFERENCIAS

(1) Farjadian, F.; Ghasemi, A.; Gohari, O.; Roointan, A.; Karimi, M.; Hamblin, M. R. Nanopharmaceuticals and Nanomedicines Currently on the Market: Challenges and Opportunities. *Nanomedicine* **2019**, *14*, 93–126.

(2) Ferrari, M. Cancer Nanotechnology: Opportunities and Challenges. *Nat. Rev. Cancer* **2005**, *5*, 161–171.

(3) Wagner, V.; Dullaart, A.; Bock, A. K.; Zweck, A. The Emerging Nanomedicine Landscape. *Nat. Biotechnol.* **2006**, *24*, 1211–1217.

(4) Ventola, C. L. Progress in Nanomedicine: Approved and Investigational Nanodrugs. *P T* **2017**, *42*, 742–755.

(5) Wicki, A.; Witzigmann, D.; Balasubramanian, V.; Huwyler, J. Nanomedicine in Cancer Therapy: Challenges, Opportunities, and Clinical Applications. *J. Control. Release* **2015**, *200*, 138–157.

(6) Venditto, V. J.; Szoka, F. C. Cancer Nanomedicines: So Many Papers and so Few Drugs! *Adv. Drug Deliv. Rev.* **2013**, *65*, 80–88.

(7) Hua, S.; de Matos, M. B. C.; Metselaar, J. M.; Storm, G. Current Trends and Challenges in the Clinical Translation of Nanoparticulate Nanomedicines: Pathways for Translational Development and Commercialization. *Front. Pharmacol.* **2018**, *9*, 790.

(8) Morigi, V.; Tocchio, A.; Bellavite Pellegrini, C.; Sakamoto, J. H.; Arnone, M.; Tasciotti, E. Nanotechnology in Medicine: From Inception to Market Domination. *J. Drug Deliv.* **2012**, *2012*, 1–7.

(9) Bobo, D.; Robinson, K. J.; Islam, J.; Thurecht, K. J.; Corrie, S. R. Nanoparticle-Based Medicines: A Review of FDA-Approved Materials and Clinical Trials to Date. *Pharm. Res.* **2016**, *33*, 2373–2387.

(10) Date, A. A.; Patil, R. R.; Panicucci, R.; Souto, E. B.; Lee, R. W. Translating Nanotechnology from Bench to Pharmaceutical Market: Barriers, Success, and Promises. *J. Drug Deliv.* **2012**, *2012*, 1–2.

(11) Hall, J. B.; Dobrovolskaia, M. A.; Patri, A. K.; McNeil, S. E. Characterization of Nanoparticles for Therapeutics. *Nanomedicine* **2007**, *2*, 789–803.

(12) Huynh, L.; Neale, C.; Pomès, R.; Allen, C. Computational Approaches to the Rational Design of Nanoemulsions, Polymeric Micelles, and Dendrimers for Drug Delivery. *Nanomedicine Nanotechnology, Biol. Med.* **2012**, *8*, 20–36.

(13) FDA. *Drug Products, Including Biological Products, That Contain Nanomaterials - Guidance for Industry*; 2017.

(14) Niu, Z.; Conejos-Sánchez, I.; Griffin, B. T.; O'Driscoll, C. M.; Alonso, M. J. Lipid-Based Nanocarriers for Oral Peptide Delivery. *Adv. Drug Deliv. Rev.* **2016**, *106*, 337–354.

(15) Duncan, R.; Gaspar, R. Nanomedicine(s) under the Microscope. *Mol. Pharm.* **2011**, *8*, 2101–2141.

(16) Patra, J. K.; Das, G.; Fraceto, L. F.; Campos, E. V. R.; Rodriguez-Torres, M. del P.; Acosta-Torres, L. S.; Diaz-Torres, L. A.; Grillo, R.; Swamy, M. K.; Sharma, S.; *et al.* Nano Based Drug Delivery Systems: Recent Developments and Future Prospects. *J. Nanobiotechnology* **2018**, *16*, 71.

(17) Eaton, M. A. W.; Levy, L.; Fontaine, O. M. A. Delivering Nanomedicines to Patients: A Practical Guide. *Nanomedicine Nanotechnology, Biol. Med.* **2015**, *11*, 983–992.

(18) Havel, H.; Finch, G.; Strode, P.; Wolfgang, M.; Zale, S.; Bobe, I.; Youssoufian, H.; Peterson, M.; Liu, M. Nanomedicines: From Bench to Bedside and Beyond. *AAPS J.* **2016**, *18*, 1373–1378.

(19) Rowe, R. C.; Sheskey, P.; Quinn, M. E. *Handbook of Pharmaceutical Excipients – 7th Edition*; Pharmaceutical Press, 2013; Vol. 18.

(20) Ingólfsson, H. I.; Melo, M. N.; van Eerden, F. J.; Arnarez, C.; Lopez, C. A.; Wassenaar, T. A.; Periole, X.; de Vries, A. H.; Tieleman, D. P.; Marrink, S. J. Lipid Organization of the Plasma Membrane. *J. Am. Chem. Soc.* **2014**, *136*, 14554–14559.

(21) Sezgin, E.; Levental, I.; Mayor, S.; Eggeling, C. The Mystery of Membrane Organization: Composition, Regulation

and Roles of Lipid Rafts. *Nat. Rev. Mol. Cell Biol.* **2017**, *18*, 361–374.

(22) Rauschert, S.; Gázquez, A.; Uhl, O.; Kirchberg, F. F.; Demmelmair, H.; Ruíz-Palacios, M.; Prieto-Sánchez, M. T.; Blanco-Carnero, J. E.; Nieto, A.; Larqué, E.; *et al.* Phospholipids in Lipoproteins: Compositional Differences across VLDL, LDL, and HDL in Pregnant Women. *Lipids Health Dis.* **2019**, *18*, 20.

(23) Dashti, M.; Kulik, W.; Hoek, F.; Veerman, E. C.; Peppelenbosch, M. P.; Rezaee, F. A Phospholipidomic Analysis of All Defined Human Plasma Lipoproteins. *Sci. Rep.* **2011**, *1*, 139.

(24) Skipski, V.; Barclay, M.; Barclay, R.; Fetzer, V.; Good, J.; Archibald, F. Lipid Composition of Human Serum Lipoproteins. *Biochem. J.* **1967**, *104*, 340–352.

(25) Hidaka, H.; Hanyu, N.; Sugano, M.; Kawasaki, K.; Yamauchi, K.; Katsuyama, T. Analysis of Human Serum Lipoprotein Lipid Composition Using MALDI-TOF Mass Spectrometry. *Ann. Clin. Lab. Sci.* **2007**, *37*, 213–221.

(26) Pons, M.; Foradada, M.; Estelrich, J. Liposomes Obtained by the Ethanol Injection Method. *Int. J. Pharm.* **1993**, *95*, 51–56.

(27) Maitani, Y.; Soeda, H.; Junping, W.; Takayama, K. Modified Ethanol Injection Method For Liposomes Containing β-Sitosterol β-D-Glucoside. *J. Liposome Res.* **2001**, *11*, 115–125.

(28) Jaafar-Maalej, C.; Diab, R.; Andrieu, V.; Elaissari, A.; Fessi, H. Ethanol Injection Method for Hydrophilic and Lipophilic Drug-Loaded Liposome Preparation. *J. Liposome Res.* **2010**, *20*, 228–243.

(29) Batzri, S.; Korn, E. D. Single Bilayer Liposomes Prepared without Sonication. *Biochim. Biophys. Acta - Biomembr.* **1973**, *298*, 1015–1019.

(30) Filipe, V.; Hawe, A.; Jiskoot, W. Critical Evaluation of Nanoparticle Tracking Analysis (NTA) by NanoSight for the Measurement of Nanoparticles and Protein Aggregates. *Pharm. Res.* **2010**, *27*, 796–810.

(31) Hou, J.; Ci, H.; Wang, P.; Wang, C.; Lv, B.; Miao, L.; You, G. Nanoparticle Tracking Analysis versus Dynamic Light Scattering: Case Study on the Effect of Ca2+and Alginate on the Aggregation of Cerium Oxide Nanoparticles. *J. Hazard. Mater.* **2018**, *360*, 319–328.

(32) Gao, X.; Lowry, G. V. Progress towards Standardized and Validated Characterizations for Measuring Physicochemical Properties of Manufactured Nanomaterials Relevant to Nano Health and Safety Risks. *NanoImpact* **2018**, *9*, 14–30.

(33) Nanosight. *Applications of Nanoparticle Tracking Analysis (NTA) in Nanoparticle Research*; 2009.

(34) ICH. Stability Testing of New Drug Substances and Products International Conference on Harmonization of Technical Requirements for Registration of Pharmaceuticals for Human Use. **2003**.

(35) Khan, M. S.; Akhtar, N. Regulation of Stability Studies to Enhance the Efficiency of Drug Registrations to Regulatory Authorities. *Arch. Pharm. Pract.* **2015**, *6*, 48.

(36) Wu, L.; Zhang, J.; Watanabe, W. Physical and Chemical Stability of Drug Nanoparticles. *Adv. Drug Deliv. Rev.* **2011**, *63*, 456–469.

(37) Heurtault, B.; Saulnier, P.; Pech, B.; Proust, J.-E.; Benoit, J.-P. Physico-Chemical Stability of Colloidal Lipid Particles. *Biomaterials* **2003**, *24*, 4283–4300.

(38) ICH. *Stability Testing of New Drug Substances and Products International Conference on Harmonization of Technical Requirements for Registration of Pharmaceuticals for Human Use*; 2003.

(39) Doktorovova, S.; Souto, E. B.; Silva, A. M. Nanotoxicology Applied to Solid Lipid Nanoparticles and Nanostructured Lipid Carriers - A Systematic Review of in Vitro Data. *Eur. J. Pharm. Biopharm.* **2014**, *87*, 1–18.

(40) Arora, S.; Rajwade, J. M.; Paknikar, K. M. Nanotoxicology and in Vitro Studies: The Need of the Hour. *Toxicol. Appl. Pharmacol.* **2012**, *258*, 151–165.

(41) Donaldson, K.; Stone, V.; Tran, C. L.; Kreyling, W.; Borm, P. J. a. Nanotoxicology : A New Frontier in Particle Toxicology Relevant to Both the Workplace and General Environment and to Consumer Safety. *Occup. Environ. Med.*

2004, *61*, 727–728.

(42) Oberdörster, G. Safety Assessment for Nanotechnology and Nanomedicine: Concepts of Nanotoxicology. *J. Intern. Med.* **2010**, *267*, 89–105.

(43) Lv, H.; Zhang, S.; Wang, B.; Cui, S.; Yan, J. Toxicity of Cationic Lipids and Cationic Polymers in Gene Delivery. *J. Control. Release* **2006**, *114*, 100–109.

(44) Stone, V.; Donaldson, K. Nanotoxicology: Signs of Stress. *Nat. Nanotechnol.* **2006**, *1*, 23–24.

(45) Yu, T.; Malugin, A.; Ghandehari, H. Impact of Silica Nanoparticle Design on Cellular Toxicity and Hemolytic Activity. *ACS Nano* **2011**, *5*, 5717–5728.

(46) Hill, A. J.; Teraoka, H.; Heideman, W.; Peterson, R. E. Zebrafish as a Model Vertebrate for Investigating Chemical Toxicity. *Toxicol. Sci.* **2005**, *86*, 6–19.

(47) Gutiérrez-Lovera, C.; Vázquez-Ríos, A.; Guerra-Varela, J.; Sánchez, L.; de la Fuente, M. The Potential of Zebrafish as a Model Organism for Improving the Translation of Genetic Anticancer Nanomedicines. *Genes (Basel).* **2017**, *8*, 349.

(48) McGrath, P.; Li, C.-Q. Zebrafish: A Predictive Model for Assessing Drug-Induced Toxicity. *Drug Discov. Today* **2008**, *13*, 394–401.

(49) OECD. *Guidelines for the Testing of Chemicals, Fish Embryo Acute Toxicity (FET) Test, Test No. 236.*; OECD, 2013.

(50) Chapman, K. L.; Holzgrefe, H.; Black, L. E.; Brown, M.; Chellman, G.; Copeman, C.; Couch, J.; Creton, S.; Gehen, S.; Hoberman, A.; *et al.* Pharmaceutical Toxicology: Designing Studies to Reduce Animal Use, While Maximizing Human Translation. *Regul. Toxicol. Pharmacol.* **2013**, *66*, 88–103.

(51) Yang, K.; Ma, Y.-Q. Computer Simulation of the Translocation of Nanoparticles with Different Shapes across a Lipid Bilayer. *Nat. Nanotechnol.* **2010**, *5*, 579–583.

(52) Ding, H. ming; Ma, Y. qiang. Computer Simulation of the Role of Protein Corona in Cellular Delivery of Nanoparticles. *Biomaterials* **2014**, *35*, 8703–8710.

(53) Ding, H. M.; Tian, W. De; Ma, Y. Q. Designing Nanoparticle Translocation through Membranes by Computer Simulations. *ACS Nano* **2012**, *6*, 1230–1238.

(54) Ding, H. M.; Ma, Y. Q. Design Strategy of Surface Decoration for Efficient Delivery of Nanoparticles by Computer Simulation. *Sci. Rep.* **2016**, *6*, 1–10.

(55) Ingólfsson, H. I.; Lopez, C. A.; Uusitalo, J. J.; de Jong, D. H.; Gopal, S. M.; Periole, X.; Marrink, S. J. The Power of Coarse Graining in Biomolecular Simulations. *Wiley Interdiscip. Rev. Comput. Mol. Sci.* **2014**, *4*, 225–248.

(56) Marrink, S. J.; Risselada, H. J.; Yefimov, S.; Tieleman, D. P.; De Vries, A. H. The MARTINI Force Field: Coarse Grained Model for Biomolecular Simulations. *J. Phys. Chem. B* **2007**, *111*, 7812–7824.

(57) Marrink, S. J.; de Vries, A. H.; Mark, A. E. Coarse Grained Model for Semiquantitative Lipid Simulations. *J. Phys. Chem. B* **2004**, *108*, 750–760.

(58) Nielsen, S. O.; Lopez, C. F.; Srinivas, G.; Klein, M. L. Coarse Grain Models and the Computer Simulation of Soft Materials. *J. Phys. Condens. Matter* **2004**, *16*, R481–R512.

(59) Ferlay, J.; Soerjomataram, I.; Dikshit, R.; Eser, S.; Mathers, C.; Rebelo, M.; Parkin, D. M.; Forman, D.; Bray, F. Cancer Incidence and Mortality Worldwide: Sources, Methods and Major Patterns in GLOBOCAN 2012. *Int. J. Cancer* **2015**, *136*, E359–E386.

(60) Arnold M, Sierra MS, Laversanne M, et al. Global Patterns and Trends in Colorectal Cancer Incidence and Mortality. *Gut* **2016**, *66*, 683–691.

(61) Anitha, A.; Maya, S.; Sivaram, A. J.; Mony, U.; Jayakumar, R. Combinatorial Nanomedicines for Colon Cancer Therapy. *Wiley Interdiscip. Rev. Nanomedicine Nanobiotechnology* **2016**, *8*, 151–159.

(62) Shi, J.; Kantoff, P. W.; Wooster, R.; Farokhzad, O. C. Cancer Nanomedicine: Progress, Challenges and Opportunities.

Nat. Rev. Cancer **2017**, *17*, 20–37.

(63) Verissimo, L. M.; Agnez Lima, L. F.; Monte Egito, L. C.; De Oliveira, A. G.; Do Egito, E. S. T. Pharmaceutical Emulsions: A New Approach for Gene Therapy. *J. Drug Target.* **2010**, *18*, 333–342.

(64) Teixeira, H.; Dubernet, C.; Puisieux, F.; Benita, S.; Couvreur, P. Submicron Cationic Emulsions as a New Delivery System for Oligonucleotides. *Pharm. Res.* **1999**, *16*, 30–36.

(65) Teixeira, H. F.; Bruxel, F.; Fraga, M.; Schuh, R. S.; Zorzi, G. K.; Matte, U.; Fattal, E. Cationic Nanoemulsions as Nucleic Acids Delivery Systems. *Int. J. Pharm.* **2017**, *534*, 356–367.

(66) Yin, H.; Kanasty, R. L.; Eltoukhy, A. A.; Vegas, A. J.; Dorkin, J. R.; Anderson, D. G. Non-Viral Vectors for Gene-Based Therapy. *Nat. Rev. Genet.* **2014**, *15*, 541–555.

(67) Mazza, M.; Alonso-Sande, M.; Jones, M.-C.; de la Fuente, M. The Potential of Nanoemulsions in Biomedicine. In *Fundamentals of Pharmaceutical Nanoscience*; Springer New York: New York, NY, 2013; pp. 117–158.

(68) Tamilvanan, S. Formulation of Multifunctional Oil-in-Water Nanosized Emulsions for Active and Passive Targeting of Drugs to Otherwise Inaccessible Internal Organs of the Human Body. *Int. J. Pharm.* **2009**, *381*, 62–76.

(69) Fischer, H. C.; Chan, W. C. Nanotoxicity: The Growing Need for in Vivo Study. *Curr. Opin. Biotechnol.* **2007**, *18*, 565–571.

(70) Ozpolat, B.; Sood, A. K.; Lopez-Berestein, G. Nanomedicine Based Approaches for the Delivery of SiRNA in Cancer. *J. Intern. Med.* **2010**, *267*, 44–53.

(71) Manoharan, M.; Johnson, L. K.; McGee, D. P. C.; Guinosso, C. J.; Ramasamy, K.; Springer, R. H.; Bennett, C. F.; Ecker, D. J.; Vickers, T.; Cowsert, L.; *et al.* Chemical Modifications to Improve Uptake and Bioavailability of Antisense Oligonucleotides. *Ann. N. Y. Acad. Sci.* **1992**, *660*, 306–309.

(72) Khvorova, A.; Watts, J. K. The Chemical Evolution of Oligonucleotide Therapies of Clinical Utility. *Nat. Biotechnol.* **2017**, *35*, 238–248.

(73) Barenholz, Y. Sphingomyelin and Cholesterol:From Membrane Biophysics and Rafts to Potential Medical Applications. In *Subcellular Biochemistry*; Springer, Boston, MA, 2004; Vol. 37, pp. 167–215.

(74) Maeda, H.; Greish, K.; Fang, J. The EPR Effect and Polymeric Drugs: A Paradigm Shift for Cancer Chemotherapy in the 21st Century. *Advances in Polymer Science*, 2006, *193*, 103–121.

(75) Teijeiro-Valiño, C.; Novoa-Carballal, R.; Borrajo, E.; Vidal, A.; Alonso-Nocelo, M.; Freire, M. D. L. F.; Lopez-Casas, P. P.; Hidalgo, M.; Csaba, N.; Alonso, M. J. A Multifunctional Drug Nanocarrier for Efficient Anticancer Therapy. *J. Control. Release* **2019**, *294*, 154–164.

(76) Wilhelm, S.; Tavares, A. J.; Dai, Q.; Ohta, S.; Audet, J.; Dvorak, H. F.; Chan, W. C. W. Analysis of Nanoparticle Delivery to Tumours. *Nat. Rev. Mater.* **2016**, *1*, 16014.

(77) Danhier, F.; Feron, O.; Préat, V. To Exploit the Tumor Microenvironment: Passive and Active Tumor Targeting of Nanocarriers for Anti-Cancer Drug Delivery. *Journal of Controlled Release*, 2010, *148*, 135–146.

(78) Byrne, J. D.; Betancourt, T.; Brannon-Peppas, L. Active Targeting Schemes for Nanoparticle Systems in Cancer Therapeutics. *Adv. Drug Deliv. Rev.* **2008**, *60*, 1615–1626.

(79) Ganta, S.; Talekar, M.; Singh, A.; Coleman, T. P.; Amiji, M. M. Nanoemulsions in Translational Research—Opportunities and Challenges in Targeted Cancer Therapy. *AAPS PharmSciTech* **2014**, *15*, 694–708.

(80) Hak, S.; Helgesen, E.; Hektoen, H. H.; Huuse, E. M.; Jarzyna, P. A.; Mulder, W. J. M.; Haraldseth, O.; Davies, C. de L. The Effect of Nanoparticle Polyethylene Glycol Surface Density on Ligand-Directed Tumor Targeting Studied in Vivo by Dual Modality Imaging. *ACS Nano* **2012**, *6*, 5648–5658.

(81) Béduneau, A.; Saulnier, P.; Hindré, F.; Clavreul, A.; Leroux, J. C.; Benoit, J. P. Design of Targeted Lipid Nanocapsules by Conjugation of Whole Antibodies and Antibody Fab' Fragments. *Biomaterials* **2007**, *28*, 4978–4990.

(82) Loureiro, A.; Nogueira, E.; Azoia, N. G.; Sárria, M. P.; Abreu, A. S.; Shimanovich, U.; Rollett, A.; Härmark, J.; Hebert, H.; Guebitz, G.; *et al.* Size Controlled Protein Nanoemulsions for Active Targeting of Folate Receptor Positive Cells. *Colloids Surfaces B Biointerfaces* **2015**, *135*, 90–98.

(83) Shi, J.; Kantoff, P. W.; Wooster, R.; Farokhzad, O. C. Cancer Nanomedicine: Progress, Challenges and Opportunities. *Nat. Rev. Cancer* **2017**, *17*, 20–37.

(84) Potter, L. R. Regulation and Therapeutic Targeting of Peptide-Activated Receptor Guanylyl Cyclases. *Pharmacol. Ther.* **2011**, *130*, 71–82.

(85) Forte, L. R. Uroguanylin and Guanylin Peptides: Pharmacology and Experimental Therapeutics. *Pharmacol. Ther.* **2004**, *104*, 137–162.

(86) Pitari, G. M.; Li, P.; Lin, J. E.; Zuzga, D.; Gibbons, A. V.; Snook, A. E.; Schulz, S.; Waldman, S. A. The Paracrine Hormone Hypothesis of Colorectal Cancer. *Clin. Pharmacol. Ther.* **2007**, *82*, 441–447.

(87) Camici, M. Guanylin Peptides and Colorectal Cancer (CRC). *Biomed. Pharmacother.* **2008**, *62*, 70–76.

(88) Buc, E.; Der Vartanian, M.; Darcha, C.; Déchelotte, P.; Pezet, D. Guanylyl Cyclase C as a Reliable Immunohistochemical Marker and Its Ligand Escherichia Coli Heat-Stable Enterotoxin as a Potential Protein-Delivering Vehicle for Colorectal Cancer Cells. *Eur. J. Cancer* **2005**, *41*, 1618–1627.

(89) Yarla, N. S.; Gali, H.; Pathuri, G.; Smriti, S.; Farooqui, M.; Panneerselvam, J.; Kumar, G.; Madka, V.; Rao, C. V. Targeting the Paracrine Hormone-Dependent Guanylate Cyclase/CGMP/Phosphodiesterases Signaling Pathway for Colorectal Cancer Prevention. *Semin. Cancer Biol.* **2018**.

(90) Giblin, M. F.; Sieckman, G. L.; Watkinson, L. D.; Daibes-Figueroa, S.; Hoffman, T. J.; Forte, L. R.; Volkert, W. A. Selective Targeting of E. Coli Heat-Stable Enterotoxin Analogs to Human Colon Cancer Cells. *Anticancer Res* **2006**, *26*, 3243–3251.

(91) Tian, X.; Michal, A. M.; Li, P.; Wolfe, H. R.; Waldman, S. A.; Wickstrom, E. STa Peptide Analogs for Probing Guanylyl Cyclase C. *Biopolym. - Pept. Sci. Sect.* **2008**, *90*, 713–723.

(92) Liu, D.; Overbey, D.; Watkinson, L. D.; Daibes-Figueroa, S.; Hoffman, T. J.; Forte, L. R.; Volkert, W. A.; Giblin, M. F. In Vivo Imaging of Human Colorectal Cancer Using Radiolabeled Analogs of the Uroguanylin Peptide Hormone. *Anticancer Res.* **2009**, *29*, 3777–3783.

(93) Liu, D.; Overbey, D.; Watkinson, L. D.; Smith, C. J.; Daibes-Figueroa, S.; Hoffman, T. J.; Forte, L. R.; Volkert, W. A.; Giblin, M. F. Comparative Evaluation of Three Cu-64-Labeled E-Coli Heat-Stable Enterotoxin Analogues for PET Imaging of Colorectal Cancer. *Bioconjug. Chem.* **2010**, *21*, 1171–1176.

(94) Brierley, S. M. Guanylate Cyclase-C Receptor Activation: Unexpected Biology. *Curr. Opin. Pharmacol.* **2012**, *12*, 632–640.

(95) Waldman, S. A.; Camilleri, M. Guanylate Cyclase-C as a Therapeutic Target in Gastrointestinal Disorders. *Gut* **2018**, *67*, 1543–1552.

(96) Aryal, S.; Hu, C. M. J.; Zhang, L. Combinatorial Drug Conjugation Enables Nanoparticle Dual-Drug Delivery. *Small* **2010**, *6*, 1442–1448.

INTRODUCTION

USC
UNIVERSIDADE
DE SANTIAGO
DE COMPOSTELA

1. Nanopharmaceuticals in clinical practice.

Over the past decades, the advances made in the field of nanotechnology together with a deeper understanding of biomedical and pharmaceutical sciences have enabled the growth of a new field, nanomedicine. The term "nanomedicine" groups altogether products for therapeutic and/or diagnostic purposes to achieve an innovation in healthcare[1–3].

Nanomedicines can be described as drug delivery systems developed to operate on a nanometer size range (without an established consensus, typically from 1 to 100 nm as defined by the UPAC), with novel properties that provide medical and pharmaceutical benefits[4–8]. Hence, the adequate use of nanotechnological properties allow new engineered nanostructures containing different molecular entities to protect their cargo, control or modify their pharmacokinetic/pharmacodynamic profile, enhance the efficacy or otherwise reduce their toxicity[9,10]. Therefore, the ultimate goal of nanomedicine-based research is the successful development of nanopharmaceuticals (both nanodrugs, nanodevices and/or nanotheranostics) able to reach clinical practice[11–13].

Application of nanotechnology in the biomedicine field is already a reality. To date, more than 50 nanopharmaceuticals have been approved and thus being available in the clinics[14–16]. Besides, a wide range of nanosystems are currently being tested in clinical trials[17,18].

In order to classify the commercialized nanopharmaceuticals we have divided them according to their nature into organic or inorganic. This introduction will be focused only in the organic-based nanopharmaceuticals divided as well into polymer, protein and lipid-based nanopharmaceuticals. A comprehensive analysis of the current state of approved nanomedicines has been done and an up-to-date list of them is provided in **table 1** (lipid-based nanosystems) and **table 2** (polymer and protein-based nanosystems). As shown below, since

1990 up to 43 organic-based nanopharmaceuticals have obtained the approval from either the U.S. Food and Drug Administration (FDA) or the European Medicines Agency (EMA).

Table 1. Lipid-based EMA and FDA-approved nanopharmaceuticals[9,17,19–24].

Commercialized product	Date of Approval	Drug	Type	Indication	Composition
Diazemuls®	1989	Diazepam	Emulsion	Anesthesia	Soybean oil Monoglycerides Egg phospholipids
Doxil®/Caelix®	1995	Doxorubicin	PEGylated Liposome	Oncology	PEG 2000-DSPE HSPC CH
Abelcet®	1995	Amphotericin B	Liposome	Anti-infective	DMPC DMPG
DaunoXome®	1996	Daunorubicin	Liposome	Oncology	DSPC CH
Diprivan®	1996	Propofol	Emulsion	Anesthesia	Soybean oil Egg lecithin
Amphotec®	1996	Amphotericin B	Lipid complex	Anti-infective	Cholesteryl sulfate
Ambisome®	1997	Amphotericin B	Liposome	Anti-infective	HSPC CH DSPG
DepoCyt®	1999	Cytarabine	Liposome	Anti-infective	DOPC DPPG CH Triolein
Curosurf®	1999	Poractant alfa	Lipid complex	Respiratory disease	Porcine lung phospholipids Hydrophobic proteins SP-B and SP-C
Visudyne®	2000	Verteporphin	Liposome	Ophthalmic	DMPC EPG

Commercialized product	Date of Approval	Drug	Type	Indication	Composition
Myocet®	2000	Doxorubicin	Liposome	Oncology	EPC CH
Restasis®	2002	Cyclosporine	Emulsion	Ophthalmic	Castor oil Polysorbate 80
Etomidate Lipuro®	2002	Etomidate	Emulsion	Anesthesia	Soybean oil Medium chain triglycerides Egg lecithin
Estrasorb™	2003	Estradiol	Emulsion	Hormone replacement	Soybean oil Polysorbate 80
DepoDur™	2004	Morphine sulfate	Liposomes	Chronic Pain	DOPC DPPG CH Triolein and Tricaprylin
Cleviprex®	2008	Clevidipine	Emulsion	Antihypertensive	Soybean oil Oleic acid Disodium edetate Egg phospholipids
Mepact™	2009	Mifamurtide	Liposome	Oncology	POPC DOPS
Exparel®	2011	Bupivacaine	Liposome	Pain management	DEPC DPPG CH Tricaprylin
Marqibo®	2012	Vincristine	Liposome	Oncology	SM CH
Lipodox™	2013	Doxorubicin hydrochloride	PEGylated Liposome	Oncology	MPEG 2000-DSPE DSPC CH
Onivyde®	2015	Irinotecan	PEGylated Liposome	Oncology	DSPC MPEG-2000-DSPE CH
Vyxeos®	2017	Cytarabine and daunorubicin	Liposome	Oncology	DSPG DSPC CH

From all approved products, polymeric conjugates based on PEGylation strategies as well as liposomes are the most represented[25]. These two modalities were also represented among the first five nanopharmaceuticals being commercialized (PEGylated enzymes Adagen® in 1990[26] and Oncaspar® in 1994, lipid-based emulsion Diazemuls® in 1989, PEGylated liposomes Doxil®[27] and non-PEGylated liposome Abelcet® in 1995). PEGylation strategy has been particularly successful in marketed products due to its ability to prevent the interaction of the nanopharmaceuticals with the mononuclear phagocyte system, therefore providing a greater stability after intravenous injection and an extended blood circulation time[28]. Additionally, two protein-based products have also been approved to date, namely Ontak® (Il-2 fusion protein, 1999)[29] and Abraxane® (Albumin nanoparticle, 2005)[30] starting a promising strategy of using natural proteins as drug carriers. Finally, in terms of indication, is remarkable that the majority of marketed organic-based nanopharmaceuticals corresponds to cancer therapies, though nanopharmaceuticals for other indications such as anti-infective, ophthalmic diseases, or pain management, have also been successfully commercialized[9,12].

Table 2. Polymer and Protein-based EMA and FDA-approved nanopharmaceuticals[9,17,19–24,31]

Commercialized product	Date of Approval	Drug	Type	Indication	Composition
Adagen®	1990	Adenosine deaminase enzyme	Polymeric conjugate	Enzyme replacement	Monomethoxypolyethylene glycol (PEG) 5kDa
Oncaspar®	1994	L-asparaginase	Polymeric conjugate	Oncology	Monomethoxypolyethylene glycol (PEG) 5kDa
Copaxone®	1996	Polypeptide	Polymeric conjugate	Multiple Sclerosis	L-glutamate L-arginine L-lysine L-tyrosine

Commercialized product	Date of Approval	Drug	Type	Indication	Composition
Ontak®	1999	Denileukin diftitox	Protein nanoparticle	Oncology	Il-2 fusion protein
Renagel®	2000	Sevelamer hydrochloride	Polymeric conjugate	Renal Disease	Cross-linked poly (allylamine hydrochloride)
PegIntron®	2001	Interferon alfa-2b	Polymeric conjugate	Anti-infective	Monomethoxypolyethylene glycol (PEG)12kDa
Pegasys®	2002	Interferon alfa-2a	Polymeric conjugate	Anti-infective	Monomethoxypolyethylene glycol (PEG) 40kDa
Neulasta®	2002	Recombinant methionyl human G-CSF (filgrastim)	Polymeric conjugate	Oncology	Monomethoxypolyethylene glycol (PEG) 20kDa
Eligard®	2002	Leuprolide acetate	Polymeric nanoparticle	Oncology	DL-lactic-co-glycolic acid (PLGA)
Somavert®	2003	Human Growth Hormone receptor antagonist	Polymeric conjugate	Hormone replacement	Monomethoxypolyethylene glycol (PEG) 5kDa
Macugen®	2004	anti-VEGF aptamer	Polymeric conjugate	Ophthalmic	Monomethoxypolyethylene glycol (PEG) 40kDa
Abraxane®	2005	Paclitaxel	Protein nanoparticle	Oncology	Albumin-bound paclitaxel
Mircera®	2007	Epoetin beta (Erythropoietin receptor activator)	Polymeric conjugate	Anemia	Monomethoxypolyethylene glycol (PEG) 30kDa
Genexol®	2007	Paclitaxel	Polymeric nanoparticle	Oncology	Monomethoxy-poly(ethylene glycol)-block-poly(D,L lactic acid) (PEG-PLA)
Cimzia®	2008	Certolizumab	Polymeric conjugate	Autoimmune disease	Polyethylene glycol (PEG) 40kDa

Commercialized product	Date of Approval	Drug	Type	Indication	Composition
Krystexxa®	2010	Porcine-like uricase	Polymeric conjugate	Pain management	Monomethoxypolyethylene glycol (PEG) 10kDa
Plegridy®	2014	Interferon beta-1a	Polymeric conjugate	Multiple sclerosis	Monomethoxypolyethylene glycol (PEG) 20kDa
VivaGel®	2014	SPL7013 antiviral dendrimer	Dendrimer	Anti-infective	3% w/w SPL7013
Adynovate®	2015	Coagulation Factor VIII	Polymeric conjugate	Hemophilia	Monomethoxypolyethylene glycol (PEG) 20kDa
Zilretta®	2017	Triamcinolone acetonide	Polymeric nanoparticle	Pain management	Poly lactic-co-glycolic acid (PLGA)
Rebinyn®	2017	Coagulation Factor IX	Polymeric conjugate	Hemophilia	Polyethylene glycol (PEG) 40kDa

Components: DMPC: Dimyristoyl-phosphatidylcholine; **DMPG:** Dimyristoyl-phosphatidylglycerol; **PEG 2000-DSPE:** N-(carbonyl-methoxypolyethylene glycol 2000)-1,2-distearoyl-sn-glycero3-phosphatidylethanolamine; **HSPC**: Fully hydrogenated soy phosphatidylcholine; **CH:** Cholesterol; **DSPC:** Distearoyl phosphatidylcholine; **DSPG:** Distearoyl phosphatidylglycerol; **DOPC:** Dioleoyl phosphatidylcholine; **DPPG:** Dipalmitoyl phosphatidylglycerol; **EPG:** Egg phosphatidylglycerol; **POPC:** 1-palmitoyl-2-oleoyl-sn-glycerol-3-phosphocholine; **DOPS:** 1,2-dioleoyl-sn-glycero-3-phosphatidylserine; **SM:** Sphingomyelin; **MPEG-2000:** Polyethylene-glycol 2000.

2. Nanocarriers as platforms for drug delivery

As illustrated in **Figure 1**, nanostructures can be classified according to their structure and composition under different terms such as micelles, liposomes, emulsions, polymeric nanoparticles, nanocrystals, dendrimers, inorganic nanoparticles, quantum dots and carbon nanotubes among others[17,32,33]. Overall, these nanostructures could be classified in two categories, inorganic or organic nanosystems. Organic materials include lipid, protein or polymer-based nanosystems. Finally, nanocrystals represent an undefined group between organic and inorganic materials.

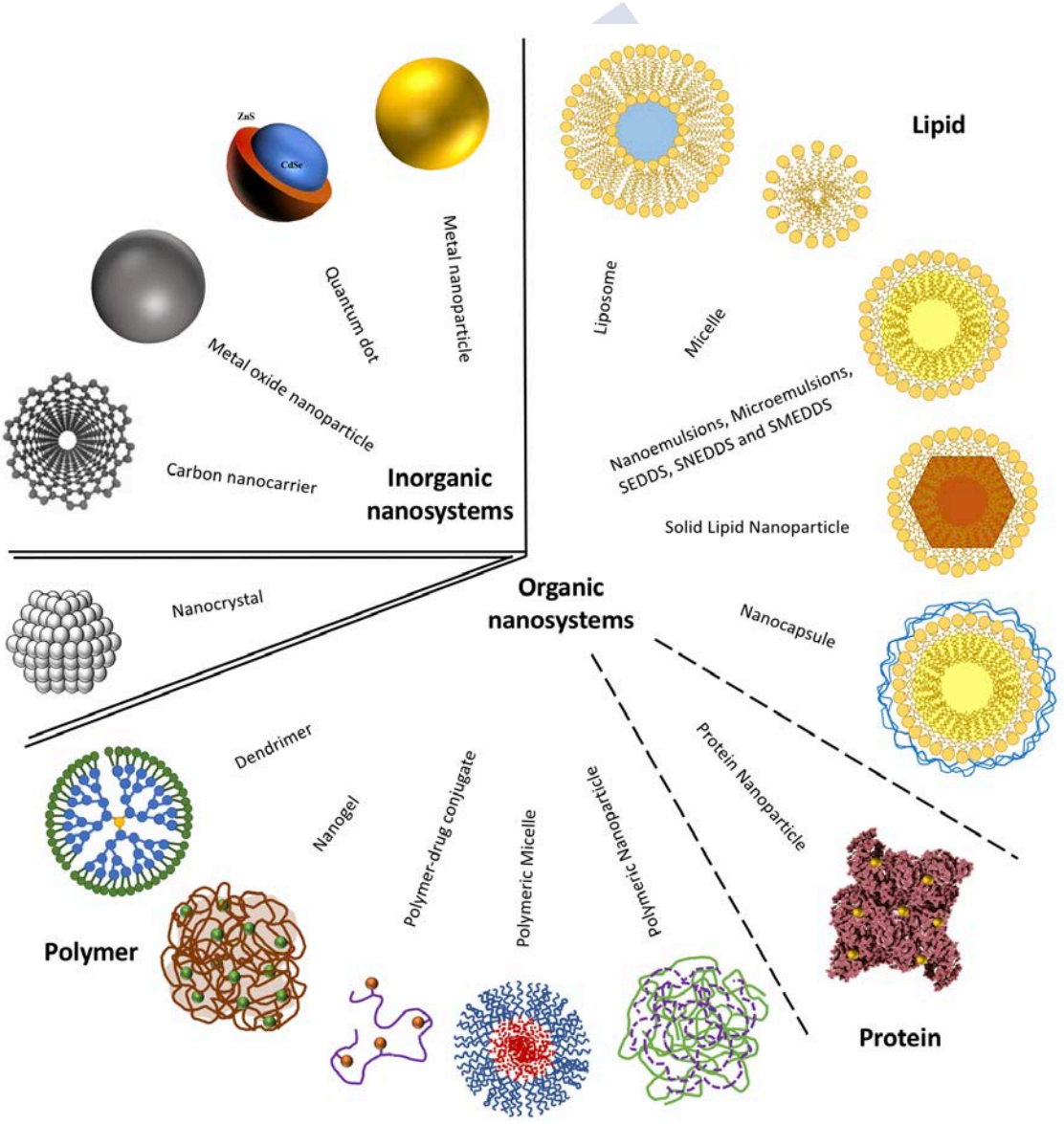

Figure 1: Schematic illustration of inorganic and organic nanocarrier platforms.

2.1. Inorganic nanosystems

Inorganic nanosystems are composed of a wide range of materials including elemental metals, metal oxides, and metal salts. They are being used for numerous applications including photo, magnetic, radio or ultrasound thermal therapy, imaging and drug delivery[34,35]. In general, these nanomaterials have been classified into different categories: carbon nanocarriers (such as fullerenes, carbon nanotubes, carbon nanohorns and carbon nanodiamonds)[36], metallic nanocarriers (gold, silver, iron, hafnium, cobalt, platinum, titanium, silicon, etc) and semiconductors so-called quantum dots[37].

To date several inorganic nanopharmaceuticals have reached the clinic for different indications such as iron deficiency and cancer. Moreover, some of them have been marketed as imaging agents (Superparamagnetic iron oxide nanoparticles, SPIONs) (Feridex®, Feraheme™, NanoTherm®, GastroMARK™, FerrLecit®, etc)[9]. For a detailed review on the subject we refer to the work of Rivera Gil et al[35].

2.2. Nanocrystals

Drug nanocrystals are solid nanosized particles, with crystalline character, mostly formed by the active pharmaceutical ingredient (API) and enfolded by a layer of stabilizers[38–40]. These systems, depending on the stabilizing materials, have also been called solid micelles (**Figure 1**). An important number of nanocrystals are already presented in the market with indications such as antiemetic, bone substitute and psychostimulant (Emend®, Ostim®, Megace®, Rapamune®, Tricor®, Vitoss®, etc)[9,41].

2.3. Organic nanosystems

Organic nanomaterials can be defined as nanomaterials founded on carbon-constructed compounds resulted of a combination with several other elements, particularly hydrogen, oxygen, nitrogen and phosphorous and originally derived from living organisms[42]. Nanosystems developed with these organic nanomaterials can be classify into three main categories such as protein, polymer, and lipid-based nanocarriers.

2.3.1. Protein-based nanosystems

The use of proteins as building elements for the development of nanopharmaceuticals is due to their interesting properties, such as molecular recognition, non-antigenicity, biocompatibility, biodegradability into amino acids and the possibility of introducing additional chemical modifications with drugs and/or ligands. However, it needs to be taken in consideration that proteins are very sensitive to physicochemical environmental changes that may lead to hydrolysis, oxidation, proteolysis and denaturation[43–45].

A wide range of proteins have been characterized and employed so far for the development of drug delivery systems. These proteins can be classified into two main categories: animal (albumin, casein, collagen, gelatin, silk protein, elastin, and whey protein) or vegetal proteins (soy protein, gliadin, legumin and zein)[46–48].

Interestingly, among these, a special type of proteins with auto-assembly capacity are the so-called protein nanocages (ferritin, small heat shock proteins and vault protein) successfully used for the encapsulation of different types of drug molecule into the template[49,50].

Protein-based nanoparticles and nanoconjugates have been reported for delivery of all kinds of drugs; from small molecule drugs[51] with its main representative FDA approved Abraxane® (albumin-bound paclitaxel[52,53]), to nucleic acids[54] and peptides/proteins[29], this last case

exemplified with the successfully commercialized product Ontak® (recombinant fusion protein composed of the diphtheria toxin catalytic domain and the sequence for human interleukin-2 (IL-2; $Ala_1 - Thr_{133}$)). A complete review on protein-based nanosystems can be found in the work published by Tarhini et al[46].

2.3.2. Polymer-based nanosystems

Polymer-based nanosystems comprise a very heterogeneous group with a long history in the biomedicine field[55,56]. Polymeric nanosystems can be constructed leading to many different types of compositions and structures like polymer-drug conjugates, polymer-protein conjugates, polymeric micelles, dendrimer and nanogels among others[57,58]. Polymeric materials that can be classified into synthetic or naturally obtained polymers[9,59]. Both natural and synthetic polymers are widely used as nanomaterials due to their optimal characteristics in terms of simple processing and design, modulable biocompatibility, and wide versatility for subsequent chemical modifications[60]. Commonly used natural polymers include alginate, chitosan, dextran cellulose and hyaluronic acid (HA), while polyethylene glycol (PEG), poly-lactic acid (PLA), poly-glycolic acid (PGA), poly-lactic-acid-co-glycolic-acid (PLGA), poly(ε-caprolactone) (PCL) and polyvinyl alcohol (PVA), are synthetic polymeric biomaterials[61,62]. A list of common polymers employed for biomedical applications in many previous studies is compiled in **Table 3**.

Initially, the use of synthetic polymers in nanotechnological applications was based on non-biodegradable polymers, such as poly (methyl methacrylate) (PMMA). However, toxicity and inflammatory reactions associated with their use favored a shift towards biodegradable polymers[63]. Nevertheless, decoration of proteins (Adagen®, Oncaspar®, PegIntron®, Pegasys®, etc.) antibodies (Cimzia®) and most recently aptamers (Macugen®) with the non-biodegradable

polymer poly(ethylene glycol) (PEG), so called PEGylation, have been particularly successful in reaching the clinical practice[64]. Additionally, polyester-based polymers are among the most widely investigated biodegradable polymers. Poly(lactic acid) (PLA), poly(glycolic acid) (PGA), as well as poly(lactic acid-co-glycolic acid) (PLGA) represent some of the preferentially selected biomaterials for nanoformulation. Examples of successful clinical translation of formulations containing these polymers are Eligard® (Leuprolide acetate with PLGA)[65] and Zilretta® (Triamcinolone acetonide with PLGA matrix).

Table 3. List of representative polymers for biomedical applications[59–62,66–69].

Natural polymers	**Synthetic polymers**	
	Biodegradable	**Non-biodegradable**
Alginate Chitosan Agarose Hyaluronic acid Starch Cellulose Polyhydroxyalkanoate (PHA) Carrageenan Cyclodextrins	**Polyester** Poly-lactic acid (PLA) Poly-glycolic acid (PGA) Poly-lactic acid-co-glycolic acid (PLGA) Poly-ε-caprolactone (PCL) Poly hydroxy butyrate (PHB) Polydioxanone (PDO) **Polyanhydrides (PAHs)** Poly sebacic acid (PSA) **Phosphorus-containing polymers** Polyphosphoesthers (PPE) Polyphosphonates (PPh) Polyphosphazenes (PPZ) **Others** Poly cyano acrylate (PCA) Poly orthoesters (POE) Poly acrylic acid (PAA)	**Cellulose derivative** Carboxymethyl cellulose (CMC) Ethyl cellulose (EC) Cellulose acetate (CA) Hydroxyl propyl methyl cellulose (HPMC) **Silicones** Polydimethyl siloxane (PDMS) Colloidal silica **Others** Polyethylene glycol (PEG) Polyoxyethylene (POE or PEO) Polyvynil pyrrolidone (PVP) Polyvynil alcohol (PVA) Ethyl vinyl acetate (EVA) Poly(ethyleneoxide-co-propyleneoxide) (PEO-PPO) (Pluronics®) Poly(ether-urethanes) (PU) Poly(methyl methacrylate) (PMMA) Poly(2-hydroxypropyl)methacrylamide (PHPMA)

Many polymer-based nanosystems are currently being investigated in clinical trials[10,57,70]. Some remarkable examples are: Opaxio®/Xyotax® (conjugate of poly(L-glutamic acid) (PLA) and the anticancer drug paclitaxel)[71], Livatag® (Transdrug™ technology, nanoparticle of poly(iso-hexyl-cyanoacrylate) with doxorubicin) and ProLindac™ ((hydroxypropylmethacrylamide) HPMA-co-DACH-platinum)[72].

2.3.3. Lipid-based nanosystems

Lipid-based nanosystems vary from simple lipid mixtures to complex combinations of oils, surfactants and co-surfactants[73]. Several nanotechnological lipid-based approaches are available such as liposomes, micelles, emulsions, nanoemulsions, microemulsions, self-emulsifying drug delivery systems (SEDDS), self-micro-emulsifying drug delivery systems (SMEDDS), self-nano-emulsifying drug delivery systems (SNEDDS), solid lipid nanoparticles (SLN) and nanocapsules (NCs)[74].

Since 1965, when Alec D. Bangham and his colleagues published a paper discovering liposomes, these vesicles have been thoroughly studied for their application in drug delivery[75,76]. Liposomes are defined as spherical vesicles composed of a lipid bilayer and containing an aqueous core with a size range around 50 nm to 1 µm. Liposomes remain the most studied nanocarriers and the most represented in pharmaceutical and cosmetic industries. They are mainly composed by phospholipids and sterols (**Table 4**) and ultimately they can be decorated with polyethylene glycol (PEG) moieties to achieve "stealth" properties[77] as well as with targeting units such as antibodies, peptides and/or aptamers[78–80]. Up to 14 nanopharmaceuticals have successfully reached the market based on liposomal design such as Doxil®/Caelix®, DaunoXome®, Ambisome®, Depocyt®, Myocet® or Marqibo® (complete list in **Table 2**).

Micelles are colloidal dispersions of amphiphilic molecules consisting of a lipidic monolayer that normally generate small spherical particles (5-100 nm)[81]. These nanosystems are spontaneously formed when the lipidic non-polar heads are oriented towards the hydrophilic interior once reached critical micelle concentration (CMC)[82]. Micelles can be found in three major subtypes, entirely polymeric (described in section 2.2.2), entirely lipidic, or lipid-polymer conjugates being one example micelles formed by the modified phospholipid polyethylene glycol-phosphatidylethanolamine (PEG-PE)[83,84].

Emulsions are thermodynamically unstable colloidal systems formed typically in a dispersion of two immiscible liquids (oil-in-water, O/W or water-in-oil, W/O) kinetically stabilized using appropriate surfactant combination and concentration[85,86]. Depending on the mean diameter of the existing nanostructures they can be also categorized into nanoemulsions (d < 300nm) or macroemulsions (coarse emulsions) (d > 300nm), having the first ones numerous advantages regarding stability towards aggregation[87–89]. These nanostructures have been investigated since long time and also in a wide range of fields like textile, food, pharmaceutical, cosmetic and agrochemical industries[86,90–95]. Unlike emulsions and nanoemulsions, microemulsions were defined by Danielsson and Lindman in 1981[96] as "a system of water, oil and amphiphile which is a single optically isotropic and thermodynamically stable liquid solution". Although they typically require similar ingredients to be developed[97], this definition pointed out the main difference between emulsion/nanoemulsion and microemulsion which falls on its thermodynamic stability[88,98]. Interestingly, microemulsions established the root for the development of self-emulsifying drug delivery systems (SEDDS), self-micro-emulsifying drug delivery systems (SMEDDS) and self-nano-emulsifying drug delivery systems (SNEDDS), novel nanosystems composed of oil, surfactants and co-surfactants that are spontaneously emulsified once entering in contact with aqueous fluids without energy imput[99–101].

Table 4. List of representative lipidic components presented in nanosystems[97,102–104].

Lipid nanosystem components	
Phospholipids	Phosphatidylcholine (PC) 1,2-Dilauroyl-sn-glycero-3-phosphocholine (DLPC) 1,2-Dimyristoyl-sn-glycero-3-phosphocholine (DMPC) 1,2-Dipalmistoyl-sn-glycero-3-phosphocholine (DPPC) 1,2-Distearoyl-sn-glycero-3-phosphocholine (DSPC) 1,2-Dioleoyl-sn-glycero-3-phosphocholine (DOPC) Phosphatidylethanolamine (PE) 1,2-Dimyristoyl-sn-glycero-3-phosphoethanolamine (DMPE) 1,2-Dipalmistoyl-sn-glycero-3-phosphoethanolamine (DPPE) 1,2-Distearoyl-sn-glycero-3-phosphoethanolamine (DSPE) 1,2-Dioleoyl-sn-glycero-3-phosphoethanolamine (DOPE) Phosphatidic acid (PA) 1,2-Dimyristoyl-sn-glycero-3-phosphate (DMPA) 1,2-Dipalmistoyl-sn-glycero-3-phosphate (DPPA) 1,2-Distearoyl-sn-glycero-3-phosphate (DSPA) Phosphatidylglycerol (PG) 1,2-Dimyristoyl-sn-glycero-3-phosphoglycerol (DMPG) 1,2-Dipalmistoyl-sn-glycero-3-phosphoglycerol (DPPG) 1,2-Distearoyl-sn-glycero-3-phosphoglycerol (DSPG) 1-Palmitoyl-2-oleoyl-sn-glycero-3-phosphoglycerol (POPG) Phosphatidylserine (PS) Phosphatidylinositol (PI)
Sphingolipids	Sphingosine, Ceramide and Sphingomyelin
Triglycerides	Castor oil, Corn oil, Cottonseed oil, Olive oil, Peanut oil, Peppermint oil, Safflower oil, Sesame oil, Soybean oil, tripalmitin, triolein Capric/Caprylic acid (Labrafac, Miglyol 810 or 812, Crodamol, Softison)
Mono- and Di- glycerides	Glycerol monostearate, glyceryl monooleate (Peceol), glyceryl monolinoleate glyceryl palmitostearate, mono/di-glycerides of caprylic acid
Fatty acids	Stearic acid, oleic acid, linoleic acid and palmitic acid
Other Surfactants	Cholesterol Bile Salts (derived from cholic acid) Cremophor EL (Polyoxyl 35 castor oil) Cremophor RH 40 (Polyoxyl 40 hydrogenated castor oil) Cremophor RH 60 (Polyoxyl 60 hydrogenated castor oil) Tween 80 or 20 (Polysorbate 80 or 20) Solutol HS-15 (Polyethyleneglycol-15-hydroxystearate) Spam 20 (Sorbitan monooleate) TPGS (D-α-tocopheryl polyethylene glycol 1000 succinate)

Marketed emulsion-based nanopharmaceuticals are generally developed to encapsulate lipophilic components so that they can be dispersed into an aqueous medium. Six examples of emulsions can be found among the commercialized products: Diazemuls® (Diazepam)

Diprivan® (Propofol), Restasis® (Cyclosporine), Etomidate-Lipuro® (Etomidate), Estrasorb™ (Estradiol) and Cleviprex® (Clevidipine).

Solid Lipid Nanoparticles (SLN) were introduced in the beginning of 90s as a new alternative of the traditional nanocarriers. The particularity of this type of nanosystems is the replacement of the liquid oil froming the particle core with a solid-state oil that remains solid at both room and body temperatures[105–107]. Moreover, a second generation of SLN have been developed. They are the so called Nanostructured Lipid Carriers (NLC), which consist on an unstructured solid core with more room available for the active components[108,109].

Another family of nanosystems is represented by the nanocapsules (NCs). They consists of an oily core stabilized by surfactants and surrounded by one or several polymeric shells. In the last years, our group has reported many papers showing the great potential of these nanocarriers for ocular diseases[110], gastrointestinal diseases[111], cancer treatment[112,113], oral drug delivery[114,115] and vaccines[116]. This type of nanocarrier exhibits several advantages over the previous mentioned drug delivery nanosystems. While its oily core permits the encapsulation of high loads of hydrophobic molecules the polymeric shell protects the nanostructure or the encapsulated drug/macromolecule against degradation and control the release profile of the encapsulated drugs[74].

Altogether, lipid-based dosage forms represent a class of drug products that have drawn considerable interest and attention from pharmaceutical scientists[102]. Lipid-based formulations are mostly developed as the best strategy for the delivery of poorly water-soluble drugs[103]. Representative lipidic compounds commonly used in developed nanopharmaceuticals are listed in **table 4**[97,102–104,117].

3. O/W Nanoemulsions concept, production technologies and impact in biomedicine

Since the first article using the term "nanoemulsion" (also called submicron emulsion, ultrafine emulsion or miniemulsion) published by Calvo et al. in 1996[118], these nanocarriers have attracted significant interest in the scientific community[88,91,119–124]. Nanoemulsions consists in a suspension of droplets not soluble in the surrounded medium, either water (O/W) or oil (W/O). With minor presence in the literature, apart from the described biphasic nanoemulsions, multiple nanoemulsions can also be obtained, such as oil-in-water-in-oil (O/W/O) or water-in-oil-in-water (W/O/W) nanoemulsions[88,89].

Oil-in-water (O/W) nanoemulsions being the most representative ones and the subject of this thesis, are going to be deeply assessed in the next section regarding production methodologies and impact in the biomedical field.

3.1. Emulsification methods

Emulsification production methods can be generally classified into two broad categories, high-energy methods or low-energy methods[85]. High-energy methods are based on the application of large disruptive forces, provided using either homogenizers, microfluidizers or ultrasonicators to produce nanosized droplets. Low-energy methods rely on the stored chemical energy instead of external forces for production of tiny droplets[88,122]. Criteria to select the appropriate emulsification method is based on the desired properties such as droplet size, homogeneity of the produced nanosystems, solvent use, disruptive forces and/or temperature[119,125].

3.1.1. High-Energy Emulsification Methods

3.1.1.1. Homogenization

High-pressure homogenization is currently the most popular technique to produce small emulsions in the industry[85,126]. This technique makes use of intense disruptive forces such as cavitation, turbulence and shear to manufacture nanoemulsions with a very small droplet size (up to 1nm particles). During the procedure (**Figure 2**), macroemulsions are forced through a small inlet orifice at very high pressure (500 to 5000 psi) resulting in a fragmentation of the pre-existing droplets. The obtained formulation can be re-subjected to the homogenization process until nanoemulsion with desired droplet size and polydispersity index is obtained[122]. Main advantages are the easily scale up process and the little batch-to-batch variations, while the high-energy consumption and reached temperature during the procedure are the main disadvantages[127].

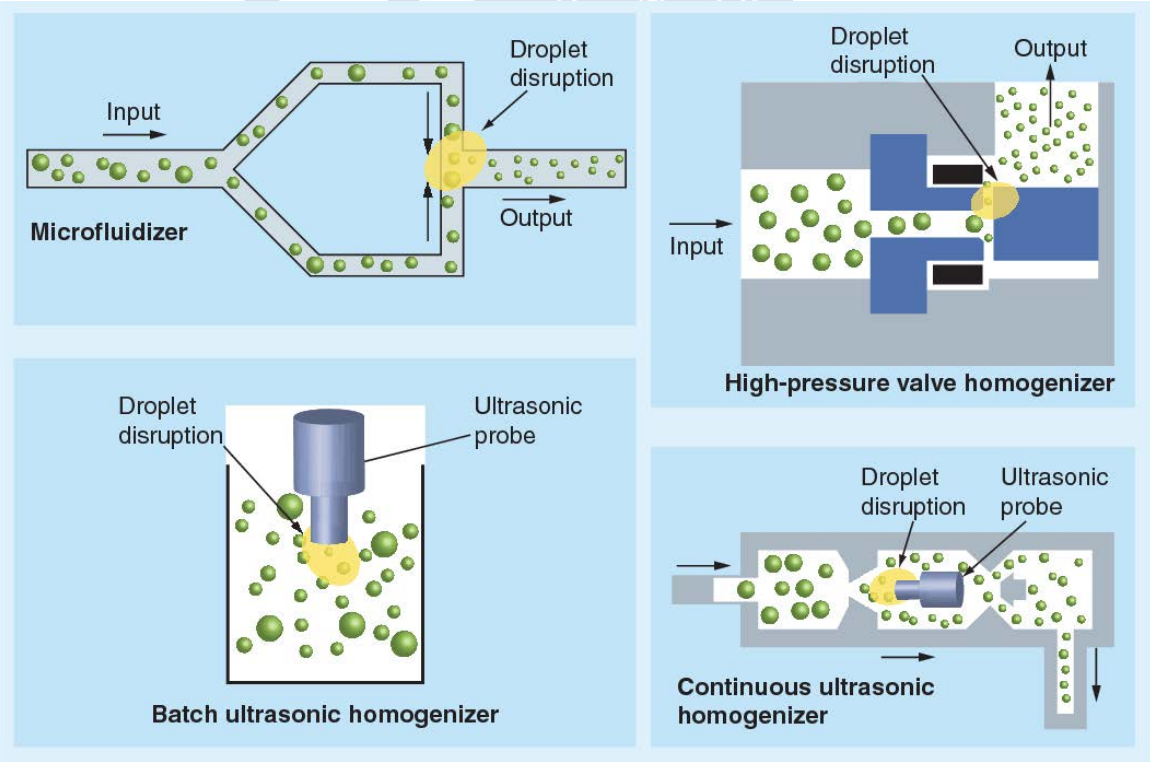

Figure 2: High-energy methods for production of nanoemulsions. Adapted with permission from[128].

3.1.1.2. Microfluidization

Microfluidization is a patented technology based on a device named Microfluidizer[86]. This device employs a high-pressure positive displacement pump operating at very high pressures (500 - 20,000 psi)[126]. Microfluidizer works on the principle of dividing a pre-existent macroemulsion into a network of microchannels and then directing two channels at each other to collide in a pressurized interaction chamber[129]. Similarly to the homogenization process, the macroemulsion is passed through the interaction chamber of the microfluidizer repeatedly until the desired particle size is obtained[122].

3.1.1.3. Ultrasonication

Ultrasonication methods utilize high-frequency sound waves (>20 kHz) to create the intense disruptive forces necessary to form nanosized emulsions[86,119]. A sonicator consists of an ultrasonic probe containing a piezoelectric crystal that converts inputted electrical waves into intense mechanical vibrations (**Figure 2**)[85,94,126]. Variation of the ultrasonic energy input and time, results in nanoemulsions with desired properties. Nevertheless, for uniform sonication it is important to ensure that the emulsion spends adequate time within the region of the ultrasonic probe[129]. Compared to other high-energy methods, ultrasonication requires less energy expenditure but undesired reactions such as protein denaturation, polysaccharide de-polymerization, or lipid oxidation as well as contamination induced by the probe have become an important concern[86].

3.1.2. Low-Energy Emulsification Methods

3.1.2.1. Spontaneous emulsification

Spontaneous emulsification is referred to a method consisting of mixing together an organic phase (containing oils, surfactants and water-miscible solvents) and an aqueous phase (containing or not additional stabilizers) at a particular temperature and without the need of an external energy input[85,130]. The physicochemical mechanism of nanoemulsion formation by this method is triggered by the rapid diffusion of both surfactants and solvents from the organic phase to the aqueous phase without involving a change in the molecular geometry of the surfactants (**Figure 3**)[92]. Several parameters can be modified in order to obtain the desired nanosystems such as composition of the organic and aqueous phases, environmental conditions (i.e., temperature, pH and/or ionic strength) and the mixing conditions (i.e., stirring speed, rate of addition, way of addition and order of addition)[119,129].

Several nomenclatures can be included into this definition, grouping methodologies with slight differences between them such as self-emulsification, emulsification-diffusion, solvent displacement, nanoprecipitation and the methodology used in this work ethanol injection[131].

3.1.2.2. Phase inversion methods

Phase inversion methods exploit changes in the spontaneous curvature of surfactants from negative (W/O) to positive (O/W) or vice versa in order to formulate nanoemulsions[85,92,130]. Several methods have been developed and they are classified into transitional methods (phase inversion temperature (PIT) and phase inversion composition (PIC)) and catastrophic methods (emulsion inversion point (EIP))[119,129,132]. Phase inversion temperature method (PIT) relies on changes in aqueous/oil solubility of non-ionic surfactants in response to temperature. As

represented in **Figure 3**, at temperatures below the PIT the surfactants head group are highly hydrated becoming soluble in water and favoring the formation of O/W nanoemulsions.

At the PIT temperature, the solubility of the surfactant is equal for water and oil and so the nanoemulsions breaks down resulting into a liquid crystalline or bicontinuous microemulsion structure. Temperatures greater than PIT make the surfactant more soluble in oil due to the dehydration of the polyoxyethylene chains present in the non-ionic surfactants thus obtaining W/O nanoemulsions[86,91,92,119,129,132,133].

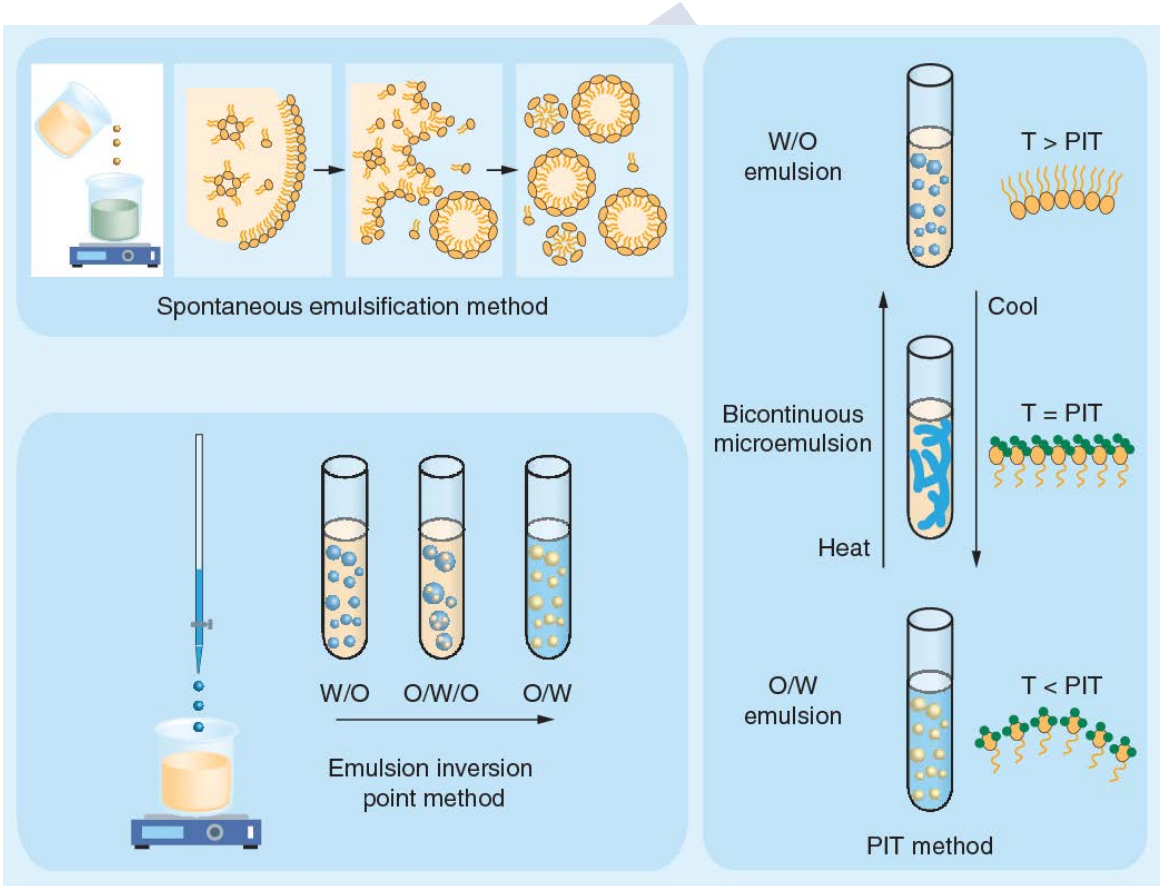

Figure 3: Low-energy methods for production of nanoemulsions. Adapted with permission from[128].

Phase inversion composition method (PIC) is alike to PIT method, but the surfactant optimum curvature is changed by altering the composition (salts, pH…), rather than the temperature. For instance, nanoemulsions formed by ionic surfactants can switch phases (W/O to O/W or vice versa) by altering the amount of electrolytes[85,88,129,132].

In the emulsion inversion point method (EIP) phase inversion occurs through a catastrophic phase inversion (CPI) rather than a transitional phase inversion as in the case of PIC and PIT. This method relies on the fact that changes in the surfactant spontaneous curvature can be obtained by changing water-to-oil volume ratio while the surfactants remain constant. For that, the continuous phase (water droplets) is slowly added over the dispersed phase (oils and surfactants) spontaneously changing from and initially W/O nanoemulsion to a O/W nanoemulsion (**Figure 3**)[85,119,125,129,132–134].

3.2. Impact of O/W nanoemulsion on the biomedical field

Great advances in biomedicine and nanotechnology have led to the development of pharmaceutical dosage forms from relatively simple systems to highly sophisticated ones[135]. Adequate selection of manufacturing techniques (described in section 3.1) and nanomaterials (lipidic components listed in **Table 4**) permits the preparation of O/W nanoemulsions with ideal physicochemical characteristics[85]. Nanoemulsions have proven themselves in the past decades to be effective drug delivery systems[135,136]. Due to their submicron size and lipidic nature, nanoemulsions are able to interact with several physiological barriers and penetrate deep into tissues through the capillaries and even cross fenestrations between cells[137]. The main advantages of nanoemulsions in the biomedicine field comprise enhancing drug solubility, increasing drug loading, improving bioavailability, controlling drug release and enhancing protection from chemical and/or enzymatic degradation[135]. Nanoemulsions can be formulated for the administration of drugs through various routes, including parenteral, oral, topical/transdermal, intranasal, pulmonary and ocular[31,85,122,125,135,138–140].

Following the classifications proposed by Collins-Gold[140] and Tamilvanan[137,141], we suggest a reformulated classification in this introduction into three generations of nanoemulsions attending to their story and progress through the years.

3.2.1. First-generation: nanoemulsions as nutrient carriers for parenteral feeding

Lipid emulsions were developed after the Second World War to serve as nutrient carriers to be administered via intravenous route. Therefore, first-generation nanoemulsions are considered primarily as sources of essential fatty acids and calories[140,142,143].

Even though the first generation of nanoemulsions has no active pharmaceutical ingredient (API) it is worthy to have a better understanding of the nature and physicochemical characteristic of the first commercialized products. After several attempts of administering oils parenterally[144] it was determined that intravenous applications of emulsions requires the nanosystem to be below the size of the smallest blood vessels (lung capillaries with diameters down to 5 μm) to avoid embolisms[140,143,145].

Commercially available intravenous nanoemulsions (representative examples listed in **Table 5**) have particle size normally around 200–500 nm[145] (fulfilling the requirements established by the U.S Pharmacopeia, USP chapter 729) and a negatively surface charge due to the main stabilization with egg phospholipids (phosphatidyl choline as principal component)[141].

Lipid nanoemulsions have been in the market for over 5 decades as the case of Intralipid®, approved in Europe in 1962. Interestingly, as shown in **Table 5**, the first developed nanoemulsions were prepared entirely (or with a high percentage) of soybean oil due to its high content of essential C18 fatty acids (Intralipid®, Lyposin® and Nutrilipid®)[31]. New oil sources were later added (as the case of Clinoelic®, SMOFlipid®, Lipoplus® and Omegaven®) to achieve the proper fatty acid balance (C8 to C22 carbon chain length) and avoid side effects associated with long intravenous feeding [31,141–143].

Table 5. List of representative commercialized emulsions for parenteral nutrition[31,140–143,146].

Commercialized product	Date of Approval	Company	Oil Composition				
			Soybean	Safflower	Coconut (MCT)	Fish	Olive
Intralipid®	1962 EU 1975 USA	Fresenius Kabi (Germany)	100%	-	-	-	-
Lyposin II®	1979 USA	Abbot laboratories Hospira Inc. (USA)	50%	50%	-	-	-
Nutrilipid®	1993 USA	B. Braun Medical Inc. (USA)	100%	-	-	-	-
Clinoleic/ Clinolipid®	1995 EU 2013 USA	Baxter Healthcare Corporation (USA)	20%	-	-	-	80%
SMOFlipid®	2000 EU 2016 USA	Fresenius Kabi (Germany)	30%	-	30%	15%	25%
Lipoplus®	2004 EU	B. Braun Medical Inc. (USA)	40%	-	50%	10%	-
Omegaven®	2012 EU 2018 USA	Fresenius Kabi (Germany)	-	-	-	100%	-

MCT: Medium chain triglycerides; EU: European Union; USA: United States of America

3.2.2. Second-generation: Stealth nanoemulsions as drug carriers for lipophilic drugs

The FDA's Biopharmaceutics Classification System (BCS, ICH Harmonization Guideline) categorize drugs based on three parameters, solubility, dissolution and permeability[147]. From this classification, class II and IV correspond to poorly soluble chemical entities that could benefit from their formulation into drug carriers[148].

Following successful commercialization of parenteral nutrition emulsions (described in the previous section) and confirmation of its safety use for years, second generation nanoemulsions appeared as a smart alternative to formulate poorly soluble drugs (class II and IV)[31].

Pioneer work using nanoemulsions to deliver class IV drug paclitaxel was carried out by Tarr et al (1987). In this study they compared the commercial parenteral nanoemulsion Intralipid® loaded with paclitaxel with a new developed nanoemulsion (composed by 50% Triacetin, 1.5% Soy Lecithin, 1.5% Pluronic F68 and 2% of Ethyl oleate). They found Intralipid® to be an inadequate carrier due to the poor solubility of the drug (0.3 mg/ml) in the soybean oil while the triacetin nanoemulsion showed a greater solubility (75 mg/ml) and greater formulation stability[149]. Later, Kan and co-workers (1999) reported also another work encapsulating the extremely low aqueous soluble drug paclitaxel (0.03mg/ml) in a nanoemulsion composed of Tricaproin and Tricaprylin oil mixture and stabilized by egg phosphatidylcholine and Tween 80. Effective anticancer activity was determined both in HeLa cells and tumor-bearing mice[150]. Clearly, there has been a strong and continuous interest in developing nanoemulsions for taxane delivery[151] (mainly paclitaxel and docetaxel as shown in **table 6**). They are well-established poorly water-soluble anticancer drugs with lack of appropriate drug delivery vehicles (Taxol® (Paclitaxel) and Taxotere® (Docetaxel)) apart from the only approved alternative to Taxol®, the protein-based nanoparticle Abraxane®.

An interesting alternative could have been the nanoemulsion named TOCOSOL™, developed in the early 2000s by SONUS Pharmaceuticals[152], however it was withdraw in Phase III clinical trials due to low primary endpoint of overall response rate when compared with the control arm[153]. This formulation corresponded to a lipid-based strategy to deliver paclitaxel. As disclosed in **Table 6**, this formulation was manufactured by High Pressure Homogenization and consisted of a vitamin E (DL-α-Tocopherol) nucleus stabilized by TPGS and Pluronic F127 with a droplet diameter of 40-80 nm and neutral charge. The formulation could be administered in only 15 minutes (instead of >3h for the approved Taxol®) and was found to accumulate in the tumor tissue, thereby improving the anticancer efficacy[139,154,155]. New works have been proposed taking this failed clinical example as a starting point[156].

Several representative examples from the last two decades investigating the potential of nanoemulsions for the solubilization of lipophilic drugs have been listed in **Table 6**. Their therapeutic application has mainly in cancer (taxanes[154,157–162], doxorubicin[163], curcumin[160], fisetin[164], lycobetaine[165], etoposide[166], camptothecin[167], 5-fluorouracil[168], chlorambucil[169] and platinum[170]), although some other drugs for different indications have also been successfully formulated into nanoemulsions such as carbamazepine[171], rifampicin[172], thalidomide[173], diazepam[174], indomethacin[175], cyclosporine A[176] or clofazimine[177] among others not listed in this introduction. Remarkably, in almost all cited studies, the methodology used to produce these nanoemulsions correspond to one or a combination of several High-Energy Methods with the High Pressure Homogenizer as the most frequently employed device (3.1.1.1 section).

Table 6. Examples from the last decade of nanoemulsions for solubilization of lipophilic drugs[139,154,155,157–180].

Drug	Composition	Method of preparation	Indication	Reference
Paclitaxel (TOCOSOL™)	Vitamin E (DL-α-Tocopherol) PEG 400 TPGS Pluronic F127	High pressure homogenization	Cancer treatment	Constantinides et al 2000, 2004 and 2008
Paclitaxel oleate	Triolein Egg phosphatidylcholine Polysorbate 80 PEG2000-DPPE	Ultrasonication	Cancer treatment	Lundberg et al 2003
Etoposide oleate	Triolein Egg phosphatidylcholine Cholesterol Cholesteryl oleate	Ultrasonication	Melanoma	Prete et al 2006
Carbamazepine	Medium Chain Triglycerides (MCT) Castor oil Lipoid S75 Polyoxyl 35 castor oil Tween 80	Spontaneous emulsification	Antiepileptic treatment	Kelmann et al 2007
Rifampicin	Sefsol 218 Tween 80 Tween 85	Aqueous phase titration method	Tuberculosis treatment	Ahmed et al 2008
Paclitaxel C_6-ceramide	Pine-nut oil Lipoid E80 PEG2000-Lipoid PE	Ultrasonication	Glioblastoma	Desai et al 2008
Paclitaxel and Curcumin	Flaxseed oil Egg lecithin PEG2000-DSPE	Homogenization + ultrasonication	Multidrug resistance in ovarian adenocarcinoma	Ganta and Amiji 2009
Chlorambucil	Soybean oil Cholesterol Egg lecithin PEG2000-DSPE	Ultrasonication	Cancer treatment	Ganta et al 2010
Thalidomide	Castor oil Soybean lecithin Tween 80	Spontaneous emulsification	Intravenous administration of thalidomide	Araújo et al 2011
Docetaxel	Medium chain triglycerides (MCT) Oleic acid Lipoid E 80 Poloxamer 188	High pressure homogenization	Cancer treatment	Li et al 2011
7-ethyl-10-hydroxycamptothecin (SN-38)	D-α-tocopherol succinyl chloride SN-38 Two surfactants non disclosed	Non disclosed	Cancer treatment	Marier et al 2011
Metotrexate (ddMTX)	Triolein Egg phosphatidylcholine Cholesterol Cholesteryl oleate	Ultrasonication	Cancer treatment	Moura et al 2011

Drug	Composition	Method of preparation	Indication	Reference
Doxorubicin (DOX)	Soybean oil Lipoid E 80 Vitamin E Oleic acid-DOX	High pressure homogenization	Cancer treatment	Zhang et al 2011
Docetaxel	Soybean oil Egg lecithin Sodium deoxycholate Poloxamer 188	High pressure homogenization	Cancer treatment	Gaoe et al 2012
Fisetin	Labrasol Tween 80 Miglyol 812 Lipoid E 80	Phase inversion + High shear mixer + Ultrasonication	Lewis Lung Carcinoma	Ragelle et al 2012
Diazepam	Soybean oil Medium chain triglycerides (MCT) Soybean Lecithin Butylhydroxytoluene Tween 80	High pressure homogenization	Diazepam pharmacokinetics	Dordevic et al 2013
Lycobetaine (LBT)	LBT-Oleic acid Lipoid E 80 Triglycerides PEG2000-DSPE	Lipid film hydration + Homogenization	Lewis Lung Carcinoma	Zhao et al 2013
Paclitaxel	Vitamin E acetate Sodium dodecyl sulphate (SDS) Soya Lecithin Tween® 80	Microfluidization	Breast Cancer	Pawar et al 2014
5-fluorouracil (5-FU)	Triolein Phosphatidylcholine Cholesterol Cholesteryl oleate Tween 80 Labrasol	Ultrasonication	Cancer treatment	Alanazi et al 2015
Cyclosporine A	Flaxseed oil Lipoid E80 Tween 80 Stearylamine	Homogenization +Ultrasonication	Brain delivery	Yadav et al 2015
Indomethacin	Olive oil DSPC PEG-DSPE Cholesterol	Film hydration + Ultrasonication	Anti-inflammatory	Kwasigroch et al 2016
Gemcitabine	γ-Tocotrienol α-T-MPEG2000	Ultrasonication	Pancreatic cancer	Abu-Fayyad et al 2017
Sylmarin	Capryol 90 Solutol HS 15 Transcutol HP	High pressure homogenization	Oral bioavailability	Nagi et al 2017
Clofazimine, Artemisone and Decoquinate	Span® 60 olive oil safflower oil Tween® 80	Spontaneous emulsification + ultrasonication	Anti-infective against Mycobacterium	Burger et al 2018
Oleic acid−Pt (II) conjugate	Lysine-tyrosine-phenylalanine (KYF) Oleic acid−Pt (II) conjugate	Nanoprecipitation method	Ovarian cancer	Dragulska et al 2018

Rapid clearance of parenterally administered nanoemulsions from the blood stream has been one of the most important problems to face[28,141]. A growing interest in overcoming this effect has led to the development of the "long-circulation concept". To achieve this, several "stealth" alternatives were developed involving mostly the use of hydrophilic co-emulsifiers like polyoxyethylene (POE) derivatives (Polysorbate or Tween®) or polyethylene glycol (PEG) modified phospholipids[141].

Liu and Liu (1995) used a modified phosphatidylethanolamine (PE) to explore the biodistribution changes of nanoemulsions composed by castor oil, phosphatidylcholine (PC) and the modified-PE with three PEG chain lengths (MW 1000, 2000 and 5000). PEG2000-PE was found to be the best candidate increasing blood circulation and therefore, a major chance for tumor accumulation[181]. Many nanoemulsions containing both POE derivatives or PEG derivatives can be found in the literature (**Table 6**). Interestingly, the commercialized nanoemulsion Estrasob™ (Estradiol) is the only emulsion approved containing polysorbate 80 (POE derivative) while other formulations types (liposomes) have been successfully formulated and translated to the clinics with PEG modifications.

Overall, this literature review has shown the enormous potential of second generation nanoemulsions for delivering poorly water-soluble drugs within the oil phase. Continuous research in this regard is still ongoing, mainly due to the fact that many of the novel therapeutic entities have poor or no water solubility[31]. In addition, surface modifications with hydrophilic moieties (POE and/or PEG) has proven to be useful in prolonging nanosystems circulation and therefore in their interaction with the desired pathological target cells, as well as evading tendency to be taken by the reticuloendothelial system (RES)[141,182].

3.2.3. Third generation: targeted nanoemulsions and nanoemulsions for emerging therapeutic approaches

After decades of nanotechnological development and a significant quantity of commercialized nanodrugs, many improvements can still be made in drug delivery systems[32]. Based on the knowledge about the first and second nanoemulsion generations in terms of rational design, drug loading and stealth properties, the third generation of nanoemulsions has been focused on two challenging directions. On one hand the development of targeted nanoemulsions and on the other hand the use of nanoemulsions as platforms for delivery of new generation biopharmaceuticals (such as peptides, proteins, antibodies and oligonucleotides)[31,141,183].

Over the past few decades, enhanced permeability and retention (EPR) effect on tumor vasculature (also termed as passive targeting)[184] was actively exploited for the passive targeted delivery of anticancer nanomedicines resulting in numerous pharmaceutical products (section 1)[183]. Moreover, passive nanosystem accumulation has also been observed in many other pathological disorders such as rheumatoid arthritis, cardiovascular diseases, obesity, inflammatory bowel disease and multiple sclerosis, mainly due to inflammatory processes involving vessel remodelling[185]. Although passive targeting constitutes the basis of current clinical therapy, it suffers from several limitations such as ubiquitous targeting and dependence on vasculature permeability degree[184].

One hundred years ago the Nobel Prize winner Paul Ehrlich postulated the concept of a "magic bullet" referring to the importance of targeting the specific drugs site of action within the body[186]. Without realizing it, he established the roots of the actual "active targeting strategies" and inspired multiple revolutionary works[183]. To address the challenge of active targeting several aspects need to be taken into consideration. First, the identification of a specific recognition motif on the target cell or tissue and, second, the definition of the adequate targeting

ligand that can specifically recognize this receptor[141]. Targeting ligands can be broadly classified into protein nature (peptides, proteins, antibodies and their fragments), oligonucleotide nature (aptamers) or other ligands (vitamins and carbohydrates)[183,184]. In the past decade, a significant number of actively targeted nanoemulsions have been developed (representative examples listed in **Table 7**).

Table 7. Examples of actively targeted nanoemulsions[187–199].

Drug	Composition	Method of preparation	Indication	Reference
Prednisolone acetate valerate (PAV)	Soybean oil DSPC PEG-DSPE **RGD-**PEG-DSPE Cy7-PEG-DSPE Oxide nanocrystals	Ultrasonication	Imaging guided therapy for colon cancer	Gianella et al 2011
-	Soybean oil DSPC PEG2000-DSPE **RGD-**PEG2000-DSPE Gd-DTPA-DSA	Film hydration + Ultrasonication	Cancer treatment	Hak et al 2012
Phosphatidylinositol 3-kinase inhibitor (PIK75) + C_6-ceramide	Flaxseed oil Egg lecithin Lipoid E80 PEG2000-DSPE **EGFRbp**-PEG2000-DSPE **Folic acid**-cys-PEG2000-DSPE	Ultrasonication	Ovarian Cancer	Talekar et al 2012
17-β-estradiol and analogues	Flaxseed oil Lipoid E80 DOTAP or PEG2000-DSPE **cysteine–arginine–glutamic acid–lysine–alanine (CREKA)** 17-β-estradiol	Microfluidization	Atherosclerosis	Deshpande et al 2013 and 2014
Myrisplatin	Flaxseed oil Myrisplatin Gd-DTPA-PE **EGFRbp (YHWYGYTPQNVIGGGGC)-PEG2000-DSPE**	Microfluidization	Ovarian Cancer	Ganta et al 2014
Docetaxel	Flaxseed oil Egg lecithin PEG2000-DSPE Gd-DTPA-PE **Folic acid**-PEG-DSPE	Homogenization + Microfluidization	Ovarian Cancer	Ganta et al 2014
Myrisplatin + C_6-ceramide	Flaxseed oil Egg lecithin PEG2000-DSPE Gd-DTPA-PE **EGFRbp**	Microfluidization	Ovarian Cancer	Ganta et al 2015

Drug	Composition	Method of preparation	Indication	Reference
Docetaxel	Olive oil Egg lecithin Cholesterol α-Tocopherol Oleic acid Stearylamine **Transferrin**	Homogenization + Ultrasonication	Cancer treatment	Afzal et al 2016
Docetaxel	Olive oil Egg lecithin Cholesterol α-Tocopherol Oleic acid PEG2000-DSPE **Folic acid**-PEG2000-DSPE	Homogenization + Ultrasonication	Cancer treatment	Afzal et al 2016
Difattyacid platin + C_6-ceramide	Safflower oil Egg lecithin PEG2000-DSPE **Folic Acid**-PEG3400-DSPE Gd-DTPA-ePE	Microfluidization	Ovarian Cancer	Patel et al 2016
Lycobetaine (LBT)	Soybean oil LBT-Oleic acid Lipoid E 80 Cholesterol mPEG2000-DSPE **RGD peptide**	Lipid film hydration + Homogenization	Lung Cancer	Chen et al 2018
Doxorubicin	α-linolenic acid (ALA) Lecithin Tween 80 Cholesterol **Folic acid**-PEG-ALA	Spontaneous emulsification + ultrasonication	Breast Cancer	Tripathi et al 2018
Docetaxel	Flaxseed oil Egg lecithin mPEG2000-DSPE **Folic Acid**-PEG2000-DSPE Gd-DTPA-ePE	Microfluidization	Ovarian Cancer	Patel et al 2018

Targeting peptides highlighted in **bold**.

In order to bring nanoemulsions more closer to pathological target tissues several ligands have been usually attached onto the particle surface by coupling the ligand to the nanosystem by chemical conjugation[200]. Selection of an appropriate conjugation strategy is not trivial since the function of the targeting moiety (sequence and structure) has to be preserved during the conjugation process. The most common strategy is the direct conjugation using existing surface functional groups in the nanocarrier such as the terminal end of a PEG chain[184]. The basis of

this conjugation lies in the distancing of the ligand from the nanoemulsion improving its flexibility and interaction with the environment to facilitate receptor recognition[182].

Until now, in the case of nanoemulsions, the most used strategies for targeted delivery to specific sites (mainly to cancer cells) is their coupling with proteins[197], peptides[187–189,193,194,196] or vitamins[190–192,195,198,199]. Particularly, as shown in **Table 7**, RGD peptide (towards $\alpha_v\beta_3$ and $\alpha_v\beta_5$ integrin)[201,202], folic acid (folate receptor)[203], EGFR binding peptide (EGF receptor) and transferrin (transferrin receptor)[204] are the most commonly used ligands to functionalize nanoemulsions[182].

Interestingly, the use of O/W nanoemulsions in drug delivery is not limited to hydrophobic compounds or functionalization with ligands[85]. Indeed, in the last decades biotech products have transformed the pharmaceutical industry reaching from 13 approved biopharmaceuticals in 1989 to 210 in 2012 and representing nearly US$ 200 billion in 2017 of the global pharmaceutical market[205,206]. Biopharmaceuticals have a high specificity and potency compared to small molecules but their structural complexity makes them difficult molecules to deliver and formulate[206]. However, several drawbacks such as high molecular weight (associated with poor permeability through membranes) and loss of activity due to environmental changes (aggregation, hydrolysis, oxidation or denaturalization) can be solved by using a nanocarrier[206]. In this regard, the use of nanoemulsions as platforms for systemic delivery of biopharmaceuticals (protein nature and nucleic acid derived) has also been explored.

Since the majority of therapeutic peptides are hydrophilic, most studies conducted on nanoemulsions as vehicles for such molecules have explored water-in-oil (W/O) nanoemulsions[97]. Studies referring to the use of O/W nanoemulsions can also be found in the literature[207–213]. Lundberg and co-workers first reported the association of an antibody anti-B cell lymphoma to a negatively charged nanoemulsion by conjugation with the phospholipid

derivative (PEG-DSPE) incorporated to the oily phase[207]. Later Goldstein et al described the coupling of several antibodies (AMB8LK or Trastuzumab (Herceptin®, Roche)) to a cationic nanoemulsion that includes stearylamine (ST) among the main components[208,209,214]. Additionally, peptide hydrophobization (modification with C8 carbon chain) has also been described by Shah et al. as another strategy to improve encapsulation of a peptide into O/W nanoemulsion core and effectively deliver it to the central nervous system (CNS)[212,213]. Several other cases encapsulating proteins[211] or peptides[210] are also listed in **Table 8**.

Gene therapy has emerged as a promising strategy for the modification of genetic material of living cells for therapeutic purposes. This new therapy involves the introduction of functional nucleic acid that replace, amplify, suppress or correct a defective gene[215].

DNA complexation with cationic compounds has been the most explored strategy to overcome enzymatic degradation of the genetic material and to promote their capability to cross biological membranes[215]. The majority of the experiments performed with non-viral vectors were done with both liposomes and DNA complexes (named lipoplexes)[215,216]. However, since the end of 1900s, positively charged oil-in-water nanoemulsions were also proposed as a potential new delivery system for nucleic acids overcoming some liposome drawbacks such as particle agregation[216,217].

To achieve substantial positive charge in the nanoemulsion surface, several cationic surfactants were added to the formulation, being the most used DOTAP (1,2-diolyoxy-3-(trimethylammonium)propane), ST (Stearylamine), DC-Chol (3β-[N-(N',N'-dimethylaminoethane)-carbamoyl] cholesterol) and CTAB (cetyltrimethylammonium bromide)[141,216].

Table 8. Examples nanoemulsions for oligonucleotide, peptide, protein or antibody delivery[207–212,217–225].

Drug	Composition	Method of preparation	Indication	Reference
LL2, murine IgG2a	Triolein DPPC Tween 80 PEG-DSPE	Ultrasonication	Hematological cancer	Lundberg et al 1999
Thymidine based oligonucleotide	Medium Chain Triglycerides (MCT) Lipoid E80 Pluronic F68 Vitamin E **Stearylamine**	Microfluidization	Systemic gene delivery	Teixeira et al 1999, 2001 and 2003
pDNA	Squalene **DOTAP** DOPE	Ultrasonication	Gene therapy	Choi et al 2002
AMB8LK Fab' or Trastuzumab	Medium Chain Triglycerides (MCT) Pluronic F68 Lipoid E80 **Stearylamine** Vitamin E	Microfluidization	Cancer treatment	Goldstein et al 2005 and 2007
MG7 peptide and CpG ODN (1645)	Soybean oil Span 80 Tween 80 PEG2000	Ultrasonication	Nanovaccine against gastric cancer	Shi et al 2005
pDNA	Oleic acid Tween 80 Span 85 **Arginine, lysine and histidine** amino acids	Ultrasonication	Gene therapy	Liu and Yu 2010
Antisense oligonucleotides	Medium Chain Triglycerides (MCT) Lipoid E80 **DOTAP**	Spontaneous emulsification	Antimalarial	Bruxel et al 2011
Antisense Oligonucleotide (ODN17)	Medium Chain Triglycerides (MCT) Pluronic F68 Lipoid E80 Vitamin E **DOTAP**	Homogenization	Ocular neovascularization	Hagigit et al 2012
Model protein BSA	Cremophor EL-35 Propylene glycol Isopropyl myristate	Phase Inversion Method (PIT)	Oral peptide delivery	Sun et al 2012
[D-Arg^2, Lys^4]-dermorphin-(1–4)-amide) (DALDA)	Lipoid E80 Tween 80 DSPE-PEG2000 *DALDA-C8 peptide*	Spontaneous emulsification + ultrasonication	Brain delivery of an analgesic peptide	Shah et al 2013 and 2014
self-amplifying mRNA, mRNA and pDNA	Squalene **DOTAP** Sorbitan trioleate Tween® 80	Homogenization + Microfluidization	RNA vaccination	Brito et al 2014

Drug	Composition	Method of preparation	Indication	Reference
pDNA for alpha-L-iduronidase (IDUA)	Medium Chain Triglycerides (MCT) **DOTAP** DOPE DSPE-PEG2000	Film hydration + High pressure homogenization	Mucopolysaccharidosis type I	Fraga et al 2015
TNFα silencing siRNA	Flaxseed oil **DOTAP** Lipoid E80 Tween® 80	Homogenization + ultrasonication	Nose-to-brain for neuroinflamation	Yadav et al 2016
pDNA for alpha-L-iduronidase (IDUA)	Medium Chain Triglycerides (MCT) **DOTAP** DOPE DSPE-PEG2000	Film hydration + ultrasonication + Homogenization	Nose-to-brain for Muco-polysaccharidosis type I (MPS I)	Schuh et al 2018

Cationic component highlighted in **bold**, peptidic component highlighted in *italics*.

Different formulation strategies have so far been employed to develop cationic nanoemulsions (**Table 8**)[210,217–225]. Since Teixeira el all in 1999 explored the capacity of cationic-modified nanoemulsions (stearylamine)[217] to bind the highly negative oligonucleotides onto the particle surface through electrostatic interactions several other studies followed the same approach. However, in such studies, stearylamine has been replaced by DOTAP, the most used cationic surfactant in the last decades [218–223,225]. Some years later, complexation of plasmid DNA (pDNA) with positive amino acids (Arginine, Lysine and Histidine) was also reported by Liu and Yu as an alternative to positive surfactants[224]. Moreover, Yadab and co-workers have recently proposed a different approach for efficient association of nucleic acids, which involves the encapsulation of preformed lipoplexes (siRNA+DOTAP) into a flaxseed oil core[221].

Overall, gene delivery has become a crucial and challenging area of research. A successful formulation will be the one that can find the equilibrium among acceptable toxicity, transfection efficiency, and stability[85,141,215,216].

4. Cancer Nanomedicine

Despite the progress in cancer therapeutics this disease still remains a leading cause of death[226]. As showed in **Figure 4** cancer is a major public-health sickness worldwide with lung, breast, colorectal and prostate cancers as globally dominant types. Lung cancer is situated at the leading position in both incidence and mortality per number of cases. Additionally, colorectal cancer ranks third in terms of incidence but second in terms of mortality relegating breast and prostate cancer to lower mortality positions due to the efforts done in the early diagnosis frequency of the latter two.

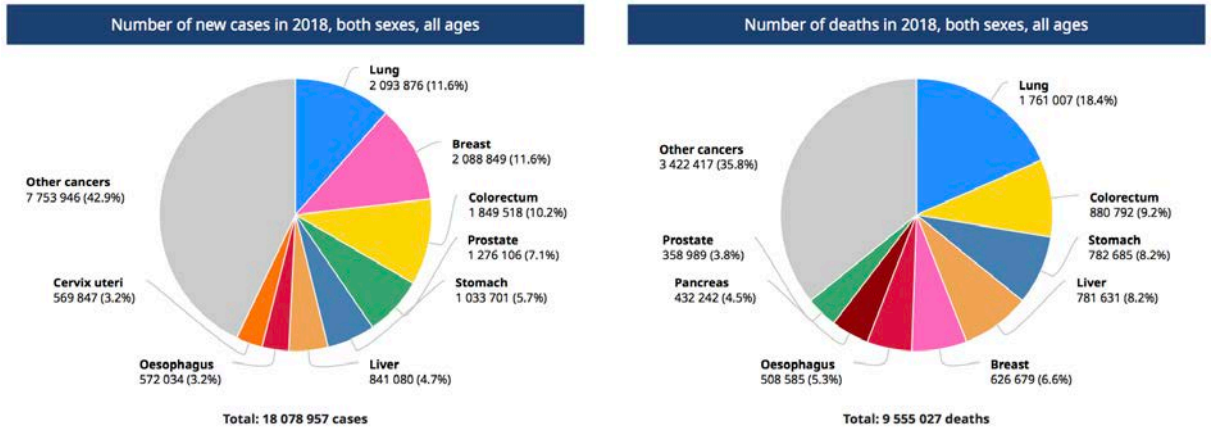

Figure 4: World statistics of cancer incidence and mortality in 2018 obtained from the International Agency for Research on Cancer – Global Cancer Observatory[227].

Innovation in the last decades, prompted by the collaboration of several disciplines including biology, pharmacy, chemistry, medicine and engineering, has given nanotechnology a variety of tools for deeply contribute to delivery, imaging and detection of cancer malignancies[228–231]. Besides, the limitations of existing therapies stimulate the development and application of various nanotechnological platforms (section 2) for more effective and safer cancer treatment[229]. Considerable success has been achieved in this field with the majority of marketed nanopharmaceuticals intended for cancer therapy (Section 1, **Figure 5**)[9,12,23,41,232].

Some key benefits of these nanomedicines include the ability to solubilize poorly soluble chemotherapeutic drugs, the capacity to accumulate into pathological areas with a characteristic defective vasculature (EPR effect) and the adequate biocompatibility profiles[230].

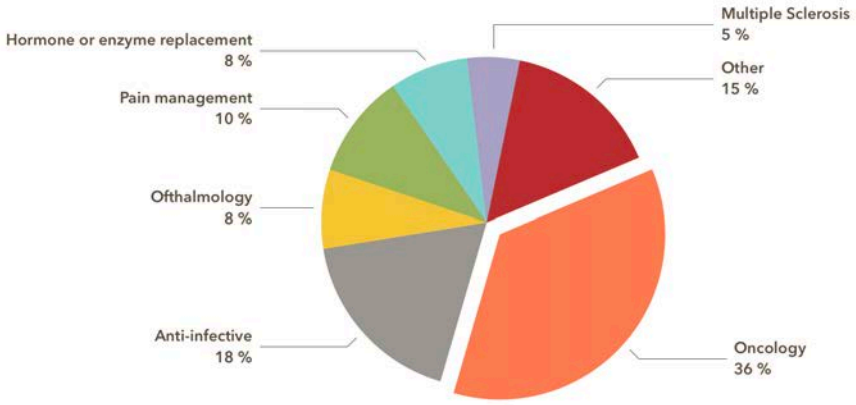

Figure 5: Indication distribution of commercialized nanopharmaceuticals (lipid, protein and polymer-based).

It is true that nanotechnology have revolutionized cancer medicine over the last decades, however deeper efforts are required from basic research to reach a deeper understanding of tumor complex biology, tumor development, cellular heterogeneity among the tumor and biomarkers definition. Filling also the gaps in our cancer knowledge regarding bio-nano interactions, systemic transport of nanosystems to tumor cells, tumor microenvironment (TME) or premetastatic niche will lead to more effective nanopharmaceuticals[229].

A lot of challenges and opportunities lie ahead for nanomedicine[183]. Although most approved nanosystems carried conventional chemotherapeutical agents, currently the tendency is to gradually incorporate new molecular entities (biological macromolecules such as peptides, proteins, antibodies, miRNAs, siRNAs or aptamers)[8]. Therefore the true goal of cancer nanomedicine is yet to come.

REFERENCES

(1) ETPN. What is nanomedicine? https://etp-nanomedicine.eu/about-nanomedicine/what-is-nanomedicine/.

(2) Couvreur, P. Nanoparticles in Drug Delivery: Past, Present and Future. *Adv. Drug Deliv. Rev.* **2013**, *65*, 21–23.

(3) Mühlebach, S. Regulatory Challenges of Nanomedicines and Their Follow-on Versions: A Generic or Similar Approach? *Adv. Drug Deliv. Rev.* **2018**, *131*, 122–131.

(4) European Commission, E. *Reccommendations on the Definition of Nanomaterial*; 2011.

(5) Whitesides, G. M. The "Right" Size in Nanobiothechnology. *Nat. Biotechnol.* **2003**, *21*, 1161–1165.

(6) Singh, R.; Lillard, J. W. Nanoparticle-Based Targeted Drug Delivery. *Exp. Mol. Pathol.* **2009**, *86*, 215–223.

(7) Klang, V.; Matsko, N. B.; Valenta, C.; Hofer, F. Electron Microscopy of Nanoemulsions: An Essential Tool for Characterisation and Stability Assessment. *Micron* **2012**, *43*, 85–103.

(8) Ferrari, M. Cancer Nanotechnology: Opportunities and Challenges. *Nat. Rev. Cancer* **2005**, *5*, 161–171.

(9) Bobo, D.; Robinson, K. J.; Islam, J.; Thurecht, K. J.; Corrie, S. R. Nanoparticle-Based Medicines: A Review of FDA-Approved Materials and Clinical Trials to Date. *Pharm. Res.* **2016**, *33*, 2373–2387.

(10) Svenson, S. Clinical Translation of Nanomedicines. *Curr. Opin. Solid State Mater. Sci.* **2012**, *16*, 287–294.

(11) Scheinberg, D. A.; Grimm, J.; Heller, D. A.; Stater, E. P.; Bradbury, M.; McDevitt, M. R. Advances in the Clinical Translation of Nanotechnology. *Curr. Opin. Biotechnol.* **2017**, *46*, 66–73.

(12) Havel, H.; Finch, G.; Strode, P.; Wolfgang, M.; Zale, S.; Bobe, I.; Youssoufian, H.; Peterson, M.; Liu, M. Nanomedicines: From Bench to Bedside and Beyond. *AAPS J.* **2016**, *18*, 1373–1378.

(13) Devalapally, H.; Chakilam, A.; Amiji, M. M. Role of Nanotechnology in Pharmaceutical Product Development. *J. Pharm. Sci.* **2007**, *96*, 2547–2565.

(14) European Medicines Agency. Find medicine - European public assessment reports http://www.ema.europa.eu/ema/index.jsp?curl=pages/medicines/landing/epar_search.jsp&mid=WC0b01ac058001d124 (accessed Sep 12, 2018).

(15) Food and Drug Administration, F. Drugs@FDA: FDA approved drug products https://www.accessdata.fda.gov/scripts/cder/daf/ (accessed Sep 12, 2018).

(16) Wagner, V.; Dullaart, A.; Bock, A. K.; Zweck, A. The Emerging Nanomedicine Landscape. *Nat. Biotechnol.* **2006**, *24*, 1211–1217.

(17) Ventola, C. L. Progress in Nanomedicine: Approved and Investigational Nanodrugs. *P T* **2017**, *42*, 742–755.

(18) Wicki, A.; Witzigmann, D.; Balasubramanian, V.; Huwyler, J. Nanomedicine in Cancer Therapy: Challenges, Opportunities, and Clinical Applications. *J. Control. Release* **2015**, *200*, 138–157.

(19) Bulbake, U.; Doppalapudi, S.; Kommineni, N.; Khan, W. Liposomal Formulations in Clinical Use: An Updated Review. *Pharmaceutics* **2017**, *9*, 1–33.

(20) Weissig, V.; Pettinger, T.; Murdock, N. Nanopharmaceuticals (Part 1): Products on the Market. *Int. J. Nanomedicine* **2014**, *9*, 4357.

(21) Havel, H. A. Where Are the Nanodrugs? An Industry Perspective on Development of Drug Products Containing Nanomaterials. *AAPS J.* **2016**, *18*, 1351–1353.

(22) Varshochian, R.; Hosseinzadeh, H.; Gandomi, N.; Tavassolian, F.; Atyabi, F.; Dinarvand, R. Utilizing Liposomes and Lipid Nanoparticles to Overcome Challenges in Breast Cancer Treatment. *Clin. Lipidol.* **2014**, *9*, 571–585.

(23) Patra, J. K.; Das, G.; Fraceto, L. F.; Campos, E. V. R.; Rodriguez-Torres, M. del P.; Acosta-Torres, L. S.; Diaz-Torres, L. A.; Grillo, R.; Swamy, M. K.; Sharma, S.; *et al.* Nano Based Drug Delivery Systems: Recent Developments and Future Prospects. *J. Nanobiotechnology* **2018**, *16*, 71.

(24) Zhang, Y.; Chan, H. F.; Leong, K. W. Advanced Materials and Processing for Drug Delivery: The Past and the Future.

Adv. Drug Deliv. Rev. **2013**, *65*, 104–120.

(25) Farokhzad, O. C.; Langer, R. Impact of Nanotechnology on Drug Delivery. *ACS Nano* **2009**, *3*, 16–20.

(26) Vellard, M. The Enzyme as Drug: Application of Enzymes as Pharmaceuticals. *Curr. Opin. Biotechnol.* **2003**, *14*, 444–450.

(27) Barenholz, Y. Doxil® - The First FDA-Approved Nano-Drug: Lessons Learned. *J. Control. Release* **2012**, *160*, 117–134.

(28) Milton Harris, J.; Chess, R. B. Effect of Pegylation on Pharmaceuticals. *Nat. Rev. Drug Discov.* **2003**, *2*, 214–221.

(29) Foss, F. Clinical Experience with Denileukin Diftitox (ONTAK). *Semin. Oncol.* **2006**, *33*, 11–16.

(30) Miele, E. E.; Spinelli, G. P.; Miele, E. E.; Tomao, F.; Tomao, S. Albumin-Bound Formulation of Paclitaxel (Abraxane® ABI-007) in the Treatment of Breast Cancer. *Int. J. Nanomedicine* **2009**, *4*, 99–105.

(31) Hörmann, K.; Zimmer, A. Drug Delivery and Drug Targeting with Parenteral Lipid Nanoemulsions - A Review. *J. Control. Release* **2016**, *223*, 85–98.

(32) Lim, S. B.; Banerjee, A.; Önyüksel, H. Improvement of Drug Safety by the Use of Lipid-Based Nanocarriers. *J. Control. Release* **2012**, *163*, 34–45.

(33) Onoue, S.; Yamada, S.; Chan, K. Nanodrugs: Pharmacokinetics and Safety. *Int. J. Nanomedicine* **2014**, *9*, 1025.

(34) Fadeel, B.; Garcia-Bennett, A. E. Better Safe than Sorry: Understanding the Toxicological Properties of Inorganic Nanoparticles Manufactured for Biomedical Applications. *Adv. Drug Deliv. Rev.* **2010**, *62*, 362–374.

(35) Rivera Gil, P.; Hühn, D.; del Mercato, L. L.; Sasse, D.; Parak, W. J. Nanopharmacy: Inorganic Nanoscale Devices as Vectors and Active Compounds. *Pharmacol. Res.* **2010**, *62*, 115–125.

(36) Cheng, R.; Xue, Y. Carbon Nanomaterials for Drug Delivery. In *Carbon Nanomaterials for Biomedical Applications*; 2016; pp. 31–80.

(37) Beik, J.; Abed, Z.; Ghoreishi, F. S.; Hosseini-Nami, S.; Mehrzadi, S.; Shakeri-Zadeh, A.; Kamrava, S. K. Nanotechnology in Hyperthermia Cancer Therapy: From Fundamental Principles to Advanced Applications. *J. Control. Release* **2016**, *235*, 205–221.

(38) Junghanns, J. U. A. H.; Müller, R. H. Nanocrystal Technology, Drug Delivery and Clinical Applications. *Int. J. Nanomedicine* **2008**, *3*, 295–309.

(39) Peltonen, L.; Hirvonen, J. Drug Nanocrystals – Versatile Option for Formulation of Poorly Soluble Materials. *Int. J. Pharm.* **2018**, *537*, 73–83.

(40) Lu, Y.; Li, Y.; Wu, W. Injected Nanocrystals for Targeted Drug Delivery. *Acta Pharm. Sin. B* **2016**, *6*, 106–113.

(41) Farjadian, F.; Ghasemi, A.; Gohari, O.; Roointan, A.; Karimi, M.; Hamblin, M. R. Nanopharmaceuticals and Nanomedicines Currently on the Market: Challenges and Opportunities. *Nanomedicine* **2019**, *14*, 93–126.

(42) Miller, S. L.; Urey, H. C. Organic Compound Synthesis on the Primitive Earth. *Science (80-.).* **1959**, *130*, 245–251.

(43) Herrera Estrada, L. P.; Champion, J. A. Protein Nanoparticles for Therapeutic Protein Delivery. *Biomater. Sci.* **2015**, *3*, 787–799.

(44) Lohcharoenkal, W.; Wang, L.; Chen, Y. C.; Rojanasakul, Y. Protein Nanoparticles as Drug Delivery Carriers for Cancer Therapy. *Biomed Res. Int.* **2014**, *2014*, 1–12.

(45) Jahanshahi, M.; Babaei, Z. Protein Nanoparticle: A Unique System as Drug Delivery Vehicles. *African J. Biotechnol.* **2008**, *7*, 4926–4934.

(46) Tarhini, M.; Greige-Gerges, H.; Elaissari, A. Protein-Based Nanoparticles: From Preparation to Encapsulation of Active Molecules. *Int. J. Pharm.* **2017**, *522*, 172–197.

(47) MaHam, A.; Tang, Z.; Wu, H.; Wang, J.; Lin, Y. Protein-Based Nanomedicine Platforms for Drug Delivery. *Small* **2009**, *5*, 1706–1721.

(48) Elzoghby, A. O.; Samy, W. M.; Elgindy, N. A. Protein-Based Nanocarriers as Promising Drug and Gene Delivery

Systems. *J. Control. Release* **2012**, *161*, 38–49.

(49) Lee, E. J.; Lee, N. K.; Kim, I.-S. Bioengineered Protein-Based Nanocage for Drug Delivery. *Adv. Drug Deliv. Rev.* **2016**, *106*, 157–171.

(50) Molino, N. M.; Wang, S.-W. Caged Protein Nanoparticles for Drug Delivery. *Curr. Opin. Biotechnol.* **2014**, *28*, 75–82.

(51) Leo, E.; Vandelli, M. A.; Cameroni, R.; Forni, F. Doxorubicin-Loaded Gelatin Nanoparticles Stabilized by Glutaraldehyde: Involvement of the Drug in the Cross-Linking Process. *Int. J. Pharm.* **1997**, *155*, 75–82.

(52) Miele, E.; Spinelli, G. P.; Miele, E.; Tomao, F.; Tomao, S. Albumin-Bound Formulation of Paclitaxel (Abraxane® ABI-007) in the Treatment of Breast Cancer. *Int. J. Nanomedicine* **2009**, *4*, 99–105.

(53) Kratz, F. Albumin as a Drug Carrier: Design of Prodrugs, Drug Conjugates and Nanoparticles. *J. Control. Release* **2008**, *132*, 171–183.

(54) Arnedo, A.; Irache, J. M.; Merodio, M.; Espuelas Millán, M. S. Albumin Nanoparticles Improved the Stability, Nuclear Accumulation and Anticytomegaloviral Activity of a Phosphodiester Oligonucleotide. *J. Control. Release* **2004**, *94*, 217–227.

(55) Duncan, R. Polymer Therapeutics: Top 10 Selling Pharmaceuticals - What Next? *J. Control. Release* **2014**, *190*, 371–380.

(56) Langer, R. Biomaterials in Drug Delivery and Tissue Engineering: One Laboratory's Experience. *Acc. Chem. Res.* **2000**, *33*, 94–101.

(57) Tang, Z.; He, C.; Tian, H.; Ding, J.; Hsiao, B. S.; Chu, B.; Chen, X. Polymeric Nanostructured Materials for Biomedical Applications. *Prog. Polym. Sci.* **2016**, *60*, 86–128.

(58) Duncan, R.; Vicent, M. J. Polymer Therapeutics-Prospects for 21st Century: The End of the Beginning. *Adv. Drug Deliv. Rev.* **2013**, *65*, 60–70.

(59) Lu, X.-Y.; Wu, D.-C.; Li, Z.-J.; Chen, G.-Q. Polymer Nanoparticles. In *Progress in molecular biology and translational science*; 2011; Vol. 104, pp. 299–323.

(60) Englert, C.; Brendel, J. C.; Majdanski, T. C.; Yildirim, T.; Schubert, S.; Gottschaldt, M.; Windhab, N.; Schubert, U. S. Pharmapolymers in the 21st Century: Synthetic Polymers in Drug Delivery Applications. *Prog. Polym. Sci.* **2018**, *87*, 107–164.

(61) Banik, B. L.; Fattahi, P.; Brown, J. L. Polymeric Nanoparticles: The Future of Nanomedicine. *Wiley Interdiscip. Rev. Nanomedicine Nanobiotechnology* **2016**, *8*, 271–299.

(62) El-Say, K. M.; El-Sawy, H. S. Polymeric Nanoparticles: Promising Platform for Drug Delivery. *Int. J. Pharm.* **2017**, *528*, 675–691.

(63) Langer, R.; Tirrell, D. A. Designing Materials for Biology and Medicine. *Nature* **2004**, *428*, 487–492.

(64) Turecek, P. L.; Bossard, M. J.; Schoetens, F.; Ivens, I. A. PEGylation of Biopharmaceuticals: A Review of Chemistry and Nonclinical Safety Information of Approved Drugs. *J. Pharm. Sci.* **2016**, *105*, 460–475.

(65) Sartor, O. Eligard: Leuprolide Acetate in a Novel Sustained-Release Delivery System. *Urology* **2003**, *61*, 25–31.

(66) Kadajji, V. G.; Betageri, G. V. Water Soluble Polymers for Pharmaceutical Applications. *Polymers (Basel).* **2011**, *3*, 1972–2009.

(67) Pillai, O.; Panchagnula, R. Biodegradable and Nondegradable Polymers. *Curr. Opin. Chem. Biol.* **2001**, *5*, 447–451.

(68) Soppimath, K. S.; Aminabhavi, T. M.; Kulkarni, A. R.; Rudzinski, W. E. Biodegradable Polymeric Nanoparticles as Drug Delivery Devices. *J. Control. Release* **2001**, *70*, 1–20.

(69) Shastri, V. Non-Degradable Biocompatible Polymers in Medicine: Past, Present and Future. *Curr. Pharm. Biotechnol.* **2003**, *4*, 331–337.

(70) Duncan, R.; Gaspar, R. Nanomedicine(s) under the Microscope. *Mol. Pharm.* **2011**, *8*, 2101–2141.

(71) Singer, J. W.; Shaffer, S.; Baker, B.; Bernareggi, A.; Stromatt, S.; Nienstedt, D.; Besman, M. Paclitaxel Poliglumex (XYOTAX; CT-2103): An Intracellularly Targeted Taxane. *Anticancer. Drugs* **2005**, *16*, 243–254.

(72) Nowotnik, D. P.; Cvitkovic, E. ProLindac™ (AP5346): A Review of the Development of an HPMA DACH Platinum Polymer Therapeutic. *Adv. Drug Deliv. Rev.* **2009**, *61*, 1214–1219.

(73) Pouton, C. W.; Porter, C. J. H. Formulation of Lipid-Based Delivery Systems for Oral Administration: Materials, Methods and Strategies. *Adv. Drug Deliv. Rev.* **2008**, *60*, 625–637.

(74) Santalices, I.; Gonella, A.; Torres, D.; Alonso, M. J. Advances on the Formulation of Proteins Using Nanotechnologies. *J. Drug Deliv. Sci. Technol.* **2017**, *42*, 155–180.

(75) Bangham, A. D.; Standish, M. M.; Watkins, J. C. Diffusion of Univalent Ions across the Lamellae of Swollen Phospholipids. *J. Mol. Biol.* **1965**, *13*, IN26–IN27.

(76) Torchilin, V. P. Recent Advances with Liposomes as Pharmaceutical Carriers. *Nat. Rev. Drug Discov.* **2005**, *4*, 145–160.

(77) Bozzuto, G.; Molinari, A. Liposomes as Nanomedical Devices. *Int. J. Nanomedicine* **2015**, *10*, 975–999.

(78) Belfiore, L.; Saunders, D. N.; Ranson, M.; Thurecht, K. J.; Storm, G.; Vine, K. L. Towards Clinical Translation of Ligand-Functionalized Liposomes in Targeted Cancer Therapy: Challenges and Opportunities. *J. Control. Release* **2018**, *277*, 1–13.

(79) Moosavian, S. A.; Sahebkar, A. Aptamer-Functionalized Liposomes for Targeted Cancer Therapy. *Cancer Lett.* **2019**, *448*, 144–154.

(80) Eloy, J. O.; Petrilli, R.; Trevizan, L. N. F.; Chorilli, M. Immunoliposomes: A Review on Functionalization Strategies and Targets for Drug Delivery. *Colloids Surfaces B Biointerfaces* **2017**, *159*, 454–467.

(81) Hanafy, N. A. N.; El-Kemary, M.; Leporatti, S. Micelles Structure Development as a Strategy to Improve Smart Cancer Therapy. *Cancers (Basel).* **2018**, *10*, 1–14.

(82) Gill, K. K.; Kaddoumi, A.; Nazzal, S. PEG-Lipid Micelles as Drug Carriers: Physiochemical Attributes, Formulation Principles and Biological Implication. *J. Drug Target.* **2015**, *23*, 222–231.

(83) Torchilin, V. P. Lipid-Core Micelles for Targeted Drug Delivery. *Curr. Drug Deliv.* **2005**, *2*, 319–327.

(84) Lasic, D. D. Mixed Micelles in Drug Delivery. *Nature* **1992**, *355*, 279–282.

(85) Mazza, M.; Alonso-Sande, M.; Jones, M.-C.; de la Fuente, M. The Potential of Nanoemulsions in Biomedicine. In *Fundamentals of Pharmaceutical Nanoscience*; Springer New York: New York, NY, 2013; pp. 117–158.

(86) Singh, Y.; Meher, J. G.; Raval, K.; Khan, F. A.; Chaurasia, M.; Jain, N. K.; Chourasia, M. K. Nanoemulsion: Concepts, Development and Applications in Drug Delivery. *J. Control. Release* **2017**, *252*, 28–49.

(87) McClements, D. J. Encapsulation, Protection, and Delivery of Bioactive Proteins and Peptides Using Nanoparticle and Microparticle Systems: A Review. *Adv. Colloid Interface Sci.* **2018**, *253*, 1–22.

(88) McClements, D. J. Nanoemulsions versus Microemulsions: Terminology, Differences, and Similarities. *Soft Matter* **2012**, *8*, 1719–1729.

(89) Callender, S. P.; Mathews, J. A.; Kobernyk, K.; Wettig, S. D. Microemulsion Utility in Pharmaceuticals: Implications for Multi-Drug Delivery. *Int. J. Pharm.* **2017**, *526*, 425–442.

(90) Gutiérrez, J. M.; González, C.; Maestro, A.; Solè, I.; Pey, C. M.; Nolla, J. Nano-Emulsions: New Applications and Optimization of Their Preparation. *Curr. Opin. Colloid Interface Sci.* **2008**, *13*, 245–251.

(91) Solans, C.; Izquierdo, P.; Nolla, J.; Azemar, N.; Garcia-Celma, M. J. Nano-Emulsions. *Curr. Opin. Colloid Interface Sci.* **2005**, *10*, 102–110.

(92) Solans, C.; Solé, I. Nano-Emulsions: Formation by Low-Energy Methods. *Curr. Opin. Colloid Interface Sci.* **2012**, *17*, 246–254.

(93) Chappat, M. Some Applications of Emulsions. *Colloids Surfaces A Physicochem. Eng. Asp.* **1994**, *91*, 57–77.

(94) Rao, J.; McClements, D. J. Food-Grade Microemulsions, Nanoemulsions and Emulsions: Fabrication from Sucrose Monopalmitate & Lemon Oil. *Food Hydrocoll.* **2011**, *25*, 1413–1423.

(95) Rao, J.; McClements, D. J. Lemon Oil Solubilization in Mixed Surfactant Solutions: Rationalizing Microemulsion & Nanoemulsion Formation. *Food Hydrocoll.* **2012**, *26*, 268–276.

(96) Danielsson, I.; Lindman, B. The Definition of Microemulsion. *Colloids and Surfaces* **1981**, *3*, 391–392.

(97) Niu, Z.; Conejos-Sánchez, I.; Griffin, B. T.; O'Driscoll, C. M.; Alonso, M. J. Lipid-Based Nanocarriers for Oral Peptide Delivery. *Adv. Drug Deliv. Rev.* **2016**, *106*, 337–354.

(98) Pouton, C. W. Self-Emulsifying Drug Delivery Systems: Assessment of the Efficiency of Emulsification. *Int. J. Pharm.* **1985**, *27*, 335–348.

(99) Pouton, C. W. Lipid Formulations for Oral Administration of Drugs: Non-Emulsifying, Self-Emulsifying and "self-Microemulsifying" Drug Delivery Systems. *Eur. J. Pharm. Sci.* **2000**, *11*, S93–S98.

(100) Vasconcelos, T.; Marques, S.; Sarmento, B. Measuring the Emulsification Dynamics and Stability of Self-Emulsifying Drug Delivery Systems. *Eur. J. Pharm. Biopharm.* **2018**, *123*, 1–8.

(101) Anton, N.; Vandamme, T. F. Nano-Emulsions and Micro-Emulsions: Clarifications of the Critical Differences. *Pharm. Res.* **2011**, *28*, 978–985.

(102) Chen, M.-L. Lipid Excipients and Delivery Systems for Pharmaceutical Development: A Regulatory Perspective. *Adv. Drug Deliv. Rev.* **2008**, *60*, 768–777.

(103) Shrestha, H.; Bala, R.; Arora, S. Lipid-Based Drug Delivery Systems. *J. Pharm.* **2014**, *2014*, 1–10.

(104) Strickley, R. G. Solubilizing Excipients in Oral and Injectable Formulations. *Pharm. Res.* **2004**, *21*, 201–230.

(105) Müller, R. Solid Lipid Nanoparticles (SLN) for Controlled Drug Delivery: A Review of the State of the Art. *Eur. J. Pharm. Biopharm.* **2000**, *50*, 161–177.

(106) Weber, S.; Zimmer, A.; Pardeike, J. Solid Lipid Nanoparticles (SLN) and Nanostructured Lipid Carriers (NLC) for Pulmonary Application: A Review of the State of the Art. *Eur. J. Pharm. Biopharm.* **2014**, *86*, 7–22.

(107) Naseri, N.; Valizadeh, H.; Zakeri-Milani, P. Solid Lipid Nanoparticles and Nanostructured Lipid Carriers: Structure Preparation and Application. *Adv. Pharm. Bull.* **2015**, *5*, 305–313.

(108) Beloqui, A.; Solinís, M. Á.; Rodríguez-Gascón, A.; Almeida, A. J.; Préat, V. Nanostructured Lipid Carriers: Promising Drug Delivery Systems for Future Clinics. *Nanomedicine Nanotechnology, Biol. Med.* **2016**, *12*, 143–161.

(109) Khosa, A.; Reddi, S.; Saha, R. N. Nanostructured Lipid Carriers for Site-Specific Drug Delivery. *Biomed. Pharmacother.* **2018**, *103*, 598–613.

(110) Reimondez-Troitiño, S.; Alcalde, I.; Csaba, N.; Íñigo-Portugués, A.; de la Fuente, M.; Bech, F.; Riestra, A. C.; Merayo-Lloves, J.; Alonso, M. J. Polymeric Nanocapsules: A Potential New Therapy for Corneal Wound Healing. *Drug Deliv. Transl. Res.* **2016**, *6*, 708–721.

(111) Jakubiak, P.; Thwala, L. N.; Cadete, A.; Préat, V.; Alonso, M. J.; Beloqui, A.; Csaba, N. Solvent-Free Protamine Nanocapsules as Carriers for Mucosal Delivery of Therapeutics. *Eur. Polym. J.* **2017**, *93*, 695–705.

(112) Abellan-Pose, R.; Rodríguez-Évora, M.; Vicente, S.; Csaba, N.; Évora, C.; Alonso, M. J.; Delgado, A. Biodistribution of Radiolabeled Polyglutamic Acid and PEG-Polyglutamic Acid Nanocapsules. *Eur. J. Pharm. Biopharm.* **2017**, *112*, 155–163.

(113) Alonso-Nocelo, M.; Abellan-Pose, R.; Vidal, A.; Abal, M.; Csaba, N.; Alonso, M. J.; Lopez-Lopez, R.; de la Fuente, M. Selective Interaction of PEGylated Polyglutamic Acid Nanocapsules with Cancer Cells in a 3D Model of a Metastatic Lymph Node. *J. Nanobiotechnology* **2016**, *14*, 51.

(114) Thwala, L. N.; Beloqui, A.; Csaba, N. S.; González-Touceda, D.; Tovar, S.; Dieguez, C.; Alonso, M. J.; Préat, V. The Interaction of Protamine Nanocapsules with the Intestinal Epithelium: A Mechanistic Approach. *J. Control. Release* **2016**, *243*, 109–120.

(115) Lollo, G.; Gonzalez-Paredes, A.; Garcia-Fuentes, M.; Calvo, P.; Torres, D.; Alonso, M. J. Polyarginine Nanocapsules as a Potential Oral Peptide Delivery Carrier. *J. Pharm. Sci.* **2017**, *106*, 611–618.

(116) González-Aramundiz, J. V.; Presas, E.; Dalmau-Mena, I.; Martínez-Pulgarín, S.; Alonso, C.; Escribano, J. M.; Alonso, M. J.; Csaba, N. S. Rational Design of Protamine Nanocapsules as Antigen Delivery Carriers. *J. Control. Release* **2017**, *245*, 62–69.

(117) Kohli, A. G.; Kierstead, P. H.; Venditto, V. J.; Walsh, C. L.; Szoka, F. C. Designer Lipids for Drug Delivery: From Heads to Tails. *J. Control. Release* **2014**, *190*, 274–287.

(118) Calvo, P.; Vila-Jato, J. L.; Alonso, M. J. Comparative in Vitro Evaluation of Several Colloidal Systems, Nanoparticles, Nanocapsules, and Nanoemulsions, as Ocular Drug Carriers. *J. Pharm. Sci.* **1996**, *85*, 530–536.

(119) McClements, D. J. Edible Nanoemulsions: Fabrication, Properties, and Functional Performance. *Soft Matter* **2011**, *7*, 2297–2316.

(120) Jaiswal, M.; Dudhe, R.; Sharma, P. K. Nanoemulsion: An Advanced Mode of Drug Delivery System. *3 Biotech* **2015**, *5*, 123–127.

(121) Sonneville-Aubrun, O.; Simonnet, J. T.; L'Alloret, F. Nanoemulsions: A New Vehicle for Skincare Products. *Adv. Colloid Interface Sci.* **2004**, *108–109*, 145–149.

(122) Lovelyn, C.; Attama, A. A. Current State of Nanoemulsions in Drug Delivery. *J. Biomater. Nanobiotechnol.* **2011**, *02*, 626–639.

(123) Sainsbury, F.; Zeng, B.; Middelberg, A. P. Towards Designer Nanoemulsions for Precision Delivery of Therapeutics. *Curr. Opin. Chem. Eng.* **2014**, *4*, 11–17.

(124) Maali, A.; Mosavian, M. T. H. Preparation and Application of Nanoemulsions in the Last Decade (2000–2010). *J. Dispers. Sci. Technol.* **2013**, *34*, 92–105.

(125) Gupta, A.; Eral, H. B.; Hatton, T. A.; Doyle, P. S. Nanoemulsions: Formation, Properties and Applications. *Soft Matter* **2016**, *12*, 2826–2841.

(126) Chime, S. A.; Kenechukwu, F. C.; Attama, A. A. Nanoemulsions — Advances in Formulation, Characterization and Applications in Drug Delivery. In *Application of Nanotechnology in Drug Delivery*; InTech, 2014; pp. 77–126.

(127) Bhatt, P.; Madhav, S. A Detailed Review on Nanoemulsion Drug Delivery System. *Int. J. Pharm. Sci. Res.* **2011**, *2*, 2292–2298.

(128) McClements, D. J. Nanoemulsion-Based Oral Delivery Systems for Lipophilic Bioactive Components: Nutraceuticals and Pharmaceuticals. *Ther. Deliv.* **2013**, *4*, 841–857.

(129) McClements, D. J.; Rao, & J. Food-Grade Nanoemulsions: Formulation, Fabrication, Properties, Performance, Biological Fate, and Potential Toxicity. *Crit. Rev. Food Sci. Nutr.* **2011**, *51*, 285–330.

(130) Solans, C.; Morales, D.; Homs, M. Spontaneous Emulsification. *Curr. Opin. Colloid Interface Sci.* **2016**, *22*, 88–93.

(131) Mora-Huertas, C. E.; Fessi, H.; Elaissari, A. Influence of Process and Formulation Parameters on the Formation of Submicron Particles by Solvent Displacement and Emulsification-Diffusion Methods: Critical Comparison. *Adv. Colloid Interface Sci.* **2011**, *163*, 90–122.

(132) Sugumar, S.; Ghosh, V.; Mukherjee, A.; Chandrasekaran, N. Essential Oil-Based Nanoemulsion Formation by Low- and High-Energy Methods and Their Application in Food Preservation against Food Spoilage Microorganisms. In *Essential Oils in Food Preservation, Flavor and Safety*; Elsevier, 2016; pp. 93–100.

(133) Perazzo, A.; Preziosi, V.; Guido, S. Phase Inversion Emulsification: Current Understanding and Applications. *Adv. Colloid Interface Sci.* **2015**, *222*, 581–599.

(134) Fernandez, P.; André, V.; Rieger, J.; Kühnle, A. Nano-Emulsion Formation by Emulsion Phase Inversion. *Colloids Surfaces A Physicochem. Eng. Asp.* **2004**, *251*, 53–58.

(135) Pathak, K.; Pattnaik, S.; Swain, K. Application of Nanoemulsions in Drug Delivery. In *Nanoemulsions*; Elsevier,

2018; pp. 415–433.

(136) Sutradhar, K. B.; Amin, L. Nanoemulsions: Increasing Possibilities in Drug Delivery. *Eur. J. Nanomedicine* **2013**, *5*, 97–110.

(137) Tamilvanan, S. Oil-in-Water Lipid Emulsions: Implications for Parenteral and Ocular Delivering Systems. *Prog. Lipid Res.* **2004**, *43*, 489–533.

(138) Kotta, S.; Khan, A. W.; Pramod, K.; Ansari, S. H.; Sharma, R. K.; Ali, J. Exploring Oral Nanoemulsions for Bioavailability Enhancement of Poorly Water-Soluble Drugs. *Expert Opin. Drug Deliv.* **2012**, *9*, 585–598.

(139) Constantinides, P. P.; Chaubal, M. V; Shorr, R. Advances in Lipid Nanodispersions for Parenteral Drug Delivery and Targeting. *Adv. Drug Deliv. Rev.* **2008**, *60*, 757–767.

(140) Collins-Gold, L. C.; Lyons, R. T.; Bartholow, L. C. Parenteral Emulsions for Drug Delivery. *Adv. Drug Deliv. Rev.* **1990**, *5*, 189–208.

(141) Tamilvanan, S. Formulation of Multifunctional Oil-in-Water Nanosized Emulsions for Active and Passive Targeting of Drugs to Otherwise Inaccessible Internal Organs of the Human Body. *Int. J. Pharm.* **2009**, *381*, 62–76.

(142) Calder, P. C.; Jensen, G. L.; Koletzko, B. V.; Singer, P.; Wanten, G. J. A. Lipid Emulsions in Parenteral Nutrition of Intensive Care Patients: Current Thinking and Future Directions. *Intensive Care Med.* **2010**, *36*, 735–749.

(143) Fell, G. L.; Nandivada, P.; Gura, K. M.; Puder, M. Intravenous Lipid Emulsions in Parenteral Nutrition. *Adv. Nutr.* **2015**, *6*, 600–610.

(144) Wretlind, A. Development of Fat Emulsions. *J. Parenter. Enter. Nutr.* **1981**, *5*, 230–235.

(145) Driscoll, D. F. Lipid Injectable Emulsions: Pharmacopeial and Safety Issues. *Pharm. Res.* **2006**, *23*, 1959–1969.

(146) Teitelbaum, D. H.; Guenter, P.; Griebel, D.; Abrams, S. A.; Bark, S.; Baker, M.; Berry, K. L.; Bistrian, B. R.; Brenna, J. T.; Bonnot, D.; *et al.* Proceedings from FDA/A.S.P.E.N. Public Workshop: Clinical Trial Design for Intravenous Fat Emulsion Products, October 29, 2013. *J. Parenter. Enter. Nutr.* **2015**, *39*, 768–786.

(147) Food and Drug Administration, F. *Waiver of In Vivo Bioavailability and Bioequivalence Studies for Immediate-Release Solid Oral Dosage Forms Based on a Biopharmaceutics Classification System Guidance for Industry*; 2017.

(148) Ghadi, R.; Dand, N. BCS Class IV Drugs: Highly Notorious Candidates for Formulation Development. *J. Control. Release* **2017**, *248*, 71–95.

(149) Tarr, B. D.; Sambandan, T. G.; Yalkowsky, S. H. A New Parenteral Emulsion for the Administration of Taxol. *Pharm. Res.* **1987**, *4*, 162–165.

(150) Kan, P.; Chen, Z. B.; Lee, C. J.; Chu, I. M. Development of Nonionic Surfactant/Phospholipid o/w Emulsion as a Paclitaxel Delivery System. *J. Control. Release* **1999**, *58*, 271–278.

(151) Feng, L.; Mumper, R. J. A Critical Review of Lipid-Based Nanoparticles for Taxane Delivery. *Cancer Lett.* **2013**, *334*, 157–175.

(152) Constantinides, P. P.; Han, J.; Davis, S. S. Advances in the Use of Tocols as Drug Delivery Vehicles. *Pharm. Res.* **2006**, *23*, 243–255.

(153) Ma, P.; Mumper, R. J. Paclitaxel Nano-Delivery Systems: A Comprehensive Review. *J. Nanomed. Nanotechnol.* **2013**, *04*.

(154) Constantinides, P. P.; Lambert, K. J.; Tustian, A. K.; Schneider, B.; Lalji, S.; Ma, W.; Wentzel, B.; Kessler, D.; Worah, D.; Quay, S. C. Formulation Development and Antitumor Activity of a Filter-Sterilizable Emulsion of Paclitaxel. *Pharm. Res.* **2000**, *17*, 175–182.

(155) Constantinides, P. P.; Tustian, A.; Kessler, D. R. Tocol Emulsions for Drug Solubilization and Parenteral Delivery. *Adv. Drug Deliv. Rev.* **2004**, *56*, 1243–1255.

(156) Abu-Fayyad, A.; Kamal, M. M.; Carroll, J. L.; Dragoi, A. M.; Cody, R.; Cardelli, J.; Nazzal, S. Development and In-Vitro Characterization of Nanoemulsions Loaded with Paclitaxel/γ-Tocotrienol Lipid Conjugates. *Int. J. Pharm.* **2018**,

536, 146–157.

(157) Pawar, V. K.; Panchal, S. B.; Singh, Y.; Meher, J. G.; Sharma, K.; Singh, P.; Bora, H. K.; Singh, A.; Datta, D.; Chourasia, M. K. Immunotherapeutic Vitamin e Nanoemulsion Synergies the Antiproliferative Activity of Paclitaxel in Breast Cancer Cells via Modulating Th1 and Th2 Immune Response. *J. Control. Release* **2014**, *196*, 295–306.

(158) Lundberg, B. B.; Risovic, V.; Ramaswamy, M.; Wasan, K. M. A Lipophilic Paclitaxel Derivative Incorporated in a Lipid Emulsion for Parenteral Administration. *J. Control. Release* **2003**, *86*, 93–100.

(159) Desai, A.; Vyas, T.; Amiji, M. Cytotoxicity and Apoptosis Enhancement in Brain Tumor Cells Upon Coadministration of Paclitaxel and Ceramide in Nanoemulsion Formulations. *J. Pharm. Sci.* **2008**, *97*, 2745–2756.

(160) Ganta, S.; Amiji, M. Coadministration of Paclitaxel and Curcumin in Nanoemulsion Formulations to Overcome Multidrug Resistance in Tumor Cells. *Mol. Pharm.* **2009**, *6*, 928–939.

(161) Li, X.; Du, L.; Wang, C.; Liu, Y.; Mei, X.; Jin, Y. Highly Efficient and Lowly Toxic Docetaxel Nanoemulsions for Intravenous Injection to Animals. *Pharmazie* **2011**, *66*, 479–483.

(162) Gaoe, H.; Pang, Z.; Pan, S.; Cao, S.; Yang, Z.; Chen, C.; Jiang, X. Anti-Glioma Effect and Safety of Docetaxel-Loaded Nanoemulsion. *Arch. Pharm. Res.* **2012**, *35*, 333–341.

(163) Zhang, X.; Sun, X.; Li, J.; Zhang, X.; Gong, T.; Zhang, Z. Lipid Nanoemulsions Loaded with Doxorubicin-Oleic Acid Ionic Complex: Characterization, in Vitro and in Vivo Studies. *Pharmazie* **2011**, *66*, 496–505.

(164) Ragelle, H.; Crauste-Manciet, S.; Seguin, J.; Brossard, D.; Scherman, D.; Arnaud, P.; Chabot, G. G. Nanoemulsion Formulation of Fisetin Improves Bioavailability and Antitumour Activity in Mice. *Int. J. Pharm.* **2012**, *427*, 452–459.

(165) Zhao, H.; Lu, H.; Gong, T.; Zhang, Z. Nanoemulsion Loaded with Lycobetaine-Oleic Acid Ionic Complex: Physicochemical Characteristics, in Vitro, in Vivo Evaluation, and Antitumor Activity. *Int. J. Nanomedicine* **2013**, *8*, 1959–1973.

(166) Prete, A. C. Lo; Maria, D. A.; Rodrigues, D. bora G.; Valduga, C. J.; Ibañez, O. C. M.; Maranhão, R. C. Evaluation in Melanoma-Bearing Mice of an Etoposide Derivative Associated to a Cholesterol-Rich Nanoemulsion. *J. Pharm. Pharmacol.* **2006**, *58*, 801–808.

(167) Marier, J.-F.; Pheng, L.; Trinh, M. M.; Burris, H. A.; Jones, S.; Anderson, K.; Warner, S.; Porubek, D. Pharmacokinetics of SN2310, an Injectable Emulsion That Incorporates a New Derivative of SN-38 in Patients with Advanced Solid Tumors. *J. Pharm. Sci.* **2011**, *100*, 4536–4545.

(168) Alanazi, F. K.; Haq, N.; Radwan, A. A.; Alsarra, I. A.; Shakeel, F. Formulation and Evaluation of Cholesterol-Rich Nanoemulsion (LDE) for Drug Delivery Potential of Cholesteryl-Maleoyl-5-Fluorouracil. *Pharm. Dev. Technol.* **2015**, *20*, 266–270.

(169) Ganta, S.; Sharma, P.; Paxton, J. W.; Baguley, B. C.; Garg, S. Pharmacokinetics and Pharmacodynamics of Chlorambucil Delivered in Long-Circulating Nanoemulsion. *J. Drug Target.* **2010**, *18*, 125–133.

(170) Dragulska, S. A.; Chen, Y.; Wlodarczyk, M. T.; Poursharifi, M.; Dottino, P.; Ulijn, R. V.; Martignetti, J. A.; Mieszawska, A. J. Tripeptide-Stabilized Oil-in-Water Nanoemulsion of an Oleic Acids-Platinum(II) Conjugate as an Anticancer Nanomedicine. *Bioconjug. Chem.* **2018**, *29*, 2514–2519.

(171) Kelmann, R. G.; Kuminek, G.; Teixeira, H. F.; Koester, L. S. Carbamazepine Parenteral Nanoemulsions Prepared by Spontaneous Emulsification Process. *Int. J. Pharm.* **2007**, *342*, 231–239.

(172) Ahmed, M.; Ramadan, W.; Rambhu, D.; Shakeel, F. Potential of Nanoemulsions for Intravenous Delivery of Rifampicin. *Pharmazie* **2008**, *63*, 806–811.

(173) Araújo, F. A.; Kelmann, R. G.; Araújo, B. V; Finatto, R. B.; Teixeira, H. F.; Koester, L. S. Development and Characterization of Parenteral Nanoemulsions Containing Thalidomide. *Eur. J. Pharm. Sci.* **2011**, *42*, 238–245.

(174) Dordević, S. M.; Radulović, T. S.; Cekić, N. D.; Randelović, D. V.; Savić, M. M.; Krajišnik, D. R.; Milić, J. R.; Savić, S. D. Experimental Design in Formulation of Diazepam Nanoemulsions: Physicochemical and Pharmacokinetic

Performances. *J. Pharm. Sci.* **2013**, *102*, 4159–4172.

(175) Kwasigroch, B.; Escribano, E.; Morán, M. del C.; Queralt, J.; Busquets, M. A.; Estelrich, J. Oil-in-Water Nanoemulsions Are Suitable for Carrying Hydrophobic Compounds: Indomethacin as a Model of Anti-Inflammatory Drug. *Int. J. Pharm.* **2016**, *515*, 749–756.

(176) Yadav, S.; Gattacceca, F.; Panicucci, R.; Amiji, M. M. Comparative Biodistribution and Pharmacokinetic Analysis of Cyclosporine-A in the Brain upon Intranasal or Intravenous Administration in an Oil-in-Water Nanoemulsion Formulation. *Mol. Pharm.* **2015**, *12*, 1523–1533.

(177) Burger, C.; Aucamp, M.; du Preez, J.; Haynes, R. K.; Ngwane, A.; du Plessis, J.; Gerber, M. Formulation of Natural Oil Nano-Emulsions for the Topical Delivery of Clofazimine, Artemisone and Decoquinate. *Pharm. Res.* **2018**, *35*, 186.

(178) Moura, J. A.; Valduga, C. J.; Tavares, E. R.; Kretzer, I. F.; Maria, D. A.; Maranhão, R. C. Novel Formulation of a Methotrexate Derivative with a Lipid Nanoemulsion. *Int. J. Nanomedicine* **2011**, *6*, 2285–2295.

(179) Abu-Fayyad, A.; Nazzal, S. Gemcitabine-Vitamin E Conjugates: Synthesis, Characterization, Entrapment into Nanoemulsions, and in-Vitro Deamination and Antitumor Activity. *Int. J. Pharm.* **2017**, *528*, 463–470.

(180) Nagi, A.; Iqbal, B.; Kumar, S.; Sharma, S.; Ali, J.; Baboota, S. Quality by Design Based Silymarin Nanoemulsion for Enhancement of Oral Bioavailability. *J. Drug Deliv. Sci. Technol.* **2017**, *40*, 35–44.

(181) Liu, F.; Liu, D. Long-Circulating Emulsions (Oil-in-Water) as Carriers for Lipophilic Drugs. *Pharm. Res.* **1995**, *12*, 1060–1064.

(182) Wang, M.; Thanou, M. Targeting Nanoparticles to Cancer. *Pharmacol. Res.* **2010**, *62*, 90–99.

(183) Peer, D.; Karp, J. M.; Hong, S.; Farokhzad, O. C.; Margalit, R.; Langer, R. Nanocarriers as an Emerging Platform for Cancer Therapy. *Nat. Nanotechnol.* **2007**, *2*, 751–760.

(184) Torchilin, V. P. Multifunctional Nanocarriers. *Adv. Drug Deliv. Rev.* **2012**, *64*, 302–315.

(185) Durymanov, M.; Kamaletdinova, T.; Lehmann, S. E.; Reineke, J. Exploiting Passive Nanomedicine Accumulation at Sites of Enhanced Vascular Permeability for Non-Cancerous Applications. *J. Control. Release* **2017**, *261*, 10–22.

(186) Strebhardt, K.; Ullrich, A. Paul Ehrlich's Magic Bullet Concept : 100 Years of Progress. *Nat. Rev. cancer* **2008**, *8*, 473–480.

(187) Gianella, A.; Jarzyna, P. A.; Mani, V.; Ramachandran, S.; Calcagno, C.; Tang, J.; Kann, B.; Dijk, W. J. R.; Thijssen, V. L.; Griffioen, A. W.; *et al.* Multifunctional Nanoemulsion Platform for Imaging Guided Therapy Evaluated in Experimental Cancer. *ACS Nano* **2011**, *5*, 4422–4433.

(188) Hak, S.; Helgesen, E.; Hektoen, H. H.; Huuse, E. M.; Jarzyna, P. A.; Mulder, W. J. M.; Haraldseth, O.; Davies, C. D. L. The Effect of Nanoparticle Polyethylene Glycol Surface Density on Ligand-Directed Tumor Targeting Studied in Vivo by Dual Modality Imaging. *ACS Nano* **2012**, *6*, 5648–5658.

(189) Chen, T.; Gong, T.; Zhao, T.; Fu, Y.; Zhang, Z.; Gong, T. A Comparison Study between Lycobetaine-Loaded Nanoemulsion and Liposome Using NRGD as Therapeutic Adjuvant for Lung Cancer Therapy. *Eur. J. Pharm. Sci.* **2018**, *111*, 293–302.

(190) Tripathi, C. B.; Parashar, P.; Arya, M.; Singh, M.; Kanoujia, J. QbD-Based Development of α -Linolenic Acid Potentiated Nanoemulsion for Targeted Delivery of Doxorubicin in DMBA-Induced Mammary Gland Carcinoma : In Vitro and in Vivo Evaluation. *Drug Deliv. Transl. Res.* **2018**, *8*, 1313–1334.

(191) Patel, N. R.; Piroyan, A.; Ganta, S.; Morse, A. B.; Candiloro, K. M.; Solon, A. L.; Nack, A. H.; Galati, C. A.; Bora, C.; Maglaty, M. A.; *et al.* In Vitro and In Vivo Evaluation of a Novel Folate-Targeted Theranostic Nanoemulsion of Docetaxel for Imaging and Improved Anticancer Activity against Ovarian Cancers. *Cancer Biol. Ther.* **2018**, *19*, 554–564.

(192) Talekar, M.; Ganta, S.; Singh, A.; Amiji, M.; Kendall, J.; Denny, W. A.; Garg, S. Phosphatidylinositol 3-Kinase

Inhibitor (PIK75) Containing Surface Functionalized Nanoemulsion for Enhanced Drug Delivery, Cytotoxicity and pro-Apoptotic Activity in Ovarian Cancer Cells. *Pharm. Res.* **2012**, *29*, 2874–2886.

(193) Deshpande, D.; Kethireddy, S.; Gattacceca, F.; Amiji, M. Comparative Pharmacokinetics and Tissue Distribution Analysis of Systemically Administered 17-β-Estradiol and Its Metabolites in Vivo Delivered Using a Cationic Nanoemulsion or a Peptide-Modified Nanoemulsion System for Targeting Atherosclerosis. *J. Control. Release* **2014**, *180*, 117–124.

(194) Ganta, S.; Singh, A.; Patel, N. R.; Cacaccio, J.; Rawal, Y. H.; Davis, B. J.; Amiji, M. M.; Coleman, T. P. Development of EGFR-Targeted Nanoemulsion for Imaging and Novel Platinum Therapy of Ovarian Cancer. *Pharm. Res.* **2014**, *31*, 2490–2502.

(195) Ganta, S.; Singh, A.; Rawal, Y.; Cacaccio, J.; Patel, N. R.; Kulkarni, P.; Ferris, C. F.; Amiji, M. M.; Coleman, T. P. Formulation Development of a Novel Targeted Theranostic Nanoemulsion of Docetaxel to Overcome Multidrug Resistance in Ovarian Cancer. *Drug Deliv.* **2014**, *23*, 1–13.

(196) Ganta, S.; Singh, A.; Kulkarni, P.; Keeler, A. W.; Piroyan, A.; Sawant, R. R.; Patel, N. R.; Davis, B.; Ferris, C.; O'Neal, S.; *et al.* EGFR Targeted Theranostic Nanoemulsion for Image-Guided Ovarian Cancer Therapy. *Pharm. Res.* **2015**, *32*, 2753–2763.

(197) Afzal, S. M.; Shareef, M. Z.; Kishan, V. Transferrin Tagged Lipid Nanoemulsion of Docetaxel for Enhanced Tumor Targeting. *J. Drug Deliv. Sci. Technol.* **2016**, *36*, 175–182.

(198) Afzal, S. M.; Shareef, M. Z.; Dinesh, T.; Kishan, V. Folate-PEG-Decorated Docetaxel Lipid Nanoemulsion for Improved Antitumor Activity. *Nanomedicine* **2016**, *11*, 2171–2184.

(199) Patel, N. R.; Piroyan, A.; Nack, A. H.; Galati, C. A.; McHugh, M.; Orosz, S.; Keeler, A. W.; O'Neal, S.; Zamboni, W. C.; Davis, B.; *et al.* Design, Synthesis, and Characterization of Folate-Targeted Platinum-Loaded Theranostic Nanoemulsions for Therapy and Imaging of Ovarian Cancer. *Mol. Pharm.* **2016**, *13*, 1996–2009.

(200) Yao, V. J.; D'Angelo, S.; Butler, K. S.; Theron, C.; Smith, T. L.; Marchiò, S.; Gelovani, J. G.; Sidman, R. L.; Dobroff, A. S.; Brinker, C. J.; *et al.* Ligand-Targeted Theranostic Nanomedicines against Cancer. *J. Control. Release* **2016**, *240*, 267–286.

(201) Kunjachan, S.; Pola, R.; Gremse, F.; Theek, B.; Ehling, J.; Moeckel, D.; Hermanns-Sachweh, B.; Pechar, M.; Ulbrich, K.; Hennink, W. E.; *et al.* Passive versus Active Tumor Targeting Using RGD- and NGR-Modified Polymeric Nanomedicines. *Nano Lett.* **2014**, *14*, 972–981.

(202) Ruoslahti, E. Tumor Penetrating Peptides for Improved Drug Delivery. *Adv. Drug Deliv. Rev.* **2017**, *110–111*, 3–12.

(203) Sudimack, J.; Lee, R. J. Targeted Drug Delivery via the Folate Receptor. *Adv. Drug Deliv. Rev.* **2000**, *41*, 147–162.

(204) Qian, Z. M.; Li, H.; Sun, H.; Ho, K. Targeted Drug Delivery via the Transferrin Receptor-Mediated Endocytosis Pathway. *Pharmacol. Rev.* **2002**, *54*, 561–587.

(205) Walsh, G. Biopharmaceuticals, an Overview. In *Biopharmaceuticals, an Industrial Perspective*; Walsh, G.; Murphy, B., Eds.; Springer, Dordrecht: Dordrecht, 1999; Vol. 34, pp. 1–19.

(206) Mitragotri, S.; Burke, P. A.; Langer, R. Overcoming the Challenges in Administering Biopharmaceuticals: Formulation and Delivery Strategies. *Nat. Rev. Drug Discov.* **2014**, *13*, 655–672.

(207) Lundberg, B. B.; Griffiths, G.; Hansen, H. J. Conjugation of an Anti-B-Cell Lymphoma Monoclonal Antibody, LL2, to Long-Circulating Drug-Carrier Lipid Emulsions. *J. Pharm. Pharmacol.* **1999**, *51*, 1099–1105.

(208) Goldstein, D.; Nassar, T.; Lambert, G.; Kadouche, J.; Benita, S. The Design and Evaluation of a Novel Targeted Drug Delivery System Using Cationic Emulsion–Antibody Conjugates. *J. Control. Release* **2005**, *108*, 418–432.

(209) Goldstein, D.; Sader, O.; Benita, S. Influence of Oil Droplet Surface Charge on the Performance of Antibody-Emulsion Conjugates. *Biomed. Pharmacother.* **2007**, *61*, 97–103.

(210) Shi, R.; Hong, L.; Wu, D.; Ning, X.; Chen, Y.; Lin, T.; Fan, D.; Wu, K. Enhanced Immune Response to Gastric Cancer

Specific Antigen Peptide by Coencapsulation with CpG Oligodeoxynucleotides in Nanoemulsion. *Cancer Biol. Ther.* **2005**, *4*, 218–224.

(211) Sun, H.; Liu, K.; Liu, W.; Wang, W.; Guo, C.; Tang, B.; Gu, J.; Zhang, J.; Li, H.; Mao, X.; *et al.* Development and Characterization of a Novel Nanoemulsion Drug-Delivery System for Potential Application in Oral Delivery of Protein Drugs. *Int. J. Nanomedicine* **2012**, *7*, 5529–5543.

(212) Shah, L.; Kulkarni, P.; Ferris, C.; Amiji, M. M. Analgesic Efficacy and Safety of DALDA Peptide Analog Delivery to the Brain Using Oil-in-Water Nanoemulsion Formulation. *Pharm. Res.* **2014**, *31*, 2724–2734.

(213) Shah, L.; Gattacceca, F.; Amiji, M. M. CNS Delivery and Pharmacokinetic Evaluations of DALDA Analgesic Peptide Analog Administered in Nano-Sized Oil-in-Water Emulsion Formulation. *Pharm. Res.* **2014**, *31*, 1315–1324.

(214) Goldstein, D.; Gofrit, O.; Nyska, A.; Benita, S. Anti-HER2 Cationic Immunoemulsion as a Potential Targeted Drug Delivery System for the Treatment of Prostate Cancer. *Cancer Res.* **2007**, *67*, 269–275.

(215) Verissimo, L. M.; Agnez Lima, L. F.; Monte Egito, L. C.; De Oliveira, A. G.; Do Egito, E. S. T. Pharmaceutical Emulsions: A New Approach for Gene Therapy. *J. Drug Target.* **2010**, *18*, 333–342.

(216) Teixeira, H. F.; Bruxel, F.; Fraga, M.; Schuh, R. S.; Zorzi, G. K.; Matte, U.; Fattal, E. Cationic Nanoemulsions as Nucleic Acids Delivery Systems. *Int. J. Pharm.* **2017**, *534*, 356–367.

(217) Teixeira, H.; Dubernet, C.; Puisieux, F.; Benita, S.; Couvreur, P. Submicron Cationic Emulsions as a New Delivery System for Oligonucleotides. *Pharm. Res.* **1999**, *16*, 30–36.

(218) Hagigit, T.; Abdulrazik, M.; Valamanesh, F.; Behar-Cohen, F.; Benita, S. Ocular Antisense Oligonucleotide Delivery by Cationic Nanoemulsion for Improved Treatment of Ocular Neovascularization: An in-Vivo Study in Rats and Mice. *J. Control. Release* **2012**, *160*, 225–231.

(219) Brito, L. A.; Chan, M.; Shaw, C. A.; Hekele, A.; Carsillo, T.; Schaefer, M.; Archer, J.; Seubert, A.; Otten, G. R.; Beard, C. W.; *et al.* A Cationic Nanoemulsion for the Delivery of Next-Generation RNA Vaccines. *Mol. Ther.* **2014**, *22*, 2118–2129.

(220) Fraga, M.; Bruxel, F.; Diel, D.; de Carvalho, T. G.; Perez, C. A.; Magalhães-Paniago, R.; Malachias, Â.; Oliveira, M. C.; Matte, U.; Teixeira, H. F. PEGylated Cationic Nanoemulsions Can Efficiently Bind and Transfect PIDUA in a Mucopolysaccharidosis Type I Murine Model. *J. Control. Release* **2015**, *209*, 37–46.

(221) Yadav, S.; Gandham, S. K.; Panicucci, R.; Amiji, M. M. Intranasal Brain Delivery of Cationic Nanoemulsion-Encapsulated TNFα SiRNA in Prevention of Experimental Neuroinflammation. *Nanomedicine Nanotechnology, Biol. Med.* **2016**, *12*, 987–1002.

(222) Schuh, R. S.; Bidone, J.; Poletto, E.; Pinheiro, C. V.; Pasqualim, G.; de Carvalho, T. G.; Farinon, M.; da Silva Diel, D.; Xavier, R. M.; Baldo, G.; *et al.* Nasal Administration of Cationic Nanoemulsions as Nucleic Acids Delivery Systems Aiming at Mucopolysaccharidosis Type I Gene Therapy. *Pharm. Res.* **2018**, *35*, 221.

(223) Choi, B. Y.; Chung, J. W.; Park, J. H.; Kim, K. H.; Kim, Y.; Koh, Y. H.; Kwon, J. W.; Lee, K. H.; Choi, H. J.; Kim, T. W.; *et al.* Gene Delivery to the Rat Liver Using Cationic Lipid Emulsion/DNA Complex: Comparison between Intra-Arterial, Intraportal and Intravenous Administration. *Korean J. Radiol.* **2002**, *3*, 194–198.

(224) Liu, C. H.; Yu, S. Y. Cationic Nanoemulsions as Non-Viral Vectors for Plasmid DNA Delivery. *Colloids Surfaces B Biointerfaces* **2010**, *79*, 509–515.

(225) Bruxel, F.; Cojean, S.; Bochot, A.; Teixeira, H.; Bories, C.; Loiseau, P. M.; Fattal, E. Cationic Nanoemulsion as a Delivery System for Oligonucleotides Targeting Malarial Topoisomerase II. *Int. J. Pharm.* **2011**, *416*, 402–409.

(226) Bray, F.; Ferlay, J.; Soerjomataram, I.; Siegel, R. L.; Torre, L. A.; Jemal, A. Global Cancer Statistics 2018: GLOBOCAN Estimates of Incidence and Mortality Worldwide for 36 Cancers in 185 Countries. *CA. Cancer J. Clin.* **2018**, *68*, 394–424.

(227) IARC - International Agency for Research on Cancer. Global Cancer Observatory https://gco.iarc.fr/.

(228) Portney, N. G.; Ozkan, M. Nano-Oncology: Drug Delivery, Imaging, and Sensing. *Anal. Bioanal. Chem.* **2006**, *384*, 620–630.

(229) Shi, J.; Kantoff, P. W.; Wooster, R.; Farokhzad, O. C. Cancer Nanomedicine: Progress, Challenges and Opportunities. *Nat. Rev. Cancer* **2017**, *17*, 20–37.

(230) Mahato, R. Nanoemulsion as Targeted Drug Delivery System for Cancer Therapeutics. *J. Pharm. Sci. Pharmacol.* **2017**, *3*, 83–97.

(231) Yingchoncharoen, P.; Kalinowski, D. S.; Richardson, D. R. Lipid-Based Drug Delivery Systems in Cancer Therapy: What Is Available and What Is Yet to Come. *Pharmacol. Rev.* **2016**, *68*, 701–787.

(232) Öztürk-Atar, K.; Eroğlu, H.; Gürsoy, R. N.; Çaliş, S. Current Advances in Nanopharmaceuticals. *J. Nanosci. Nanotechnol.* **2019**, *19*, 3686–3705.

BACKGROUND, HYPOTHESIS AND OBJECTIVES

USC
UNIVERSIDADE
DE SANTIAGO
DE COMPOSTELA

Background

Despite the recognized role of nanotechnology in the development of advanced therapies, there is still much room for improvement[1,2]. The definition of the chapters of this work has been made taking into the following background:

Chapter 1 *"Application of an in vitro-in silico modeling approach for the development of sphingomyelin nanosystems for personalized medicine"*

In the era of personalized medicine there is a growing interest towards the development of versatile treatments that can accommodate several drugs depending on every patient needs. Nanosystems can represent a promising alternative towards this application considering its remarkable capability for the co-association of several drugs (small molecules as well as macromolecules)[3]. Nanosystems can be prepared using natural occurring lipids (such as sphingomyelin) and employing soft and mild methodologies that do not use high energies and high amounts or organic solvents.

A key requirement to design versatile nanosystems is an accurate understanding of the molecular properties associated with the carrier and the cargo. However, experimental biophysical techniques and principles correlating drug affinity towards a nanosystem and its composition are hard to elucidate. In silico methodologies such as molecular dynamics computational simulation can be useful tools to predict the affinity of certain drugs for a given nanocarrier at a molecular scale, thereby helping the rational design of versatile nanomedicines[4–6].

Chapter 2 "*Sphingomyelin-based nanosystems for cancer gene therapy*"

Nanostructures can be engineered using simple and scalable methodologies. Their appropriate composition and physicochemical properties such as size, shape, surface charge, stability, chemical composition, surface modification and toxicity are critical in order to assure their correct interactions with biological barriers and targeted cells/organs[7].

The national cancer institute (NCI, National Institute of Health) defines cancer as a term given to a collection of related diseases characterized by an accelerated and indiscriminate cell growth, with the capacity to spread through the blood and or the lymphatic system, invade surrounding organs and distal organs. The high incidence of cancer makes this disease one of the leading causes of death worldwide, highlighting the need to find more effective and powerful treatments[8,9]. In recent years, the development of biomolecular therapies aimed at interfering with specific processes related to tumor progression and metastasis has gained importance. Therapies based on miRNAs, key molecules in the regulation of cellular processes such as cell dissemination, tumorigenesis and chemoresistance, have gained enormous interest for the treatment of metastatic disease[10,11]. Nanotechnology allows the successful delivery of this type of biomolecules by avoiding their degradation in biological environments and facilitating their transport to the intracellular compartments of the target cells[12].

Chapter 3 "*Development of a nanocarrier based on a uroguanylin derivative for targeting metastatic colorectal cancer*"

Cancer remains the second leading cause of death worldwide and metastases are the responsible of 90% of the deaths[13]. Despite its clinical importance, very little have been achieved in this regard, rendering management of metastatic cancer cells an unmet clinical need[14].

Guanylyl Cyclase C receptor (GCC) is a receptor expressed at the apical membrane of enterocytes and also on primary and metastatic colorectal cancer cells[15]. Three natural ligands are known to activate GCC in an agonist manner, i.e. UroG, Uroguanylin; Gn Guanylin and ST, *Escherichia coli* Heat Stable Enterotoxin[16–19]. Exploiting the existence of biomarkers that are expressed on the surface of disseminated cells enables the preparation of decorated nanosystems to achieve recognition and specific tumor homing by means of active targeting[20]. Moreover, the development of a combinatory therapy can also provide additional advantages to treat cancer by enhancing efficacy compared to monotherapy approach since it could target key signaling pathways in a synergistic or additive manner.

REFERENCES

(1) Wagner, V.; Dullaart, A.; Bock, A. K.; Zweck, A. The Emerging Nanomedicine Landscape. *Nat. Biotechnol.* **2006**, *24*, 1211–1217.

(2) Farjadian, F.; Ghasemi, A.; Gohari, O.; Roointan, A.; Karimi, M.; Hamblin, M. R. Nanopharmaceuticals and Nanomedicines Currently on the Market: Challenges and Opportunities. *Nanomedicine* **2019**, *14*, 93–126.

(3) Farokhzad, O. C. Nanotechnology for Drug Delivery: The Perfect Partnership. *Expert Opin. Drug Deliv.* **2008**, *5*, 927–929.

(4) Glotzer, S. C.; Nordlander, P.; Fernandez, L. E. Theory, Simulation, and Computation in Nanoscience and Nanotechnology. *ACS Nano* **2017**, *11*, 6505–6506.

(5) Ding, H. M.; Tian, W. De; Ma, Y. Q. Designing Nanoparticle Translocation through Membranes by Computer Simulations. *ACS Nano* **2012**, *6*, 1230–1238.

(6) Huynh, L.; Neale, C.; Pomès, R.; Allen, C. Computational Approaches to the Rational Design of Nanosystems, Polymeric Micelles, and Dendrimers for Drug Delivery. *Nanomedicine Nanotechnology, Biol. Med.* **2012**, *8*, 20–36.

(7) Niu, Z.; Conejos-Sánchez, I.; Griffin, B. T.; O'Driscoll, C. M.; Alonso, M. J. Lipid-Based Nanocarriers for Oral Peptide Delivery. *Adv. Drug Deliv. Rev.* **2016**, *106*, 337–354.

(8) World Health Organisation. WHO | Cancer http://www.who.int/mediacentre/factsheets/fs297/en/ (accessed Apr 10, 2018).

(9) Siegel, R. L.; Miller, K. D.; Jemal, A. Cancer Statistics, 2019. *CA. Cancer J. Clin.* **2019**, *69*, 7–34.

(10) Chen, Z.; Zeng, H.; Guo, Y.; Liu, P.; Pan, H.; Deng, A.; Hu, J. MiRNA-145 Inhibits Non-Small Cell Lung Cancer Cell Proliferation by Targeting c-Myc. *J. Exp. Clin. Cancer Res.* **2010**, *29*, 151.

(11) Ibrahim, A. F.; Weirauch, U.; Thomas, M.; Grunweller, A.; Hartmann, R. K.; Aigner, A. MicroRNA Replacement Therapy for MiR-145 and MiR-33a Is Efficacious in a Model of Colon Carcinoma. *Cancer Res.* **2011**, *71*, 5214–5224.

(12) Wang, K.; Kievit, F. M.; Zhang, M. Nanoparticles for Cancer Gene Therapy: Recent Advances, Challenges, and Strategies. *Pharmacol. Res.* **2016**, *114*, 56–66.

(13) Mehlen, P.; Puisieux, A. Metastasis: A Question of Life or Death. *Nat. Rev. Cancer* **2006**, *6*, 449–458.

(14) Vázquez-Ríos, A. J.; Alonso-Nocelo, M.; Bouzo, B. L.; Ruiz-Bañobre, J.; de la Fuente, M. Nanotheranostics and Their Potential in the Management of Metastatic Cancer. In *Handbook of Nanomaterials for Cancer Theranostics*; Conde, J., Ed.; Elsevier: USA, 2018; pp. 199–244.

(15) Buc, E.; Der Vartanian, M.; Darcha, C.; Déchelotte, P.; Pezet, D. Guanylyl Cyclase C as a Reliable Immunohistochemical Marker and Its Ligand Escherichia Coli Heat-Stable Enterotoxin as a Potential Protein-Delivering Vehicle for Colorectal Cancer Cells. *Eur. J. Cancer* **2005**, *41*, 1618–1627.

(16) Potter, L. R. Regulation and Therapeutic Targeting of Peptide-Activated Receptor Guanylyl Cyclases. *Pharmacol. Ther.* **2011**, *130*, 71–82.

(17) Forte, L. R. Uroguanylin and Guanylin Peptides: Pharmacology and Experimental Therapeutics. *Pharmacol. Ther.* **2004**, *104*, 137–162.

(18) Pitari, G. M.; Li, P.; Lin, J. E.; Zuzga, D.; Gibbons, A. V.; Snook, A. E.; Schulz, S.; Waldman, S. A. The Paracrine Hormone Hypothesis of Colorectal Cancer. *Clin. Pharmacol. Ther.* **2007**, *82*, 441–447.

(19) Camici, M. Guanylin Peptides and Colorectal Cancer (CRC). *Biomed. Pharmacother.* **2008**, *62*, 70–76.

(20) Torchilin, V. P. Passive and Active Drug Targeting: Drug Delivery to Tumors as an Example. In *Tissue Engineering: Principles and Practices*; Fisher, J. P.; Mikos, A. G.; Bronzino, J. D.; Peterson, D. R., Eds.; CRC Press, 2010; pp. 3–53.

Hypothesis

The main hypothesis (H) of this thesis is that it is possible to design and develop novel types of nanosystems that can be exploited as targeted delivery of anticancer therapies using biodegradable materials with a well-known safety record and simple and scalable manufacturing process. This main hypothesis can be divided as following:

H1. It is possible to design nanostructures based on natural occurring components such as sphingomyelin, a lipid present in cell membranes, which are simple in composition, safe-by-design, easy to prepare, biocompatible and biodegradable.

H2. It is possible to use *in silico* strategies to facilitate the rational design of drug delivery nanocarriers. Computational simulation studies can be of high utility as predictive tools to determine if a specific drug would be successfully associated to a given nanosystem with a particular composition.

H3. Neutral nanosystems based on natural occurring components such as sphingomyelin can also be of utility for the development of RNA-based therapies. Nucleic acids can be modified with cholesterol to improve stability in biological fluids and increase their association to lipidic nanocarriers.

H4. Nanosystems composted by natural occurring lipids such as sphingomyelin can be loaded with therapeutic peptides, upon modification of these biomolecules with a amphiphilic PEGylated aliphatic (C_{18}) chain. Since peptides will be exposed onto the surface of the

nanosystems, they can also meditate an interaction with specific cell surface receptors characteristic of cancer cells.

H5. It is possible to developed combinatory therapies upon co-association of biomolecules and anticancer drugs within the same type of nanostructure.

Objectives

Based on the background and hypothesis outlined, the main goal of this work has been the development of versatile biodegradable nanosystems for the targeted delivery of improved anticancer treatments. This broad objective (O), could be divided in the following objectives:

O1. *In silico/In vitro* approach for the development of sphingomyelin nanosystems (SNs) and evaluation of their potential as anticancer therapies

- Development and characterization of nanosystems composed by sphingomyelin in combination with vitamin E.
- Development of an in silico methodology by Molecular Dynamics (MD) Simulation to determine the supramolecular properties of SNs and their capacity to associate drugs and macromolecules.

Results corresponding to this objective are presented in Chapter 1 *"Application of an in vitro-in silico modeling approach for the development of sphingomyelin nanosystems for personalized medicine"*

O2. Evaluation of the potential of sphingomyelin nanosystems for oligonucleotide delivery

- Evaluation of the toxicological properties of neutral SNs and their potential in for the development of anticancer gene therapies
- Evaluation of the ability of SNs to associate oligonucleotides and their capacity to deliver them to the target cancer cells.

Results corresponding to this objective are presented in Chapter 2 "*Sphingomyelin-based nanosystems for cancer gene therapy*"

O3. Development of targeted nanotherapeutics based on uroguanylin hormone combined with cytostatic drug etoposide as strategy to metastatic colorectal cancer treatment

- Preparation of a derivative of Uroguanylin (UroG), a natural ligand of the Guanylyl Cyclase C (GCC), to mediate its association to SNs as a targeted delivery nanocarrier against metastatic colorectal cancer.
- Assessment of the potential of the targeted SNs for the development of a combinatorial therapy with a conventional cytostatic drug to treat metastatic colorectal cancer.

Results corresponding to this objective are presented in Chapter 3 "*Development of a nanotherapy based on a uroguanylin derivative for targeting metastatic colorectal cancer*"

CHAPTER 1

Application of an in *vitro/in silico* modelling approach for the development of sphingomyelin nanosystems for personalized medicine

USC
UNIVERSIDADE
DE SANTIAGO
DE COMPOSTELA

ABSTRACT

Personalized medicine requires the development of versatile nanocarriers for different types of drugs, depending on every patient's need. Nanotechnology platforms for drug delivery are typically complex, composed of a plethora of materials and engineered following different methodologies. We present here a new type of nanocarrier prepared by emulsification of vitamin E (V) using sphingomyelin (SM) for stabilization. Nanosystems (SNs) were characterized in the present work using a number of computational and physicochemical methods. It is shown that, regardless the amount of SM, the nanostructure is compartmentalized, with a water pocket enclosed by a V membrane-like structure. The interaction of a battery of heterogeneous drugs with the proposed nanosystem was studied, aiming to determine their versatility of the nanocarrier to associate different molecules. The average diameter of the nanosystem is approximately 100 nm with a low polydispersity index and an almost neutral surface charge. Additionally, they presented colloidally stable over short and long time periods and in biologically relevant media. Overall, our results suggest that SNs nanosystems are promising carriers for personalized medicine, and particularly interesting for anticancer therapies. The biocompatibility of the employed molecules and the simple preparation of the nanocarriers are clear advantages of the proposed platform. Additionally, our synergistic *in silico*/*in vitro* approach based on laboratory experiments combined with multiscale Molecular Dynamics simulations showed the predictive power of computational simulations for the structural characterization of nanosystems as well as for the description of internal interaction mechanisms.

USC
UNIVERSIDADE
DE SANTIAGO
DE COMPOSTELA

1. INTRODUCTION

For the treatment of diseases, and in line with the personalized medicine concept, which mainly applies in cancer but also in many other scenarios, there is a growing interest towards the development of versatile nanocarriers that can accommodate more than one type of drug depending on every patient's needs[1,2]. This includes not only conventional low molecular weight drugs but also biotechnological drugs such as gene therapies, antitumor peptides and mononuclear antibodies[3–5]. Drug delivery systems could offer several advantages by improving the access of drugs to the tumor, decreasing secondary effects related to toxicity and offering additional potential for the successful delivery of labile biotechnological drugs[6–8].

The development of effective drug delivery systems is considered one of the major milestones nowadays. In disease states, such as cancer, the delivery of a drug can be as important as the drug itself. Since the first cancer nanoformulation approval in 1995 (Doxil®), many others have made this way into clinics[9]. However, the number of nanomedicines in the market is still limited in comparison to the experimental growth that the nanomedicine field has experimented over the last decades[10,11]. From a translational perspective, we believe it is very important to develop nanocarriers that are simple in composition, easily adapted to industrial requirements, stable, and highly versatile, so that they can be useful for the association of different payloads increasing their therapeutic potential[12].

On the other hand, drug association to nanosystems has been extensively studied and is by far, the most advanced area on nanomedicine application. This rely on the ability of nanosystems to associate several drugs and modify their properties such as solubility, release profiles, diffusivity, bioavailability and even immunogenicity[13]. However, this evaluation has been mainly carried out at experimental level by trial and error procedures. In this regard, a variety of computational methods can be employed to predict small molecules physicochemical

properties including lipophilicity and interaction patterns with formulated nanomaterials[15]. Among them, molecular simulations are the most suitable techniques for a greater comprehension of the relationship between the structure of the nanosystems and the association mechanisms with the drugs, which will ultimately enable the rational design of new drug delivery materials. Without the ability to understand dynamic structural changes the design and creation of new nanosystems must rely on empirical rule-based approaches as well as a fair degree of serendipity. Obtaining high resolution (temporal and spatial) information about dynamic processes, absent or incomplete in analytical models, is extremely challenging and it is still unattainable by most experimental techniques known today. In this regard, molecular modelling techniques, mainly Molecular Dynamics (MD) simulations, may provide the necessary bridges to shed light into the structural and dynamical properties of nanosystems and its interaction with different drugs at atomistic or molecular levels detail[14–17], affording a potential fast pre-screening tool during nanosystems development. Recent advances in biomolecular simulation have allowed to study the fusion of complete vesicles[18,19]. In the last years it has been shown that using simulation studies with simplified models, under appropriate conditions, and from disordered solutions, small spontaneous vesicles can be formed[20–23]. In addition, it has been proven that MD simulations allow real-time observation of spontaneous assembly of lipids into vesicles at molecular level and even at the atomistic level[23–26]. Generally, a realistic representation of a nanosystem comprises millions of atoms including explicit solvent. Atomistic resolution simulations (AT) may not be feasible due to the limitation of computer resources. To overcome computational limitations, molecular simulations using Coarse-grained (CG) resolution can be applied[27]. These simulations, where groups of several atoms are represented by single particles, allow increasing the system size and the total simulation timescales by 2-3 orders of magnitude due to the largely reduced number of explicit

particles considered to the consequent reduction of the number of degrees of freedom and the smoothening of the energy landscape[28]. This allows significantly increasing the time step employed for the integration of the equation of motion. Thus, the spontaneous formation of large vesicles, the equilibrium or molecular exchange between different supramolecular structures or the assembly of large macromolecules can be studied at this resolution level. The loss of resolution associated to CG simulations entails a loss of information and, in some cases, artefacts that could lead to misinterpretations of the real molecular system behavior. A good solution for this is performing multiscale simulations taking advantage of the best features of each simulation level, i.e. CG simulations would be done for relatively large scale self-assembly studies, and AT simulations would be then done to go into details at atomic level. At this regard, we have recently developed a new method to switch between different representations of systems consisting of discrete and flexible objects, that has been validated by recovering AT representations of a number of molecular systems, starting from CG level representations[29]. Bearing this in mind, we decided to develop a new type of nanosystems based on only two components, vitamin E (V), an antioxidant and a widely used GRAS-listed excipient with a well-known safety record[30] and sphingomyelin (SM), a major component of cell membranes that has already been used in the preparation and commercialization of nanoformulations (Marqibo®)[31]. We proposed the preparation of Sphingomyelin Nanosystems (SNs) by adapting the ethanol injection methodology in order to obtain them in a simple way without needing additional organic solvents and/or co-surfactants. Following a translational approach, and bearing in mind that experimental determination of drug loading on a one-to-one bases became costly and time-consuming[32] we decided to follow a synergistic *in vitro-in silico* modelling approach for the development of predictive tools that can speed-up the process and suppose a shift paradigm for the rational design of nanotechnologies as drug delivery systems.

2. MATERIALS AND METHODS

2.1. Chemicals

Vitamin E (V, DL-α-Tocopherol) was purchased from Calbiochem (Merck-Millipore, Darmstadt, Germany). Sphingomyelin (SM, Lipoid E SM) was kindly provided by Lipoid GmbH (Ludwigshafen, Germany). Curcumin was acquired from Acros Organics (Madrid, Spain). Gemcitabine and Resveratrol were obtained from Sigma Aldrich (Madrid, Spain). Hydrophilic peptide LDFI (LAPI) (635 Da) and its hydrophobized derivative LDFIK-PEG_6-C_{18} (LAPIK) were obtained from China Peptides Co., Ltd (Shanghai, China). Double stranded miRNA (21bp; 5' UUC UCC GAA CGU GUC ACG UUU 3') was obtained from Eurofins MWG Operon (Ebersberg, Germany). HPLC-grade Acetonitrile (ACN), Ethanol (EtOH), Isopropanol (IPA) and Water were obtained from Fisher Chemicals (Thermo Fisher Scientific, USA). Trifluoroacetic acid (TFA) was provided by Sigma-Aldrich (Madrid, Spain). Triethylamine (TEA) was purchased from (Panreac Applichem S.A.U., Barcelona, Spain).

2.2. Preparation of SNs, physicochemical characterization, and morphological examination.

SNs were prepared by conveniently adapting the ethanol injection method[33–35]. Briefly, vitamin E (V) and sphingomyelin (SM) were dissolved in ethanol at a concentration of 200 mg/mL and 100 mg/mL respectively. Next, volumes of both solutions were subsequently mixed to obtain different mass ratios of both components (V:SM 1:1 to 1:0.05), taking as constant the amount of vitamin E (10mg, 5mg, or 2.5 mg). The resulting volume was completed up to 100µl with ethanol and the total mixture injected to 1mL of ultrapure water under continuous magnetic stirring (<10% of ethanol in the final suspension medium).

Particle size and polydispersity index (PdI) of the nanoemulsions were determined by dynamic light scattering (DLS) after a dilution 1:20 in water. Surface charge (Z-potential, ZP) values were obtained by Laser Doppler Anemometry (LDA) (Zetasizer NanoZS®, Malvern Instruments, Worcestershire, United Kingdom). Additionally, extended nanoemulsion characterization was performed by Nanoparticle Tracking Analysis (NTA) after particle dilution 1:1000 in water (NanoSight LM20, Amesbury, United Kingdom). Data collection was settled with 3 repeats/60s capture time and both shutter and gain were manually determined for each sample. NTA 2.0 Build 127 software was used for measurement and subsequent data analysis.

Morphological examination was performed by both Transmission Electron Microscopy (TEM) and Cryogenic Transmission Electron Microscopy (CryoTEM). TEM images were obtained using a JEOL JEM-2010 High-Resolution Microscope (Peabody, MA, USA) operating between 120 and 200 kV accelerating voltage and configured with a high brightness LaB_6 filament. Preparation of TEM samples were performed as follows, 10µL of 10-20 times diluted nanoemulsion suspension were placed in a copper grid and stained with 2% (w/v) phosphotungstic acid for 1 minute, washed with 0.2mL of water and dried overnight under vacuum. CryoTEM samples were initially vitrified according to the method developed by Dubochet and collaborators[36]. Briefly, 3.5µL aliquots of the different samples were applied to glow-discharged holey grids for 1 min, blotted, and frozen rapidly in liquid ethane at −180 °C and kept at this temperature throughout the whole procedure. Images were obtained at 0°-tilt under minimum dose conditions using a field emission gun Tecnai 20 G2 Microscope (FEI, Eindhoven, The Netherlands) equipped with a Gatan cold stage operated at 200 keV. Images were taken at a magnification of 50,000X by using a FEI Eagle CCD camera with a step size of 15µm; thus, the original pixel size of the acquired images was 2.74Å.

2.3. Stability

Colloidal stability was assessed in various conditions, i.e. short-term stability, accelerated long-term stability and stability in relevant biological medium. Short-term stability was performed for early determination of immediate instability behavior. Particle size, PdI and surface charge were measured at time 0, 4 and after 24h. Colloidal stability was also determined in relevant biological medium, i.e. human plasma and supplemented cell culture medium. Briefly, SNs were diluted 1/10 v/v with the correspondent medium for incubation reaching a final concentration of 1mg/mL. Nanosystems then were incubated at 37ºC under constant horizontal shaking for up to 24h. For measuring purposes, the previous mixture was further diluted 1/10 in water and analyzed by DLS. Lastly accelerated long-term storage stability studies were performed according to the International Council for Harmonization (ICH) guidelines (at 40ºC ± 2ºC, 75% RH ± 5% RH for storage in general case and at 25ºC ± 2ºC, 60% RH ± 5% RH for storage in a refrigerator)[37].

2.4. Drug association and encapsulation efficiency

Therapeutically active molecules with different nature, physicochemical characteristics, and mechanisms of action, were selected for association to SNs, as shown in **Table 1**. Theoretical loading was fixed in all cases at 0.5% w/w (weight of the active molecule with respect to the total weight of the components). The hydrophobic drugs, curcumin and resveratrol, were incorporated directly to the oily phase from ethanol stock solutions at concentrations of 1mg/mL and 10mg/mL respectively (based on their different solubilities in ethanol). The hydrophilic drug gemcitabine was incorporated directly into the aqueous phase. In the case of the amphiphilic molecule LAPIK, preliminary tests were carried out to find the optimum solubilization conditions. Firstly, a dissolution in 10/90 v/v water:ethanol mixture containing

the SM was chosen. Subsequently the correspondent proportion of Vitamin E was added obtaining a limited water proportion of <10%. In order to compare, the unmodified LAPI peptide was included following the same procedure, as well as the double stranded RNA (dsRNA).

Table 1. Description of the active therapeutic molecules (small and biotechnological drugs) to be associated to SNs.

	Gemcitabine	**Resveratrol**	**Curcumin**	**dsRNA**	**LAPI**	**LAPIK**
Water Solubility	Hydrophilic	Hydrophobic		Hydrophilic		Amphiphilic
LogP	-1.5	3.1	3.2	N/A	N/A	N/A
Mass unit	263.201g/mol	228.2 g/mol	368.4 g/mol	21 bp	507 Da	1153 Da
IP	N/A	N/A	N/A	≈ 5	3.81	6.25

LAPI: peptide with the following aminoacidic sequence LDFI; LAPIK: LAPI-derivative LDFIK-PEG$_6$-C$_{18}$; LogP: Partition coefficient; g/mol: grams per mole; bp: base pair; Da: Dalton; IP: Isoelectric Point; N/A: not applicable

Analytic methodologies were optimized for each particular drug. HPLC methods were applied for analysis of gemcitabine, resveratrol, LAPI, LAPIK and dsRNA (LaChrom Elite®, VWR-Hitachi, Barcelona, Spain) as disclosed in **Table S1** (supplementary information). In the case of curcumin, quantification was done by fluorescence spectroscopy. Lamp was settled at λex 420 and the detector at λem 525 (EnVision® Multilabel Plate Reader, Perkin Elmer, Massachusetts, MA, USA). Encapsulation efficiencies (EE%) for the six selected molecules were experimentally determined after separation of the drug loaded into SNs from the free drug present in the suspension media. Conditions were adapted according to each formulation.

Briefly, SNs loaded with gemcitabine, LAPI, LAPIK or dsRNA, were separated by ultracentrifugation (84035 RCF, 1h, 15ºC, OptimaTM L-90K Ultracentrifuge, Beckman Coulter; Fullerton, CA) and then resuspended in water to a final volume of 0.25mL for subsequent quantification. In the case of SNs loaded with curcumin or resveratrol, to avoid aggregation, isolation was done by conventional centrifugation (20000 RCF, 1h, 15ºC, Eppendorf 5430R, Germany), after addition of the loaded SNs on top of a 20% w/v sucrose solution. Encapsulation values were referred in all cases to a pre-determination of the total amount of drug present in the suspension of non-isolated SNs (100% of the drug added) following the described analytical methodologies, for a more accurate determination. Then, the amount of drug encapsulated, as well as the free fraction, were quantified, and encapsulation efficiencies in percentage (EE%) was determined according to **Equation 1A** (direct measurement of the encapsulated fraction) and **Equation 1B** (indirect measurement of the free fraction).

A) B)

$$Direct\ EE\% = \frac{Associated\ \mu g}{Total\ \mu g} \qquad Indirect\ EE\% = \frac{Total\ \mu g\ - Free\ \mu g}{Total\ \mu g}$$

Equation 1: Direct (A) and indirect (B) formula for the determination of encapsulation efficiencies (EE) in percentage (%) with respect to the total amount of drug that was determine in the nanosystems suspension.

2.5 Cellular internalization of fluorescent nanosystems

Nile Red, a hydrophobic dye (λex 552 nm, λem 636 nm) that links specifically to the phospholipids and triglycerides was associated to the nanosystems in order to obtain fluorescent particles. Briefly, to achieve a loading of 0.1% of the dye 5.5µg of Nile Red was added to 100µL of the organic phase and nanoemulsions were produced and characterized as previously described. The release of the fluorescent molecule from the nanosystems was assessed by

incubation in cell culture medium (2h at 37ºC) and during storage (4 days 4ºC). After the estimated period of incubation, nanosystems were isolated by ultracentrifugation and then diluted in methanol to determine the encapsulation efficiency by fluorescence spectroscopy (EnVision® Multilabel Plate Reader, Perkin Elmer, Massachusetts, MA, USA).

Fluorescent nanoemulsions uptake was tested in immortalized cancer cells lines (SW480, MiaPaCa-2, and PC3 cancer cells). Nanosystem uptake by the three cell lines was evaluated using confocal microscopy (Leica SP5, Germany). Cells were seeded on a glass coverslip in a 24-well plate and incubated with 100ng of Nile Red per well (0.1mg of nanoemulsion). After two washes with PBS, cell nuclei were stained with DAPI dye (1mg/mL in PBS) by adding 0.5 mL to each well during 5 minutes. Then, cells were washed three times and, finally, the coverslips containing the attached cells were mounted over the slides in presence of paraformaldehyde (4% w/v, Sigma Aldrich).

2.6. NMR analysis

SNs prepared at a w/w ratios 1:0.1 and 1:0.5 were diluted to a final volume of 300µL consisting on H_2O:D_2O 90:10. Each sample was transferred to a Varian style *Shigemi* NMR tube (*Shigemi inc.*) for the analysis. NMR spectra were acquired on a Varian Inova 750 MHz equipped with an inverse HCP probe and triax PFG gradients. The only exception is the ^{13}C NMR spectra that were measured on a Varian Mercury 300 MHz spectrometer. The spectra were measured at a temperature of 25°C, and the chemical shifts reported are referenced to the lock deuterium solvent. Spectra were processed and analysed with Mestrenova software v11.0 (*Mestrelab. inc.*). Non-linear fits to determine diffusion coefficients were carried out with Origin 8.0 software (*Originlab inc.*).

1D ^{13}C-NMR spectrum was acquired with 12000 (6 hours) and 20000 (10 hours) scans for samples SNs 1:0.1 and SNs 1:0.5, respectively.

1D ^{1}H-watergate quantitative spectra (1D ^{1}Hwg) were measured for each sample with strong suppression of the water peak with the Perfect-Echo watergate sequence[38]. The spectra were measured with quantitative conditions with an inter-scan delay d_1 of 10s and 128 scans. Residual signals of ethanol in these samples were attenuated by applying 1.5s of signal presaturation over the center frequency of the two resonances of ethanol during the d_1 period.

1D ^{1}H quantitative NMR spectra (1D ^{1}H) were acquired with the standard one pulse sequence and using a low angle excitation pulse to detect the intense signal of H_2O. The tilt angle of the pulse was 0.1º, the inter-scan delay d_1 was 4 s and the number of scans was 4. The receiver gain was reduced close to the minimum to avoid the saturation of the receiver by the strong water signal of the samples studied.

A DOSY spectrum was measured with the BPP-STE-LED scheme sequence[39] incorporating a watergate scheme for the strong suppression of the water peak. The diffusion delay Δ was 0.5s, the bipolar gradient pulses (δ) used to encode/decode diffusion have a total duration of 5ms. Their power was varied linearly between 2.5 and 50.3 G/cm to detect 32 points in the diffusion dimension with 16 scans per point. The intensities were non-linearly fitted to the Stejskal-Tanner equation governing the experiment to determine the self-diffusion coefficient (*D*). The hydrodynamic radius (r_H) was calculated from the self-diffusion coefficient using the SEGWE model[40].

2.7. Molecular Dynamics simulations

2.7.1. CG/AT structures and parameters

The CG simulations were performed with the standard simulation parameters associated with the MARTINI force-field[41,42]. The atomistic structures of curcumin, resveratrol and gemcitabine were obtained from PubChem database[43]. LAPI structure was generated with Avogadro[44] and joined to the non-protein segment in LAPIK, generated with the ChemOffice software. Vitamin E and sphingomyelin AT-structures were also generated with ChemOffice. The RNA was generated with the Make-na Server[45], using the sequences 5' UUC UCC GAA CGU GUC ACG UUU 3' and 3' AAG AGG CTT GCA CTG TGC AAA 5´. The mapping to CG was carried out with Auto_MARTINI in the case of gemcitabine[46]. For LAPI and RNA we used the script *martinize.py.*[47]. For LAPIK, the protein part was combined with the PEG parameters obtained from Panizon et al.[48] and those for the hydrophobic chain obtained from Auto_MARTINI[46]. They were merged using the script *molmaker.py*[49]. The CG structure and parameters for curcumin and resveratrol were directly taken from Ingolfsson et al.[50]. CG parameters for vitamin E (V) were generated from known fragments, following MARTINI combination rules. For sphingomyelin (SM) we took the parameters for C(18:1/18:0)[28,41,51] deleting one of the beads to make it more similar to the one used experimentally [C(18:0/16:0)]. The CG systems were mapped back to AT resolution using GADDLE Maps, a novel algorithm implemented recently in our group[29]. After the re-solvation with pre-equilibrated water, AT-simulations were carried out using different force fields, depending on the system: GROMOS54a7_atb[52] for all the mapped systems except for those participating in the simulation with RNA, which were mapped to AMBER99SB[53].

2.7.2. Preparation of the initial simulation boxes: the computational experiment

A high local concentration of the V:SM mixture was set in order to favor the spontaneous formation of SNs. The following computational protocol was employed (**Figure S1**): (i) 1000 V molecules and 67 SM molecules were randomly distributed in a (11x11x11 nm^3) cubic box; (ii) the drug (6 curcumin, 10 resveratrol, 1 RNA, 6 LAPI or 6 LAPIK) was added to the mixture; (iii) the resulting mixture was centered in a truncated octahedron shaped box with the walls at a minimum distance of 3.5 nm; (iv) the system was then solvated using 104 MARTINI water molecules. The simulations using gemcitabine were prepared in a slightly different way: instead of step (ii), 9 molecules of this drug were added directly to the truncated octahedron box, just before solvation. So, gemcitabine molecules were introduced in the water rich region, in contrast to the other drugs that were introduced in region were the concentration of V and SM is larger. In any case, the number of drug molecules introduced in the simulation box was based on the proportion of drug employed experimentally.

2.7.3. CG and AT simulation conditions

All the systems were minimized and simulated for 500ns, except RNA, which was simulated for 250ns. Five replications were made for each drug and two replicates without any drug. In order to keep the double-helix shape of the RNA elastic network restraints (ElNeDyn) were applied[54]. All CG calculations were carried out at a temperature of 300K, using the Berendsen thermostat with isotropic pressure coupling[55]. AT simulations were carried out at 300K using the V-rescale thermostat. Besides, Berendsen thermostat with isotropic pressure coupling was used to control pressure[55]. All simulations were done using GROMACS 5.1.2.[56].

3. RESULTS AND DISCUSSION

3.1 Preparation and characterization of SNs

SNs composed by vitamin E and sphingomyelin were prepared by adapting the ethanol injection method, a low-energy manufacturing technique traditionally used for the preparation of liposomes, consisting in adding a constant volume of an ethanol solution that contain the lipids onto a fixed volume of water. In our case, after some preliminary experiments, the amount of ethanol was kept below 10% in the final nanosystem suspension (100μL of the ethanol mixture were added onto 1mL of water (1:10 v/v) for the preparation of SNs), a percentage that, according to the pharmacopeia, is accepted to parenteral administration[57].

Initial experiments were addressed to determine the optimal formulation components concentration (the amount of vitamin E was varied from 2 to 10 mg) and composition (V:SM mass ratios from 1:0.05 to 1:1) in order to obtain SNs with optimal characteristics for targeting tumors. Ideally, a mean size below 100nm and a neutral surface charge is desired, which will improve penetration into the tumors and association of different anticancer drugs[58].

Physicochemical characterization of SNs was initially performed by DLS (Dynamic Light Scattering) and LDA (Laser Droplet Anemometry), methods of reference in nanocharacterization[59–62] (**Table 2**). Results indicate that almost all developed formulations presented a particle size under 200nm with the exception of the ones of 10mg vitamin E with the ratio V:SM 1:1, 1:0.5 and 1:0.2. In all cases, SNs exhibit monodisperse populations (polydispersity index ≤0,3), with neutral or slightly negative surface charges. According to this results, we have selected for the next set of experiments SNs prepared with an intermediate concentration of V comprising two different amounts of SM (V:SM 1:0.1 and 1:0.5) for further studies.

Table 2. Nanoemulsion physicochemical characterization by Dynamic Light Scattering (DLS) and Laser Doppler Anemometry (LDA).

	Total amount of Vitamin E (mg)								
	2			**5**			**10**		
Mass Ratio (V:SM)	**Size (nm)**	**PdI**	**ZP (mV)**	**Size (nm)**	**PdI**	**ZP (mV)**	**Size (nm)**	**PdI**	**ZP (mV)**
1:1	119 ± 20	0.3	0 ± 1	187 ± 16	0.2	-2 ± 3	Aggregated		
1:0.5	72 ±12	0.3	-1 ± 2	101 ± 10	0.2	-3 ± 2	254 ± 33	0.3	-9 ± 0
1:0.2	58 ± 18	0.2	-2 ± 0	123 ± 14	0.2	-4 ± 4	239 ± 18	0.2	-4 ± 0
1:0.1	63 ± 7	0.1	-5 ± 2	85 ± 7	0.1	-3 ± 1	169 ± 5	0.2	-1 ± 0
1:0.05	64 ± 7	0.2	-4 ± 1	97 ± 6	0.2	-2 ± 0	162 ± 2	0.2	-3 ± 2

V: Vitamin E; SM: Sphingomyelin; nm: nanometer; PdI: Polydispersity index; ZP: surface charge; mV: millivolts. Total volume of the nanoparticle suspension: 1 mL Ethanol to water ratio: 1:10 v/v . Results presented in mean ± SD, n=3. Size refers to diameter.

Physicochemical characterization was complemented by NTA measurements. While DLS determine particle size from fluctuations in scattered light intensity due to the Brownian movement of the particles, NTA allow identifying and tracking individual nanoparticles moving under Brownian motion, relating this movement to a particle size and a calculation of a precise particle concentration[60,63]. Data acquired by NTA (**Table 3, Figure S1**), are consistent with DLS results, on view of the reported average size, D-values (D_{10}, D_{50}, and D_{90}, are indicative of the particle diameter at 10 %, 50 %, and 90 % cumulative distribution[64]), and the resulting SPAN value, ≤ 1 (indicative of a homogeneous sample).

Table 3. Physicochemical characterization of SNs 1:0.1 and 1:0.5 by Nanoparticle Tracking Analysis (NTA) showing mean particle size, D-values (D_{10}, D_{50}, D_{90}), calculated SPAN value and sample concentration in particles per milliliter (particle/mL) *(mean ± SD, n=3)*. Size refers to diameter.

Ratio (V:SM)	Size (nm)	D_{10}	D_{50}	D_{90}	SPAN	Concentration (particles/mL)
1:0.1	98 ± 1	89 ± 0	116 ± 2	191 ± 10	0.88	9.85×10^8
1:0.5	82 ± 2	71 ± 0	92 ± 1	130 ± 3	0.64	1.12×10^9

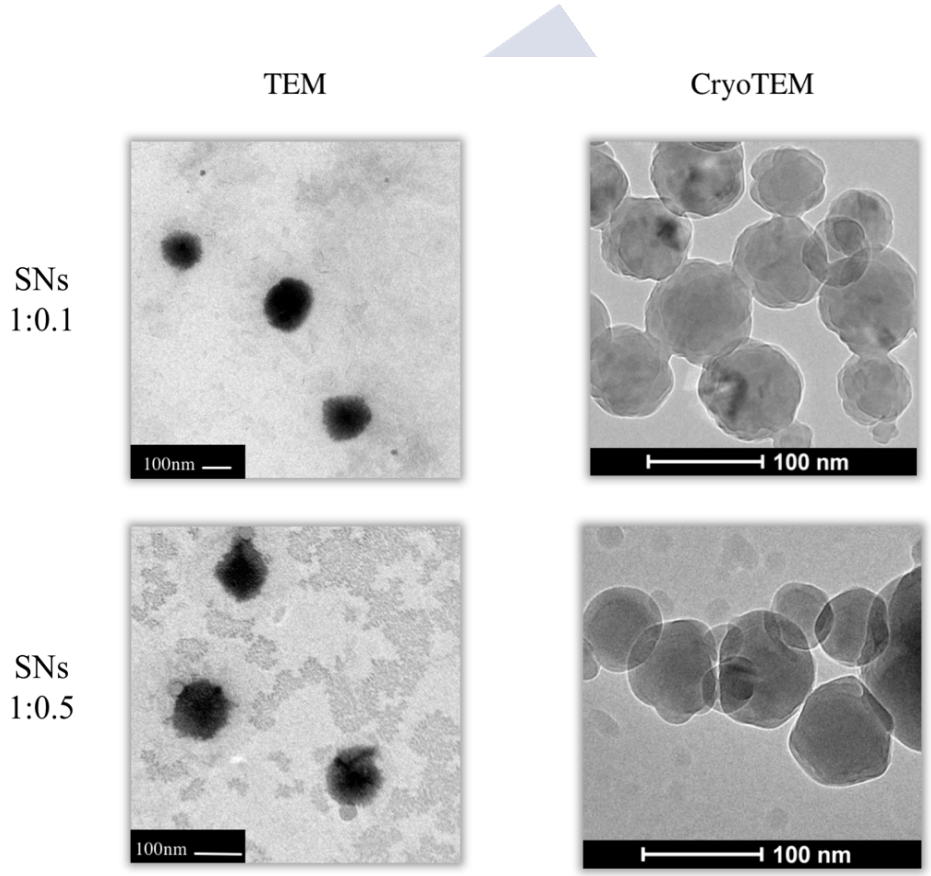

Figure 1. Transmission Electron Microscopy (TEM) and Cryogenic Transmission Electron Microscopy (CryoTEM) images of SNs nanoemulsions prepared at two different ratios, 1:0.1 and 1:0.5.

Additional morphological characterization of SNs was completed with Transmission Electron Microscopy (TEM), the most frequently used technique for the morphological examination of

colloidal drug carriers. Knowing that staining and drying processes may result in structural alterations of the nanosystems that always need to be taken into consideration when interpreting negative staining TEM images, Cryogenic Transmission Electron Microscopy (CryoTEM) was also used as complementary morphological information. CryoTEM allows direct investigation of nanosystems in vitrified medium (frozen-hydrated state) which could be consider the closest condition to their native state[65–67]. TEM and CryoTEM images (**Figure 1**) showed homogeneous populations of spherical and regular particles, and corroborate the values of mean particle size and particle size distribution previously determined by DLS and NTA.

Stability of nanocarriers is a very important property for the adequate handling of pharmaceutical products[68,69]. Colloidal short-term stability of SNs was determined after 24h in the suspension media, upon incubation with cell culture medium and human plasma (**Figure 2A**). Moreover long-term accelerated stability following the International Council for Harmonization (ICH) guidelines was assesed[70] (**Figure 2B-C**). Short-term stability of SNs indicate that besides an initial increase in size both in plasma and cell culture medium, SNs maintain their size throughout the entire study. This size increase could be related to protein adsorption and formation of a protein corona, a fact that should be investigated in consecutive studies.

Long-term stability results indicate that SNs 1:0.1 and SNs 1:0.5 maintain the initial size after 24 weeks. **Figure 2B** corresponds to the evaluation of product stability when stored in a refrigerator (25ºC ± 2ºC, 60% RH ± 5%). On the other side, **Figure 2C** refers to the stability of the product under general temperature conditions (RT). Overall, our results show that colloidally stable SNs against gravitational separation and particle aggregation can be successfully prepared following a simple and soft methodology, and with only two components. Few examples can be found in literature stating the formulation of nanometric emulsions

following low-energy methods with such a simple composition and stable over time, which mainly refer to the preparation of emulsions with mixtures of naturally derived phospholipids such as lecithin[71]. Additionally, we have proved that SNs do not show intrinsic toxicity for concentrations as high as 10mg/mL, and can efficiently interact with cancer cells (**Figure S2**), facts that highlight their potential for the further development of anticancer nanotherapeutics.

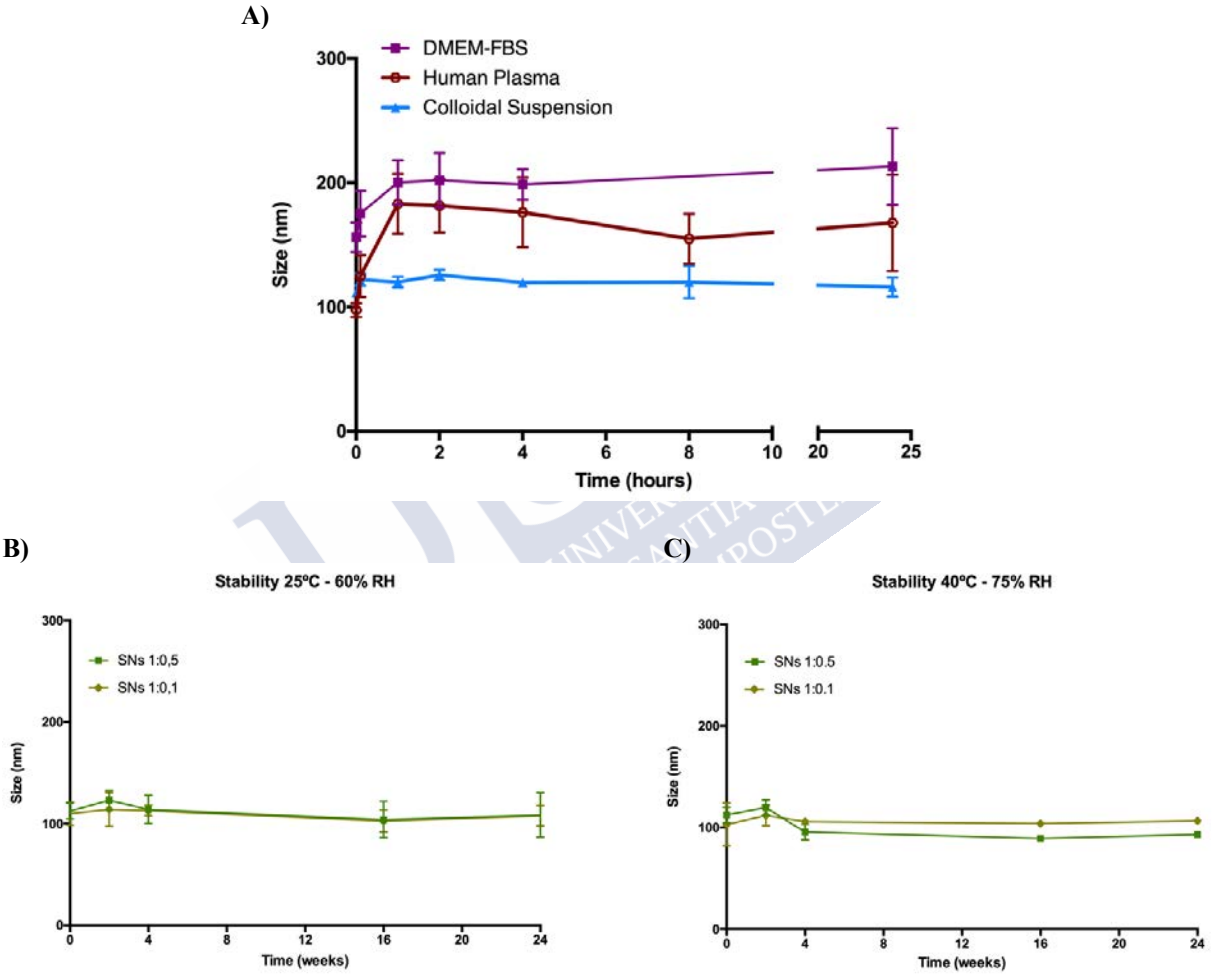

Figure 2. (A) Stability of SNs at ratio V:SM 1:0.1 in cell culture medium, human plasma and colloidal suspension. **(B-C)** ICH long-term stability of SNs composed of Vitamin E and sphingomyelin at ratio V:SM 1:0.1 and 1:0.5.

3.2. MDs simulations of SNs

Spontaneous formation of nanosystems composed of 1000 molecules of V and 67 SM molecules (1:0.1 w/w ratio) initially at random positions and orientations was investigated using CG-MD simulations (section 2.5.2). The spontaneous formation of a unilamellar vesicle was observed under the simulation time (500 ns) in the two replicas studied (**Figure 3A and Figure S4**). Different V:SM ratios (1:0.5 and 1:1) led to similar results (**Figure S5 and S6).** In all cases, the vesicle is composed by V forming a compartmentalized structure with an outer diameter of ~10 nm (**Figure 3C-F**). The hydroxyl groups of V point towards the water in both inner and outer sides of the V-membrane. The SM molecules are randomly distributed in the nanovesicle, with the PO_4 group oriented also towards the inner and outer water (**Figure 3D, E, G**). The Radial Distribution Function (RDF) calculations, considering the center of mass of the encapsulated water as a reference, show that this behavior is clearer increasing the proportion of SM (**Figure S7**).

Although a classical nanoemulsion-type structure had been initially envisaged for these formulations, the formation of such nanosystem containing at least one water pocket into the structure should not be, in fact, something unexpected. It is known that, due to its amphipathic structure, both V and its analogues can be easily incorporated into nanosystems and even forming vesicles by themselves at appropriate concentrations[72]. However, such vesicles become easily unstable in the presence of divalent cations, acidic pH, and serum. Considering our concentration range, the absence of SM leads to the formation of nanosystems with size over 200nm and marked negative charge that are not stable for more than a few hours, **Figure S8**). Nevertheless, this destabilization effect is not measurable in the time scales (500 ns) of the MD simulations. It should be thus expected that the presence of SM stabilizes such a type of nanostructures.

The number of V and SM particles used in the simulation is too small to obtain nanostructures comparable in size to experimental conditions under equilibrium. Larger nanovesicles could be formed by coalescence from the formed nanosystems in **Figure 3**. Nonetheless, we will assume that the basic structure of these vesicles can be extrapolated to those obtained in the laboratory experiments.

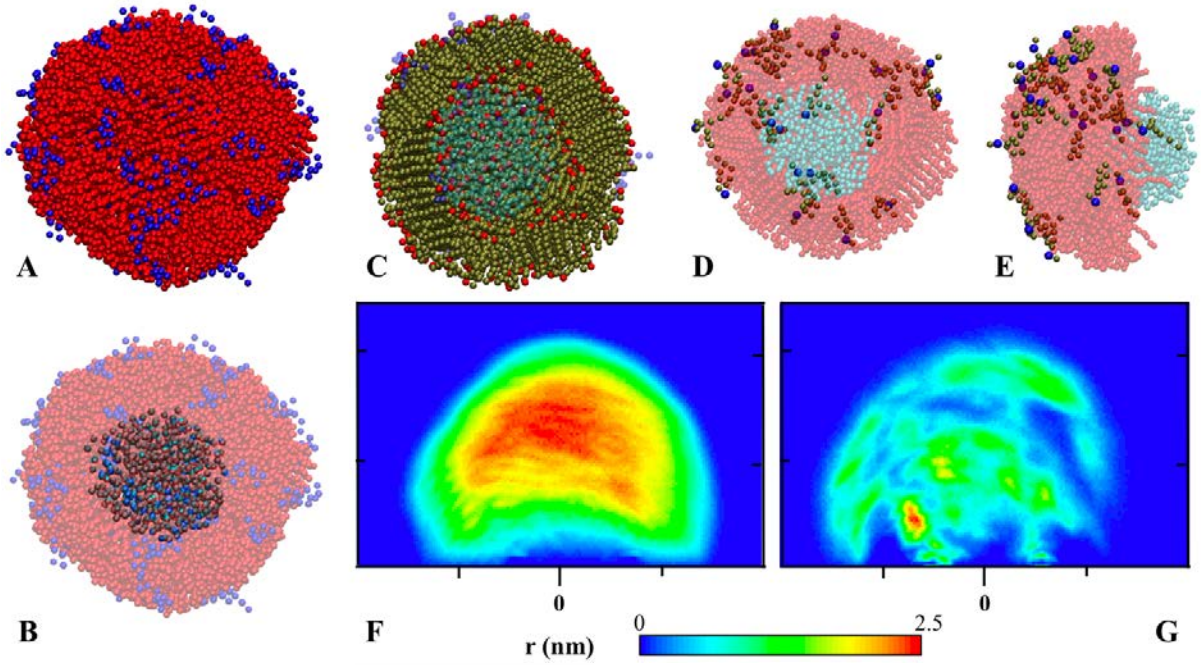

Figure 3. Last snapshot (t=500ns) of a simulation without any drug added A) representing V in red and sphingomyelin in blue, B) representing V in red and SM in blue, emphasizing the encapsulated water, C) representing the hydroxyl groups of the V in red and the rest of the molecule in brown, D) representing the PO_4 groups of SM in blue and the rest of the molecule in brown, E) one-half of the nanosystem representing the water inside in cyan, the PO_4 groups of the SM in blue and the rest of the molecule in brown. 2-D number-density maps for F) V and G) SM, taking as reference the center of the nanovesicle.

3.3. The existence of inner water revealed from MD simulations and NMR experiments

Interestingly, in all the simulated replicas (**Figure 3B,D,E**) the presence of a small amount of water was observed inside the SNs. This fact, suggested by the simulations, was not initially contemplated as a possibility based on the available experimental data.

NMR analysis were subsequently performed to experimentally validate simulation results. Firstly, a 1D ^{13}C NMR spectra of SNs (ratios 1:0.5 and 0.1) was performed, as shown in **Figure 4**. Carbon signals from V appeared with considerably lower intensity than SM signals despite of the same larger concentration of V presented in each sample (5mg/mL). A clear evidence of this effect is seen in the aromatic region 115-150 ppm (dotted region) where only the peaks of V can be expected (**Figure 4A,B**). On the other hand, the sensitivity of these two ^{13}C spectra was enough to detect with much higher intensity the peaks of the lower concentrated component SM in the two samples (0,5mg/mL in ratio 1:0.1 and 2.5mg/mL in ratio 1:0.5). Interestingly, if the aromatic carbon signals of V are compared, the reduction of their peak intensity is inversely proportional to the concentration of SM in the sample.

To assist the interpretation of the aforementioned changes, a brief summary of some key points on NMR relaxation is provided. It is well stablished in NMR that the linewidth of a certain peak in the spectrum depends on a property of the peak that is its T_2 transversal relaxation time. The linewidth of a peak at half height (LWHH) is related to the T_2 by the formula $LWHH=1/(\pi \cdot T_2)$. Therefore any shortening of the T_2's cause line-broadening and loss of the peak (maximum) intensity. From the several NMR mechanisms potentially modulating the T_2, the only relevant to our system is dipolar relaxation[73]. Under this mechanism, the T_2's of the peaks of a molecular specie are dependent on its molecular mobility in solution, in particular on the rate of its molecular tumbling and the extend of its internal motions also known as flexibility.

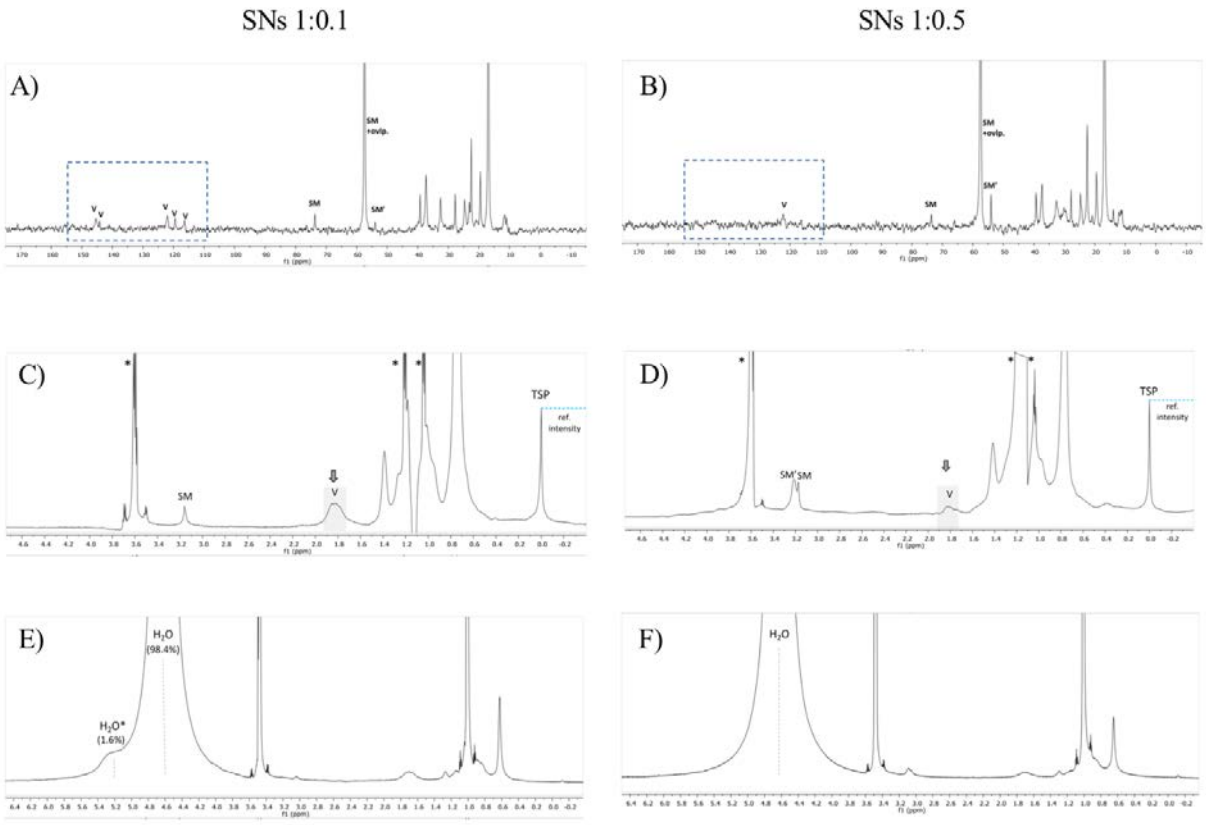

Figure 4. 1D ^{13}C NMR spectra of samples (A) SNs 1:0.1 measured with 12000 scans and (B) SNs 1:0.5 measured with 20000 scans. 1D ^{1}H-watergate quantitative spectra of samples (C) SNs 1:0.1 and (D) SNs 1:0.5. (Vertical intensities in the two spectra are normalized respect to the signal of TSP). 1D ^{1}H quantitative spectra of samples (E) SNs 1:0.1 and (F) SNs 1:0.5. The relative integral of the H_2O and H_2O* peaks that is reported in spectrum E) was determined by signal deconvolution. *Indicated peaks correspond to V, SM and (*) ethanol*

Any event lowering the molecular mobility parameters shortens the T_2's of the molecule causing peak line-broadening. According to these considerations, it is possible to do the following interpretation of the spectra of **Figure 4A**; at small concentrations of SM (ratio 1:0.1), the aromatic signals of V are visible in the ^{13}C spectrum suggesting that such component is still in the fast molecular mobility regime, characterized by large enough T_2's to provide visible peaks. However, at the higher concentration of SM (maintaining V constant, ratio 1:0.5) signals of V are not (or barely) detectable in ^{13}C spectrum, indicating that the component V experiences

a slower molecular mobility and/or a more rigid chemical environment which shortens the T_2's and broadens its aromatic peaks below detection level thereby creating an "invisible NMR zone" (**Figure 4B**)[74]. Another interesting observation occurring in the ^{13}C and ^{1}H spectra of the samples SNs 1:0.1 and SNs 1:0.5 (**Figure 4C and D**) is the appearance of two set of signals for the component NMe_3 group of SM. It is an indication that the molecules of SM are experiencing two different environments with slow or no exchange among them. Overall, these considerations point out to an effect of entrapment of the V component into a nanosystems, a result that is in agreement with the prediction of the MD calculations (**Figure 3**).

The 1D ^{1}H quantitative spectrum of the samples SNs 1:0.1 and SNs 1:0.5 is given in **Figure 4E and F**. These spectra were acquired under suitable conditions to observe the intense water peak for samples with high H_2O content. The two spectra have some features in common such as the appearance of several broad peaks in the region 3.5-0.5 ppm that correspond to the components V and SM, the presence of two narrow peaks at ~3.5 and ~1.0 ppm due to traces of ethanol, and the expected strong peak of the water (labelled as H_2O) at ~4.7 ppm. Interestingly, in the spectrum of SNs 1:0.1 (**Figure 4E**), partially overlapping with the mentioned H_2O peak, there is a peak at 5.14 ppm (labelled as H_2O^*), that it is not seen for sample SNs 1:0.5 (**Figure 4F**) in contrast with the observations made in MD simulations for the same sample (**Figure S5**). According to the analysis of the integral represents the 1.6 % of the total water content, which concords with the presence of a minor fraction of water molecules that are obtained in the MD simulations. The H_2O^* peak was assigned to water molecules residing in vesicles in the nanosystem formed by the SM and V components (discussed in the study by 1D ^{13}C NMR). The de-shielding caused by the nanosystem environment explains its different chemical shift respect to the bulk-water molecules that are represented by the intense H_2O peak. Overall, NRM experiments can confirm that SNs at ratio 1:0.1 contain a measurable amount of internalized

water, superior than in the case of SNs 1:0.5, which could be a fact of interest for the encapsulation of hydrophilic macromolecules. On view of the previous results from NRM and CG-MD, SNs with a ratio V:SM 1:0.1 were further explored for their potential action as tunable drug delivery systems for personalized medicine.

3.4. Association of active therapeutic molecules to SNs and use of Molecular Dynamics simulations as predictive tools

In this work we have described the development of a novel type of nanosystems of interest for anticancer therapies, SNs. Next, we evaluated the interaction and affinity of SNs with several drugs, namely curcumin, resveratrol, gemcitabine, dsRNA, a natural peptide (LAPI) and a hydrophobically modified peptide (LAPIK) (**Figure 5**) using both biophysical experiments and CG-MD/AT-MD simulations. Physicochemical properties of drug-loaded SNs were evaluated experimentally as described in section 2.3. and are reported in **Table 4**. Remarkably, no major changes were observed regarding particle size (with a maximum increasing size up to 150nm) or PdI values in loaded nanosystems. Slight variations in the surface charge of the nanosystems were also observed towards more negative values when the drugs and biomolecules were incorporated, which evidence changes in the surface properties. Variations in surface charge towards more negative values were observed for the formulations loaded nucleic acids (justified by the presence of functional phosphate [PO_4^-] groups in DNA/RNA chemical structure), curcumin and resveratrol (could be explained by the presence of protonated forms of both drugs[75–77]). Moreover, just in the case of the hydrophobic derivative of the selected peptide (LAPIK) a slight positive charge can be found due to the presence of the amino acid lysine (K) in the structure of this peptide derivative. Regarding encapsulation efficiencies of all drugs, curcumin and resveratrol exhibit the most efficient association to SNs, (98 and 93% respectively). This was somehow expected considering the markedly hydrophobic character of these drugs (LogP values 3.2 and 3.1 showed in **Table 1**), as well as by comparison with previous works in literature[78–81].

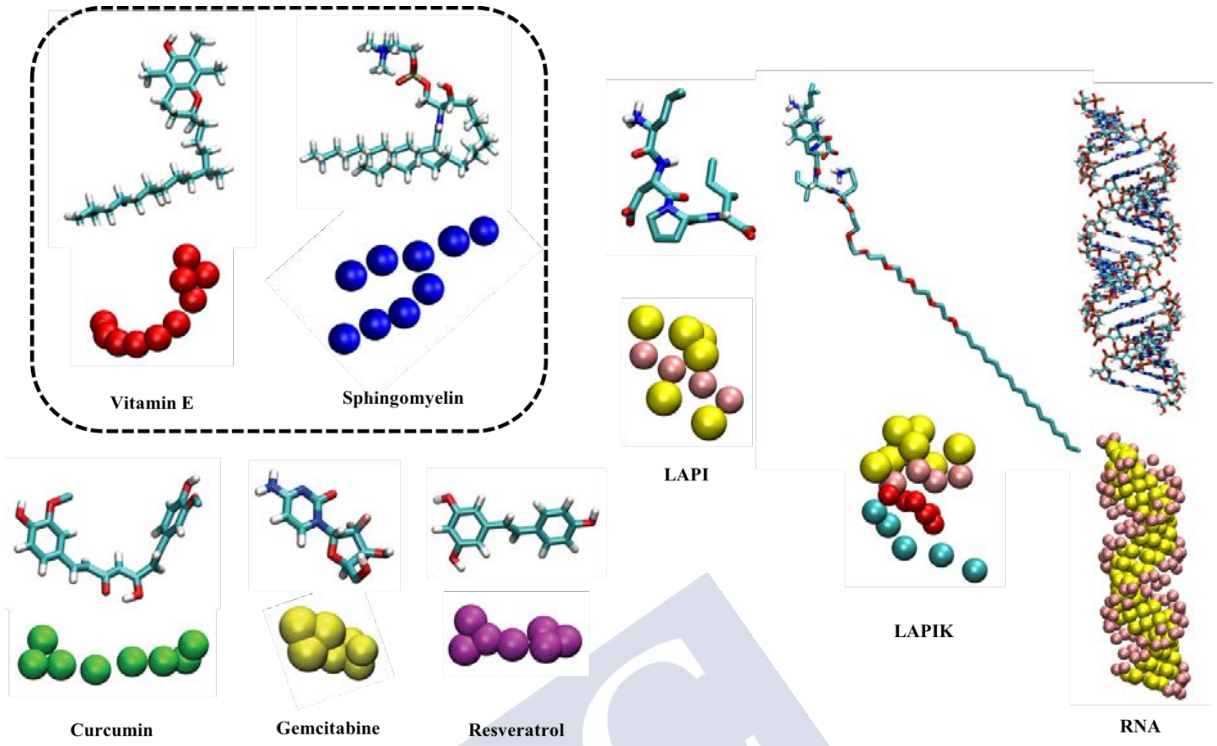

Figure 5. Molecular representation of the nanoemulsion forming compounds (dotted black area) and the associated drugs and biomolecules.

Table 4. Physicochemical characterization of SNs associating the six selected molecules.

Drug	Size (nm)	PdI	Surface charge (mV)	EE%
Curcumin	121 ± 2	0.1	-21 ± 2	98 ± 0
Resveratrol	134 ± 2	0.1	-13 ± 3	93 ± 8
Gemcitabine	104 ± 1	0.1	-4 ± 4	12 ± 1
dsRNA	144 ± 10	0.1	-10 ± 0	14 ± 2
LAPI	110 ± 8	0.1	-9 ± 2	15 ± 3
LAPIK	127 ± 3	0.2	+4 ± 2	85 ± 4

nm: nanometer; PdI: polydispersity index; mV: millivolts; EE%: encapsulation/association efficiency (mean ± SD, n=6)

CG-MD simulations show that a high percentage of the curcumin is found inside the vesicle, interacting with the inner water of the nanostructure in all the replicas simulated (**Figure 6A-B and S9**), in good agreement with the high %EE found experimentally (**Table 4**). The RDF of each component with respect to the center of the water pocket confirms this observation (**Figure S9**). The concentration of SM is also more abundant in the inner layer, exposed to the encapsulated water than in the outer layer of the V-membrane. Mapping to AT resolution using the GADDLE maps algorithm [see Methods] and the GROMOS force-field and subsequent AT-MD simulation during 20 ns confirmed the stability of the supramolecular assembly at the studied time scale (**Figure 6C-D**). The atomistic resolution revealed that curcumin molecules exhibit, in average, 1 H-bond with SM, 4 H-bonds with water molecules and practically no H-bonds with V molecules. Curiously, in some of the replicas the formation of two inner pockets of water was observed, and they were even maintained after 20 ns of AT-MD (**Figure S9**). In the same way, CG-MD simulations in presence of resveratrol led again to a spontaneous formation of the nanovesicle with a good association of the drug (**Figure 6E-F and S10**), also in consent with experimental findings (**Table 4**). Resveratrol mainly locates near the inner water, as it can be also observed in the RDF graphics (Figure S10), with some molecules also in the bulk water region interacting with the nanosystem surface. Mapping to AT resolution and subsequent AT-MD simulations using the GROMOS force-field during 20 ns confirmed the stability of the supramolecular assembly at the studied time scale (**Figure 6G-H and S10**), leading to ~1H-bonds per molecule of resveratrol with SM and about 3 H-bonds with water.

Experimental association efficiencies for the hydrophilic drug gemcitabine (LogP value -1.5), were around 10%, as expected due to its high hydrophilicity character. This molecule could be mainly expected not to interact with the nanostructure or be minimally accommodated onto the surface of the nanosystems, mainly mediated for the establishment of ionic interactions with

phosphate and amine groups presented in the hydrophilic head of the SM molecule[82]. Both CG-MD and AT-MD also suggest a lower association to the nanosystem in all the replica studied. (**Figure 6I-L and S11**) All the gemcitabine molecules are placed outside the nanosystem. No drug was observed in the interior water pocket, as it can be clearly observed from the RDFs (**Figure S11**). In addition, it is worth to mention that the gemcitabine is the drug that stablish a larger number of H-bonds per molecule with water (~8), a clear indication of its hydrophilic character. Regarding the non-modified biomolecules (i.e. dsRNA and LAPI) we have also observed a moderate association efficiency (close to 15%) which was expected considering the challenge of incorporating negatively charged macromolecules into almost neutral lipophilic nanosystems (**Table 4**). From CG-MD simulation, the dsRNA was found to interact just in the external zone of the nanosystem (**Figure 6M-N and Figure S12**), slightly penetrating the hydrophobic part of the membrane in two of the five replicas simulated with a CG resolution (**Figure S11**). Mapping to AT resolution and the AT-MD simulation using the AMBER99SB confirmed the stability of this association pattern, where the dsRNA is interacting with the external zone of the nanovesicle, although a distortion of its structure is observed, mainly in one of the replica (**Figure 6O-P and Figure S12**). Experimental results obtained for the hydrophobically modified peptide (i.e. LAPIK) (**Table 4**) showed even five times more encapsulation efficiency than the original molecule (LAPI) rendering these hydrophobic modifications promising alternatives for maximizing encapsulation efficiency of hydrophilic drug into lipidic nanostructures. However, our CG MD simulations does not show differences between both peptide systems, obtaining a good encapsulation in all cases. These results suggest that a more accurate resolution or a better description of the interactions in these systems is needed for reproducing the experimental conclusions.

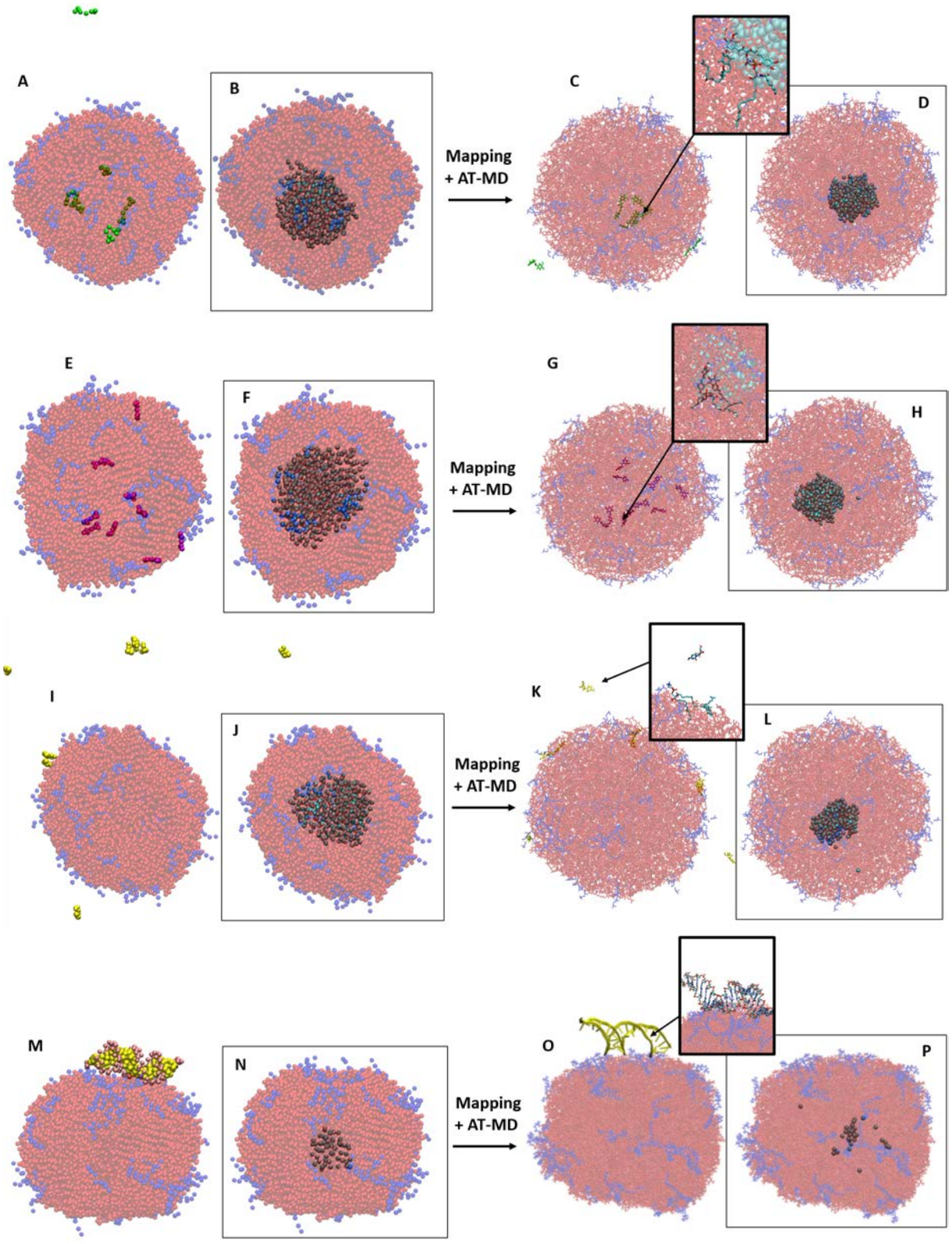
A
B
Mapping
+ AT-MD
C
D
E
F
Mapping
+ AT-MD
G
H
I
J
Mapping
+ AT-MD
K
L
M
N
Mapping
+ AT-MD
O
P

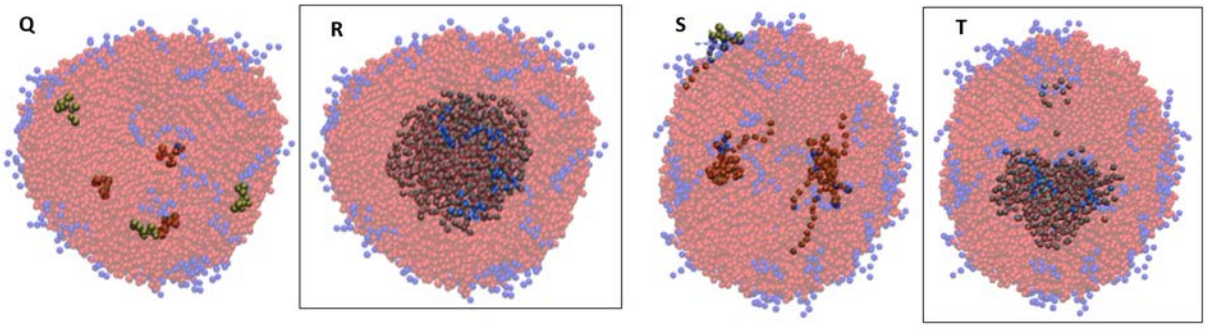

Figure 6. Molecular representation of the nanovesicle loading curcumin (A-D), resveratrol (E-H), gemcitabine (I-L), dsRNA (M-P), LAPI (Q-R) and LAPIK (S-T). Snapshot of the last structure of one of the CG-MD simulations (A, I, M, Q, S) together with the structure mapped to atomistic resolution after 20 ns of MD simulation (C, G, K, O). V is represented in transparent-red, SM in blue, and drugs in different colors. A detail of the trapped water molecules inside the vesicle are shown in the boxed snapshots, corresponding to CG or AT resolution.

CONCLUSIONS

In the present study we have successfully developed SNs, a very simple and stable nanosystem, composed of just one oil (Vitamin E) and one surfactant (Sphingomyelin), which also show a good biocompatibility and ability to interact with cancer cells. The characterization of these systems, using a number of computational and physicochemical methods, showed a high compartmentation of the nanosystem, with a water pocket enclosed among the nanostructure. Additionally, the potential of SNs for drug delivery applications was evaluated by associating different therapeutic molecules. Using a synergistic *in-vitro*/*in-silico* strategy based on laboratory experiments and multiscale CG-MD/AT-MD simulations we were able to study the fundamental interactions governing the assembly, structural and dynamical characteristics of SNs, together with their drug loading capacity, drug distribution/localization in the nanosystem and dominant drug–nanosystem interactions. Our results suggest that SNs are promising carriers for the development of anticancer therapies for personalized medicine and can be further optimized and fully exploited making use of predictive computer simulation tools. This strategy is a very promising instrument for the rational design of tailored nanosystems for specific applications. The validation of such a methodology begins the road towards the development of a virtual screening platform to address the future development of personalized medicine.

SUPPLEMENTARY INFORMATION

Table S1. Detailed HPLC methods conditions.

	Small Drugs		Biotechnological Drugs	
	Gemcitabine	**Resveratrol**	**dsRNA**	**LAPI / LAPIK**
Column	Kinetex C8 2.6µm 2.1x100mm Phenomenex	Kinetex C8 2.6µm 4.6x150mm Phenomenex	Sunfire C18 5µm 4.6x250 mm Waters	Kinetex C8 5µm 4.6x150 mm Phenomenex
Flow	0.2 mL/min	0.2 mL/min	0.6 mL/min	1 mL/min
Wavelength	248 nm	325 nm	260 nm	220 nm
Mobil Phases	A: Water B: MetOH	A: Water 2%IPA B: MetOH 2%IPA	A: 95mL TEAAc 855mL H2O 50mL ACN B: 30mL TEAAc 270mL H2O 700mL ACN	A: Water 0.1%TFA B: ACN 0.1%TFA
Method Gradient (t=min)	t=0.0. B=90% t=1.0 .B=90% t=4.0 B=10% t=5.0 B=10%	t=0.0 B=50% t=5.0 B=100% t=6.0 B=100% t=10.0 B=50%	t=0.0 B=15% t=5.0 B=15% t=6.0 B=100% t=10.0 B=15% t=15.0 B=15%	t=0.0 B=20% t=0.5 B=20% t=1.0 B=35% t=1.5 B=35% t=3.0 B=92% t=8.0 B=20% t=10.0 B=20%

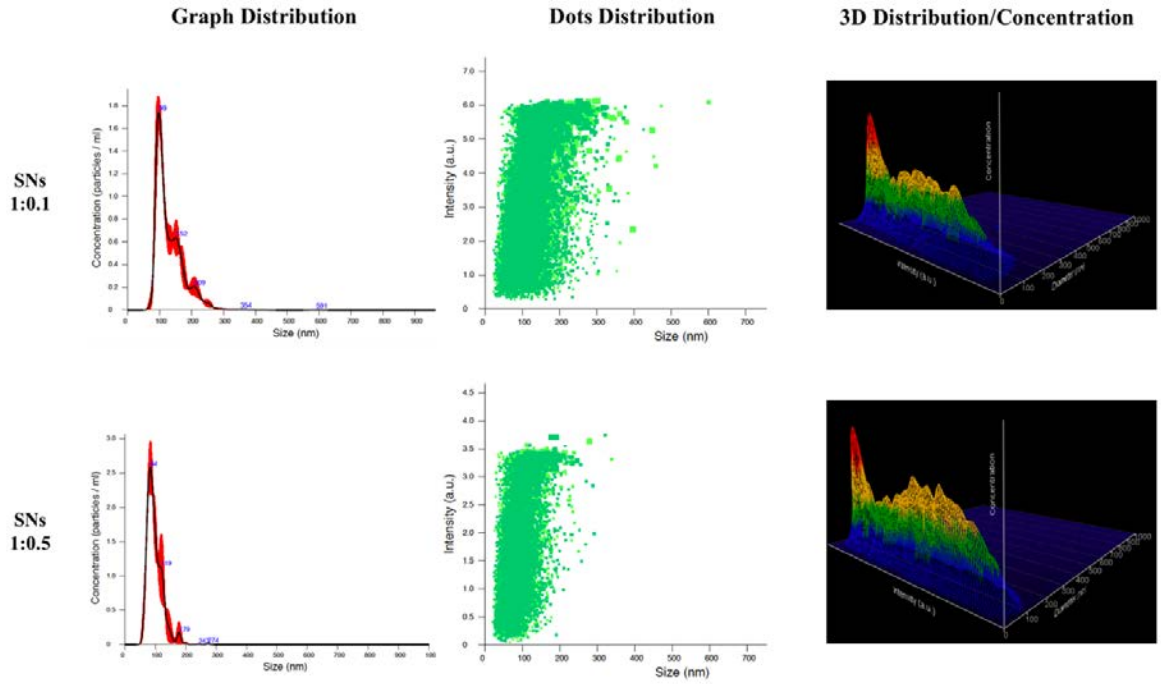

Figure S1. Physicochemical characterization of SNs 1:0.1 and 1:0.5 by Nanoparticle Tracking Analysis (NTA).

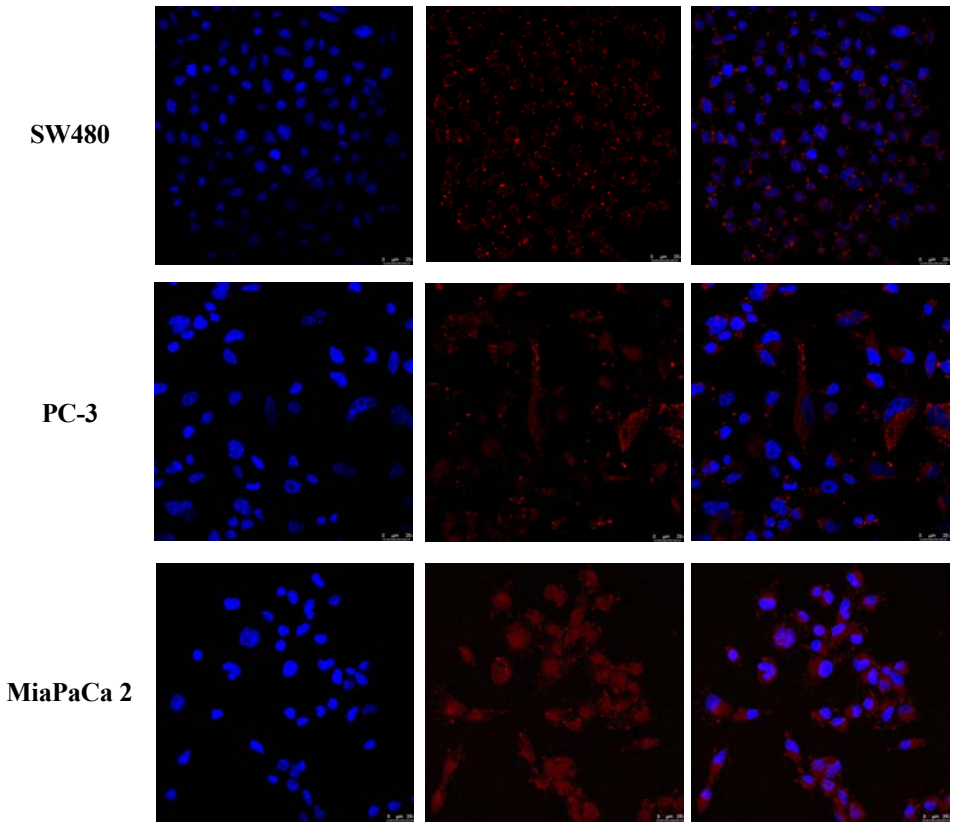

Figure S2. Cellular uptake observed under the confocal microscope of SNs (red channel) upon 4h incubation at 37ºC in SW480 colorrectal cancer cells, MiaPaCa 2 pancreatic adenocarcinoma cancer cells, and PC3 prostate cancer cells (cell nuclei stained with DAPI, blue channel). Merged channels correspond to the right column.

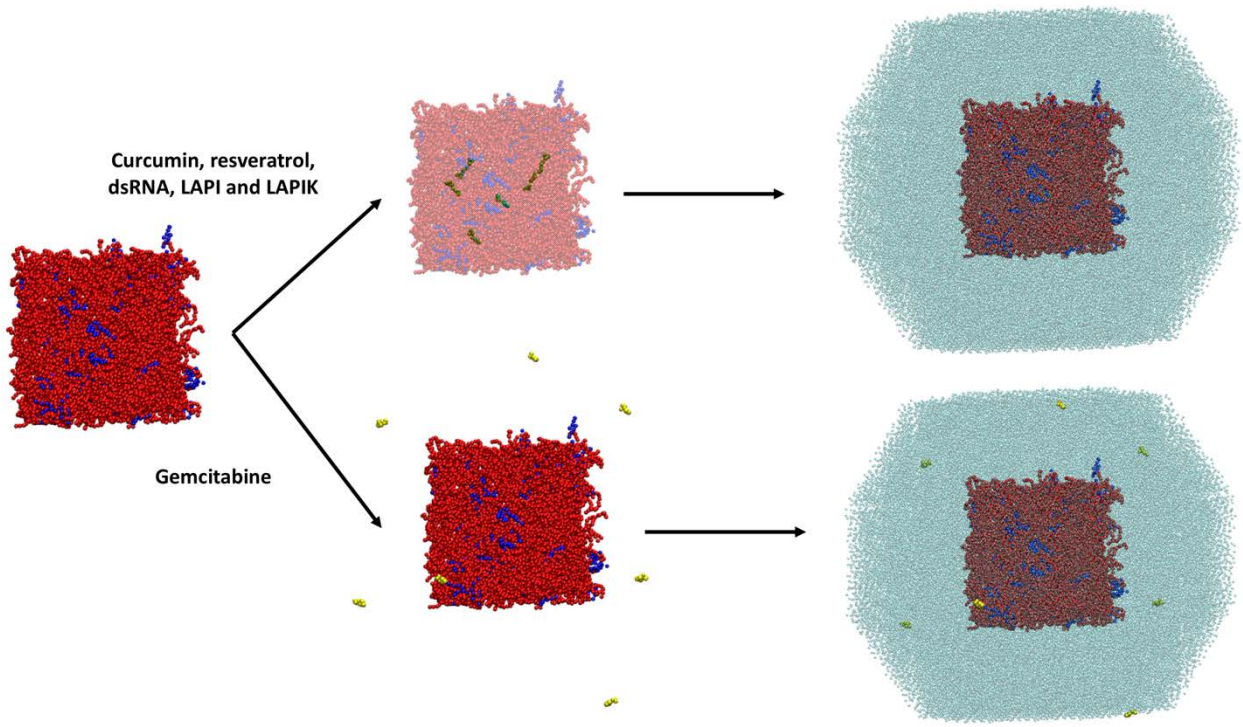

Figure S3. Preparation of the initial simulation boxes.

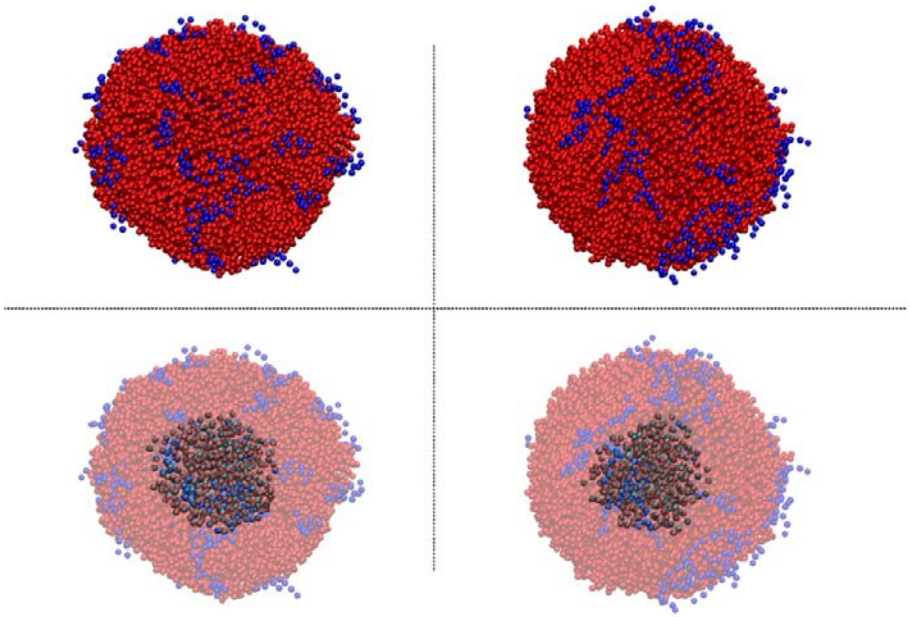

Figure S4. Simulation of a blank nanoemulsion composed of vitamin E nucleus (V, red) and surrounded by sphingomyelin molecules (SM, blue) at a **ratio 1:0.1**.

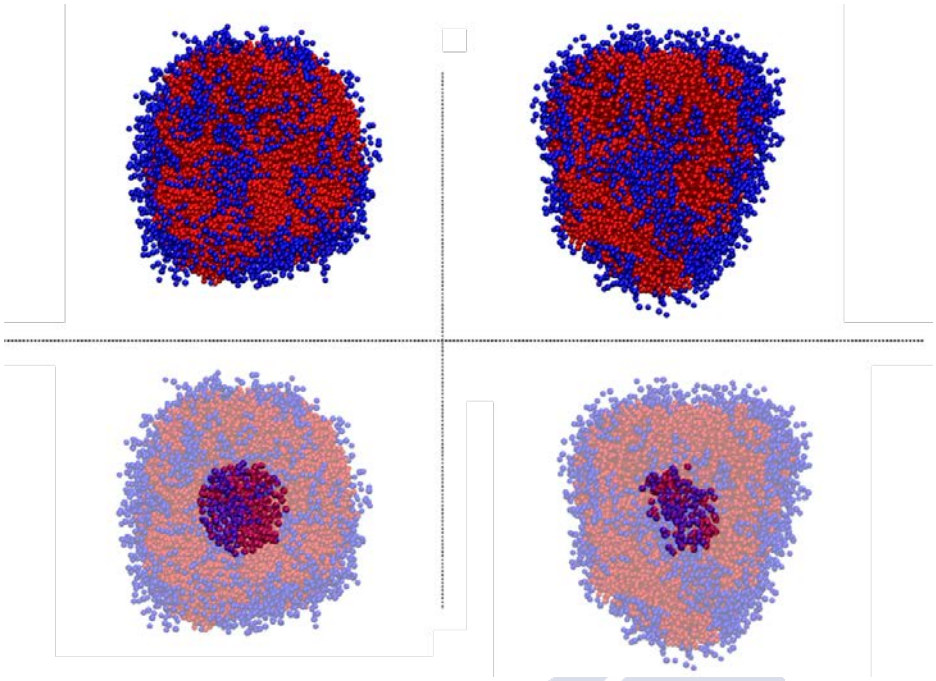

Figure S5. Simulation of a blank nanoemulsion composed of vitamin E nucleus (V, red) and surrounded by sphingomyelin molecules (SM, blue) at a **ratio 1:0.5**.

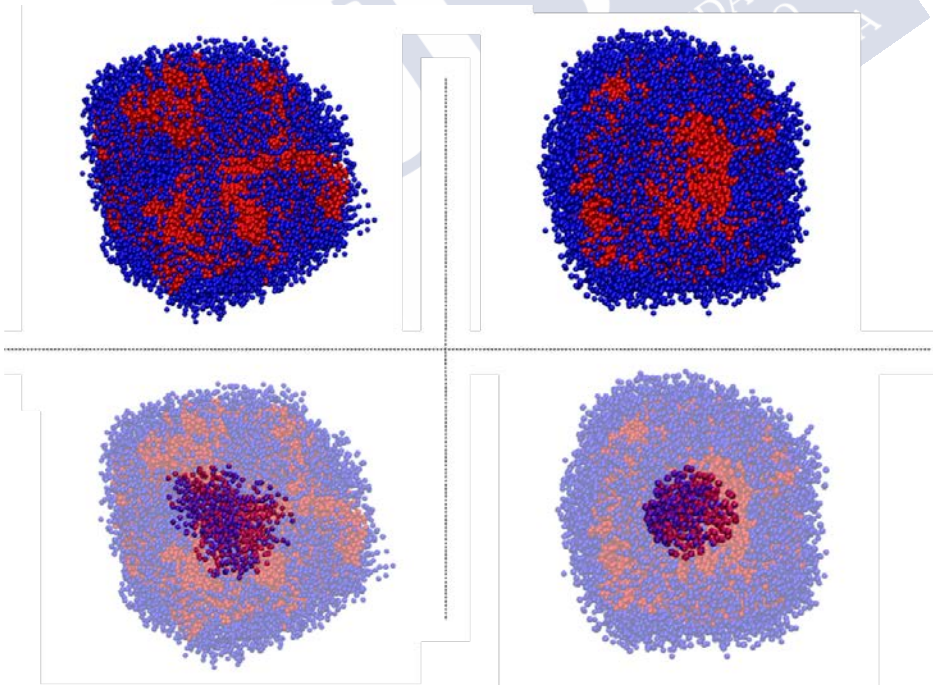

Figure S6. Simulation of a blank nanoemulsion composed of vitamin E nucleus (V, red) and surrounded by sphingomyelin molecules (SM, blue) at a **ratio 1:1**.

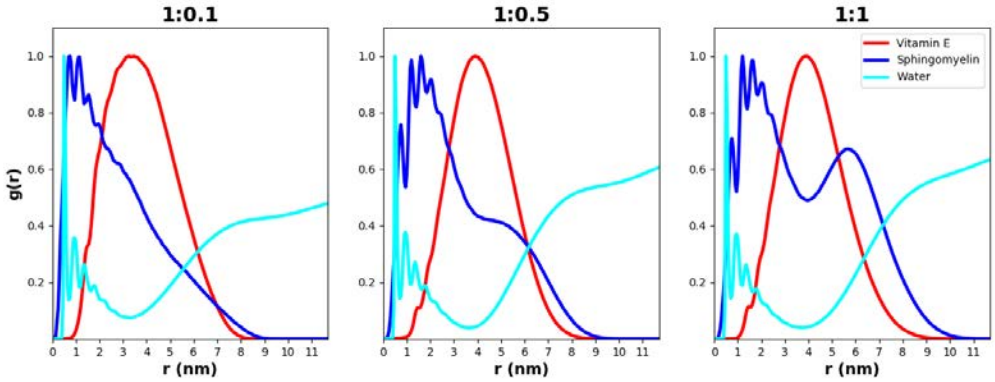

Figure S7. Radial Distribution Functions of Vitamin E (red), Sphingomyelin (blue) and water (cyan) from the center of the inner water pocket for the different V:SM ratios, considering the last 50ns of the simulation.

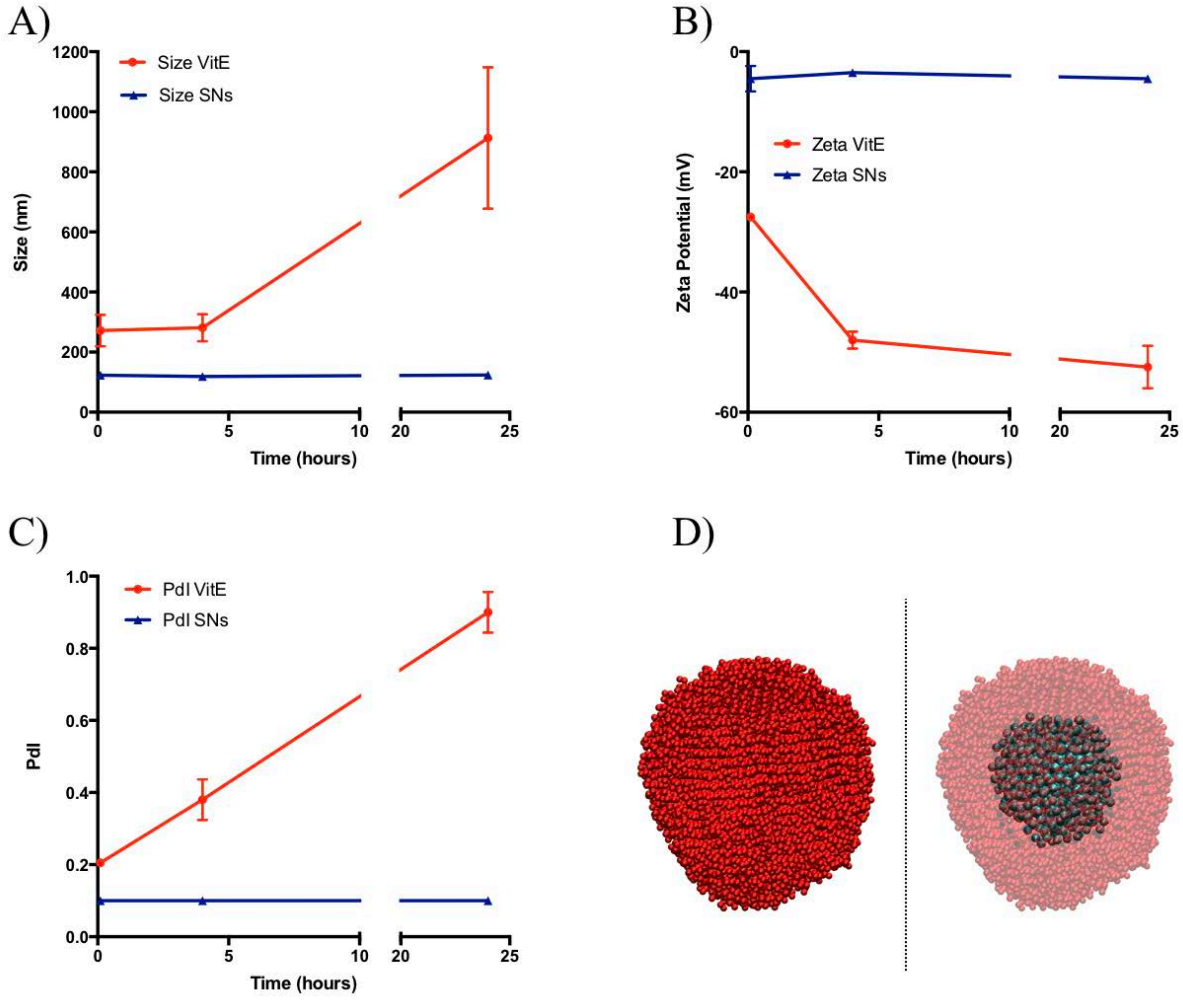

Figure S8. Evaluation of physicochemical characteristics in terms of size (A), zeta potential (B) and homogeneity of nanosystems (C) formed solely by vitamin E during a 24h period. Structure simulated using coarse-grained (D).

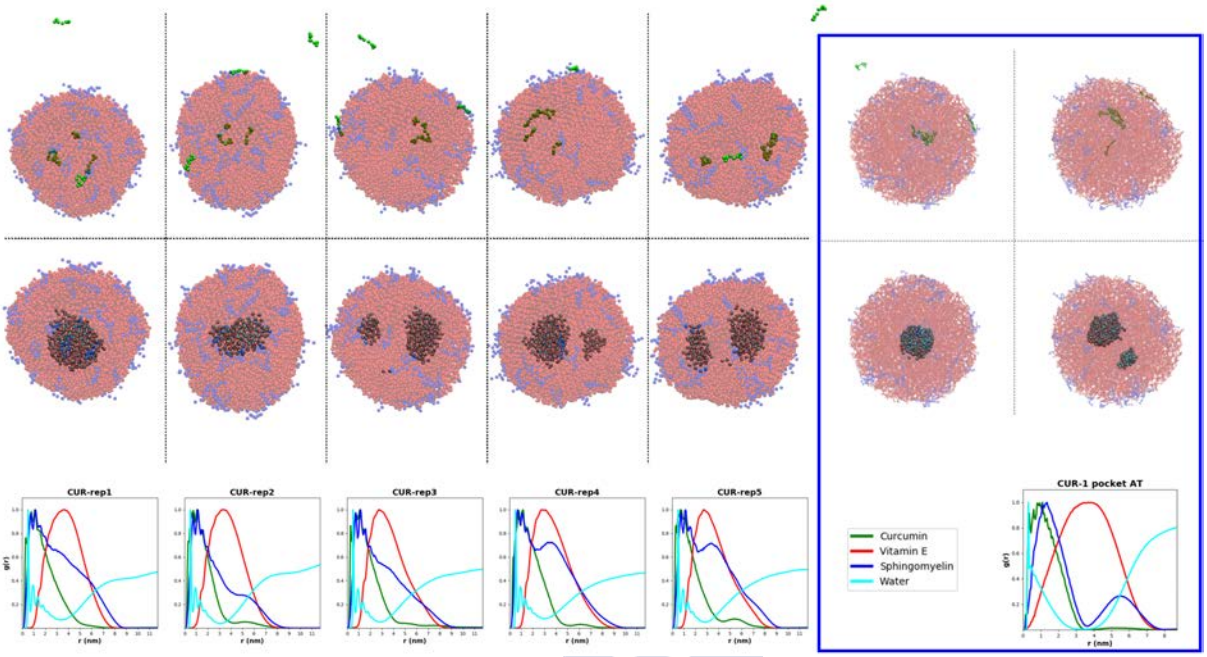

Figure S9. Last snapshot from the CG-MD simulation (t = 500 ns) and AT-MD simulations (t = 20 ns, blue square) including 6 molecules of curcumin in a fixed ratio 1:0.1 (Vitamin E (1000) and Sphingomyelin (67)). Radial distribution function from the center of the inner water pocket for the 5 CG-MD replicas, considering the last 50ns of the simulation, or the AT-MD simulation (blue square).

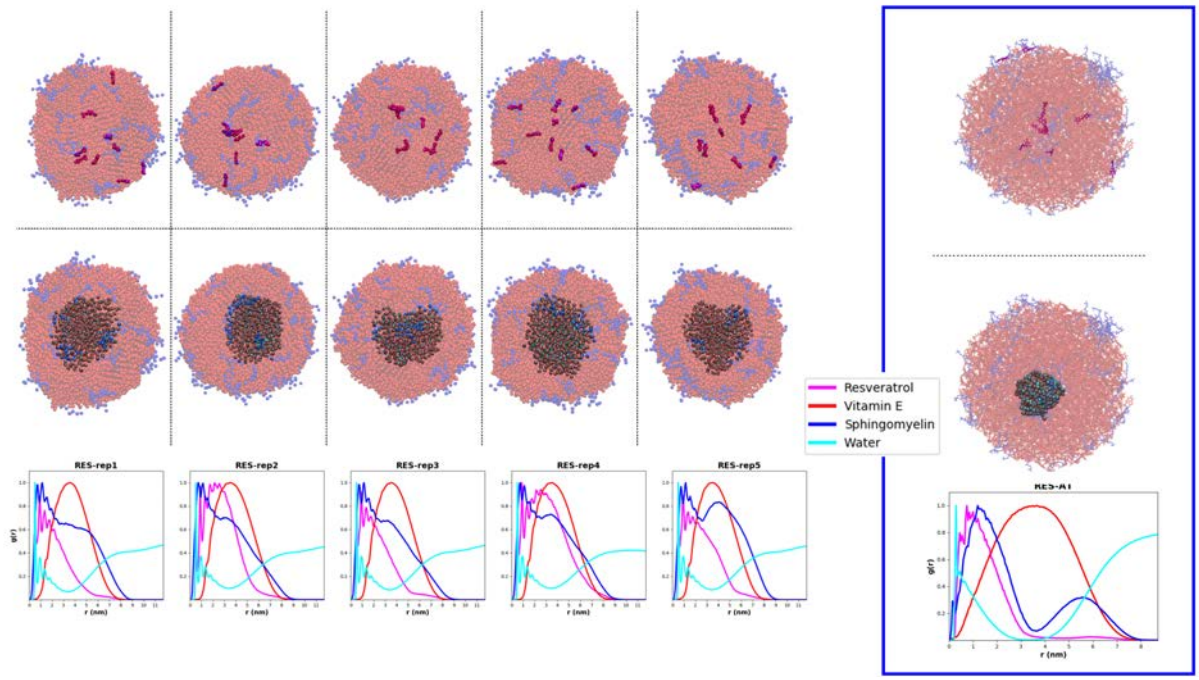

Figure S10. Last snapshot from the CG-MD simulation (t = 500 ns) and AT-MD simulations (t = 20 ns, blue square) including 10 molecules of resveratrol in a fixed ratio 1:0.1 (Vitamin E (1000) and Sphingomyelin (67)). Radial distribution function from the center of the inner water pocket for the 5 CG-MD replicas, considering the last 50ns of the simulation, or the AT-MD simulation (blue square).

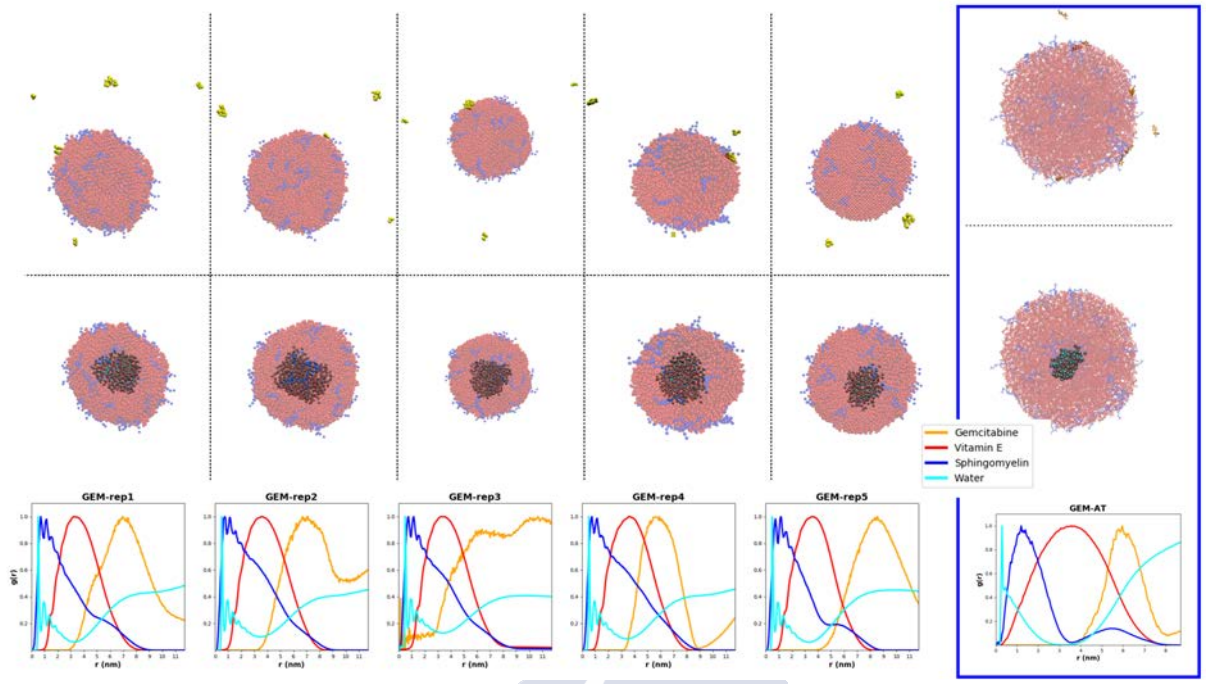

Figure S11. Last snapshot from the CG-MD simulation (t = 500 ns) and AT-MD simulations (t = 20 ns, blue square) including 9 molecules of gemcitabine in a fixed ratio 1:0.1 (Vitamin E (1000) and Sphingomyelin (67)). Radial distribution function from the center of the inner water pocket for the 5 CG-MD replicas, considering the last 50ns of the simulation, or the AT-MD simulation (blue square).

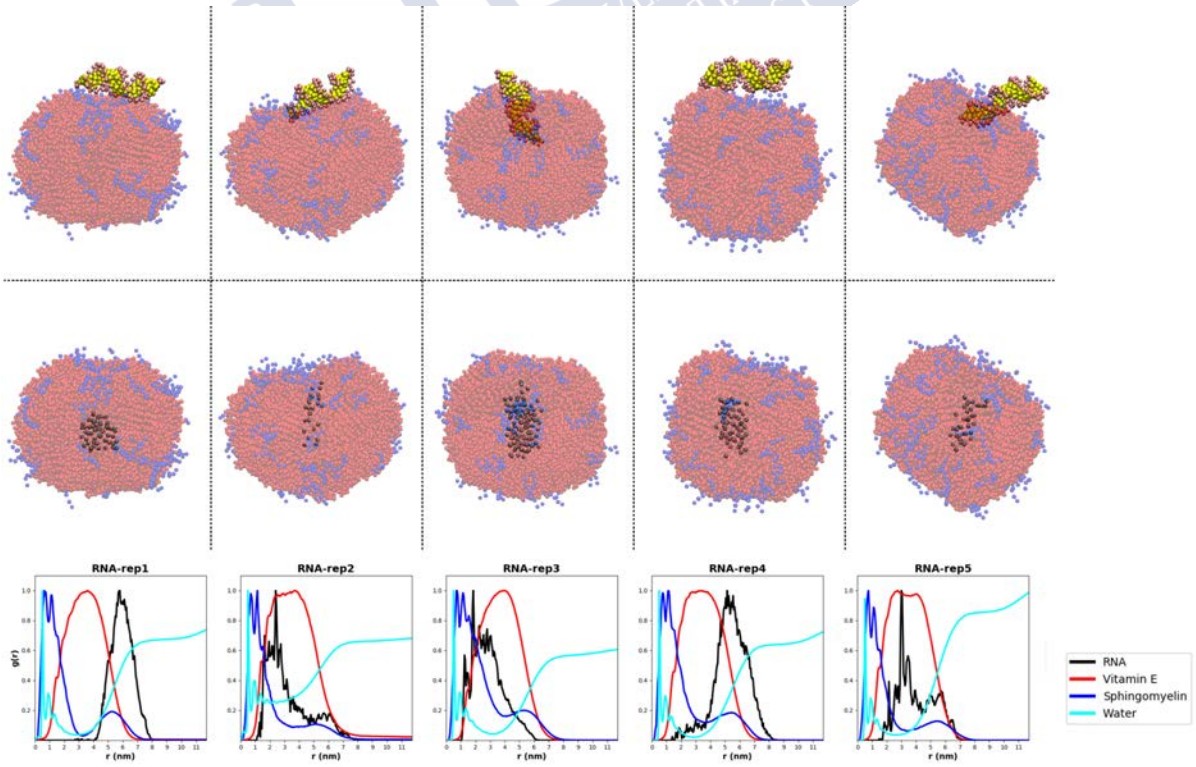

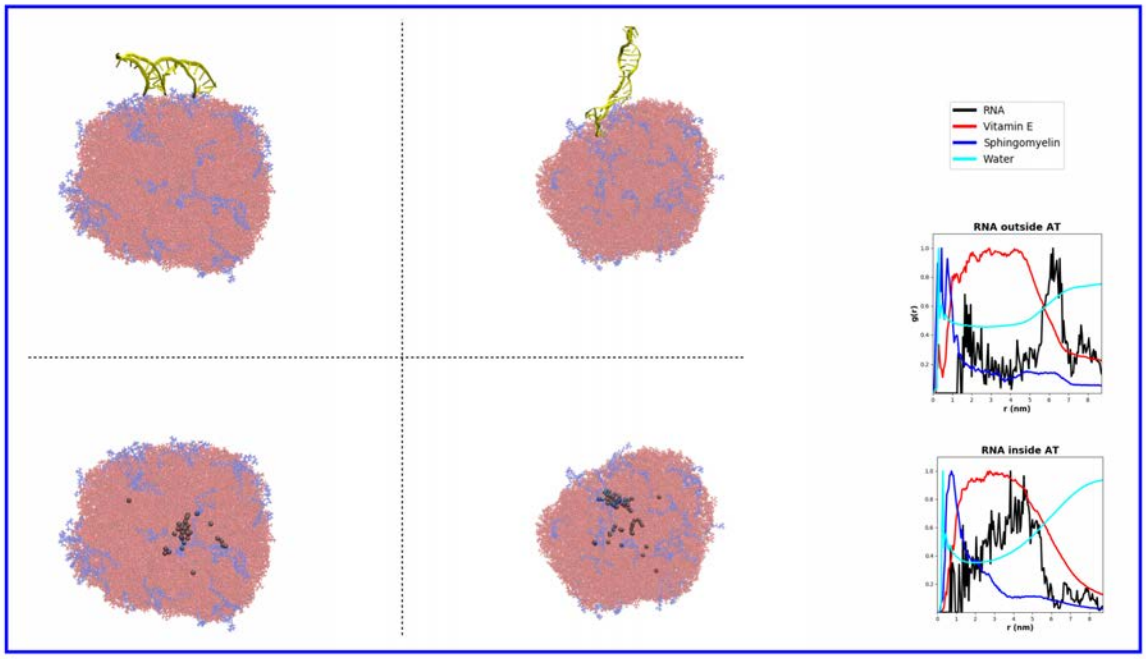

Figure S12. Last snapshot from the CG-MD simulation (t = 250 ns) and AT-MD simulations (t = 20 ns, blue square) including 1 molecules of ds-RNA in a fixed ratio 1:0.1 (Vitamin E (1000) and Sphingomyelin (67)). Radial distribution function from the center of the inner water pocket for the 5 CG-MD replicas, considering the last 50ns of the simulation, or the AT-MD simulation (blue square).

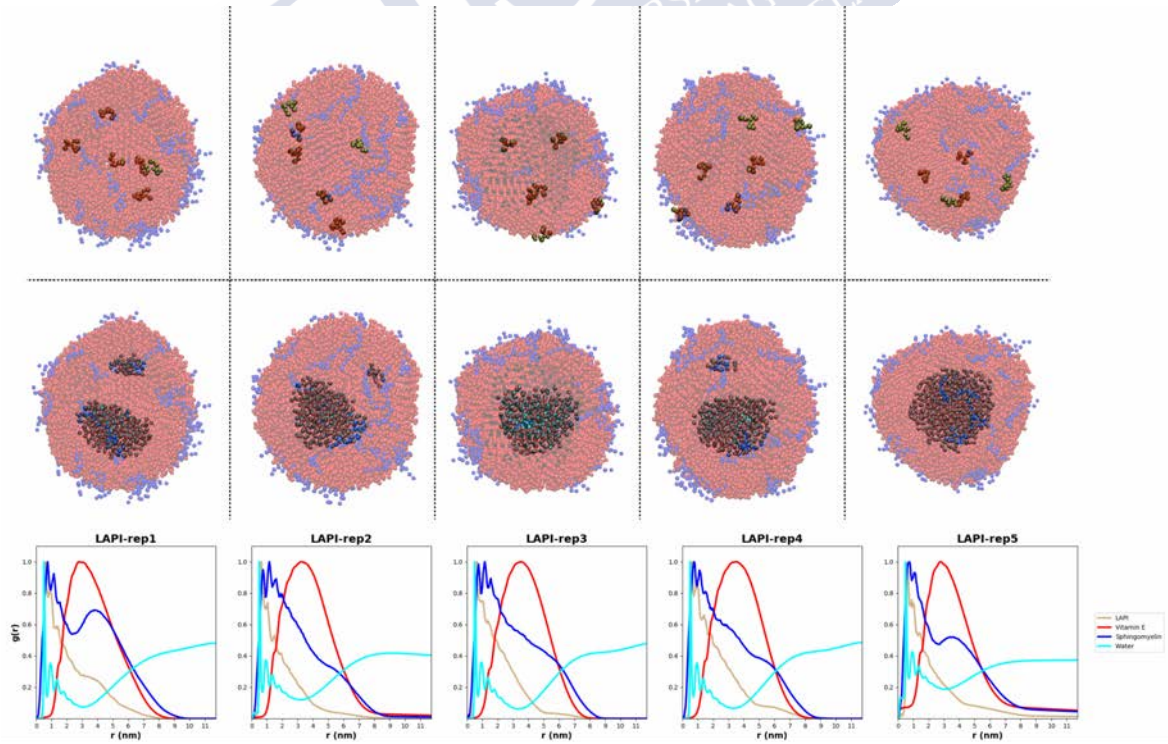

Figure S13. SNs simulation including 6 molecules of LAPI in a fixed ratio 1:0.1 (Vitamin E (1000) and Sphingomyelin (67)). Radial distribution function from the center of the inner water pocket for the 5 CG-MD replicas, considering the last 50ns of the simulation.

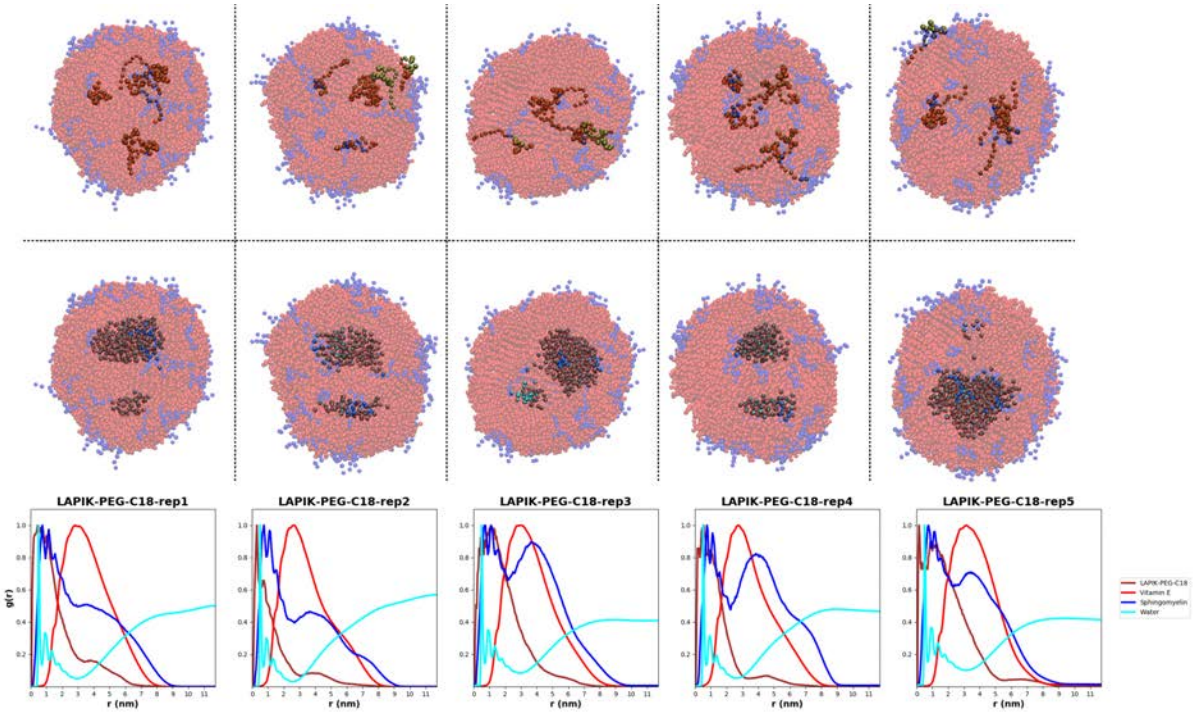

Figure S14. SNs simulation including 6 molecules of LAPIK in a fixed ratio 1:0.1 (Vitamin E (1000) and Sphingomyelin (67)). Radial distribution function from the center of the inner water pocket for the 5 CG-MD replicas, considering the last 50ns of the simulation.

REFERENCES

(1) Marchant, G. Small Is Beautiful: What Can Nanotechnology Do for Personalized Medicine? *Curr. Pharmacogenomics Person. Med.* **2012**, *7*, 231–237.

(2) Jane, K. Role of Nanobiotechnology in the Development of Personalized Medicine. *Nanomedicine* **2009**, *4*, 249–252.

(3) Chabner, B. A.; Roberts, T. G. Timeline: Chemotherapy and the War on Cancer. *Nat. Rev. Cancer* **2005**, *5*, 65–72.

(4) Tabassum, S.; Pettinari, C. Chemical and Biotechnological Developments in Organotin Cancer Chemotherapy. *J. Organomet. Chem.* **2006**, *691*, 1761–1766.

(5) Schrama, D.; Reisfeld, R. A.; Becker, J. C. Antibody Targeted Drugs as Cancer Therapeutics. *Nat. Rev. Drug Discov.* **2006**, *5*, 147–159.

(6) Orive, G.; Hernández, R. M.; Gascón, A. R.; Domínguez-Gil, A.; Pedraz, J. L. Drug Delivery in Biotechnology: Present and Future. *Curr. Opin. Biotechnol.* **2003**, *14*, 659–664.

(7) Allen, T. M. Drug Delivery Systems: Entering the Mainstream. *Science (80-.).* **2004**, *303*, 1818–1822.

(8) Hu, Q.; Sun, W.; Wang, C.; Gu, Z. Recent Advances of Cocktail Chemotherapy by Combination Drug Delivery Systems. *Adv. Drug Deliv. Rev.* **2016**, *98*, 19–34.

(9) Farjadian, F.; Ghasemi, A.; Gohari, O.; Roointan, A.; Karimi, M.; Hamblin, M. R. Nanopharmaceuticals and Nanomedicines Currently on the Market: Challenges and Opportunities. *Nanomedicine* **2019**, *14*, 93–126.

(10) Satalkar, P.; Elger, B. S.; Hunziker, P.; Shaw, D. Challenges of Clinical Translation in Nanomedicine: A Qualitative Study. *Nanomedicine Nanotechnology, Biol. Med.* **2016**, *12*, 893–900.

(11) Pierce, R. L. Translational Nanomedicine – through the Therapeutic Window. *Nanomedicine* **2015**, *10*, 3249–3260.

(12) Hall, J. B.; Dobrovolskaia, M. A.; Patri, A. K.; McNeil, S. E. Characterization of Nanoparticles for Therapeutics. *Nanomedicine* **2007**, *2*, 789–803.

(13) Patra, J. K.; Das, G.; Fraceto, L. F.; Campos, E. V. R.; Rodriguez-Torres, M. del P.; Acosta-Torres, L. S.; Diaz-Torres, L. A.; Grillo, R.; Swamy, M. K.; Sharma, S.; *et al.* Nano Based Drug Delivery Systems: Recent Developments and Future Prospects. *J. Nanobiotechnology* **2018**, *16*, 71.

(14) Karplus, M.; McCammon, J. A. Molecular Dynamics Simulations of Biomolecules. *Nat. Struct. Biol.* **2002**, *9*, 646–652.

(15) van Gunsteren, W. F.; Dolenc, J.; Mark, A. E. Molecular Simulation as an Aid to Experimentalists. *Curr. Opin. Struct. Biol.* **2008**, *18*, 149–153.

(16) Marrink, S. J.; de Vries, A. H.; Tieleman, D. P. Lipids on the Move: Simulations of Membrane Pores, Domains, Stalks and Curves. *Biochim. Biophys. Acta - Biomembr.* **2009**, *1788*, 149–168.

(17) Bond, P. J.; Holyoake, J.; Ivetac, A.; Khalid, S.; Sansom, M. S. P. Coarse-Grained Molecular Dynamics Simulations of Membrane Proteins and Peptides. *J. Struct. Biol.* **2007**, *157*, 593–605.

(18) Baoukina, S.; Tieleman, D. P. Direct Simulation of Protein-Mediated Vesicle Fusion: Lung Surfactant Protein B. *Biophys. J.* **2010**, *99*, 2134–2142.

(19) Risselada, H. J.; Grubmüller, H. How SNARE Molecules Mediate Membrane Fusion: Recent Insights from Molecular Simulations. *Curr. Opin. Struct. Biol.* **2012**, *22*, 187–196.

(20) Drouffe, J. M.; Maggs, A. C.; Leibler, S. Computer Simulations of Self-Assembled Membranes. *Science (80-.).* **2001**, *254*, 1353–1356.

(21) Noguchi, H.; Takasu, M. Self-Assembly of Amphiphiles into Vesicles: A Brownian Dynamics Simulation. *Phys. Rev. E - Stat. Physics, Plasmas, Fluids, Relat. Interdiscip. Top.* **2001**, *64*, 7.

(22) Yamamoto, S.; Maruyama, Y.; Hyodo, S. Dissipative Particle Dynamics Study of Spontaneous Vesicle Formation of Amphiphilic Molecules. *J. Chem. Phys.* **2002**, *116*, 5842–5849.

(23) Marrink, S. J.; Mark, A. E. The Mechanism of Vesicle Fusion as Revealed by Molecular Dynamics Simulations. *J. Am. Chem. Soc.* **2003**, *125*, 11144–11145.

(24) Markvoort, A. J.; Pieterse, K.; Steijaert, M. N.; Spijker, P.; Hilbers, P. A. J. The Bilayer−Vesicle Transition Is Entropy Driven. *J. Phys. Chem. B* **2005**, *109*, 22649–22654.

(25) De Vries, A. H.; Mark, A. E.; Marrink, S. J. Molecular Dynamics Simulation of the Spontaneous Formation of a Small DPPC Vesicle in Water in Atomistic Detail. *J. Am. Chem. Soc.* **2004**, *126*, 4488–4489.

(26) Ramezanpour, M.; Leung, S. S. W.; Delgado-Magnero, K. H.; Bashe, B. Y. M.; Thewalt, J.; Tieleman, D. P. Computational and Experimental Approaches for Investigating Nanoparticle-Based Drug Delivery Systems. *Biochim. Biophys. Acta - Biomembr.* **2016**, *1858*, 1688–1709.

(27) Ingólfsson, H. I.; Lopez, C. A.; Uusitalo, J. J.; de Jong, D. H.; Gopal, S. M.; Periole, X.; Marrink, S. J. The Power of Coarse Graining in Biomolecular Simulations. *Wiley Interdiscip. Rev. Comput. Mol. Sci.* **2014**, *4*, 225–248.

(28) Marrink, S. J.; de Vries, A. H.; Mark, A. E. Coarse Grained Model for Semiquantitative Lipid Simulations. *J. Phys. Chem. B* **2004**, *108*, 750–760.

(29) Otero-Mato, J. M.; Montes-Campos, H.; Calvelo, M.; García-Fandino, R.; Gallego, L. J.; Pineiro, Á.; Varela, L. M. GADDLE Maps: General Algorithm for Discrete Object Deformations Based on Local Exchange Maps. *J. Chem. Theory Comput.* **2018**, *14*, 466–478.

(30) Rowe, R. C.; Sheskey, P.; Quinn, M. E. *Handbook of Pharmaceutical Excipients – 7th Edition*; Pharmaceutical Press, 2013; Vol. 18.

(31) Silverman, J. A.; Deitcher, S. R. Marqibo® (Vincristine Sulfate Liposome Injection) Improves the Pharmacokinetics and Pharmacodynamics of Vincristine. *Cancer Chemother. Pharmacol.* **2013**, *71*, 555–564.

(32) Huynh, L.; Neale, C.; Pomès, R.; Allen, C. Computational Approaches to the Rational Design of Nanoemulsions, Polymeric Micelles, and Dendrimers for Drug Delivery. *Nanomedicine Nanotechnology, Biol. Med.* **2012**, *8*, 20–36.

(33) Pons, M.; Foradada, M.; Estelrich, J. Liposomes Obtained by the Ethanol Injection Method. *Int. J. Pharm.* **1993**, *95*, 51–56.

(34) Jaafar-Maalej, C.; Diab, R.; Andrieu, V.; Elaissari, A.; Fessi, H. Ethanol Injection Method for Hydrophilic and Lipophilic Drug-Loaded Liposome Preparation. *J. Liposome Res.* **2010**, *20*, 228–243.

(35) Batzri, S.; Korn, E. D. Single Bilayer Liposomes Prepared without Sonication. *Biochim. Biophys. Acta - Biomembr.* **1973**, *298*, 1015–1019.

(36) Dubochet, J.; Adrian, M.; Chang, J. J.; Homo, J. C.; Lepault, J.; McDowall, A. W.; Schultz, P. Cryo-Electron Microscopy of Vitrified Specimens. *Q. Rev. Biophys.* **1988**, *21*, 129–228.

(37) ICH. *Stability Testing of New Drug Substances and Products International Conference on Harmonization of Technical Requirements for Registration of Pharmaceuticals for Human Use*; 2003.

(38) Adams, R. W.; Holroyd, C. M.; Aguilar, J. A.; Nilsson, M.; Morris, G. A. "perfecting" WATERGATE: Clean Proton NMR Spectra from Aqueous Solution. *Chem. Commun.* **2013**, *49*, 358–360.

(39) Johnson Jr, C. S. Diffusion Ordered Nuclear Magnetic Resonance Spectroscopy: Principles and Applications. *Prog. Magn. Reson. Spectrosc.* **1999**, *34*, 203–256.

(40) Evans, R.; Dal Poggetto, G.; Nilsson, M.; Morris, G. A. Improving the Interpretation of Small Molecule Diffusion Coefficients. *Anal. Chem.* **2018**, *90*, 3987–3994.

(41) Marrink, S. J.; Risselada, H. J.; Yefimov, S.; Tieleman, D. P.; De Vries, A. H. The MARTINI Force Field: Coarse Grained Model for Biomolecular Simulations. *J. Phys. Chem. B* **2007**, *111*, 7812–7824.

(42) MARTINI. Coarse Grain Force field for Biomolecules http://www.cgmartini.nl.

(43) Kim, S.; Thiessen, P. A.; Bolton, E. E.; Chen, J.; Fu, G.; Gindulyte, A.; Han, L.; He, J.; He, S.; Shoemaker, B. A.; *et al.* PubChem Substance and Compound Databases. *Nucleic Acids Res.* **2016**, *44*, D1202–D1213.

(44) Hanwell, M. D.; Curtis, D. E.; Lonie, D. C.; Vandermeersch, T.; Zurek, E.; Hutchison, G. R. Avogadro: An Advanced Semantic Chemical Editor, Visualization, and Analysis Platform. *J. Cheminform.* **2012**, *4*, 17.

(45) Stroud, J. Make-na Server http://structure.usc.edu/make-na/server.htmL (accessed Feb 18, 2019).

(46) Bereau, T.; Kremer, K. Automated Parametrization of the Coarse-Grained Martini Force Field for Small Organic Molecules. *J. Chem. Theory Comput.* **2015**, *11*, 2783–2791.

(47) De Jong, D. H.; Singh, G.; Bennett, W. F. D.; Arnarez, C.; Wassenaar, T. A.; Schäfer, L. V.; Periole, X.; Tieleman, D. P.; Marrink, S. J. Improved Parameters for the Martini Coarse-Grained Protein Force Field. *J. Chem. Theory Comput.* **2013**, *9*, 687–697.

(48) Panizon, E.; Bochicchio, D.; Monticelli, L.; Rossi, G. MARTINI Coarse-Grained Models of Polyethylene and Polypropylene. *J. Phys. Chem. B* **2015**, *119*, 8209–8216.

(49) MolMaker. Graph-theoretical 3D design https://github.com/mnmelo/molmaker.

(50) Ingólfsson, H. I.; Thakur, P.; Herold, K. F.; Hobart, E. A.; Ramsey, N. B.; Periole, X.; De Jong, D. H.; Zwama, M.; Yilmaz, D.; Hall, K.; *et al.* Phytochemicals Perturb Membranes and Promiscuously Alter Protein Function. *ACS Chem. Biol.* **2014**, *9*, 1788–1798.

(51) Wassenaar, T. A.; Ingólfsson, H. I.; Böckmann, R. A.; Tieleman, D. P.; Marrink, S. J. Computational Lipidomics with Insane: A Versatile Tool for Generating Custom Membranes for Molecular Simulations. *J. Chem. Theory Comput.* **2015**, *11*, 2144–2155.

(52) Malde, A. K.; Zuo, L.; Breeze, M.; Stroet, M.; Poger, D.; Nair, P. C.; Oostenbrink, C.; Mark, A. E. An Automated Force Field Topology Builder (ATB) and Repository: Version 1.0. *J. Chem. Theory Comput.* **2011**, *7*, 4026–4037.

(53) Hornak, V.; Abel, R.; Okur, A.; Strockbine, B.; Roitberg, A.; Simmerling, C. Comparison of Multiple Amber Force Fields and Development of Improved Protein Backbone Parameters. *Proteins Struct. Funct. Bioinforma.* **2006**, *65*, 712–725.

(54) Periole, X.; Cavalli, M.; Marrink, S. J.; Ceruso, M. A. Combining an Elastic Network with a Coarse-Grained Molecular Force Field: Structure, Dynamics, and Intermolecular Recognition. *J. Chem. Theory Comput.* **2009**, *5*, 2531–2543.

(55) Berendsen, H. J. C. C.; Postma, J. P. M. M.; Van Gunsteren, W. F.; Dinola, A.; Haak, J. R. Molecular Dynamics with Coupling to an External Bath. *J. Chem. Phys.* **1984**, *81*, 3684–3690.

(56) Abraham, M. J.; Murtola, T.; Schulz, R.; Páll, S.; Smith, J. C.; Hess, B.; Lindahl, E. GROMACS: High Performance Molecular Simulations through Multi-Level Parallelism from Laptops to Supercomputers. *SoftwareX* **2015**, *1–2*, 19–25.

(57) European Medicines Agency, E. *Questions and Answers on Ethanol in the Context of the Guideline on "Excipients in the Label and Package Leaflet of Medicinal Products for Human Use" (CPMP/463/00)*; 2014.

(58) Wilhelm, S.; Tavares, A. J.; Dai, Q.; Ohta, S.; Audet, J.; Dvorak, H. F.; Chan, W. C. W. Analysis of Nanoparticle Delivery to Tumours. *Nat. Rev. Mater.* **2016**, *1*, 16014.

(59) Ribeiro, L. N. D. M.; Couto, V. M.; Fraceto, L. F.; De Paula, E. Use of Nanoparticle Concentration as a Tool to Understand the Structural Properties of Colloids. *Sci. Rep.* **2018**, *8*, 982.

(60) Filipe, V.; Hawe, A.; Jiskoot, W. Critical Evaluation of Nanoparticle Tracking Analysis (NTA) by NanoSight for the Measurement of Nanoparticles and Protein Aggregates. *Pharm. Res.* **2010**, *27*, 796–810.

(61) Hou, J.; Ci, H.; Wang, P.; Wang, C.; Lv, B.; Miao, L.; You, G. Nanoparticle Tracking Analysis versus Dynamic Light Scattering: Case Study on the Effect of Ca2+and Alginate on the Aggregation of Cerium Oxide Nanoparticles. *J. Hazard. Mater.* **2018**, *360*, 319–328.

(62) Gao, X.; Lowry, G. V. Progress towards Standardized and Validated Characterizations for Measuring Physicochemical Properties of Manufactured Nanomaterials Relevant to Nano Health and Safety Risks. *NanoImpact*

2018, *9*, 14–30.

(63) Nanosight. *Applications of Nanoparticle Tracking Analysis (NTA) in Nanoparticle Research*; 2009.

(64) Kang, Y.-T.; Kim, Y. J.; Bu, J.; Cho, Y.-H.; Han, S.-W.; Moon, B.-I. High-Purity Capture and Release of Circulating Exosomes Using an Exosome-Specific Dual-Patterned Immunofiltration (ExoDIF) Device. *Nanoscale* **2017**, *9*, 13495–13505.

(65) Bibi, S.; McNeil, S. E.; Christensen, D.; Henriksen-Lacey, M.; Mohammed, A. R.; Wilkhu, J.; Perrie, Y.; Kaur, R.; Lattmann, E. Microscopy Imaging of Liposomes: From Coverslips to Environmental SEM. *Int. J. Pharm.* **2010**, *417*, 138–150.

(66) Kuntsche, J.; Horst, J. C.; Bunjes, H. Cryogenic Transmission Electron Microscopy (Cryo-TEM) for Studying the Morphology of Colloidal Drug Delivery Systems. *Int. J. Pharm.* **2011**, *417*, 120–137.

(67) Klang, V.; Matsko, N. B.; Valenta, C.; Hofer, F. Electron Microscopy of Nanoemulsions: An Essential Tool for Characterisation and Stability Assessment. *Micron* **2012**, *43*, 85–103.

(68) Heurtault, B.; Saulnier, P.; Pech, B.; Proust, J.-E.; Benoit, J.-P. Physico-Chemical Stability of Colloidal Lipid Particles. *Biomaterials* **2003**, *24*, 4283–4300.

(69) Wu, L.; Zhang, J.; Watanabe, W. Physical and Chemical Stability of Drug Nanoparticles. *Adv. Drug Deliv. Rev.* **2011**, *63*, 456–469.

(70) ICH. Stability Testing of New Drug Substances and Products International Conference on Harmonization of Technical Requirements for Registration of Pharmaceuticals for Human Use. **2003**.

(71) Klang, V.; Valenta, C. Lecithin-Based Nanoemulsions. *J. Drug Deliv. Sci. Technol.* **2011**, *21*, 55–76.

(72) Neophytou, C. M.; Constantinou, A. I. Drug Delivery Innovations for Enhancing the Anticancer Potential of Vitamin E Isoforms and Their Derivatives. *Biomed Res. Int.* **2015**, *2015*, 1–16.

(73) Kowalewski, J.; Mäler, L. *Nuclear Spin Relaxation in Liquids: Theory, Experiments, and Applications, Second Edition*; CRC Press: Second edition. | Boca Raton, FL : CRC Press, Taylor & Francis Group, [2018], 2017.

(74) Novoa-Carballal, R.; Fernandez-Megia, E.; Jimenez, C.; Riguera, R. NMR Methods for Unravelling the Spectra of Complex Mixtures. *Nat. Prod. Rep.* **2011**, *28*, 78–98.

(75) Wang, Z.; Leung, M. H. M.; Kee, T. W.; English, D. S. The Role of Charge in the Surfactant-Assisted Stabilization of the Natural Product Curcumin. *Langmuir* **2010**, *26*, 5520–5526.

(76) López-Nicolás, J. M.; García-Carmona, F. Effect of Hydroxypropyl-β-Cyclodextrin on the Aggregation of (E)-Resveratrol in Different Protonation States of the Guest Molecule. *Food Chem.* **2010**, *118*, 648–655.

(77) Baur, J. A.; Sinclair, D. A. Therapeutic Potential of Resveratrol: The in Vivo Evidence. *Nat. Rev. Drug Discov.* **2006**, *5*, 493–506.

(78) Ganta, S.; Amiji, M. Coadministration of Paclitaxel and Curcumin in Nanoemulsion Formulations to Overcome Multidrug Resistance in Tumor Cells. *Mol. Pharm.* **2009**, *6*, 928–939.

(79) Yu, H.; Huang, Q. Improving the Oral Bioavailability of Curcumin Using Novel Organogel-Based Nanoemulsions. *J. Agric. Food Chem.* **2012**, *60*, 5373–5379.

(80) Donsì, F.; Sessa, M.; Mediouni, H.; Mgaidi, A.; Ferrari, G. Encapsulation of Bioactive Compounds in Nanoemulsion-Based Delivery Systems. *Procedia Food Sci.* **2011**, *1*, 1666–1671.

(81) Pangeni, R.; Sharma, S.; Mustafa, G.; Ali, J.; Baboota, S. Vitamin E Loaded Resveratrol Nanoemulsion for Brain Targeting for the Treatment of Parkinson's Disease by Reducing Oxidative Stress. *Nanotechnology* **2014**, *25*, 485102.

(82) Hankins, J. L.; Doshi, U. A.; Haakenson, J. K.; Young, M. M.; Barth, B. M.; Kester, M. The Therapeutic Potential of Nanoscale Sphingolipid Technologies. In *Handbook of Experimental Pharmacology*; Springer, Vienna, 2013; Vol. 215, pp. 197–210.

USC
UNIVERSIDADE
DE SANTIAGO
DE COMPOSTELA

CHAPTER 2

Sphingomyelin-based nanosystems for cancer gene therapy

USC
UNIVERSIDADE
DE SANTIAGO
DE COMPOSTELA

ABSTRACT

The application of nanotechnology to the delivery of anticancer polynucleotides has been generally based on the ionic interaction of the polynucleotide with cationic biomaterials. Such interaction has often led to the instability and premature delivery of the polynucleotide. The objective of this work was to develop an innovative nanocarrier, which may entrap hydrophobically modified oligonucleotides. The nanocarrier was composed of two lipidic ingredients, sphingomyelin (SM), a natural lipid widely distributed in our body, and vitamin E (V). The biocompatibility of Sphingomyelin Nanosystems (SNs) was determined in different *in vitro* and *in vivo* models and compared with that of reference lipid-based nanosystems used in gene delivery (DOTAP) . *In vitro* cell toxicity experiments proved that SNs do not affect cell viability up to concentrations as high as 10 mg/mL. SNs also show a good toxicity profile in terms of hemolytic activity in the same concentration range. Additionally, *in vivo* toxicity studies performed with zebrafish embryos also indicate that neutral SNs are well tolerated nanosystems at a concentration of 3 mg/mL and do not cause loss in body weight of healthy mice after repeated intravenous administration (3 consecutive doses of 60 mg/Kg). With respect to the ability of SNs to incorporate polynucleotides, we evaluate the positive effect of oligonucleotides modified with cholesterol. Results showed that SNs can associate these modified oligonucleotides and deliver them to cancer cells. In conclusion, the overall result of this study supports the idea that SNs are promising nanocarriers for the delivery of oligonucleotides in the context of cancer gene therapy.

USC
UNIVERSIDADE
DE SANTIAGO
DE COMPOSTELA

1. INTRODUCTION

Cancer remains the second leading cause of death. According to the statistics from National Cancer Institute (NCI) and the World Health Organization (WHO), worldwide cancer cases are expected to increase from 14 million to 24 million by 2035 and cancer related deaths will accordingly increase from 8 million to 13 million[1,2].

The number of nanotherapeutic products intended to treat cancer has increased over the last two decades[3,4]. Nanopharmaceuticals products, with approximately 250 nanoproducts including those that are commercialized and in clinical trials, represents nearly 15% of the total pharmaceutical market and the profits estimated by 2019 amount to $400 billion[5]. Among the nanodelivery systems approved by the FDA, the majority of them are liposomes and emulsions[6–9]. Besides, other types of lipid-based nanostructures such as nanocapsules (NCs) and solid lipid nanoparticles (SLN), currently under preclinical investigation, are also attracting significant interest[10]. In this sense, the design of nanosystems with both, appropriate composition[11] and physicochemical properties such as size, shape, surface charge, stability, chemical composition, hydrophilicity/hydrophobicity ratio and surface modification are critical in order to assure their correct interactions with biological systems.

With regard to the utility of nanocarriers for the delivery of polynucleotides[12,13], the majority of them are composed of cationic polymers or lipids that can efficiently complex anionic nucleic acids[14]. However, there are some problems related to this type of formulations. Cationic nanocarriers typically interact with serum proteins, lipoproteins, extracellular matrix, and complement system, leading to aggregation, early release of the associated nucleic acids and/or rapid clearance by the reticuloendothelial system. In addition, toxicity associated to the use of cationic biomaterials has limited their therapeutic potential[15].

Considering the aforementioned information, the main goal of this work has been the evaluation of a new oil-in-water (O/W) neutral nanosystem for the association of oligonucleotides. The key features of the proposed nanosystems are the quick and easy preparation method (avoiding the use of additional surfactants and organic solvents other than ethanol) and the simplicity of the composition (formed just by one oil nuclei, vitamin E, and one stabilizing surfactant, sphingomyelin). Sphingomyelin represents a 2-5% of the total amount of lipids of cell membranes, and has already been successfully used for the preparation of vincristine-loaded liposomes[16], approved for the FDA in 2012 for the treatment of acute lymphoblastic leukemia (Marqibo®). With respect to the oil, vitamin E has a long-track record in pharmaceutical preparations and has additionally been shown to have antioxidant and immunomodulating properties[17,18]. Here we report data supporting the potential utility of neutral SNs for cancer gene therapy applications, a system that could potentially enlighten the design of new therapies avoiding cationic compounds.

2. Materials and methods

2.1. Chemicals

Sphingomyelin (SM, LIPOID E SM) and cationic lipid 1,2-Dioleoyloxy-3-Trimethylammoniumpropanchloride (DOTAP, LIPOID DOTAP) were kindly provided by Lipoid GmbH (Ludwigshafen, Germany). Vitamin E (DL-α-Tocopherol) was purchased from Calbiochem (Merck-Millipore, Darmstadt, Germany). HPLC-grade solvents, acetonitrile and acetic acid 100% were purchased to Fisher Chemicals (Thermo Fisher Scientific, USA) and trimethylamine was provided by Sigma-Aldrich (Madrid, Spain). 3-(4,5-Dimethylthiazol-2-yl)-2,5-Diphenyltetrazolium Bromide was purchased to Thermo Fisher Scientific (Madrid, Spain). Tetraethylthiuram disulphide (TETD) was purchased to Applied Biosystems (Thermo Fisher Scientific) (Madrid, Spain). CPG supports functionalized with C16 (Palmitate SynBase™ CPG 1000/110, cat. Number 2393) and Chol1 (3'-Cholesterol SynBase™ CPG 1000/110, cat. Number 2394) were obtained from Link Technologies (Scotland, UK). CPG support functionalized with CH (3'-Cholesteryl-TEG CPG, cat. Number 20-2975) was obtained from Glen Research (USA). For the introduction of Cy3 cyanine dye we used the Cy3 phosphoramidite (Cyanine-3-CE Phosphoramidite (Cyanine 540), cat. Number 2520) from Link Technologies (Scotland, UK).

2.2. Nanosystem preparation

Sphingomyelin nanosystems (SNs) composed by vitamin E (V) and sphingomyelin (SM) were prepared by adapting a very mild technique previously described in literature for liposome production, the ethanol injection method[19–22]. Briefly, 5mg of V and 0.5mg of SM were dissolved in ethanol in a volume of 100 µl. This ethanol stock solution was next injected to

1mL of ultrapure water under continuous magnetic stirring and nanosystems spontaneously obtained. Moreover, nanosystems containing the most common cationic lipid used in gene therapy, DOTAP, were also prepared for comparison purposes. The ethanolic phase of these nanosystems consisted on 5mg of V, 0.5mg of SM and 0,5 or 0,05mg of DOTAP (10% and 1% respectively), all dissolved in 100µL of ethanol. The addition of components was inverted in this formulation and 1mL of the aqueous phase was added over the 100µL of the ethanolic phase by pouring the one over the other. Nanosystems were then homogenized using a high speed homogenizer (UltraTurrax T10, IKA Labotechnik, Germany) at 8000 rpm for 15 seconds.

Physicochemical characterization

SNs were characterized for their mean particle size and polydispersity index (PdI), by dynamic light scattering (DLS), after a dilution 1:20 in water, and for their zeta potential, by Laser Doppler Anemometry (LDA), using a Zetasizer NanoZS® (Malvern Instruments). Morphological examination of the nanosystems was performed by transmission electron microscopy (TEM) using a JEOL JEM-2010 high-resolution microscope (Peabody, MA, USA) operating between 120 and 200 kV accelerating voltage and configured with a high brightness LaB_6 filament. For the preparation of TEM samples, 10µL of the nanosystem suspension were placed in a copper grid and stained with 1% (w/v) phosphotungstic acid for 10s, washed with 1mL of water and dried overnight under vacuum before TEM analysis.

2.3. Stability

Nanosystems stability was evaluated in several media considered appropriate for further *in vitro* and *in vivo* testing purposes. Firstly, colloidal stability was measured in Phosphate Buffer Saline

(PBS) and Dulbecco's Modified Eagle Medium (DMEM) both non-supplemented and supplemented with Fetal Bovine Serum (FBS) 1%, relevant medium used for cell culture assays. Secondly, stability was determined in human plasma, appropriate evaluation for *in vivo* testing. All stability studies were conducted at 37ºC, under constant horizontal shaking, for up to 24h. In all cases, nanosystems were diluted 1/10 v/v reaching a final nanosystem concentration of 1mg/mL. Subsequently, for measuring reasons, SNs were further diluted 1/10 in water.

2.1. *In vitro* and *in vivo* toxicity evaluation

2.1.1. Cellular viability

MTT assay was used to determine cell cytotoxicity/viability in immortalized cancer cell lines (SW480, colorectal cancer cells, ATCC® CCL-228™). Cells were seeded at a density of 10.000 cells/well and cultured in DMEM supplemented with 10% (v/v) fetal bovine serum (FBS) and 1% (v/v) penicillin/streptomycin, at 37ºC in 5% CO_2 atmosphere. Cells were then incubated at a dilution 1/5 v/v with different concentrations of nanosystems (from 0.01 to 10 mg/mL) in a final volume of 125 µL. After 4 and 24 hours 10 µL of MTT dye solution (5mg/mL in PBS, MTT Alfa Aesar, Germany) was added to each well after dilution 1/10 with non-supplemented medium. After 3 hours of incubation, this solution was removed and formazan crystals were solubilized with 100 µL of DMSO. The absorbance was measured at 570 nm in a microplate spectrophotometer (Multiskan EX, Thermo Labsystems). Cell cytotoxicity/viability (%) was calculated in percentage related to untreated control wells.

2.1.2. Blood compatibility

Hemolytic assay was performed as follows, 100µL of a 3% w/v suspension of heparin-stabilized erythrocytes were plated in a rounded bottom 96 well plate and incubated with nanosystem for 4h at a concentrations from 0.1 to 10 mg/mL (added in a 50µL total volume). Positive and negative controls were 50µL/well of 1% Triton X-100 and PBS respectively. After incubation time, the plate was centrifuged at 1000 RPM for 10 minutes at 4ºC. Subsequently, 80µL of the supernatant were transferred to another 96 well plate and read at 570 nm (absorption maxima of deoxyhemoglobin and oxyhemoglobin). Hemolysis percentage was calculating following the next equation.

Equation 1: Formula for calculation of hemolytic percentage.

$$Hemolysis\ \% = \frac{Sample - PBS\ control}{Triton\ X{-}100\ control - PBS\ control}\ x\ 100$$

2.1.3. Toxicity evaluation in zebrafish embryo

Wild-type zebrafish (*Danio rerio*) embryos were maintained in a controlled aquatic facility with purified and dechlorinated water by a reverse osmosis system, with the following conditions: 27ºC (± 1ºC), pH 7 (± 0.5), 14/10 hours light/dark photoperiod and conductivity 650µS/cm. Embryos were collected and washed with osmosis water in Petri dishes and 0-4hours post fertilization (hpf) were selected with an inverted optical microscope (Nikon TMS) and placed in 96-well plate with 200 µL/well of the different concentrations of the formulations previously diluted in osmosis water (from 0,2 to 2 mg/mL). At least three replicates of the same condition were performed (60 embryos in total) and 24 embryos were used as a negative control (with osmosis water). Zebrafish embryos were observed under inverted optical microscope (Nikon TMS) at 24, 48, 72 and 96h of treatment to analyze development alterations,

malformations, effects on hatching rate and mortality of ones treated with different drug concentrations[26].

2.1.4. *In vivo* toxicity in healthy mice

Dose ranging pilot studies were also carried out in Swiss female mice, with an average weight of 28 g. Body weight and behavior were recorded thorough the study. Animals were dosed with the nanosystems at a concentration of 10 mg/mL (one single dose of 30mg/Kg) (day 1). A second group of animals was injected at day 2 with the nanosystems at a concentration of 20 mg/mL (three consecutive doses of 60mg/Kg every second day). All procedures were approved by the Bioethics Committee for animal experimentation of the University of Santiago of Compostela (CEEA-LU).

2.2. Synthesis of oligonucleotides

To study the encapsulation efficiency in the SNs, we have used a model oligonucleotide (Rlas) correspondent to 18bp DNA oligonucleotides carrying phosphorothioate linkages. In order to increase the interaction of the oligonucleotide with the lipid nanosystem we have modified the Rlas oligonucleotide with relevant lipids moieties such as cholesterol (Rlas-CH). We selected the 3'-position for the introduction of the CH as it is one of the most frequent position in synthetic oligonucleotides to introduce the lipids. In addition, the complementary sequence (Rlas-Com) was prepared together with the same oligonucleotides carrying the fluorescent cyanine dye Cy3 located at the 5' position of the oligonucleotide (Cy3-Rlas-Com). These oligonucleotides have natural phosphodiester linkages and hybridized with the Rlas oligonucleotide forming DNA duplexes[27,28]. Characteristics of the oligonucleotides are shown in **Table 1**.

Table 1. Characteristics of synthesized oligonucleotides (Rlas), modified with CH (Rlas-CH) and with a Cy3 (Rlas-Cy3).

Oligonucleotide	Sequence (5'- 3')	MS Calculated	MS Found
Rlas	CpsGpsTpsTpsTpsCpsCpsTpsTpsTpsGpsTpsTpsCpsTpsGpsGpsA	5732	5753
Rlas-CH	CpsGpsTpsTpsTpsCpsCpsTpsTpsTpsGpsTpsTpsCpsTpsGpsGpsAps-CH	6457	6454
Cy3-Rlas-Com	Cy3-TCCAGAACAAAGGAAACG	6041	6039

ps: phosphorothioate linkage; CH: cholesterol linker; MS: mass spectra

2.3. Association of oligonucleotides to SNs

For the preparation of SNs loaded with the modified oligonucleotides (Rlas-CH and Cy3-Rlas-CH), a variable volume of the oligonucleotide aqueous solution, between 2.5µl and 5µl (depending on the starting oligonucleotide concentration) was incorporated into the 100µL of the organic phase. Theoretical concentration of oligonucleotides into SNs was maintained in 12.5µg/formulation (0.5% in weight with respect to the total weight of the components). Rlas-loaded SNs were isolated by ultracentrifugation to separate the components that do not form part of the nanosystems using an OptimaTM L-90K Ultracentrifuge (Beckman Coulter, 84035xg for 1h at 15ºC) and then resuspended in water to a final volume of 0.2mL. Encapsulation efficiencies (EE%) were determined both directly and indirectly by HPLC quantification (**Equation 2**). Briefly, HPLC analyses were performed in a HPLC System (LaChrom Elite®, VWR-Hitachi) equipped with an autosampler L-2200, pump model L-2130, oven L-2300 and a UV-detector L-2400 settled at 220 nm wavelength with a SunFire C18 (Waters, 5µm, 100Å pore size, 4.6 mm × 250 mm) operating at RT. The mobile phases used were (A) 5% ACN in 0.1 M aqueous TEAA and (B) 70% ACN in 0.1 M aqueous TEAA with

a flow rate of 0.6 mL/min. The chromatographic separation followed the next solvent gradient; t=0, 15%B; t=2min 15%B; t=10min 100%B t=12 15%B, t=15min 15%B.

Equation 2: Indirect and Direct formula for encapsulation efficiency (EE%) calculation.

$$Indirect\ EE\% = \frac{Total\ Rlas\ - Free\ Rlas}{Total\ Rlas} \qquad Direct\ EE\% = \frac{Associated\ Rlas}{Total\ Rlas}$$

2.4. Cell uptake

The internalization of Cy3-Rlas-CH loaded SNs was evaluated in GFP expressing SW480 colorectal cancer cells by confocal laser scan microscopy (Leica TCS SP5, Leica Microsystems, Germany). Cells were seeded onto a 12mm glass coverslips in a 24-well plate 24h before the experiment. After 4h incubation at 37ºC with SNs loading Cy3-Rlas-CH (500ng/well), cells were fixed with PFA 4 % (w/v) (15 min, room temperature) prior to observation under the confocal microscope. Finally, the coverslips containing the fixed cells were mounted over into microscopy slides with Mowiol™ mounting medium (Calbiochem, UK) and stored at -20ºC until visualization.

3. RESULTS AND DISCUSSION

The design of nanosystems intended to deliver anticancer drugs, and notably polynucleotides, has made significant progress over the last decades[29]. The engineering of nanosystems with specific properties such as colloidal stability and safety profiles are critical to further advance in this field and eventually reach the clinics[30]. Nanocarriers designed to deliver polynucleotides have been typically composed of cationic polymers or lipids that can efficiently complex anionic nucleic acids[14]. However, there are some problems related to this type of formulations. In particular, cationic nanocarriers are known to interact with serum proteins, blood cells, and also with the components of the extracellular matrix of tissues and intracellular nucleic acids and proteins. These interactions promote their aggregation and recognition by the mononuclear phagocytic system and the complement activation, hamper their access to cancer cells, and can lead to undesired off-target effects[31]. Overall, this toxicity problem has limited the therapeutic potential of cationic nanosystems[15]. Based on this background information, the main objective of this work has been to determine the potential of neutral SNs regarding to their biocompatibility and capacity to associate polynucleotides and deliver them to cancer cells.

3.1. Nanosystem preparation and physicochemical characterization

Success of cancer nanomedicine has as its main ally an abnormal blood and lymphatic architecture, also known as the enhanced permeability and retention (EPR) effect, which allow the nanosystems to extravasate from leaky vasculature[32,33]. However, it is well documented that the physicochemical properties and composition of nanocarriers play a crucial role in their ability to reach and accumulate in the tumor[32–36].

Sphingomyelin Nanosystems (SNs) were prepared by a previously described ethanol injection technique, schematically represented in **Figure 1**. Following this procedure, SNs can be obtained in a very fast (a few seconds) and reproducible way.

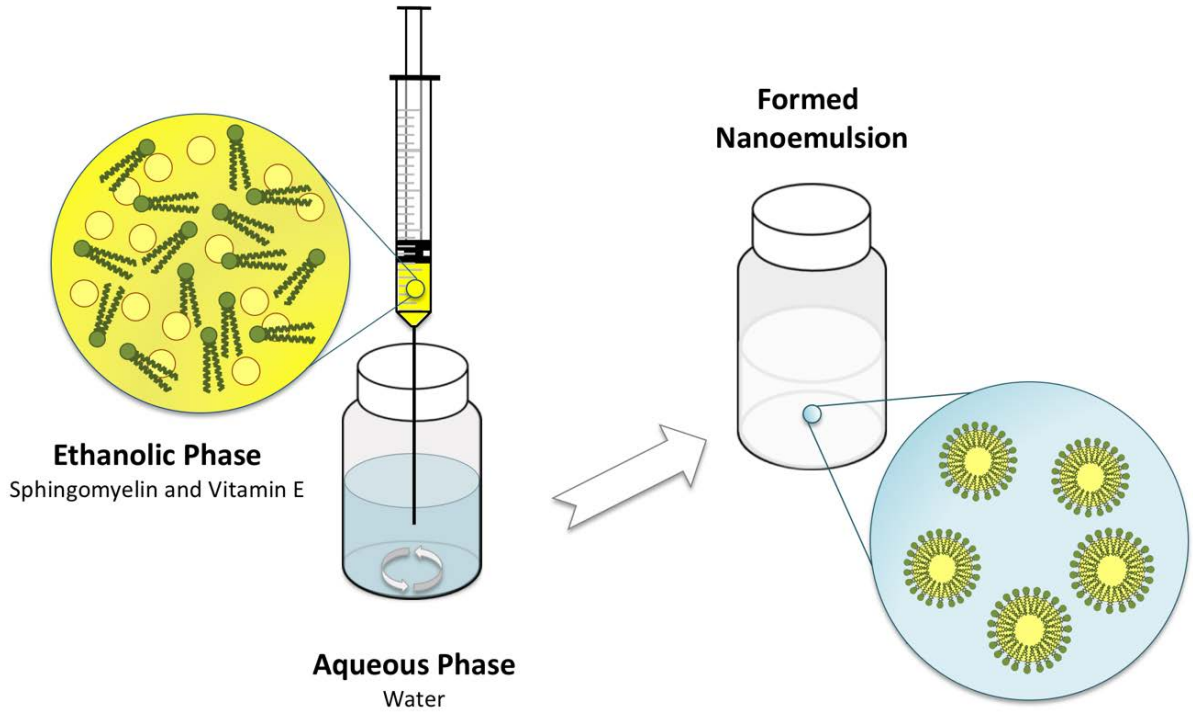

Figure 1: Schematic representation of the ethanol injection method used for nanosystem preparation.

In this work, a full characterization has been done in the particular case of SNs with a composition of vitamin E (V) and sphingomyelin (SM), at a mass ratio 1:0.1 (V:SM 1:0.1). As shown in **Figure 2A-B**, after isolation by ultracentrifugation, SNs presented a mean particle size of 125 ± 15 nm and a zeta potential close to neutral values (-6 ± 3) (**Table 2**). Transmission electron microscope (TEM) images showed a spherical and regular morphology, coherent with the previous physicochemical characterization (**Figure 2C**).

The nanocarrier's size and surface charge are the most widely accepted key parameters in their biological performance. It has been reported that, after intravenous administration, small nanosystems with size <20–30 nm are rapidly cleared by renal excretion, while particles over 200 nm are more efficiently taken up by the mononuclear phagocytic system along with liver,

spleen and bone marrow. Interesting is also the fact that tumor blood vessels present fenestrations ranging between 0.2 and 1.2 μm so that nanosystems with particle size within the 30-200 nm frame can take advantage of the EPR effect[35]. On the other hand, *in vivo*, surface charge determines a number of events such as non-specific cellular uptake, protein corona absorption, circulation half-life, tumor penetration and drug bioability[36,37]. Based on this previous knowledge, the formulation developed in this work having a particle distribution below 200nm and neutral charge could display optimum desirable characteristics for an injectable nanomedicine.

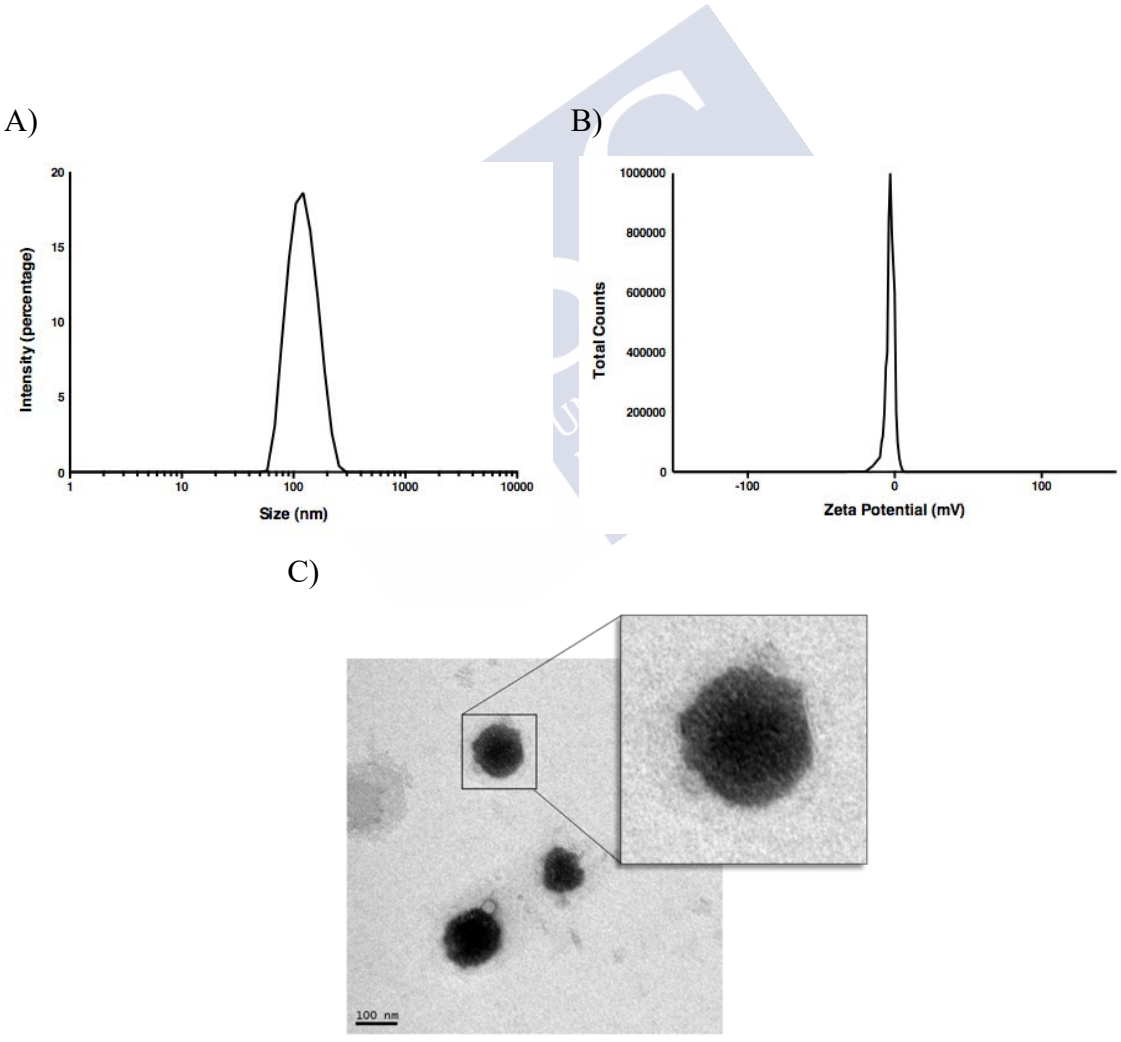

Figure 2. Representative histogram of the average size (A) and zeta potential (B) of SNs. Transmission electron microscopy (TEM) image of SNs (C). SNs were prepared at a V:SM 1:0.1 w/w ratio.

3.2. Stability studies

The assessment of the stability of nanocarriers is critical from the pharmaceutical standpoint[38,39]. The stability of SNs was assessed in different relevant media, namely Phosphate Buffer Saline (PBS) and Dulbecco's Modified Eagle Medium (DMEM) (supplemented or not with Fetal Bovine Serum) and human plasma (**Figure 3**). The results indicate that SNs were only stable in PBS and cell culture medium in the presence of proteins (FBS). The observed increase in the mean size (final particle size 254 ± 12 and 212 ± 24 nm for SNs incubated in PBS-FBS 1% and DMEM-FBS 1% respectively), might be associated to the adsorption of proteins to the nanosystems surface, despite their neutral charge, and the subsequent stabilizing role of the adsorbed proteins. This behavior was also observed upon incubation in plasma. Complementary results (**Figure S1**), indicate that the stability of the formulation in saline could be increased by incorporating a higher amount of SM to the formulation (i.e., V:SM 1:0.2).

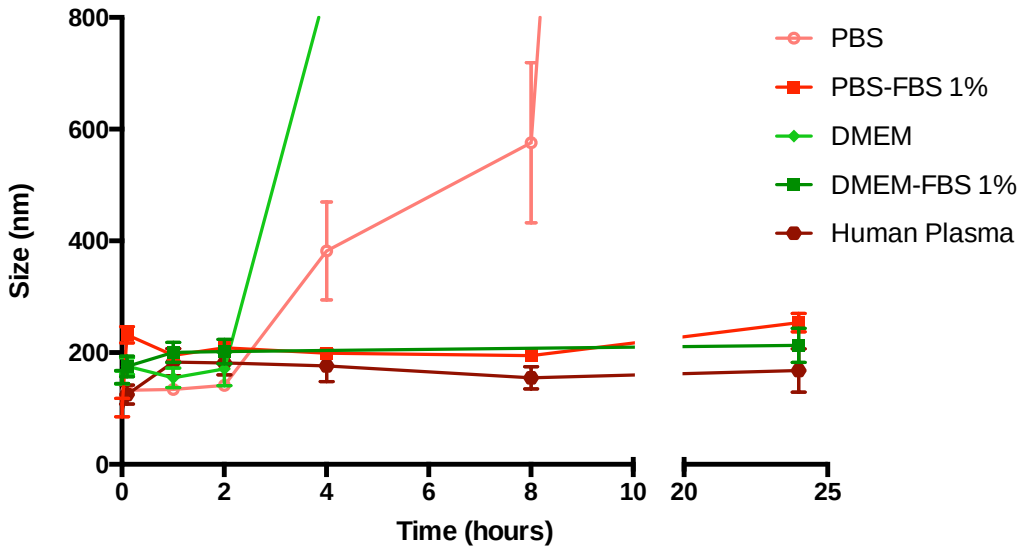

Figure 3: Stability of the nanosystem composed of vitamin E and sphingomyelin (V:SM) at ratio 1:0.1 in different relevant media. PBS: Phosphate Buffer Saline; FBS: Fetal Bovine Serum; DMEM: Dulbecco's Modified Eagle Medium.

3.3. Toxicity studies

The study of toxicity of the developed nanocarriers was thought to be crucial [40–43]. In the case of polynucleotide nanocarriers, complexation with cationic compounds has been the most explored strategy[44]. For this reason, and for the seek of comparison, we developed a nanosystem composed by V and SM in the same ratio than the formulation previously describe, but adding two percentages of the most commonly used cationic lipid in gene therapy applications, DOTAP. Physicochemical properties of formulations containing DOTAP, disclosed in **Table 2,** present a particle size distribution around 110-120nm and a marked positive charge >50mV.

Table 2. Physicochemical characteristics of the three tested nanosystems.

SNs	Ratio	Size (nm)	PdI	Surface Charge (mV)
V:SM	**1:0.1**	125 ± 15	0.1	-6 ± 3
V:SM:DOTAP	**1:0.1:0.01** (1% DOTAP)	122 ± 8	0.2	+51 ± 2
	1:0.1:0.1 (10% DOTAP)	110 ± 3	0.2	+56 ± 5

V: vitamin E; SM: Sphingomyelin; nm: nanometer; PdI: polydispersity index; mV: millivolts.

Two *in vitro* (cytotoxic studies in SW480 colorectal cancer cells and blood compatibility) and two *in vivo* assays (zebrafish embryo model and mice) were selected for the assessment of the toxicity of the developed nanocarriers. Results presented in **Figure 4A**, corresponding to MTT assay, indicate that the exposure of SNs (V:SM) to SW480 cells up to a concentration of 10 mg/mL did not lead to any cytotoxicity, irrespective of the incubation time (4h and 24h). However, considering the same exposure time and concentration, the formulation containing increasing amount of DOTAP (1% and 10%) leads to a dose dependent cell mortality even at

short incubation periods (4h). These results highlight the low cytotoxicity exhibited by the SNs formulation in comparison to the positive charged nanosystem. These results were expected since sphingomyelin is a natural occurring lipid present in high quantity in cell membranes and extracellular vesicles[39,45] and vitamin E is a GRAS-listed oil with a well-known safety track record[46,47]. However, the addition of DOTAP to the SNs, led to an increase of the SNs toxicity due to the intrinsic properties of the cationic lipid[15].

We additionally assessed the blood compatibility of two SNs (V:SM and V:SM:DOTAP 1%) by hemolytic activity. Red blood cells (RBCs)-induced hemolysis is considered to be a simple and reliable measure for evaluating nanosystems related toxicity regarding composition, porosity, geometry and surface functionality. Therefore, quantification of free hemoglobin present in the supernatant of nanosystem-RBCs mixture represent and accurate estimated blood compatibility[23–25]. Results presented in **Figure 4B** indicate that the haemolytic activity of the V:SM formulation remains below the 20% at concentrations equal or below 2.5 mg/mL however, SNs containing DOTAP at 1% exhibited 20% hemolysis from the first concentration tested (0.1mg/mL). This behavior pointed out the importance of the nanosystems surface charge regarding cellular toxicity to erythrocytes.

Concentration as high as 2.5mg/mL are not expected to be found after administration of the formulation to humans or animal models[24,25,48]. Nevertheless, concentrations up to 10 mg/mL were tested showing less than 40% of hemolysis.

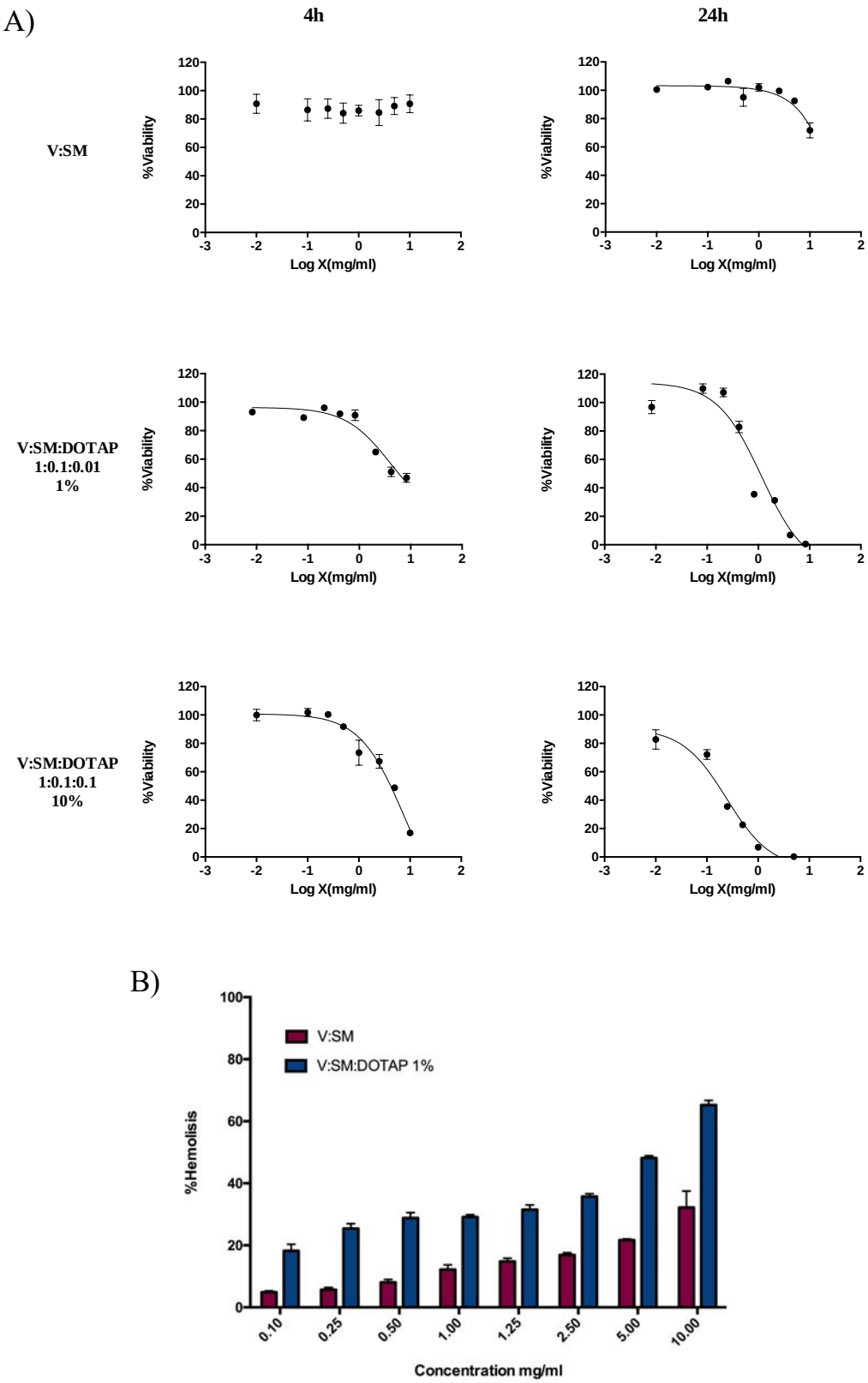

Figure 4: *In vitro* toxicity evaluation of the three developed SNs, i.e. V:SM, 1:0.1, V:SM:DOTAP 1% and V:SM:DOTAP 10% in terms of: (A) Cell viability of SW480 colorectal cancer cells upon exposure to nanosystems for 4h and 24h. (B) Dose dependent hemolysis represented in percentage.

The *in vivo* toxicity evaluation was performed in a zebrafish model, an interesting animal model that allows to test a great amount of conditions being less expensive and less time-consuming than rodents[49]. Results shown in **Figure 5A** indicate that the toxicity of V:SM was very low (<20% zebrafish death, comparable to the negative control consisting in zebrafish embryos with the intact chorion), up to 3 mg/mL concentration. Interestingly, this non-toxic nanosystems presented however, effective interaction with zebrafish embryo (with and without chorionic membrane) confirming its ability to penetrate the embryo without causing apparent damages or death (**Figure S2**). As expected, the nanosystems containing DOTAP presented a marked dose dependent toxicity when compared to the neutral formulation and also among them. Particularly, at a concentration of 3mg/mL, V:SM presented 15% death, V:SM:DOTAP 1% 40% death and V:SM:DOTAP 10% 65% death.

Finally, the nanocarriers toxicity was evaluated in the mice model. Toxicity data measured in terms of body weight, presented in **Figure 5B** indicate that the administration of three consecutive doses of the VSM 1:0.1 at a dose of 60 mg/Kg (cumulant dose of 180mg/kg) did not result in any apparent toxicity. This fact indicates that in the tested range we have not reached the maximum tolerated dose (MTD), so we still have a wide toxicity margin rendering this a promising non-toxic formulation for cancer gene delivery.

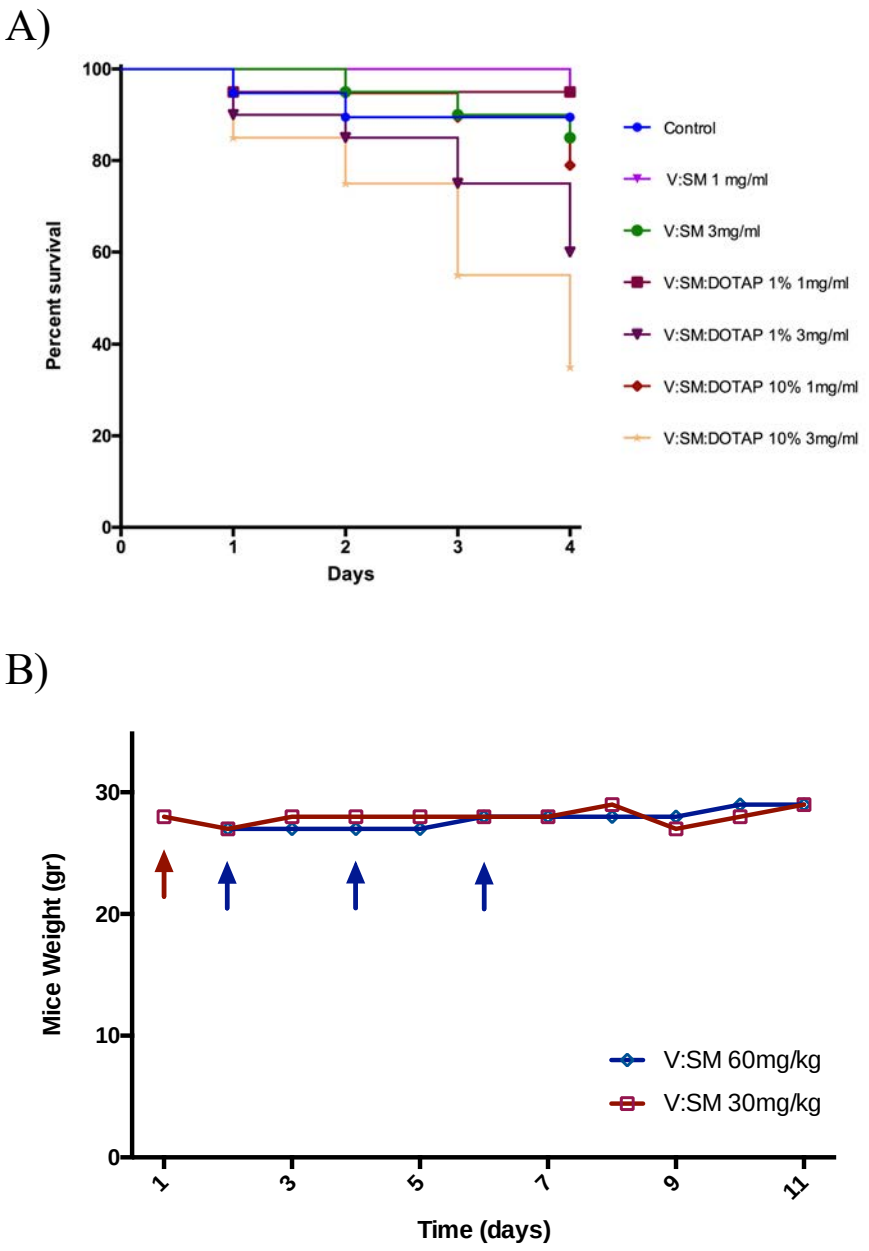

Figure 5: *In vivo* toxicity evaluation of the three developed SNs (V:SM, 1:0.1, V:SM:DOTAP 1% and V:SM:DOTAP 10%) assessed in zebrafish embryo with chorionic membrane (A). Evolution of body weight in mice injected with neutral SNs composed by V:SM 1:0.1. Red arrows: injection of the nanosystem at a concentration of 10 mg/mL nanosystems (dose 30 mg/kg) at day 1. Blue arrows: injection of nanosystems at a concentration of 20 mg/mL (dose 60 mg/kg) at days 2, 4 and 6 (cumulative dose 180mg/Kg) (B).

3.4. Oligonucleotide association and interaction with cancer cells

Next experiments were aimed to associate oligonucleotides (Rlas) to the SNs. For this purpose, we used non-modified Rlas oligonucleotides (wild type, WT) and oligonucleotides chemically modified with cholesterol (Rlas-CH). Modification with CH is an interesting approach due to the amphiphilic character provided to the resulting molecule and to the natural affinity presented between CH and SM as they form liquid ordered phase domains in biological membranes, known as lipid rafts[45]. Indeed, CH modifications have been previously used to incorporate DNA molecules into simulated cell membranes[50]. Therefore, modification of oligonucleotides with CH residues seems to be a coherent strategy to improve their association with neutral nanosystems.

Table 3: Physicochemical properties of V:SM 1:0.1 nanosystems loaded with Rlas-CH and Rlas-WT.

SNs		**Physicochemical Characterization**			
Ratio V:SM	**Oligonucleotide**	**Size**	**PdI**	**ZP**	**AE%**
1:0.1	-	125 ± 15	0.1	-6 ± 3	-
	Rlas-CH	100 ± 8	0.2	-16 ± 2	**19 ± 3**
	Rlas-WT	117 ± 2	0.1	-17 ± 1	**14 ± 0**

PdI: polydispersity index; ZP: zeta potential; AE%: association efficiency represented in percentage; Rlas-CH: oligonucleotide modified with cholesterol moiety; Rlas-WT: non-modified wildtype oligonucleotide. Quantity of vitamin E maintained constant (5mg/formulation).

Results displayed in **Table 3** show the physicochemical properties and association efficiency of Rlas-loaded SNs. Contrary to our expectations, the results indicate that both types of oligonucleotides were associated with the nanosystem. The presence of CH slightly facilitated the association of the oligonucleotides, probably because of the insertion of CH in the interface, acting as a surfactant due to the amphiphilic character of the molecule. It can be observed as

well a decrease in the zeta potential when the oligonucleotides were associated to the nanosystems. Since one of the hypothesis was that the CH residue could favor the disposition of the oligonucleotides at the interface of the nanosystem due to a potential interaction with the SM and to its ability to act as a surfactant, a second experiment was aimed to determine if decreasing the amount of SM (nanosystems were prepared at V:SM ratios lower than 1:0.1), could have a positive effect on the encapsulation efficiency. The results, depicted in **Table 2**, indicate that the association of Rlas-CH to the nanosystem was not dependent on the amount of SM in the formulation.

Table 4. Evaluation of the physicochemical properties of SNs prepared with low amounts of SM and loaded with Rlas-CH and Rlas-WT

Nanosystem components		**Physicochemical Characterization**			
Ratio V:SM	**Rlas Type**	**Size**	**PdI**	**ZP**	**AE%**
1:0.05	**Rlas-CH**	88 ± 2	0.2	-23 ± 1	17 ± 2
1:0.02		105 ± 20	0.2	-25 ± 2	20 ± 3
1:0.01		88 ± 1	0.2	-23 ± 1	19 ± 0
1:0.004		113 ± 2	0.2	-34 ± 1	25 ± 0
1:0.002		111 ± 2	0.2	-37 ± 5	20 ± 0
1:0		102 ± 12	0.2	-34 ± 3	21 ± 3
1:0.002	**Rlas-WT**	**Aggregated**			
1:0					

PdI: polydispersity index; ZP: zeta potential AE%: association efficiency represented in percentage; Rlas-CH: oligonucleotide modified with cholesterol moiety; Rlas-WT: non-modified wildtype oligonucleotide. Theoretical oligonucleotide loading: 0.5%. Quantity of vitamin E maintained constant (5mg/formulation).

Interestingly, we also observed that cholesterol modified oligonucleotides (Rlas-CH) were able to form nanosystem in absence of sphingomyelin, acting that way as the only surfactant

(however studies regarding the stability of these formulations were no performed, and measurements with respect to their size and zeta potential were taken only after preparation). This was not the case for the formulations prepared with the unmodified oligonucleotides (Rlas-WT) in which the lack of the amphiphilic character could not stabilize the oily droplets leading to massive aggregation.

Last experiments were carried out to determine the ability of V:SM 1:0.1 SNs to deliver the associated oligonucleotides to cancer cells. SNs were prepared with Cy3-labelled oligonucleotides. For this purpose, Rlas-CH was covalently linked to Cy3 prior to its incorporation into the nanosystem. Cy3-Rlas-CH loaded SNs had a mean size of 109 ± 5nm, a polydispersity index of 0.1 and a negative zeta potential of -31 ± 2.

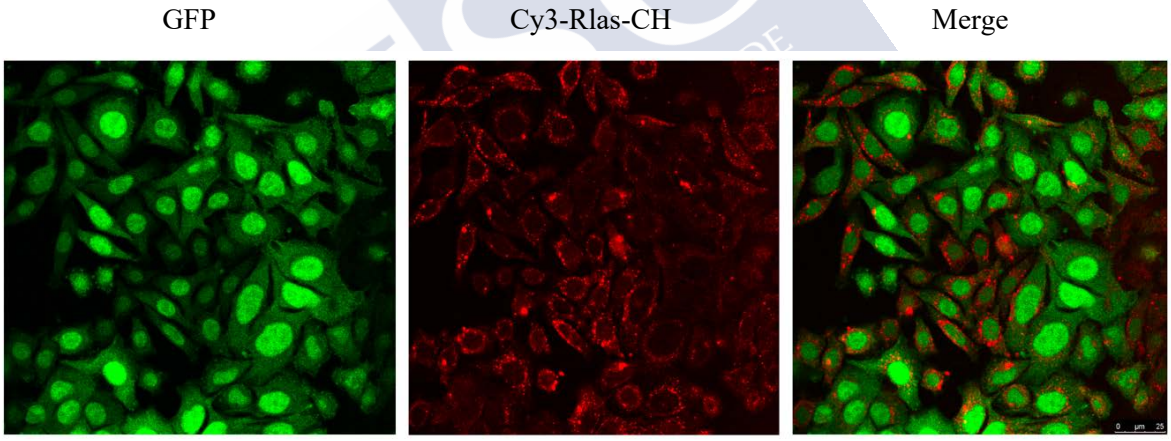

Figure 6: Uptake studies showing 500ng of Cy3-Rlas-CH loaded nanosystems (red) efficiently internalized in SW480 colorectal cancer cells expressing GFP (green).

Figure 6 show the efficient internalization of the Cy3-RIas-CH into the SW480 colorectal cancer cells expressing GFP. Successful internalization into cancer cells confirm the ability of this nanosystems to load and delivery negatively charge oligonucleotides and highlight the potential of neutral nanosystems (based on zwitterionic stabilizing surface) with a safety and stable profile to act as a gene delivery carriers[37,51,52].

4. CONCLUSIONS

Here, we describe the potential of neutral Sphingomyelin Nanosystems (SNs) for the association and delivery of oligonucleotides to cancer cells. Modification of the oligonucleotides with a hydrophobic moiety allow us to moderately improve its association to the SNs and more importantly, it showed the ability to stabilize the organic phase leading to a surfactant-free nanoformulation. SNs presented stable profile in several biological media and did not show toxicity *in vitro* an *in vivo*.

REFERENCES

(1) World Health Organisation. WHO | Cancer http://www.who.int/mediacentre/factsheets/fs297/en/ (accessed Apr 10, 2018).

(2) The National Cancer Institute. Cancer Statistics - National Cancer Institute https://www.cancer.gov/about-cancer/understanding/statistics (accessed Apr 10, 2018).

(3) Bertrand, N.; Wu, J.; Xu, X.; Kamaly, N.; Farokhzad, O. C. Cancer Nanotechnology: The Impact of Passive and Active Targeting in the Era of Modern Cancer Biology. *Adv. Drug Deliv. Rev.* **2014**, *66*, 2–25.

(4) Ferrari, M. Cancer Nanotechnology: Opportunities and Challenges. *Nat. Rev. Cancer* **2005**, *5*, 161–171.

(5) Ragelle, H.; Danhier, F.; Préat, V.; Langer, R.; Anderson, D. G. Nanoparticle-Based Drug Delivery Systems: A Commercial and Regulatory Outlook as the Field Matures. *Expert Opin. Drug Deliv.* **2017**, *14*, 851–864.

(6) Venditto, V. J.; Szoka, F. C. Cancer Nanomedicines: So Many Papers and so Few Drugs! *Adv. Drug Deliv. Rev.* **2013**, *65*, 80–88.

(7) Park, K. Facing the Truth about Nanotechnology in Drug Delivery. *ACS Nano* **2013**, *7*, 7442–7447.

(8) Weissig, V.; Pettinger, T. K.; Murdock, N. Nanopharmaceuticals (Part 1): Products on the Market. *Int. J. Nanomedicine* **2014**, *9*, 4357–4373.

(9) Bulbake, U.; Doppalapudi, S.; Kommineni, N.; Khan, W. Liposomal Formulations in Clinical Use: An Updated Review. *Pharmaceutics* **2017**, *9*, 1–33.

(10) Santalices, I.; Gonella, A.; Torres, D.; Alonso, M. J. Advances on the Formulation of Proteins Using Nanotechnologies. *J. Drug Deliv. Sci. Technol.* **2017**, *42*, 155–180.

(11) Niu, Z.; Conejos-Sánchez, I.; Griffin, B. T.; O'Driscoll, C. M.; Alonso, M. J. Lipid-Based Nanocarriers for Oral Peptide Delivery. *Adv. Drug Deliv. Rev.* **2016**, *106*, 337–354.

(12) Marchant, G. Small Is Beautiful: What Can Nanotechnology Do for Personalized Medicine? *Curr. Pharmacogenomics Person. Med.* **2012**, *7*, 231–237.

(13) Jane, K. Role of Nanobiotechnology in the Development of Personalized Medicine. *Nanomedicine* **2009**, *4*, 249–252.

(14) Ozpolat, B.; Sood, A. K.; Lopez-Berestein, G. Nanomedicine Based Approaches for the Delivery of SiRNA in Cancer. *J. Intern. Med.* **2010**, *267*, 44–53.

(15) Lv, H.; Zhang, S.; Wang, B.; Cui, S.; Yan, J. Toxicity of Cationic Lipids and Cationic Polymers in Gene Delivery. *J. Control. Release* **2006**, *114*, 100–109.

(16) Semple, S. C.; Leone, R.; Wang, J.; Leng, E. C.; Klimuk, S. K.; Eisenhardt, M. L.; Yuan, Z. N.; Edwards, K.; Maurer, N.; Hope, M. J.; *et al.* Optimization and Characterization of a Sphingomyelin/Cholesterol Liposome Formulation of Vinorelbine with Promising Antitumor Activity. *J. Pharm. Sci.* **2005**, *94*, 1024–1038.

(17) Lu, J.; Zhao, W.; Liu, H.; Marquez, R.; Huang, Y.; Zhang, Y.; Li, J.; Xie, W.; Venkataramanan, R.; Xu, L.; *et al.* An Improved D-α-Tocopherol-Based Nanocarrier for Targeted Delivery of Doxorubicin with Reversal of Multidrug Resistance. *J. Control. Release* **2014**, *196*, 272–286.

(18) Kang, T. H.; Knoff, J.; Yeh, W.-H.; Yang, B.; Wang, C.; Kim, Y. S.; Kim, T. W.; Wu, T.-C.; Hung, C.-F. Treatment of Tumors with Vitamin E Suppresses Myeloid Derived Suppressor Cells and Enhances CD8+ T Cell-Mediated Antitumor Effects. *PLoS One* **2014**, *9*, e103562.

(19) Pons, M.; Foradada, M.; Estelrich, J. Liposomes Obtained by the Ethanol Injection Method. *Int. J. Pharm.* **1993**, *95*, 51–56.

(20) Maitani, Y.; Soeda, H.; Junping, W.; Takayama, K. Modified Ethanol Injection Method for Liposomes Containing SS-Sitosterol ß-d-Glucoside. *J. Liposome Res.* **2001**, *11*, 115–125.

(21) Batzri, S.; Korn, E. D. Single Bilayer Liposomes Prepared without Sonication. *BBA - Biomembr.* **1973**, *298*, 1015–

1019.

(22) Jaafar-Maalej, C.; Diab, R.; Andrieu, V.; Elaissari, A.; Fessi, H. Ethanol Injection Method for Hydrophilic and Lipophilic Drug-Loaded Liposome Preparation. *J. Liposome Res.* **2010**, *20*, 228–243.

(23) Lee, D. W.; Powers, K.; Baney, R. Physicochemical Properties and Blood Compatibility of Acylated Chitosan Nanoparticles. *Carbohydr. Polym.* **2004**, *58*, 371–377.

(24) Yu, T.; Malugin, A.; Ghandehari, H. Impact of Silica Nanoparticle Design on Cellular Toxicity and Hemolytic Activity. *ACS Nano* **2011**, *5*, 5717–5728.

(25) Khullar, P.; Singh, V.; Mahal, A.; Dave, P. N.; Thakur, S.; Kaur, G.; Singh, J.; Singh Kamboj, S.; Singh Bakshi, M. Bovine Serum Albumin Bioconjugated Gold Nanoparticles: Synthesis, Hemolysis, and Cytotoxicity toward Cancer Cell Lines. *J. Phys. Chem. C* **2012**, *116*, 8834–8843.

(26) OECD. *Guidelines for the Testing of Chemicals, Fish Embryo Acute Toxicity (FET) Test, Test No. 236.*; OECD, 2013.

(27) Ugarte-Uribe, B.; Grijalvo, S.; Pertíñez, S. N.; Busto, J. V; Martín, C.; Alagia, A.; Goñi, F. M.; Eritja, R.; Alkorta, I. Lipid-Modified Oligonucleotide Conjugates: Insights into Gene Silencing, Interaction with Model Membranes and Cellular Uptake Mechanisms. *Bioorganic Med. Chem.* **2017**, *25*, 175–186.

(28) Grijalvo, S.; Ocampo, S. M.; Perales, J. C.; Eritja, R. Synthesis of Lipid-Oligonucleotide Conjugates for RNA Interference Studies. *Chem. Biodivers.* **2011**, *8*, 287–299.

(29) Cho, K.; Wang, X.; Nie, S.; Chen, Z.; Shin, D. M. Therapeutic Nanoparticles for Drug Delivery in Cancer. *Clin. Cancer Res.* **2008**, *14*, 1310–1316.

(30) Havel, H.; Finch, G.; Strode, P.; Wolfgang, M.; Zale, S.; Bobe, I.; Youssoufian, H.; Peterson, M.; Liu, M. Nanomedicines: From Bench to Bedside and Beyond. *AAPS J.* **2016**, *18*, 1373–1378.

(31) Liang, X.; Liu, L.; Wei, Y.-Q.; Gao, G.-P.; Wei, X.-W. Clinical Evaluations of Toxicity and Efficacy of Nanoparticle-Mediated Gene Therapy. *Hum. Gene Ther.* **2018**, *29*, 1227–1234.

(32) Jain, R. K.; Stylianopoulos, T. Delivering Nanomedicine to Solid Tumors. *Nat. Rev. Clin. Oncol.* **2010**, *7*, 653–664.

(33) Sykes, E. A.; Chen, J.; Zheng, G.; Chan, W. C. W. Investigating the Impact of Nanoparticle Size on Active and Passive Tumor Targeting Efficiency. *ACS Nano* **2014**, *8*, 5696–5706.

(34) He, C.; Hu, Y.; Yin, L.; Tang, C.; Yin, C. Effects of Particle Size and Surface Charge on Cellular Uptake and Biodistribution of Polymeric Nanoparticles. *Biomaterials* **2010**, *31*, 3657–3666.

(35) Desai, N. Challenges in Development of Nanoparticle-Based Therapeutics. *AAPS J.* **2012**, *14*, 282–295.

(36) Wang, H. X.; Zuo, Z. Q.; Du, J. Z.; Wang, Y. C.; Sun, R.; Cao, Z. T.; Ye, X. D.; Wang, J. L.; Leong, K. W.; Wang, J. Surface Charge Critically Affects Tumor Penetration and Therapeutic Efficacy of Cancer Nanomedicines. *Nano Today* **2016**, *11*, 133–144.

(37) García, K. P.; Zarschler, K.; Barbaro, L.; Barreto, J. A.; O'Malley, W.; Spiccia, L.; Stephan, H.; Graham, B. Zwitterionic-Coated "Stealth" Nanoparticles for Biomedical Applications: Recent Advances in Countering Biomolecular Corona Formation and Uptake by the Mononuclear Phagocyte System. *Small* **2014**, *10*, 2516–2529.

(38) Wu, L.; Zhang, J.; Watanabe, W. Physical and Chemical Stability of Drug Nanoparticles. *Adv. Drug Deliv. Rev.* **2011**, *63*, 456–469.

(39) Barenholz, Y. Sphingomyelin and Cholesterol:From Membrane Biophysics and Rafts to Potential Medical Applications. In *Subcellular Biochemistry*; Springer, Boston, MA, 2004; Vol. 37, pp. 167–215.

(40) Reipa, V.; Atha, D. Nanomaterials and Oxidative Stress. *Challenges* **2018**, *9*, 17.

(41) Laurent, S.; Burtea, C.; Thirifays, C.; Häfeli, U. O.; Mahmoudi, M. Crucial Ignored Parameters on Nanotoxicology: The Importance of Toxicity Assay Modifications and "Cell Vision." *PLoS One* **2012**, *7*.

(42) Donaldson, K.; Stone, V.; Tran, C. L.; Kreyling, W.; Borm, P. J. a. Nanotoxicology : A New Frontier in Particle Toxicology Relevant to Both the Workplace and General Environment and to Consumer Safety. *Occup. Environ. Med.*

2004, *61*, 727–728.

(43) Azhdarzadeh, M.; Saei, A. A.; Sharifi, S.; Hajipour, M. J.; Alkilany, A. M.; Sharifzadeh, M.; Ramazani, F.; Laurent, S.; Mashaghi, A.; Mahmoudi, M. Nanotoxicology: Advances and Pitfalls in Research Methodology. *Nanomedicine* **2015**, *10*, 2931–2952.

(44) Verissimo, L. M.; Agnez Lima, L. F.; Monte Egito, L. C.; De Oliveira, A. G.; Do Egito, E. S. T. Pharmaceutical Emulsions: A New Approach for Gene Therapy. *J. Drug Target.* **2010**, *18*, 333–342.

(45) Sezgin, E.; Levental, I.; Mayor, S.; Eggeling, C. The Mystery of Membrane Organization: Composition, Regulation and Roles of Lipid Rafts. *Nat. Rev. Mol. Cell Biol.* **2017**, *18*, 361–374.

(46) Rowe, R. C.; Sheskey, P.; Quinn, M. E. *Handbook of Pharmaceutical Excipients – 7th Edition*; Pharmaceutical Press, 2013; Vol. 18.

(47) Duhem, N.; Danhier, F.; Préat, V. Vitamin E-Based Nanomedicines for Anti-Cancer Drug Delivery. *J. Control. Release* **2014**, *182*, 33–44.

(48) Dobrovolskaia et al. Method for Analysis of Nanoparticle Heolytic Properties In Vitro. *Nano Lett.* **2008**, *8*, 2180–2187.

(49) Gutiérrez-Lovera, C.; Vázquez-Ríos, A.; Guerra-Varela, J.; Sánchez, L.; de la Fuente, M. The Potential of Zebrafish as a Model Organism for Improving the Translation of Genetic Anticancer Nanomedicines. *Genes (Basel).* **2017**, *8*, 349.

(50) Pfeiffer, I.; Höök, F. Bivalent Cholesterol-Based Coupling of Oligonucletides to Lipid Membrane Assemblies. *J. Am. Chem. Soc.* **2004**, *126*, 10224–10225.

(51) Yuan, Y. Y.; Mao, C. Q.; Du, X. J.; Du, J. Z.; Wang, F.; Wang, J. Surface Charge Switchable Nanoparticles Based on Zwitterionic Polymer for Enhanced Drug Delivery to Tumor. *Adv. Mater.* **2012**, *24*, 5476–5480.

(52) Landen, C. N.; Chavez-Reyes, A.; Bucana, C.; Schmandt, R.; Deavers, M. T.; Lopez-Berestein, G.; Sood, A. K. Therapeutic EphA2 Gene Targeting In Vivo Using Neutral Liposomal Small Interfering RNA Delivery. *Cancer Res.* **2005**, *65*, 6910–6918.

SUPPLEMENTARY INFORMATION

Nanosystem stability

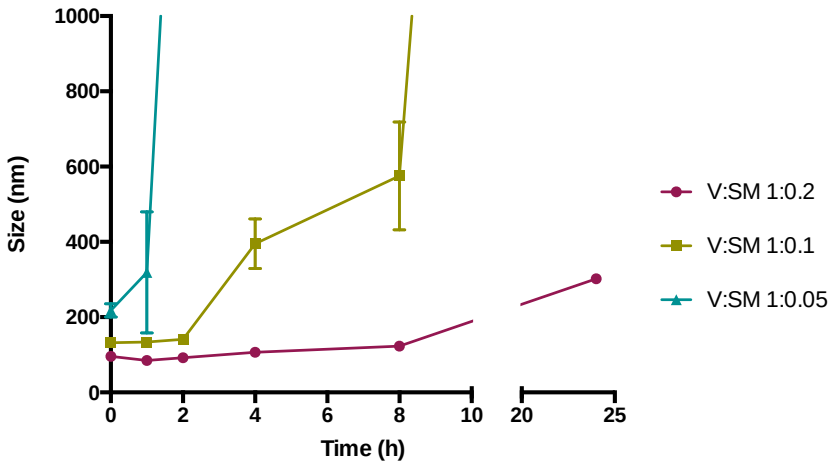

Figure S1. Stability of nanosystems composed by vitamin E (V) and sphingomyelin (SM) prepared at a ratio 1:0.2, 1:0.1 and 1:0.05 upon incubation in PBS. Increasing the amount of sphingomyelin (1:0.05<1:0.1<1:0.2) translates into an increase in PBS stability.

Nanosystem internalization in zebrafish embryo

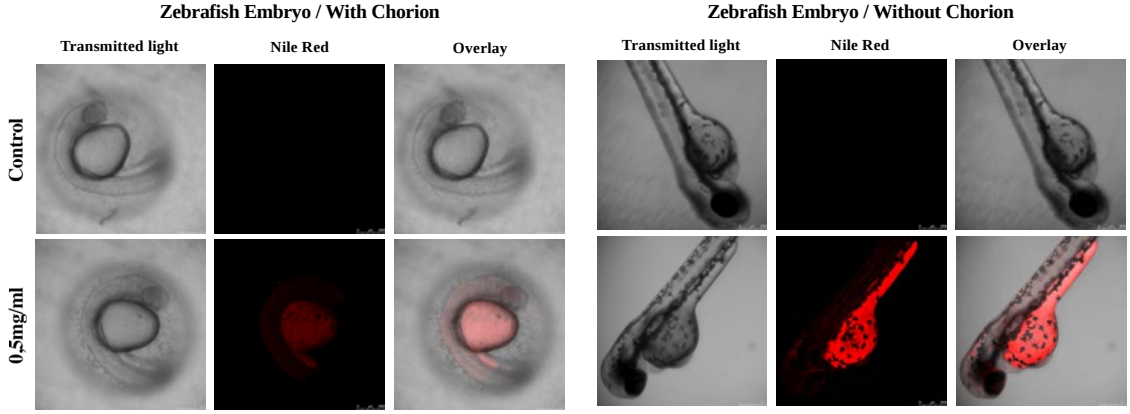

Figure S2. Internalization of Nile red-loaded SNs (V:SM 1:0.1) in zebrafish embryo model with and without the chorionic membrane removed.

CHAPTER 3

Development of a nanotherapy based on a uroguanylin derivative for the treatment of metastatic colorectal cancer

USC
UNIVERSIDADE
DE SANTIAGO
DE COMPOSTELA

ABSTRACT

Colorectal cancer (CRC) is the third most frequently diagnosed cancer malignancy and the second leading cause of cancer-related deaths worldwide. Guanylyl Cyclase C (GCC), a membrane receptor being expressed in 95% primary and metastatic colorectal cancer tumors, is a promising target for the treatment of colorectal cancer. The hormone Uroguanylin (UroG) has been identified as a drug candidate for the GCC target. The objective of this work has been the development of a combination nanotherapy involving UroG and the anticancer drug etoposide. For this purpose, we produced sphingomyelin nanoemulsions (SNs) that were functionalized with a Uroguanylin hydrophobic derivative (UroGm) and loaded with etoposide. The SNs were characterized with regard to their physicochemical properties, the UroG functionalization degree and drug loading. The synergistic effect of both drugs was evaluated *in vitro* and *in vivo*, in a xenograft SW620 mice model. In conclusion, the results showed that UroGm-etoposide-loaded SNs are a potential combination therapy for the treatment of colorectal cancer.

USC
UNIVERSIDADE
DE SANTIAGO
DE COMPOSTELA

1. INTRODUCTION

According to World Health Organization (WHO), cancer causes more deaths than all heart diseases or strokes[1]. Colorectal cancer (CRC) is the third most frequently diagnosed cancer malignancy and the second leading cause of cancer-related deaths in the world, causing approximately 10% of deaths with an increase over 20 million new cancer cases expected annually by 2025[2,3]. Moreover, the presence of local or distant metastasis remains the leading cause of death among cancer patients, with an overall mortality superior to 50%. These facts emphasize an unmet clinical requirement for effective targeting of colorectal cancer metastasis[4].

Guanylyl Cyclase C receptor (commonly referred as GCC or GUCY2C) is expressed at the apical membrane of enterocytes from duodenum to distal rectum and also by primary and metastatic colorectal cancer cells, but not by healthy extraintestinal tissue such as liver and lungs where colorectal cancer cells usually metastasize[5–9]. GCC is activated upon binding to the paracrine hormones Guanylin (Gn) and Uroguanylin (UroG) as well as with the enterotoxigenic *Escherichia coli* heat stable enterotoxin (ST)[10]. GCC-paracrine hormones axis is considered a key regulator of several cellular processes such as differentiation, apoptosis, proliferation and migration[10,11]. Interestingly, numerous works have reported that the levels of mRNA of both guanylin and uroguanylin hormones were markedly downregulated in adenocarcinomas[6,12]. Thus, colorectal tumors, even at first stages, were found to be deficient in the production of guanylin and uroguanylin hormones, but continue expressing high levels of the GCC receptor[13,14]. Moreover, it has been shown that activation of GCC receptor plays a protective role against colorectal cancers[15]. With respect to its use in therapy, Gn, UroG and the ST enterotoxin, have been proposed to inhibit cell proliferation based on GCC activation in

T84, HT29 and CaCo2 cells and its effects were also showed in GCC-/- knockout model[7,16]. In line with these discoveries, some authors have reported the development of radiotracers, based on the chemical modification with the endogenous agonists (UroG, Gn and ST), and exploited the ability to target GCC for PET and SPECT molecular diagnosis[17–20]. Up to date Linaclotide (Gn/UroG mimic peptide produced by Ironwood Pharmaceuticals, approved in 2012 with the commercial name Linzess®/Constella®)) and Plecanatide (UroG derivative synthesized by Synergy Pharmaceuticals, approved in 2017 as Trulance®) are the only two drugs FDA-approved as GCC agonists for the treatment of chronic idiopathic constipation[21,22]. This clinical evidence prompted several GCC agonists (Linaclotide, Plecanatide and Dolcanatide) regarding their potential use for oral cancer chemoprevention[7,14,23,24].

However, to the best of our knowledge, nanosystems designed for targeting GCC have not been reported to date. The advantage of using a nanotherapeutic approach relies on its potential versatility for incorporation of a variety of anticancer drugs, alone or in combinations with biomolecules.

In this work, we propose the preparation of a derivative from the natural hormone uroguanylin (UroG) upon conjugation to a PEG-lipid moiety (UroGm) for its facile incorporation to sphingomyelin nanoemulsions (SNs)[25] with the aim of targeting and treating metastatic colorectal cancer cells expressing the Guanylyl Cyclase C (GCC) receptor. After characterization of the conjugate and preparation of UroGm-SNs, we additionally associated the anticancer drug etoposide (a hydrophobic classical cytostatic drug that inhibits Topoisomerase II enzyme[26]) and studied the potential of this combination therapy for interfering with the proliferation of metastatic colorectal cells.

2. MATERIALS AND METHODS

2.1. Chemicals

C_{18}-PEG_{12}-COOH (MW 825 g/mol) was obtained from Creative PEGWorks (Winston Salem, NC, USA). 4-(4,6-dimethoxy[1,3,5]triazin-2-yl)-4-methylmorpholinium chloride salt (DMTMM·Cl, MW 276.72 g/mol) was purchased from Sigma Aldrich (Madrid, Spain). Uroguanylin (UroG, MW 1667.9 Da; NDDCELCVNACTGCL) was purchased from Bachem (King of Prusia, PA, USA). Oleic Acid was acquired from Sigma Aldrich (Madrid, Spain). Sphingomyelin (Lipoid E SM) was kindly provided by Lipoid GmbH (Ludwigshafen, Germany). Etoposide (purity≥98%) was purchased from Cayman Chemical Company (Ann Arbor, MI, USA). MiniDyalisis Kit, 1kDa cut-off was obtained from GE Healthcare (GE Healthcare Bio-Science Corp., NJ, USA). HPLC grade Acetonitrile (ACN) and Ethanol (EtOH) were obtained from Fisher Chemicals (Thermo Fisher Scientific, USA) and Trifluoroacetic acid (TFA) was provided by Sigma-Aldrich (Madrid, Spain). DMSO (99.8% D) was purchased from (Cortecnet Inc., Paris, France). All other chemicals used were HPLC or UPLC purity grade.

2.2. Synthesis of a uroguanylin derivative with a PEGylated-lipid

Uroguanylin (UroG) was covalently linked to C_{18}-PEG_{12}-COOH through an amide linker. As carboxyl activating agent, DMTMM was used[27,28]. Firstly, stock solutions of all single reagents were prepared: C_{18}-PEG_{12}-COOH and DMTMM were dissolved at 40mg/mL in MilliQ water and UroG was dissolved at 1mg/mL in HEPES 300mM buffer (pH=8)[19]. DMTMM (120eq, 276.72 g/mol) was added over C_{18}-PEG_{12}-COOH solution (100eq, 825 g/mol) under magnetic stirring and left 10 minutes at room temperature (RT) to promote the activation of the carboxylic groups. Then, 200µL of UroG stock solution (1eq, 1667,9 Da) were added dropwise. pH was adjusted by adding HEPES buffer obtaining a final concentration of HEPES 150mM and a pH

of 7.6. The reaction was allowed to proceed for 8h at RT. For purification, the reaction volume was dialyzed against deionized water 3 times for 20h by using a MiniDyalisis Kit (MWCO 1kDa) and then analysed by HPLC, NMR and MALDI-TOF techniques.

2.3. Characterization of the UroG-PEG$_{12}$-C$_{18}$ derivative (UroGm)

2.3.1 NMR

NMR experiments were conducted at 25˚C on a Varian (Agilent) Inova 17.6 T spectrometer (proton resonance 750 MHz), equipped with a 1H/13C/31P triple resonance probe and shielded PFG gradients. The spectrometer control software was VNMRJ 3.2. All the spectra were processed with MestreNova software v11.0 (Mestrelab Research Inc.). The chemical shifts were referenced automatically with respect to the deuterium lock. Samples were prepared in standard 5 mm NMR tubes by dissolving 5 to 10 mg of the product in 50 µL of D_2O and 550 µL of H_2O.

1D proton spectrum (^1H) were acquired for each sample using strong suppression of the water peak with the WET scheme[29]. The spectrum was measured with 64 scans with an inter-scan delay (d1) of 1.4 s and the acquisition time (at) was 0.4 s.

DOSY spectrum were performed with the sequence Doneshot[30]. The sequence is based in the Bipolar Pulse STimulated Echo and was modified to incorporate a watergate 3-9-19 scheme[31] for the suppression of the strong H_2O solvent peak at ~ 4.71 ppm. Each PFG gradient had a rectangular shape and after its application it was followed by stabilization delay 0.4 ms. The pair of bipolar PFG gradients for encoding/decoding diffusion had a total duration (δ) of 3 ms. The diffusion delay (Δ) was set to 300 ms. The diffusion dimension was obtained by linearly varying the strength of the bipolar gradients in 32 steps from 2.5 to 50 G cm^{-1}. Sixteen scans were measured per each point in the diffusion dimension. The intensity of each peak in the 1D

sub-spectrum was fitted to the Stejskal-Tanner equation to determine the diffusion coefficients of the signals[32] by using the analysis module of MestreNova software.

A 2D TOCSY spectrum was measured for UroG-PEG_{12}-C_{18} (UroGm) and UroG samples with a TOCSY sequence that includes a flipback pulse and watergate scheme for the suppression of the strong water signal[31]. The TOCSY period was based on a DIPSI-2 scheme and was applied with a field strength of 8.3 kHz during a mixing time of 80 ms. The spectrum was registered with 48 scans per t1 increment and the number of complex points registered were 4096 and 180 for the T2 and T1 dimensions.

2.3.2 MALDI-TOF

Mass spectra analyses were carried out in an ULTRAFLEX III MALDI TOF/TOF mass spectrometer (Bruker Daltonics, Bremen, Germany) equipped with a 200-Hz smartbeam laser. Samples were spotted onto a HCCA matrix (α-Cyano-4-hydroxycinnamic acid). Calibration of the mass spectra was performed using a standard peptide mixture. MS spectra were acquired in the reflectron positive ion mode within a mass range from 700 to 2000 Da and voltage settled at 25kV.

2.3.3 HPLC

HPLC analyses were performed in a HPLC System LaChrom Elite®, VWR-Hitachi, equipped with an autosampler L-2200, pump model L-2130, oven L-2300 and a UV-detector L-2400 settled at 220nm wavelength. A column Kinetex C8 (Phenomenex, 5µm, 100Å pore size, 4.6 mm × 150 mm) operating at 40ºC was used. Mobile phases were: Solvent A (water 98%, ACN 2%, 0.1% TFA) and Solvent B (ACN 95%, water 5%, 0.1% TFA). Flow rate was settled in 0,6 mL/min. The detection method was optimized obtaining the detailed conditions: t=0,

0%B; t=1min, 0%B; t=2min, 10%B; t=5, 23%B; t=9min, 34%B; t= 11min, 80%B; t=12min, 0%B and t=15min, 0%B.

2.4. Preparation and characterization of UroGm-SNs

Sphingomyelin nanoemulsions incorporating the modified Uroguanylin (UroGm) were prepared by ethanol injection technique. Briefly, UroGm was dissolved in water at a concentration of 0.5mg/mL. On the other hand, oleic acid and sphingomyelin were dissolved in ethanol at a concentration of 200 mg/mL and 40 mg/mL respectively. Subsequently, 50µL of the oily phase (composed by 2.5mg of oil and 0.5mg of surfactant) were subsequently injected into 450µL of ultrapure water (containing the appropriate quantity of UroGm) under continuous magnetic stirring and nanoemulsions were spontaneously formed. Increasing amounts of UroGm were added to the formulation in order to explore the maximum loading capacity (data not shown) establishing a final amount of 10µg of UroGm per formulation as the best condition. Formulations were then isolated by centrifugation (20000 RFC, 45 minutes at 15ºC) using an Eppendorf 5417R centrifuge (Eppendorf, Germany) to eliminate the components that do not form part of the nanosystem.

2.4.1 Physicochemical characterization

Particle size and polydispersity index (PdI) were determined by Dynamic Light Scattering (DLS), and Z-potential values by Laser Doppler Anemometry (LDA), using a Zetasizer NanoZS® (Malvern Instruments). Measurements were performed at 25ºC with a detection angle of 173º upon 1/10 dilution with ultrapure water (MilliQ®).

Nanoemulsions were additionally characterized by Nanoparticle Tracking Analysis (NTA) a method to measure particle size based on imaging of individual nanosystems. Experiments were

conducted with a NanoSight NS3000 System (laser operating at λ=488nm) (Malvern Instruments, Worcestershire, UK). Briefly, nanoemulsions were injected in the sample chamber with a 1000-fold dilution in ultrapure water. Five captures, with a camera level of 14, were used to determine several parameters such as average size, homogeneity and concentration of nanoemulsion particles.

Colloidal stability of the nanoemulsions was determined after being stored at 4º and 37ºC, as well as in biological media (DMEM high glucose) supplemented or not with 1% v/v fetal bovine serum (FBS).

2.4.2. Morphological examination

Morphological examination of the formulation was performed by Field Emission Scanning Electron Microscopy (FESEM) Ultra Plus (Zeiss, Germany) configured with a InLens and STEM mode and operating at 20kV. For the preparation of STEM samples, 20µL of the nanoemulsion suspension were mixed with 20µL of phosphotungstic acid 2% (w/v) and stained during 6 hours. The mixture was placed onto a copper grid with a formvar-carbon film, washed with 500µL of ultrapure water and dried overnight in a desiccator under vacuum.

2.4.3. UroGm density calculation

Efficient incorporation of UroGm into the nanoemulsions surface was determined by NMR. For an accurate quantification, a fraction of the non-isolated UroGm-SNs (total) were collected to quantify the precise amount of the UroGm presented in the formulation. After the isolation of the nanoemulsion, both the supernatant (where the decorated UroGm-SNs are located) and the undernatant (containing the free compounds that remained in solution) were collected for further analysis. These three fractions (i.e. total, supernatant and undernatant) were freeze dried

to remove traces of ethanol that was found to interfere with the analysis (peaks of ethanol overlap with the peak of the PEG in the ^{1}H-NMR spectrum), and eventually dissolved in 500µL of deuterated DMSO (99.8% D). NMR experiments were conducted at 25˚C on a Bruker NEO 17.6 T spectrometer (proton resonance 750 MHz), equipped with a ^{1}H/^{13}C/^{15}N triple resonance probe and shielded PFG z-gradient. All the spectra were processed with MestreNova software v12.0 (Mestrelab Research Inc.). The chemical shifts were referenced automatically with respect to the deuterium lock. Samples were prepared in 5 mm thin wall NMR tubes. A 1D proton spectra (^{1}H) was acquired for each sample using the pulse-acquisition sequence. The spectrum was acquired under quantitative conditions by using a low excitation tilt pulse angle of only 30 degrees, an inter-scan delay (d_1) of 6s and an acquisition time (*aq*) of 2.75s. The proton spectrum was processed with Fourier transformation and the phase and baseline were carefully corrected. For control, plain SNs were also prepared and characterized following the same methodologies as described above without the addition of the UroGm in the aqueous phase. Surface density of UroGm molecules was subsequently calculated as the number of molecules per surface unit of nanoemulsion (nm^2). Firstly, the number of UroGm particles were calculated with **equation 1A** relating to the previously NMR determined concentration. On the other side, surface area of nanoemulsions were calculated following **equation 1B** considering SNs morphology as spheres with the concentration and radium parameters obtained by NTA measurements.

Equation 1: Formulas for calculation of number or particles (A) and surface area of a sphere (B).

$$\text{A)}\quad N_{UroGm} = \frac{Mass\ x\ N_A}{MW} \qquad \text{B)}\quad SA_{SNs} = 4\,\pi\,r^2$$

N_{UroGm}: number of UroGm molecules; NA: Avogadro Constant; MW: molecular weight; SA_{SNs}: SNs Surface Area; r^2: radius squared.

2.5. Preparation of etoposide (Etp) loaded UroGm- SNs

UroGm functionalized sphingomyelin nanoemulsions (UroGm-SNs) were loaded with the chemotherapeutic drug etoposide (UroGm-Etp-SNs). In this case 250µg of etoposide (40mg/mL in DMSO) were placed into the organic phase (section 2.4) within the 50µL of ethanol and injected over the 450µL of ultrapure water containing UroGm. Nanoemulsions were isolated using the same conditions as previously described. Encapsulation efficiency was determined by direct quantification of etoposide in the nanoemulsion using an isocratic HPLC method optimized from a previous reported methodology[33]. Analysis were performed in an HPLC system 1260 Infinity II, Agilent equipped with a pump G7111A, an autosampler G7129A and UV-Vis detector G7114A set at 254nm. Separation was achieved on an InfinityLab Poroshell 120 EC-C18 (100 mm x 4.6 mm, 4 µm pore size) Agilent column. Mobile phases corresponds with a mixture of water an acetonitrile (H_2O:ACN,70:30 v/v) and a flow rate of 1 mL/min. Standard calibration curves were linear in the range of 1 to 15 µg/mL (R^2 = 0.9999).

2.6. *In vitro* studies

2.6.1 Expression of GCC in SW620 and HT29 colorectal cancer cells

Two colorectal cancer cell lines were evaluated regarding the expression of Guanylyl Cyclase C receptor (GCC). HT29 cell lines (ATCC® HTB-38™) were cultured in McCoy 5A medium (Sigma Aldrich, Spain) while SW620 cells (ATCC® CCL-227™) were cultured in Dulbecco's Modified Eagle's Medium (DMEM) High glucose (Sigma Aldrich, Spain). Both mediums were supplemented with 10% (v/v) Fetal Bovine Serum (FBS, Gibco®, LifeTechnologies) and 1% (v/v) penicillin/streptomycin (Sigma Aldrich, Spain) and cells were maintained at 37ºC in 5% CO_2 atmosphere.

For analysis of the expression of the GCC receptor, 100.000 to 150.000 cells were seeded in a 8 wells µ-chamber slides (PCL30108, SPL LifeScience). After 24 h, cells were fixed using paraformaldehyde 4% (PFA 4%) at room temperature for 15 minutes, permeabilized during 10 minutes with Triton X-100 0.2% and blocking with BSA 5% in PBS during 1 hour. Then, the polyclonal antibody rabbit anti-human GCC 1:1000 (ab213430, Abcam, UK) was incubated for 1hour. Secondary antibody Alexa Fluor® 488 polyclonal antibody goat anti-rabbit IgG (ab150077, Abcam, UK) were incubated for 1h at room temperature in the dark. Cell nuclei were stained with Hoechst 33342 (ThermoFisher®) (1:1000). Finally, cells were analyzed under the confocal microscope (Leica SP8, Germany) (Figure S2A). Cells only counter-stained with Hoechst and cells incubated with the secondary antibody, were respectively used as control and negative staining for green secondary antibody signal.

Western blot analysis was also performed to determine the GCC expression levels of the four cell lines (Figure S2B). For that 25 µg of extracted proteins (from 1million cells) were loaded and resolved using 10% SDS polyacrylamide gel electrophoresis (SDS-PAGE). Separated proteins were subsequently transferred to a nitrocellulose membrane 0.45 µm (#1620115, *BIO-RAD*) by electroblotting and probed with the same antibody used for immunofluorescent assay (rabbit anti-human GCC (ab213430, Abcam, UK)). Protein bands were detected by chemiluminescence using kit Pierce ECL (Thermo Fisher ®) for detection reagents.

2.6.2 Cell viability studies

Cell toxicity analyses (MTT) were performed to determine the viability of metastatic colorectal cancer cells SW620 (ATCC® CCL-227™) upon exposure to increasing concentrations of SNs (from 0,01 to 10 mg/mL) in a final volume of 150µL (50µL corresponded to nanoemulsion and 100µL to complete medium). Moreover, Etp-SNs were also tested to evaluate the effect of the

encapsulation of the cytostatic drug. Cells were seeded at a density of 10.000 cells/well in 96-well plates 24h before the experiment. After 48 hours of incubation with SNs and Etp-SNs medium was removed and 100µL of MTT dye solution (5mg/mL in PBS, MTT Alfa Aesar, Germany) were added to each well. After 3-4 hours of incubation this solution was also removed and formazan crystals were solubilised with 100µL of DMSO and maintained at 37ºC for 10 minutes protected from light. Results were obtained by measuring absorbance at 570 nm in a microplate spectrophotometer (Multiskan EX, Thermo Labsystems). Cell viability in percentage (%) was calculated referred to control wells containing cells without treatment.

2.6.3 Internalization studies

Internalization studies in SW620 metastatic cancer cells were performed by confocal microscopy analysis (Leica SP8, Germany). In order to follow the nanosystems, fluorescent UroGm-SNs were prepared by adding the modified lipid TopFluor®-Sphingomyelin in their composition (0.5µg/nanoemulsion). To evaluate cellular uptake 200.000 cells were seeded on a 24-well plate over a glass coverslip. After 24h, cells were washed with PBS and then incubated up to 4h with Etp-SNs, UroGm-SNs and UroGm-Etp-SNs at a concentration of 0.13mg/mL per well (added onto 500 µL of supplemented cell culture medium). After this period, cell medium was removed and cells were washed twice with PBS. Then, they were fixed with paraformaldehyde (4% w/v) for 15 minutes. Cellular nuclei were stained with Hoescht for 5 minutes and afterwards cells were washed three times with PBS. Finally, the coverslips were mounted over microscope slides using Mowiol mounting medium (8µL). Coverslips were dried in the dark overnight.

2.6.4 Colony forming assay

SW620 colorectal cancer cells were plated per triplicate at a density of 600 cells/well in 12-well plates and cultured in a humidified 37ºC incubator with an atmosphere of 5% CO_2. Drug treatments were maintained in contact with cells for the hole duration of the experiment (15 days). After this period cells were stained with MTT solution (5mg/mL) for 3-4 hours and subsequently dried and scanned. Obtained images were analyzed using ImageJ software.

2.7. *In vivo* efficiency of UroGm-Etp-SNs in mice bearing SW620 xenografts

In order to perform the *in vivo* assays, $5x10^6$ SW620 colon cancer cells (ATCC® CCL-227™) dispersed in 100µL of growth media and Matrigel® (BD Bioscences) (3:1) were injected in both flanks of female NMRI-nu mice 4-6 weeks old. Tumor growth was quantified by serial caliper measurements, body weights were recorded, and tumor volumes were calculated ($V = \pi d3/6$). UroGm-Etp-SNs (with a UroGm dose 0.05mg/kg and Etp 0.5mg/kg) were administer at days 4, 7, 11 and 15 of the study.

2.8 Statistical analysis

I*n vitro* differences were statistically determined by one-way ANOVA (GraphPad PRISM, version 6.0, GraphPad Software, Inc.). Besides, *in vivo* statistical analysis were performed with multiple Student's t test. When differences were detected from t test, Wilcoxon signed rank test was used for pairwise differences between control and treatment groups.

3. RESULTS AND DISCUSSION

The design and development of a novel nanocarrier effective in targeting and treating metastatic cancer cells still represent a challenge nowadays[34]. The need to optimize cancer management with treatments that affect cancer cells versus healthy tissues has led to idea of a nanocarrier that could act as the "magic bullet" described by Paul Ehrlich[35]. In this work we propose the synthesis of a Uroguanylin derivative in order to provide a firmer association to functionalize SNs. The nanocarrier was investigated with regard to its toxicity and bioactivity *in vitro*. In addition, upon loading the anticancer drug etoposide, the efficacy of this combination nanotherapy was evaluated both *in vitro* and *in vivo* in a mice model.

3.1. Synthesis and characterization of UroG derivative with a PEGylated lipid

The conjugation of UroG to an amphiphilic molecule, poly(ethylene glycol) (PEG) with a hydrophobic stearic acid derivative (C_{18}), was expected to facilitate the insertion/anchoring of the peptide into SNs while exposing UroG linked to the PEG section in the outer part, thus making it accessible for receptor-recognition. PEGylated lipids, and particularly PEG-DSPE (phosphatidylethanolamine), have been widely used in nanoformulations as surface stabilizers, mainly to improve half-life time in circulation[36,37]. In the last decade, the bifunctionality of PEG has allowed further exploitation for the conjugation of bioactive molecules such as antibodies or peptides as through a great variety of linkers constructing cell-specific targeting nanocarriers[38,39]. Furthermore, peptide-PEG-lipid conjugates can be exhaustively characterized, a fact positively contributes to address later regulatory processes and clinical translation[40].

The primary amino group of UroG were linked to the carboxylic group of the amphiphilic surfactant COOH-PEG_{12}-C_{18}. Activation of the carboxyl group through DMTMM is a simple

reaction where DMTMM chloride generates the activated ester with the release of 4-methylmorpholine in the first step. An amide bond is then formed between the activated ester and the amine present (**Figure 1**). The selection of an amide bond as the linkage functional group was based on its simplicity and non-immunogenicity. Besides, the amide group provides a stable union among peptide and the PEGylated lipid, avoiding a prompt release of the targeting from the nanoemulsion under multiple biological scenarios.

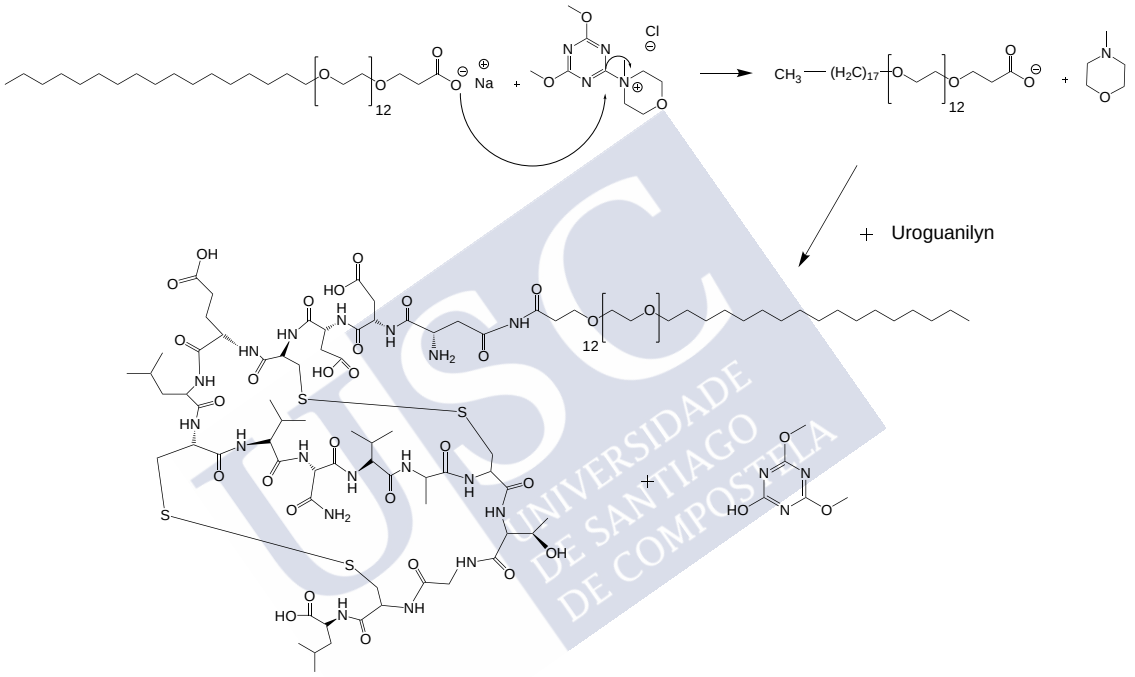

Figure 1. Scheme of the chemical synthesis of the UroG-PEG$_{12}$-C$_{18}$ conjugate (UroGm) through DMTMM-carboxyl activation mechanism.

Uroguanylin reaction progress was monitored by HPLC, evidenced by a decreasing intensity of the original peptide peak along reaction time and its shifting from (tR(UroG) = 13.8 min to tR(UroG-PEG$_{12}$-C$_{18}$) = 14 min (**Figure S1**). Once purification of the reaction was done, HPLC analysis indicated a 75.45% of conjugation yield.

In order to certify the conjugation and the identity of the conjugate, MALDI-TOF analysis were

subsequently carried out. These data provided the MW of the conjugate, approximately 2560 Da, which corresponds to the formation of the 1:1 conjugate (**Figure 2**).

Next, we corroborated this data by NMR analysis experiments: ^{1}H-NMR (**Figure S2A**) and TOCSY (**Figure S2B**) experiments. Moreover, by diffusion NMR (DOSY-NMR) experiments, it was determined the diffusion coefficients (D) of the single reagents (UroG and PEG_{12}-C_{18}) and the reaction product (UroG-PEG_{12}-C_{18} conjugate, UroGm) in D_2O. This parameter is directly related with many intrinsic properties of the molecule such as MW, size, shape or charge. Briefly, the application of NMR field gradients allows to "label" the spins along the direction of the applied gradient. Upon the use of certain pulse sequences, the spectra of the components in a mixture (chemical shifts) can be separated according to their diffusion coefficient, similarly to a size-exclusion chromatography[41,42]. This technique has been used in diverse contexts such bioconjugation studies among others[43]. In the present study, a lower D value of the conjugate was obtained in comparison with non-modified peptide (D_{UroG} = 3.7x10^{-10} m^{2}s^{-1}, D_{UroGm}= 0.45x10^{-10} m^{2}s^{-1}, $D_{C18\text{-}PEG12}$= 0.46x10^{-10} m^{2}s^{-1}) as expected: lower diffusion coefficients correspond to higher MW species (**Figure 3A**). Although in the UroGm sample was not possible to calculate the coefficient through the peptide peaks due to a deficient signal-noise ratio, the PEG-lipid signals were highly robust to calculate the coefficient in a consistent manner. Finally, by TOCSY analysis it was proved the presence of UroG in the conjugate sample (**Figure 3B**). Conjugation is also proved due to the observation of broader peaks, a well-established characteristic after polymer conjugation, as well as the shifting of NH-signals of the UroG in respect of the pure peptide.

Overall, the results of the three characterization techniques led us to conclude that conjugation prompted in a structurally well-defined peptide-PEG-lipid (UroG-PEG_{12}-C_{18}) certifying that UroG peptide was successfully conjugated through an amide bond.

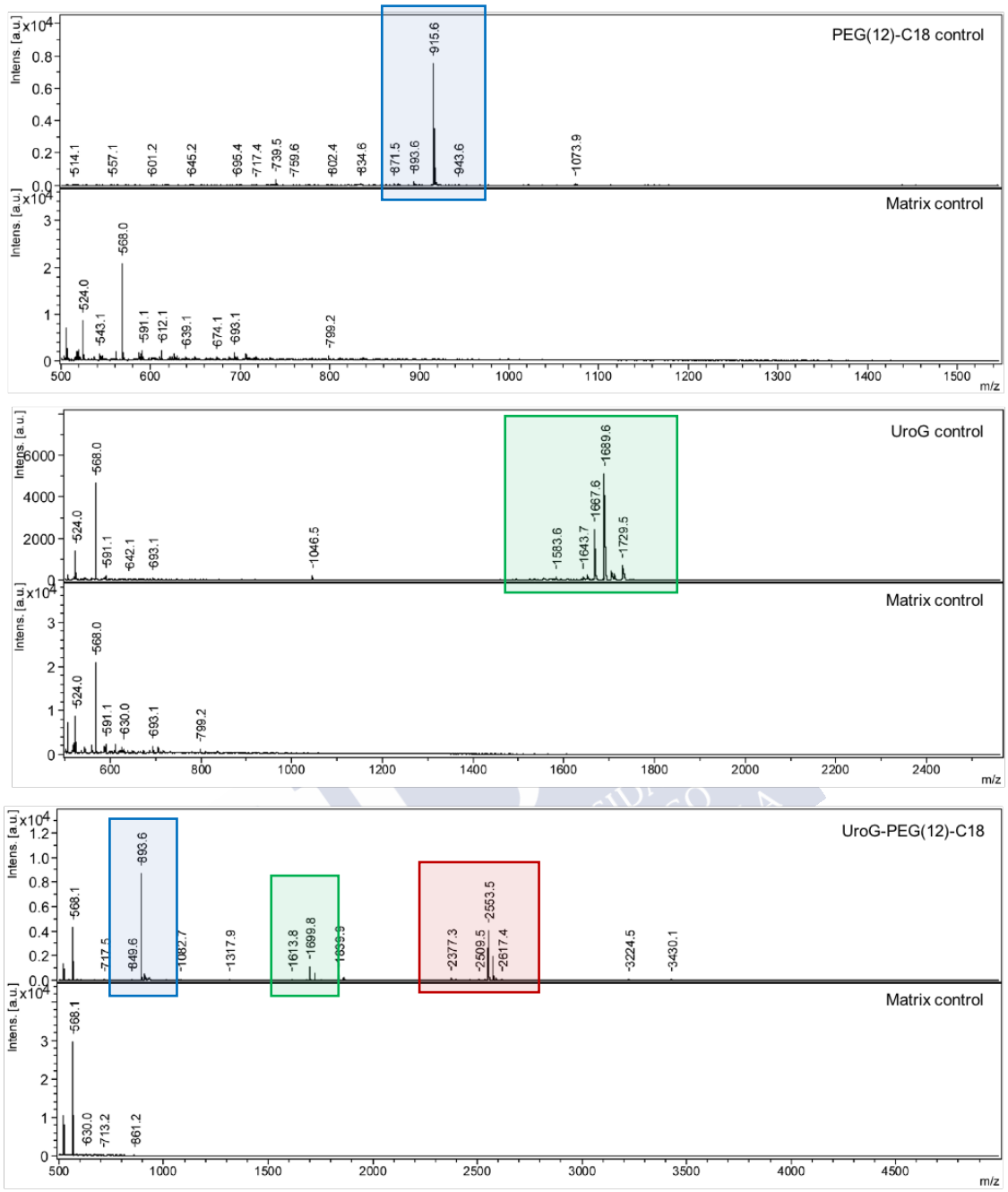

Figure 2. MALDI-TOF signals of COOH-PEG$_{12}$-C$_{18}$ control (blue area), UroG non-modified peptide (green area) and purified conjugate UroGm (red area).

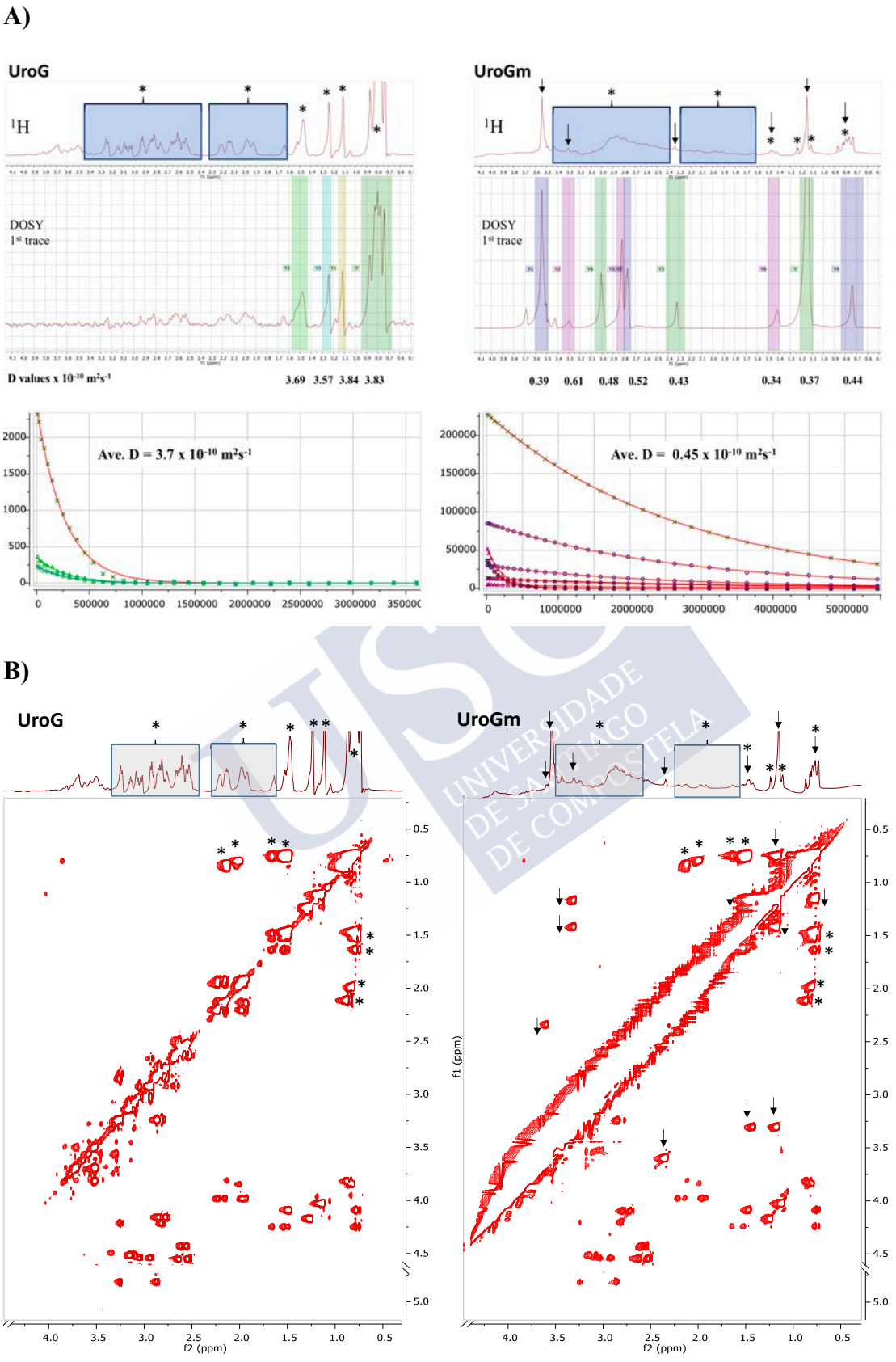

Figure 3. (A) DOSY and (B) TOCSY analysis of the parent peptide UroG (left) and its conjugate UroGm (right) (* = *UroG signals*, ↓=*PEG*$_{12}$-*C*$_{18}$ *signals*).

3.2. Therapeutic activity of UroGm

Uroguanylin have shown in literature not only a targeting capacity to GCC receptor but also a tumor-suppressor function regulating progression of GCC expressing cancer cells and induction of their apoptosis via cyclic GMP (cGMP)[44]. According to this fact tumor colony forming assay was used to evaluate in a quantitative manner the capacity of UroGm to impede the ability of a single cell to grow into a large colony through clonal expansion[45]. Clonogenic (or colony forming) assay is an *in vitro* cell survival assay established for more than 50 years after the publication of Puck and Marcus work in 1956[46]. Fundamentally, the assay enables an assessment of the ability of a single cell to produce a large number of progeny (50 or more cells) after undergoing treatments that can cause cell reproductive death (exposure to ionizing radiation, cytotoxic compounds, genetic manipulation, etc.)[45,47]. Experiments were carried out in a metastatic colorectal cancer cell line constitutively expressing the GCC receptor, SW620[48], as determined by immunofluorescence and western blot assays (**Figure S3**).

After addition of increasing concentrations of UroGm, from 50nm to 1μM, it was observed that the number of colonies significantly decreased as the concentration of UroGm increased (**Figure 4**). Indeed, the anticancer activity of UroG has been previously described mainly for T84 and CaCo-2 colorectal cancer cells for concentrations in the same order of magnitude[44,49]. We, therefore, proved that the hydrophobized derivative (UroGm) preserves the ability of UroG to decrease cell tumorigenicity. This fact is of considerable importance confirming that the biological function of the hormone remains intact. Our modification strategy was consistent with other authors works considering the importance of the carboxy-terminal conserved domain (cysteine domain) for the proper folding and bioactivity of the hormone[19,62].

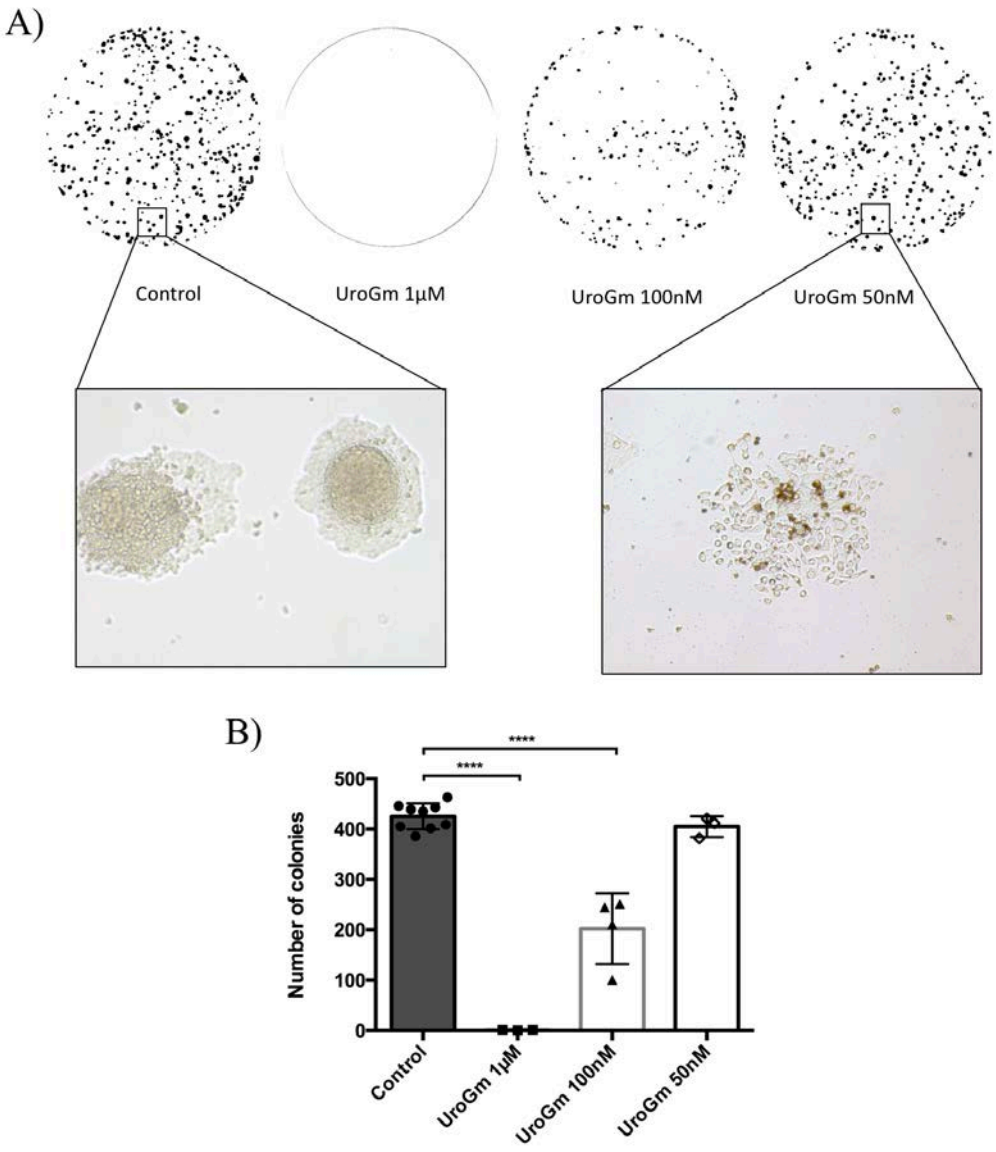

Figure 4. Evaluation of cell proliferation activity by colony forming assay. (A) Image of macroscopic colonies photographed from P12 well plates and cellular detail of control and UroGm 50nM conditions. (B) Graphical representation of the results obtained for cells treated with increasing concentrations of UroGm (**** *P* value < 0.0001)

3.3 Development and characterization of UroGm-SNs

Next experiments were directed to associate UroGm to SNs, previously developed by our group. SNs, composed by a core of oleic acid and stabilized by sphingomyelin, were prepared by ethanol injection method[50–53]. UroGm was incorporated into the aqueous phase following the addition of the lipids dissolved in ethanol. The inclusion of the targeting molecule into the system was expected to happen through its C_{18} lipophilic segment of the conjugate[54–58]. In that way the hydrophilic targeting moiety would be oriented towards the external aqueous phase[59]. Physicochemical properties of the obtained UroGm-SNs (i.e. size, particle homogeneity (PdI and SPAN values), surface charge and concentration) were assessed by Dynamic Light Scattering (DLS), Laser Doppler Anemometry (LDA) and Nanoparticle Tracking Analysis (NTA) techniques (**Table 1)**. UroGm-SNs showed a nanometric size below 150 nm and a negative surface charge due to the presence of oleic acid into the nanoemulsion nuclei. Besides, a slight decrease in the mean particle size were observed for the decorated UroGm-SNs with respect to plain SNs. This variation could be associated to the compaction of the resulting nanosystem as the conjugated peptide could behave as a new surfactant molecule (PEG_{12}-C_{18}) due to its amphiphilic character. Moreover, a change towards more negative values was also observed for the surface charge indicating an efficient association of the negatively charge UroGm conjugate to the nanoemulsion surface. Monodisperse populations were obtained for all developed nanoemulsions being indicated by both PdI $\leq$0.2 and SPAN values $\leq$1. Particle concentration measurements established an average of 5.25 x 10^{11} particles/mL, irrespective of the presence of the peptide. Additionally, morphological examination was investigated by Field Emission Scanning Electron Microscopy (FESEM) (**Figure 5**). Images showed a defined spherical shape which corroborate the same size values observed by the other technics (DLS and NTA). Interestingly, the morphology of the UroGm-SNs was found to be more irregular

than non-decorated SNs, which maybe due to the presence of a more hydrophilic part (corresponding with the PEG chain and the UroG peptide moieties) decorating the surface of the nanostructures.

Table 1. Physicochemical characterization of SNs and UroGm-SNs.

	Zetasizer (DLS and LDA)			Nanosight (NTA)					
Formulation	**Size (nm)**	**PdI**	**ZP (mV)**	**Size (nm)**	**D_{10}**	**D_{50}**	**D_{90}**	**SPAN**	**Conc. (particles/mL)**
SNs	149 ± 10	0.2	-23 ± 5	151 ± 3	107 ± 1	139 ± 3	208 ± 9	0.73	$4.9x10^{11} \pm 3.7x10^{10}$
UroGm-SNs	131 ± 12	0.2	- 44 ± 4	110 ± 2	72 ± 1	95 ± 1	152 ± 4	0.84	$5.6x10^{11} \pm 2.8x10^{10}$

nm: nanometer, PdI: polydispersity index, ZP: zeta potential in millivolts (mV), UroG: Uroguanylin

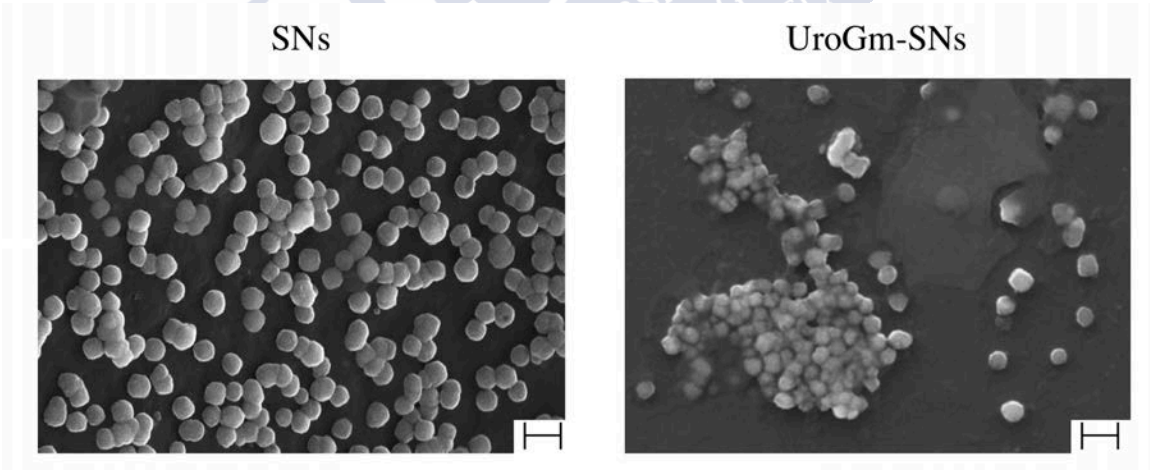

Figure 5. Scanning transmission electron microscope images of SNs and UroGm-decorated SNs using InLens (immersion lens) mode. Scale bar = 200nm

Stability of SNs and UroGm-SNs was next assessed at 37ºC (4 hours) and at storage conditions in refrigerator (4ºC) (50 days). Results presented in **Figure 6** show a good colloidal stability in suspension at the tested conditions as no changes in size were observed over the evaluated

periods. Significant differences were found in the case of SNs and UroGm-SNs incubated in supplemented and non-supplemented cell culture medium (DMEM). As shown in **Figure 6A**, SNs suffered an increase in size during the first hour of incubation in these media, thus suggesting that there is an interaction with the serum proteins (FBS). However, results presented in **Figure 6B** showed that the size of decorated nanoemulsions (UroGm-SNs) remain constant at the tested conditions, showing improved stabilities due to the presence of the amphiphilic UroGm at the interface. Nanosystems coating with both proteins and PEG chains are well known to prevent aggregation and stabilize the particles in cellular mediums by steric hydration repulsions, avoiding the adsorption of further proteins (opsonization)[60].

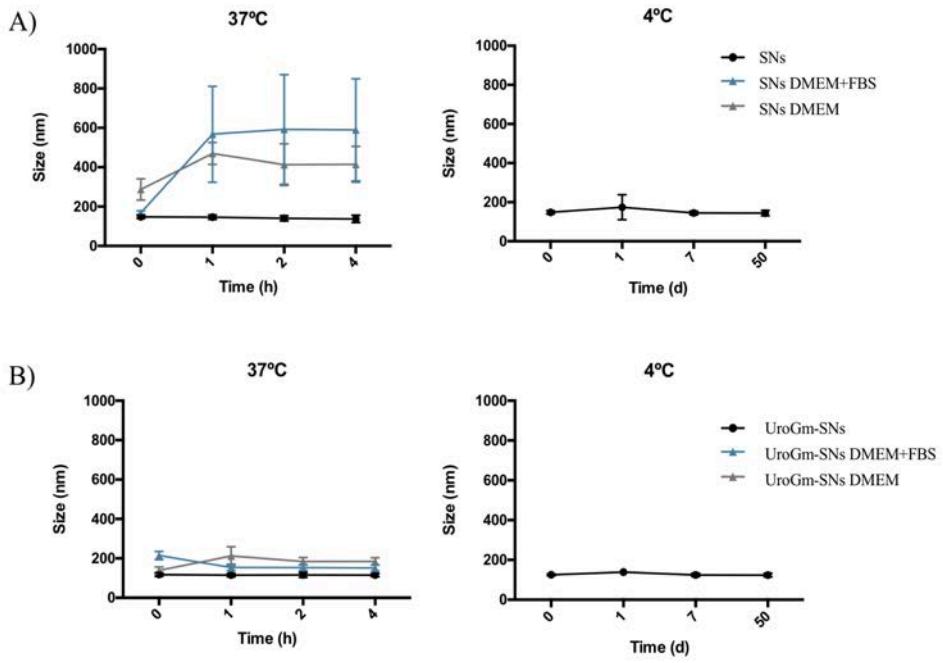

Figure 6. Colloidal stability of non-decorated (SNs) (A) and decorated (UroGm-SNs) (B) at 37ºC in different mediums (supplemented or not with FBS) and at 4ºC in suspension. DMEM: Dulbecco's Modified Eagle Medium; FBS: Fetal Bovine Serum.

Additional evidence of the incorporation of UroGm to SNs was obtained by NMR analysis. **Figure 7** shows the appearance of a signal from the PEG_{12} peak (δ:3.69-3.71) in the spectra of the UroGm, which is also observed in spectra of the functionalized UroGm-SNs, but not in the

spectra of blank SNs. For an accurate integration of UroGm NMR, signals corresponding to PEG_{12} peak were normalized to an internal control (TSP). Calculation of the precise amount of UroGm was done as well by RNM revealing a real UroGm concentration in the formulation of 2.08 ± 0.14 µg/mL.

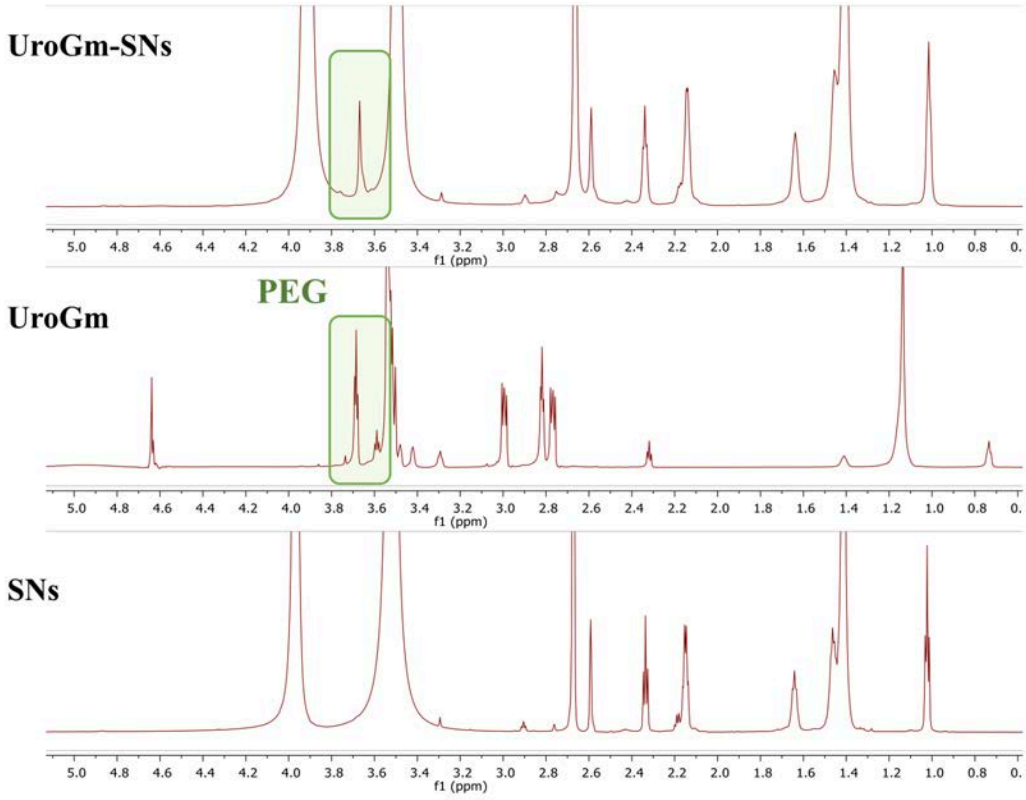

Figure 7. Comparison of the ^{1}H-NMR spectrum between functionalized nanoemulsions (UroG-SNs), UroG-PEG_{12}-C_{18} spectrum and the sphingomyelin nanoemulsions(SNs).

Following **equation 1A and B** (as detailed in section 2.4.3), we estimated a density of 0.012 UroGm molecules/nm^2 of SNs. Many reports in the literature have shown diverse ways to conjugate ligands to nanosystems surface and suggested that increasing conjugated ligands on particles often increases cellular uptake but no specific ligand density has been established for a surface area[61–66]. Calculation of ligand density although is not well established in the literature it could be an interesting parameter to evaluate effective receptor-ligand interaction.

Suitable for comparison with the ligand density presented in this work just a few articles were found in the literature. Values of ligand density in nanostructures calculated in molecules/nm^2 oscillate from 0.225 to 0.005 being in the range with the ones obtained in this work[62,66].

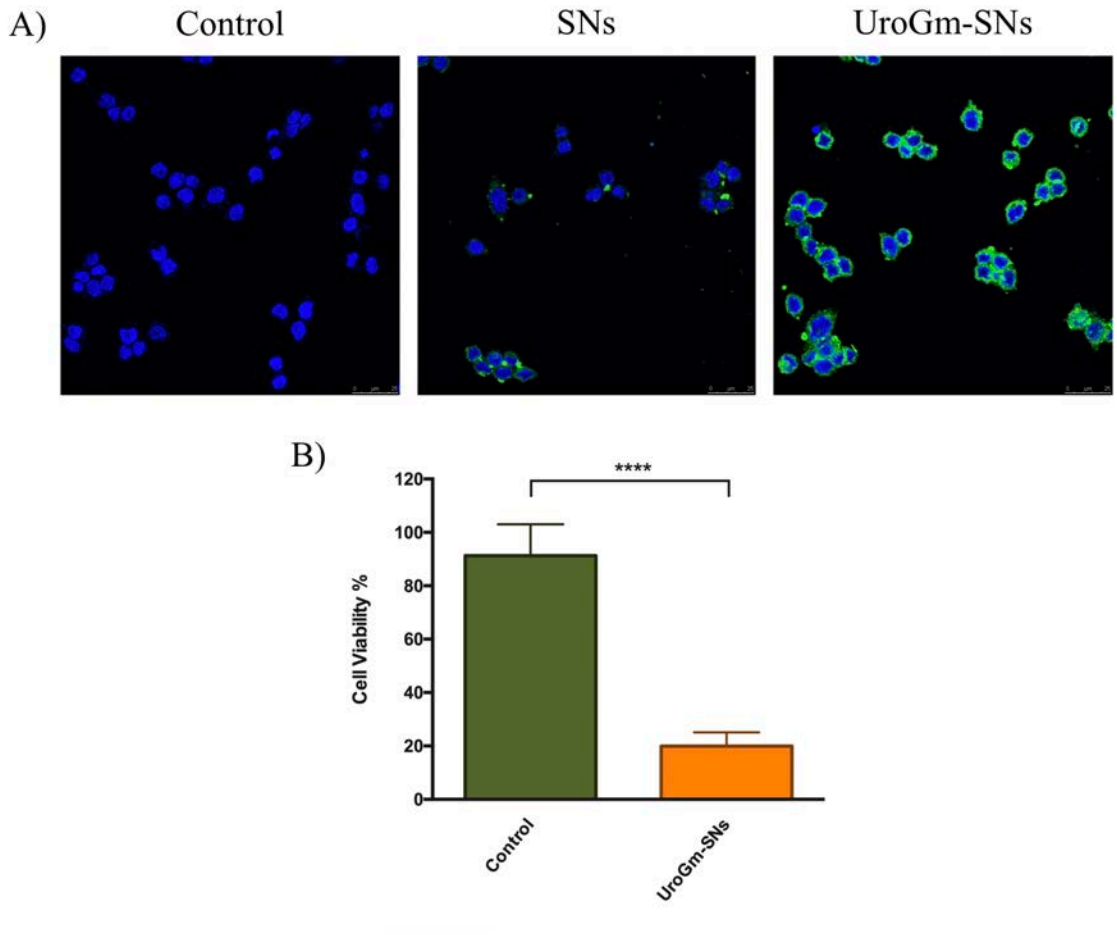

Figure 8. (A) Confocal microscopy images showing the internalization of SNs and UroGm-SNs in SW620 cells after 1 hour incubation. Green channel: TopFluor®–sphingomyelin (TopFluor®–SM) labelled nanoemulsions. Blue channel: nuclei staining with DAPI. (B) MTT results showing the antiproliferative effect of nanoemulsions loading UroGm at a concentration of 0.1mg/mL of SNs. *P value* **** $p < 0.0001$

The effect of the functionalization of SNs with UroGm was evaluated in SW620 metastatic colorectal cancer cells expressing the GCC receptor. We observed that, after 1h incubation, the intensity of the green fluorescence was superior for cells incubated with UroGm-SNs (labeled with TopFluor®–sphingomyelin) than for cells incubated with non-decorated SNs (**Figure 8A**). Additionally, cell viability studies show a decrease in cell viability of SW620 cells treated with

UroGm-SNs proving the potential of this formulation for treating metastatic colorectal cancer (**Figure 8B**). A dose concentration assay with blank SNs show that there is no effect at the tested concentration (**Figure S4**).

3.4 Development of a combination nanotherapy based on UroGm-SNs co-encapsulating cytostatic drug etoposide.

Considering the therapeutic potential of UroGm-SNs, we decided to determine if the loading of this functionalized nanocarrier with an anti-cancer drug would work as a combination therapy. For this, we chose the Topoisomerase II inhibitor, etoposide (Etp), indicated for the treatment of metastatic colorectal cancer [67]. Due to its hydrophobic nature Etp could be dissolved in the inner oily core of the nanoemulsions. The resulting etoposide-loaded UroGm-SNs (UroGm-Etp-SNs) showed a homogeneous distribution of nanoparticles (PdI:0.2, SPAN:0.85) with a similar size to UroGm-SNs (126±14 nm as measured by DLS and 122±2 nm as determined by NTA), and a negative zeta potential (-45±5 mV). Effective incorporation of the conjugated peptide (UroGm) and the anticancer drug etoposide (Etp) into the nanoemulsion was studied respectively by NMR (following PEG signal as previously reported) and HPLC. With respect to the concentration of UroGm, results show similar data in UroGm-Et-SNs with respect to UroGm-SNs (concentration of 2.30±0.12 µg/mL). Being the nanoparticle concentration in UroGm-Etp-SNs of $5.6x10^{11}$ particles/mL, according to NTA measurements, ligand density was calculated as well for the drug-loaded SNs obtaining in this case a value of 0.010 molecules/nm^2. Regarding etoposide, the drug concentration in UroGm-Etp-SNs resulted to be 40.51±5 µg/mL. Therefore, is possible to conclude that etoposide could be successfully included in the formulation, without modifying substantially the ligand density and the properties of UroGm-SNs. Additionally, UroGm-Etp-SNs preserved their capacity to

mediate an improved interaction with colorectal SW620 cells (**Figure S5**).

Experiments were next carried out to explore if the combination of UroGm and etoposide in the same formulation (UroGm-Etp-SNs) could represent a competitive advantage for the treatment of metastatic colorectal cancer. After probing that both UroGm (**Figure 4**) and Etoposide (**Figure S6**) exhibit concentration dependent colony inhibition capacity, we observed that by combining both molecules at subtherapeutic concentrations (as determined, lower than 1.7μM of etoposide and 1μM of UroGm), a potentiated effect could be appreciated (**Figure S7**). This effect could be expected after the joint activation of cGMP-AKT axis by the UroGm and the DNA damage response triggered by Etp[68–70]. Cell viability studies performed with SNs loaded with Etp, UroGm or both molecules in combination, confirmed the therapeutic interest of having both molecules in the same formulation (UroGm-Etp-SNs) (**Figure 9A and B**).

In order to determine the *in vivo* efficacy of the UroG-functionalized drug-loaded SNs, we administered UroGm-Etp-SNs to mice bearing SW620 xenografts, a metastatic colorectal cancer model[71,72]. UroGm-Etp-SNs were administered intravenously as described in **Figure 9C**. Four doses (cumulative dose of 60 mg/kg) were injected at days 4, 7, 11 and 15 (corresponding with dose of 0.2 mg/kg UroG and 2mg/kg Etoposide per mouse). The results of the relative tumor volume shown in **Figure 9D**, indicate that the combination therapy resulted in a moderate but significant reduction of the tumor growth. On the other hand, the results indicated that mice body weight at the end point of the study did not differ between control and treated groups reflecting a good overall health status for both groups (**Figure S8**).

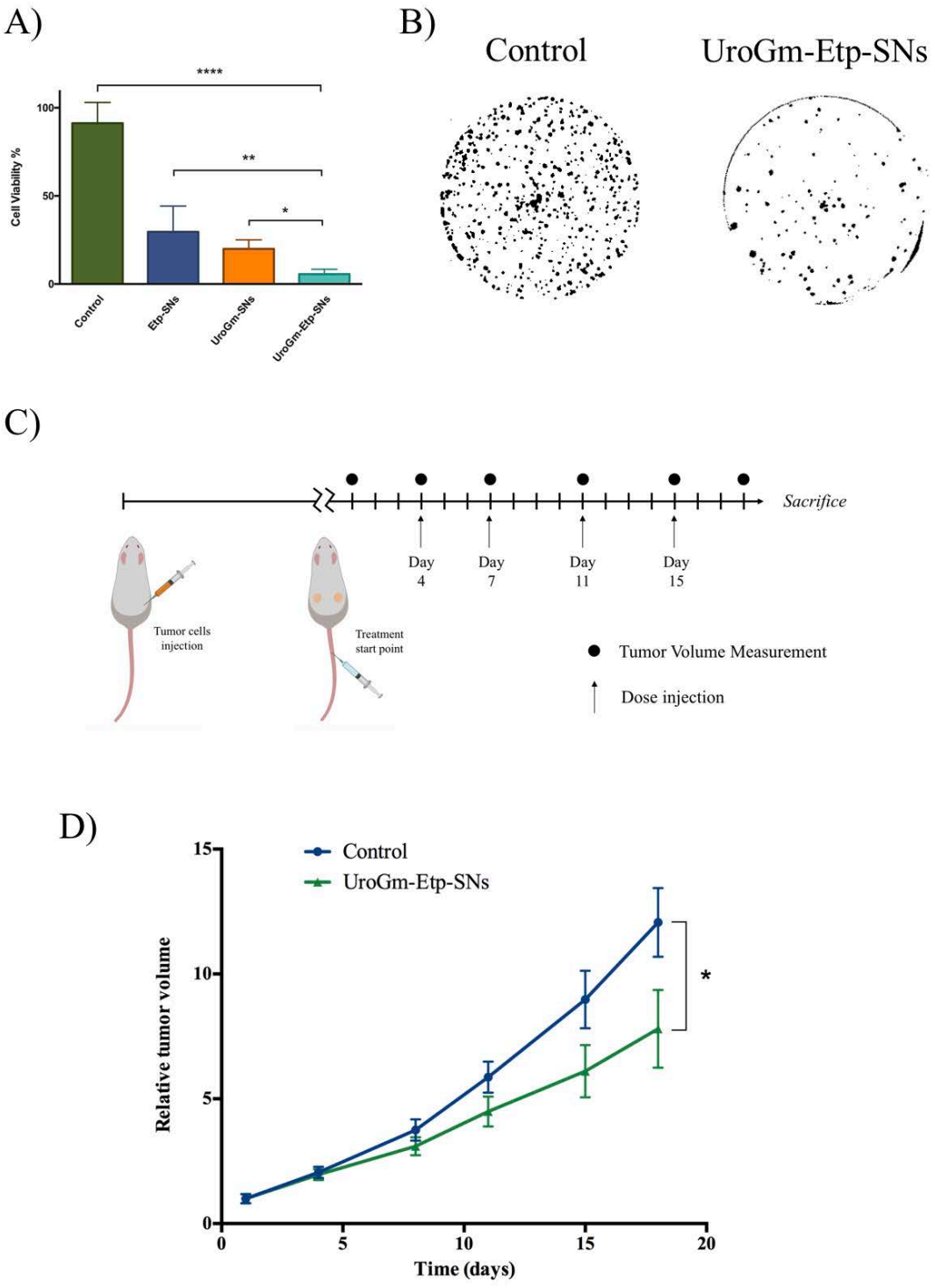

Figure 9. (A) Cell viability results showing the antiproliferative effect of nanoemulsions loading Etp, UroGm and the combination of both at a concentration of 0.1mg/mL of SNs. *P value* **** $p < 0.0001$; ** $p < 0.01$; * $p < 0.1$ **(B)** Macroscopic photograph captured from control well and UroGm-Etp-SNs well at a concentration of 500nM Etp and 50nM UroGm **(C)** Experimental *in vivo* timeline schedule of multiple dose **(D)** Antitumor effect in terms of relative tumor volume growth. Data presented for control mice (n=7) and UroGm-Etp-SNs treated mice (n=6).

4. Conclusions

In this work we have successfully proved the potential of sphingomyelin nanosystems (SNs) to act as a carrier for combination therapy against metastatic colorectal cancer. From our knowledge there is no studies using the UroG hormone either alone or in combination with other drugs as a therapy associated with nanosystems. Therefore, the combination of a new biological therapy (based on UroG replacement) with a chemotherapeutic drug (etoposide) might represent a new line of treatment of metastatic colorectal cancer.

REFERENCES

(1) World Health Organisation. WHO | Cancer http://www.who.int/mediacentre/factsheets/fs297/en/.

(2) Ferlay, J.; Soerjomataram, I.; Dikshit, R.; Eser, S.; Mathers, C.; Rebelo, M.; Parkin, D. M.; Forman, D.; Bray, F. Cancer Incidence and Mortality Worldwide: Sources, Methods and Major Patterns in GLOBOCAN 2012. *Int. J. Cancer* **2015**, *136*, E359–E386.

(3) Arnold M, Sierra MS, Laversanne M, et al. Global Patterns and Trends in Colorectal Cancer Incidence and Mortality. *Gut* **2016**, *66*, 683–691.

(4) Chang, C.; Marszlowicz, G.; Waldman, Z.; Li, P.; Snook, A. E.; Lin, J. E.; Schulz, S.; Waldman, S. A. Guanylyl Cyclase C as a Biomarker for Targeted Imaging and Therapy of Metastatic Colorectal Cancer. *Biomark Med* **2009**, *3*, 33–45.

(5) Potter, L. R. Regulation and Therapeutic Targeting of Peptide-Activated Receptor Guanylyl Cyclases. *Pharmacol. Ther.* **2011**, *130*, 71–82.

(6) Forte, L. R. Uroguanylin and Guanylin Peptides: Pharmacology and Experimental Therapeutics. *Pharmacol. Ther.* **2004**, *104*, 137–162.

(7) Pitari, G. M.; Li, P.; Lin, J. E.; Zuzga, D.; Gibbons, A. V.; Snook, A. E.; Schulz, S.; Waldman, S. A. The Paracrine Hormone Hypothesis of Colorectal Cancer. *Clin. Pharmacol. Ther.* **2007**, *82*, 441–447.

(8) Camici, M. Guanylin Peptides and Colorectal Cancer (CRC). *Biomed. Pharmacother.* **2008**, *62*, 70–76.

(9) Buc, E.; Der Vartanian, M.; Darcha, C.; Déchelotte, P.; Pezet, D. Guanylyl Cyclase C as a Reliable Immunohistochemical Marker and Its Ligand Escherichia Coli Heat-Stable Enterotoxin as a Potential Protein-Delivering Vehicle for Colorectal Cancer Cells. *Eur. J. Cancer* **2005**, *41*, 1618–1627.

(10) Yarla, N. S.; Gali, H.; Pathuri, G.; Smriti, S.; Farooqui, M.; Panneerselvam, J.; Kumar, G.; Madka, V.; Rao, C. V. Targeting the Paracrine Hormone-Dependent Guanylate Cyclase/CGMP/Phosphodiesterases Signaling Pathway for Colorectal Cancer Prevention. *Semin. Cancer Biol.* **2018**.

(11) Kuhn, M. Molecular Physiology of Membrane Guanylyl Cyclase Receptors. *Physiol. Rev.* **2016**, *96*, 751–804.

(12) Shailubhai, K.; Yu, H. H.; Karunanandaa, K.; Wang, J. Y.; Eber, S. L.; Wang, Y.; Joo, N. S.; Kim, H. D.; Miedema, B. W.; Abbas, S. Z.; *et al.* Uroguanylin Treatment Suppresses Polyp Formation in the Apc Min / ⅞ Mouse and Induces Apoptosis in Human Colon Adenocarcinoma Cells via Cyclic GMP. *Cancer Res.* **2000**, *60*, 5151–5157.

(13) Wilson, C.; Lin, J. E.; Li, P.; Snook, A. E.; Gong, J.; Sato, T.; Liu, C.; Girondo, M. A.; Rui, H.; Hyslop, T.; *et al.* The Paracrine Hormone for the GUCY2C Tumor Suppressor, Guanylin, Is Universally Lost in Colorectal Cancer. *Cancer Epidemiol. Biomarkers Prev.* **2014**, *23*, 2328–2337.

(14) Nikolaou, S.; Qiu, S.; Fiorentino, F.; Rasheed, S.; Tekkis, P.; Kontovounisios, C. The Prognostic and Therapeutic Role of Hormones in Colorectal Cancer: A Review. *Mol. Biol. Rep.* **2018**, *1*, 3.

(15) Brierley, S. M. Guanylate Cyclase-C Receptor Activation: Unexpected Biology. *Curr. Opin. Pharmacol.* **2012**, *12*, 632–640.

(16) Basu, N.; Bhandari, R.; Natarajan, V. T.; Visweswariah, S. S. Cross Talk between Receptor Guanylyl Cyclase C and C-Src Tyrosine Kinase Regulates Colon Cancer Cell Cytostasis. *Mol. Cell. Biol.* **2009**, *29*, 5277–5289.

(17) Giblin, M. F.; Sieckman, G. L.; Watkinson, L. D.; Daibes-Figueroa, S.; Hoffman, T. J.; Forte, L. R.; Volkert, W. A. Selective Targeting of E. Coli Heat-Stable Enterotoxin Analogs to Human Colon Cancer Cells. *Anticancer Res* **2006**, *26*, 3243–3251.

(18) Tian, X.; Michal, A. M.; Li, P.; Wolfe, H. R.; Waldman, S. A.; Wickstrom, E. STa Peptide Analogs for Probing Guanylyl Cyclase C. *Biopolym. - Pept. Sci. Sect.* **2008**, *90*, 713–723.

(19) Liu, D.; Overbey, D.; Watkinson, L. D.; Daibes-Figueroa, S.; Hoffman, T. J.; Forte, L. R.; Volkert, W. A.; Giblin, M.

F. In Vivo Imaging of Human Colorectal Cancer Using Radiolabeled Analogs of the Uroguanylin Peptide Hormone. *Anticancer Res.* **2009**, *29*, 3777–3783.

(20) Liu, D.; Overbey, D.; Watkinson, L. D.; Smith, C. J.; Daibes-Figueroa, S.; Hoffman, T. J.; Forte, L. R.; Volkert, W. A.; Giblin, M. F. Comparative Evaluation of Three Cu-64-Labeled E-Coli Heat-Stable Enterotoxin Analogues for PET Imaging of Colorectal Cancer. *Bioconjug. Chem.* **2010**, *21*, 1171–1176.

(21) Góngora-Benítez, M.; Tulla-Puche, J.; Albericio, F. Constella™(EU)-Linzess™(USA): The Last Milestone in the Long Journey of the Peptide Linaclotide and Its Implications for the Future of Peptide Drugs. *Future Med. Chem.* **2013**, *5*, 291–300.

(22) Thomas, R. H.; Allmond, K. Linaclotide (Linzess) for Irritable Bowel Syndrome with Constipation and for Chronic Idiopathic Constipation. *P T* **2013**, *38*, 154–160.

(23) Blomain, E. S.; Pattison, A. M.; Waldman, S. A. GUCY2C Ligand Replacement to Prevent Colorectal Cancer. *Cancer Biol. Ther.* **2016**, *17*, 713–718.

(24) Pattison, A. M.; Merlino, D. J.; Blomain, E. S.; Waldman, S. A. Guanylyl Cyclase C Signaling Axis and Colon Cancer Prevention. *World J. Gastroenterol.* **2016**, *22*, 8070–8077.

(25) PCT/EP2019/050979. Nanosystems as Selective Vehicles. PCT/EP2019/050979, 2019.

(26) Nitiss, J. L. Targeting DNA Topoisomerase II in Cancer Chemotherapy. *Nat. Rev. Cancer* **2009**, *9*, 338–350.

(27) Kunishima, M.; Kawachi, C.; Morita, J.; Terao, K.; Iwasaki, F.; Tani, S. 4-(4,6-Dimethoxy-1,3,5-Triazin-2-Yl)-4-Methylmorpholinium Chloride: An Efficient Condensing Agent Leading to the Formation of Amides and Esters. *Tetrahedron* **1999**, *55*, 13159–13170.

(28) Pelet, J. M.; Putnam, D. An In-Depth Analysis of Polymer-Analogous Conjugation Using DMTMM. *Bioconjug. Chem.* **2011**, *22*, 329–337.

(29) Smallcombe, S. H.; Patt, S. L.; Keifer, P. A. WET Solvent Suppression and Its Applications to LC NMR and High-Resolution NMR Spectroscopy. *J. Magn. Reson. Ser. A* **1995**, *117*, 295–303.

(30) Pelta, M. D.; Morris, G. A.; Stchedroff, M. J.; Hammond, S. J. A One-Shot Sequence for High-Resolution Diffusion-Ordered Spectroscopy. *Magn. Reson. Chem.* **2002**, *40*, 147–152.

(31) Liu, M.; Mao, X. A.; Ye, C.; Huang, H.; Nicholson, J. K.; Lindon, J. C. Improved Watergate Pulse Sequences for Solvent Suppression in NMR Spectroscopy. *J. Magn. Reson.* **1998**, *132*, 125–129.

(32) Koay, C. G.; Özarslan, E. Conceptual Foundations of Diffusion in Magnetic Resonance. *Concepts Magn. Reson. Part A Bridg. Educ. Res.* **2013**, *42*, 116–129.

(33) Dave, R. M.; Patel, R. K.; Patel, J. K. RP-HPLC Method Development and Validation of Etoposide. *J. Pharm. Res.* **2012**, *5*, 3618–3620.

(34) Bazak, R.; Houri, M.; El Achy, S.; Kamel, S.; Refaat, T. Cancer Active Targeting by Nanoparticles: A Comprehensive Review of Literature. *J. Cancer Res. Clin. Oncol.* **2015**, *141*, 769–784.

(35) Strebhardt, K.; Ullrich, A. Paul Ehrlich's Magic Bullet Concept: 100 Years of Progress. *Nat. Rev. Cancer* **2008**, *8*, 473–480.

(36) Nag, O. K.; Awasthi, V. Surface Engineering of Liposomes for Stealth Behavior. *Pharmaceutics*, 2013, *5*, 542–569.

(37) Zhao, C.; Deng, H.; Xu, J.; Li, S.; Zhong, L.; Shao, L.; Wu, Y.; Liang, X. "Sheddable" PEG-Lipid to Balance the Contradiction of PEGylation between Long Circulation and Poor Uptake. *Nanoscale* **2016**, *8*, 10832–10842.

(38) Ryan, S. M.; Mantovani, G.; Wang, X.; Haddleton, D. M.; Brayden, D. J. Advances in PEGylation of Important Biotech Molecules: Delivery Aspects. *Expert Opin. Drug Deliv.* **2008**, *5*, 371–383.

(39) Howard, M. D.; Jay, M.; Dziubla, T. D.; Lu, X. PEGylation of Nanocarrier Drug Delivery Systems: State of the Art. *Journal of Biomedical Nanotechnology*, 2008, *4*, 133–148.

(40) Duncan, R.; Gaspar, R. Nanomedicine(s) under the Microscope. *Molecular Pharmaceutics*, 2011, *8*, 2101–2141.

(41) Novoa-Carballal, R.; Fernandez-Megia, E.; Jimenez, C.; Riguera, R. NMR Methods for Unravelling the Spectra of Complex Mixtures. *Nat. Prod. Rep.* **2011**, *28*, 78–98.

(42) Macchioni, A.; Ciancaleoni, G.; Zuccaccia, C.; Zuccaccia, D. Determining Accurate Molecular Sizes in Solution through NMR Diffusion Spectroscopy. *Chem. Soc. Rev.* **2008**, *37*, 479–489.

(43) Duncan, R.; Gilbert, H. R. P.; Carbajo, R. J.; Vicent, M. J. Polymer Masked−Unmasked Protein Therapy. 1. Bioresponsive Dextrin−Trypsin and −Melanocyte Stimulating Hormone Conjugates Designed for α-Amylase Activation. *Biomacromolecules* **2008**, *9*, 1146–1154.

(44) Shailubhai, K.; Yu, H. H.; Karunanandaa, K.; Wang, J. Y.; Eber, S. L.; Wang, Y.; Joo, N. S.; Kim, H. D.; Miedema, B. W.; Abbas, S. Z.; *et al.* Uroguanylin Treatment Suppresses Polyp Formation in the Apc Min / ⅞ Mouse and Induces Apoptosis in Human Colon Adenocarcinoma Cells via Cyclic GMP. *Cancer Res.* **2000**, *60*, 5151–5157.

(45) Rajendran, V.; Jain, M. V. In Vitro Tumorigenic Assay: Colony Forming Assay for Cancer Stem Cells. In *Encyclopedia of Cell Biology*; 2018; Vol. 3, pp. 89–95.

(46) Puck, T. T.; Marcus, P. I. Action of X-Rays on Mammalian Cells. *J. Exp. Med.* **1956**, *103*, 653–666.

(47) Franken, N. A. P.; Rodermond, H. M.; Stap, J.; Haveman, J.; van Bree, C. Clonogenic Assay of Cells in Vitro. *Nat. Protoc.* **2006**, *1*, 2315–2319.

(48) Waldman, S. A.; Barber, M.; Pearlman, J.; Park, J.; George, R.; Parkinson, S. J. Heterogeneity of Guanylyl Cyclase C Expressed by Human Colorectal Cancer Cell Lines in Vitro. *Cancer Epidemiol. Biomarkers Prev.* **1998**, *7*, 505–514.

(49) Pitari, G. M.; Di Guglielmo, M. D.; Park, J.; Schulz, S.; Waldman, S. A. Guanylyl Cyclase C Agonists Regulate Progression through the Cell Cycle of Human Colon Carcinoma Cells. *Proc. Natl. Acad. Sci. U. S. A.* **2001**, *98*, 7846–7851.

(50) Batzri, S.; Korn, E. D. Single Bilayer Liposomes Prepared without Sonication. *BBA - Biomembr.* **1973**, *298*, 1015–1019.

(51) Pons, M.; Foradada, M.; Estelrich, J. Liposomes Obtained by the Ethanol Injection Method. *Int. J. Pharm.* **1993**, *95*, 51–56.

(52) Maitani, Y.; Soeda, H.; Junping, W.; Takayama, K. Modified Ethanol Injection Method for Liposomes Containing SS-Sitosterol ß-d-Glucoside. *J. Liposome Res.* **2001**, *11*, 115–125.

(53) Jaafar-Maalej, C.; Diab, R.; Andrieu, V.; Elaissari, A.; Fessi, H. Ethanol Injection Method for Hydrophilic and Lipophilic Drug-Loaded Liposome Preparation. *J. Liposome Res.* **2010**, *20*, 228–243.

(54) Béduneau, A.; Saulnier, P.; Hindré, F.; Clavreul, A.; Leroux, J. C.; Benoit, J. P. Design of Targeted Lipid Nanocapsules by Conjugation of Whole Antibodies and Antibody Fab' Fragments. *Biomaterials* **2007**, *28*, 4978–4990.

(55) Ganta, S.; Singh, A.; Patel, N. R.; Cacaccio, J.; Rawal, Y. H.; Davis, B. J.; Amiji, M. M.; Coleman, T. P. Development of Egfr-Targeted Nanoemulsion for Imaging and Novel Platinum Therapy of Ovarian Cancer. *Pharm. Res.* **2014**, *31*, 2490–2502.

(56) Wu, Y.; Sefah, K.; Liu, H.; Wang, R.; Tan, W. DNA Aptamer-Micelle as an Efficient Detection/Delivery Vehicle toward Cancer Cells. *Proc. Natl. Acad. Sci.* **2010**, *107*, 5–10.

(57) Talekar, M.; Ganta, S.; Singh, A.; Amiji, M.; Kendall, J.; Denny, W. A.; Garg, S. Phosphatidylinositol 3-Kinase Inhibitor (PIK75) Containing Surface Functionalized Nanoemulsion for Enhanced Drug Delivery, Cytotoxicity and pro-Apoptotic Activity in Ovarian Cancer Cells. *Pharm. Res.* **2012**, *29*, 2874–2886.

(58) Zou, A.; Huo, M.; Zhang, Y.; Zhou, J.; Yin, X.; Yao, C.; Zhu, Q.; Zhang, M.; Ren, J.; Zhang, Q. Octreotide-Modified N-Octyl-O, N-Carboxymethyl Chitosan Micelles as Potential Carriers for Targeted Antitumor Drug Delivery. *J. Pharm. Sci.* **2012**, *101*, 627–640.

(59) Storm, G.; Belliot, S. O.; Daemen, T.; Lasic, D. D. Surface Modification of Nanoparticles to Oppose Uptake by the Mononuclear Phagocyte System. *Advanced Drug Delivery Reviews*, 1995, *17*, 31–48.

(60) Rabanel, J. M.; Hildgen, P.; Banquy, X. Assessment of PEG on Polymeric Particles Surface, a Key Step in Drug Carrier Translation. *J. Control. Release* **2014**, *185*, 71–87.

(61) Gindy, M. E.; Ji, S.; Hoye, T. R.; Panagiotopoulos, A. Z.; Prud'Homme, R. K. Preparation of Poly(Ethylene Glycol) Protected Nanoparticles with Variable Bioconjugate Ligand Density. *Biomacromolecules* **2008**, *9*, 2705–2711.

(62) Elias, D. R.; Poloukhtine, A.; Popik, V.; Tsourkas, A. Effect of Ligand Density, Receptor Density, and Nanoparticle Size on Cell Targeting. *Nanomedicine Nanotechnology, Biol. Med.* **2013**, *9*, 194–201.

(63) Tang, Z.; Li, D.; Sun, H.; Guo, X.; Chen, Y.; Zhou, S. Quantitative Control of Active Targeting of Nanocarriers to Tumor Cells through Optimization of Folate Ligand Density. *Biomaterials* **2014**, *35*, 8015–8027.

(64) Colombo, M.; Fiandra, L.; Alessio, G.; Mazzucchelli, S.; Nebuloni, M.; De Palma, C.; Kantner, K.; Pelaz, B.; Rotem, R.; Corsi, F.; *et al.* Tumour Homing and Therapeutic Effect of Colloidal Nanoparticles Depend on the Number of Attached Antibodies. *Nat. Commun.* **2016**, *7*, 1–14.

(65) Fakhari, A.; Baoum, A.; Siahaan, T. J.; Le, K. B.; Berkland, C. Controlling Ligand Surface Density Optimizes Nanoparticle Binding to ICAM-1. *J. Pharm. Sci.* **2011**, *100*, 1045–1056.

(66) Teijeiro-Valiño, C.; Novoa-Carballal, R.; Borrajo, E.; Vidal, A.; Alonso-Nocelo, M.; Freire, M. D. L. F.; Lopez-Casas, P. P.; Hidalgo, M.; Csaba, N.; Alonso, M. J. A Multifunctional Drug Nanocarrier for Efficient Anticancer Therapy. *J. Control. Release* **2019**, *294*, 154–164.

(67) Jacob, S.; Aguado, M.; Fallik, D.; Praz, F. The Role of the DNA Mismatch Repair System in the Cytotoxicity of the Topoisomerase Inhibitors Camptothecin and Etoposide to Human Colorectal Cancer Cells. *Cancer Res.* **2001**, *61*, 6555–6562.

(68) Rappaport, J. A.; Waldman, S. A. The Guanylate Cyclase C—CGMP Signaling Axis Opposes Intestinal Epithelial Injury and Neoplasia. *Front. Oncol.* **2018**, *8*, 1–17.

(69) Lin, J. E.; Li, P.; Snook, A. E.; Schulz, S.; Dasgupta, A.; Hyslop, T. M.; Gibbons, A. V.; Marszlowicz, G.; Pitari, G. M.; Waldman, S. A. The Hormone Receptor GUCY2C Suppresses Intestinal Tumor Formation by Inhibiting AKT Signaling. *Gastroenterology* **2010**, *138*, 241–254.

(70) Montecucco, A.; Biamonti, G. Cellular Response to Etoposide Treatment. *Cancer Lett.* **2007**, *252*, 9–18.

(71) Stragand, J. J.; Drewinko, B.; Barlogie, B.; White, R. A. Biological Properties of the Human Colonic Adenocarcinoma Cell Line Sw 620 Grown as a Xenograft in the Athymic Mouse. *Cancer Res.* **1981**, *41*, 3364–3369.

(72) Yoo, W.; Yoo, D.; Hong, E.; Jung, E.; Go, Y.; Singh, S. V. B.; Khang, G.; Lee, D. Acid-Activatable Oxidative Stress-Inducing Polysaccharide Nanoparticles for Anticancer Therapy. *J. Control. Release* **2018**, *269*, 235–244.

SUPPLEMENTARY MATERIAL

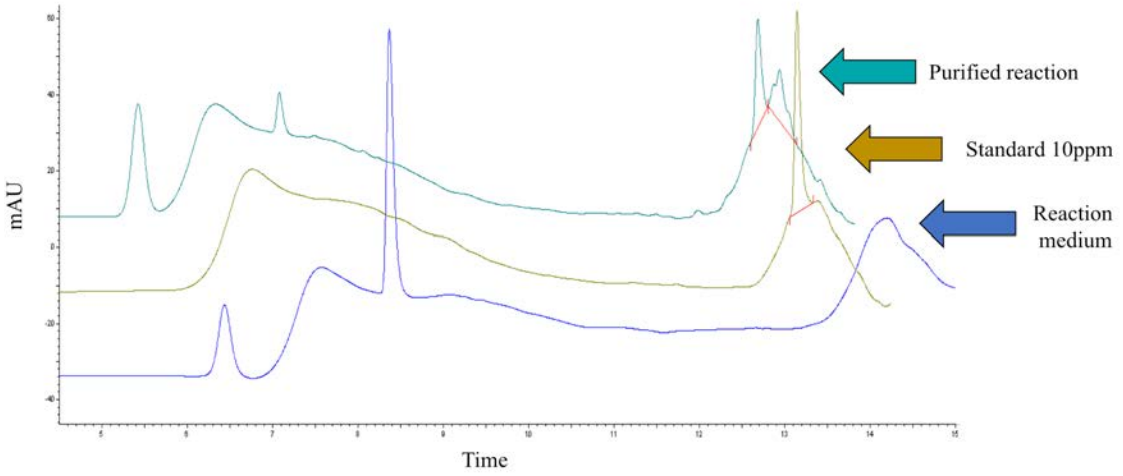

Figure S1. HPLC obtained chromatograms for: reaction medium: COOH-PEG$_{12}$-C$_{18}$ and DMTMM•Cl dissolved in HEPES 150mM (blue line), 10ppm standard of the non-modified peptide UroG (yellow line) and the purified compounds UroG + UroGm conjugate (turquoise line).

A)

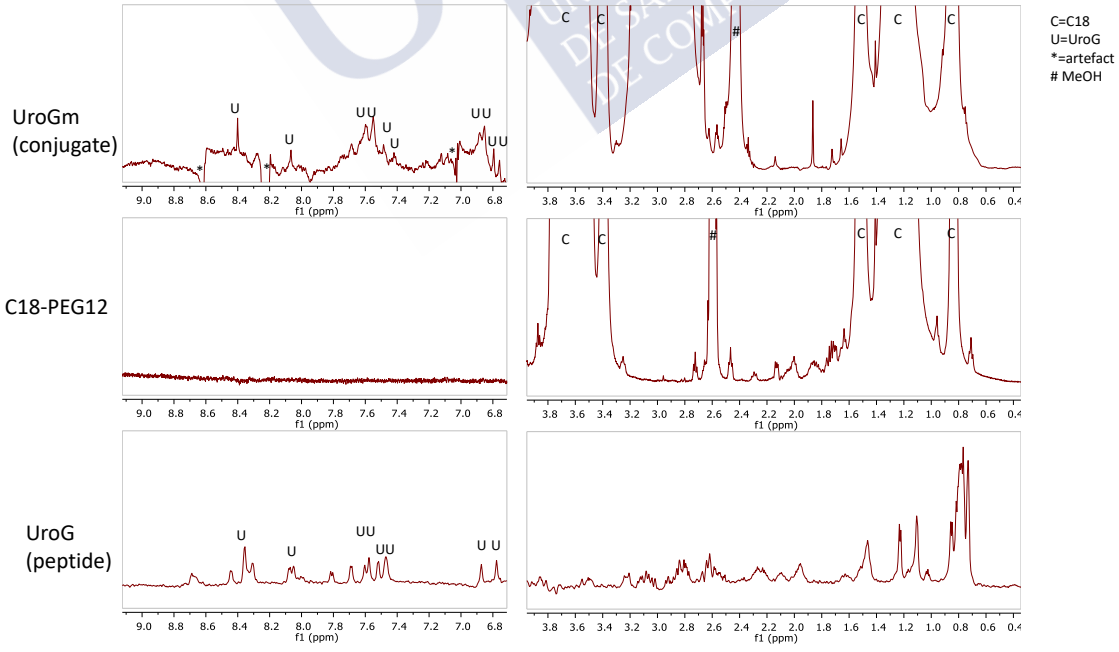

B)

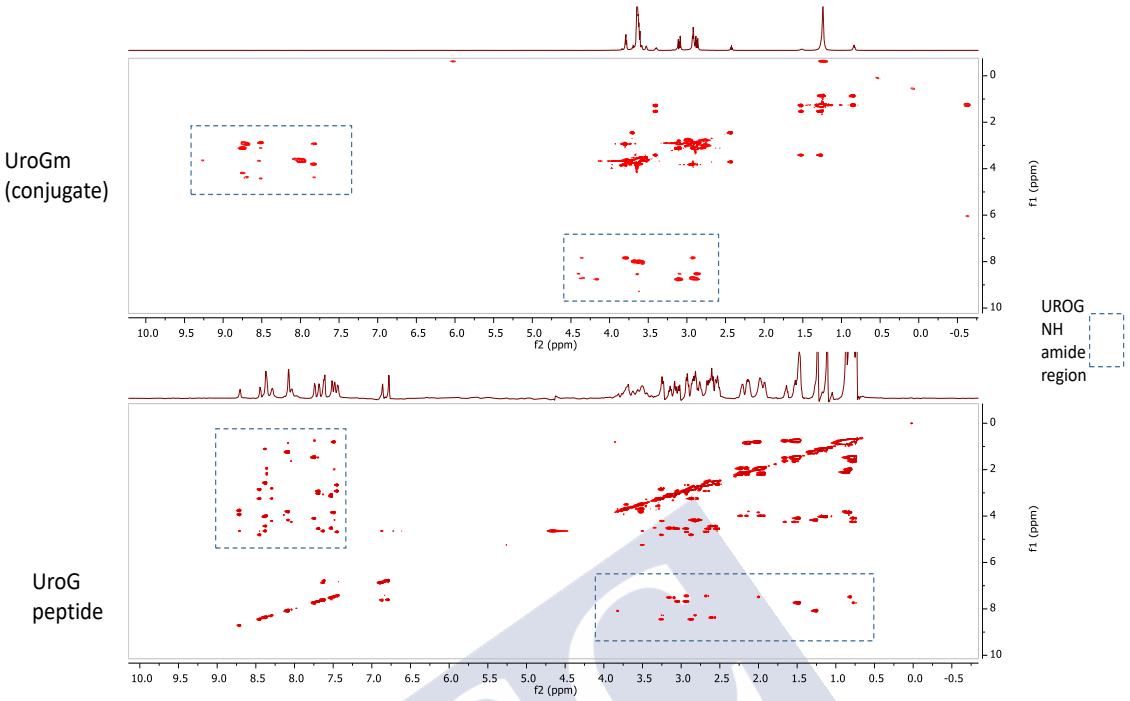

Figure S2.**(A)** ^{1}H-NMR analysis of the reaction reagents and product. **(B)** TOCSY analysis of the amide region.

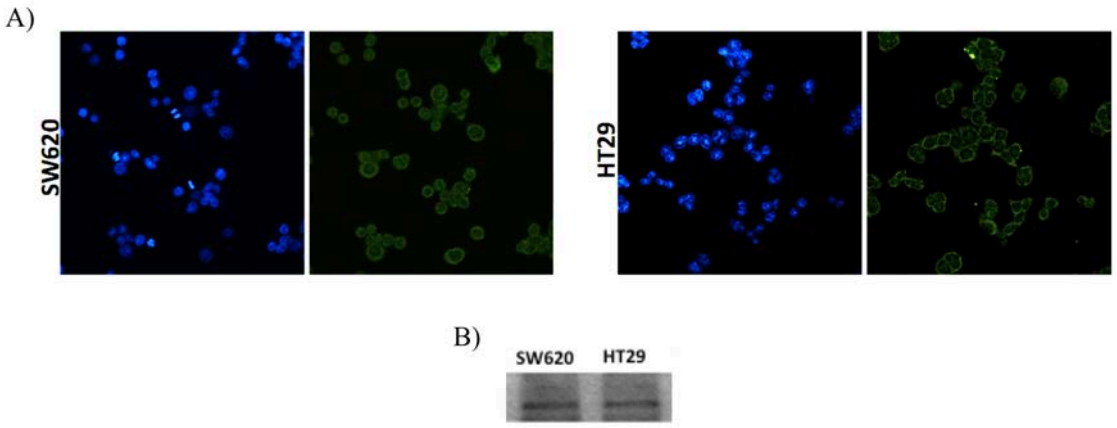

Figure S3. (A) Immunohistochemistry of GCC receptor in SW620 and HT29 colon cancer cell lines and **(B)** western blot confirmation of the same GCC expression levels.

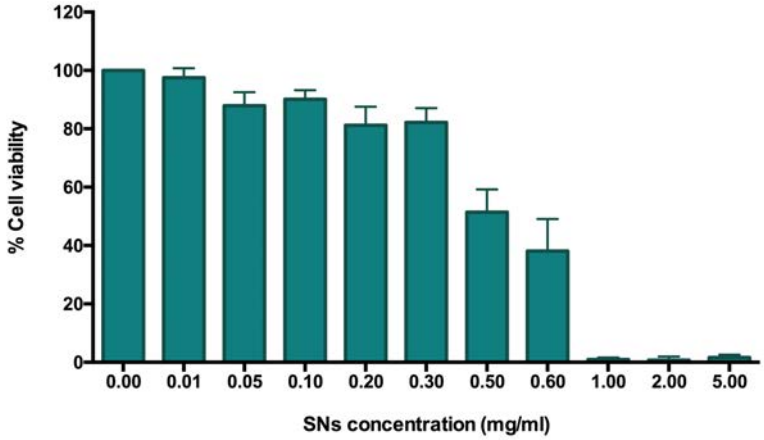

Figure S4. MTT toxicity assay of sphingomyelin nanoemulsions (SNs).

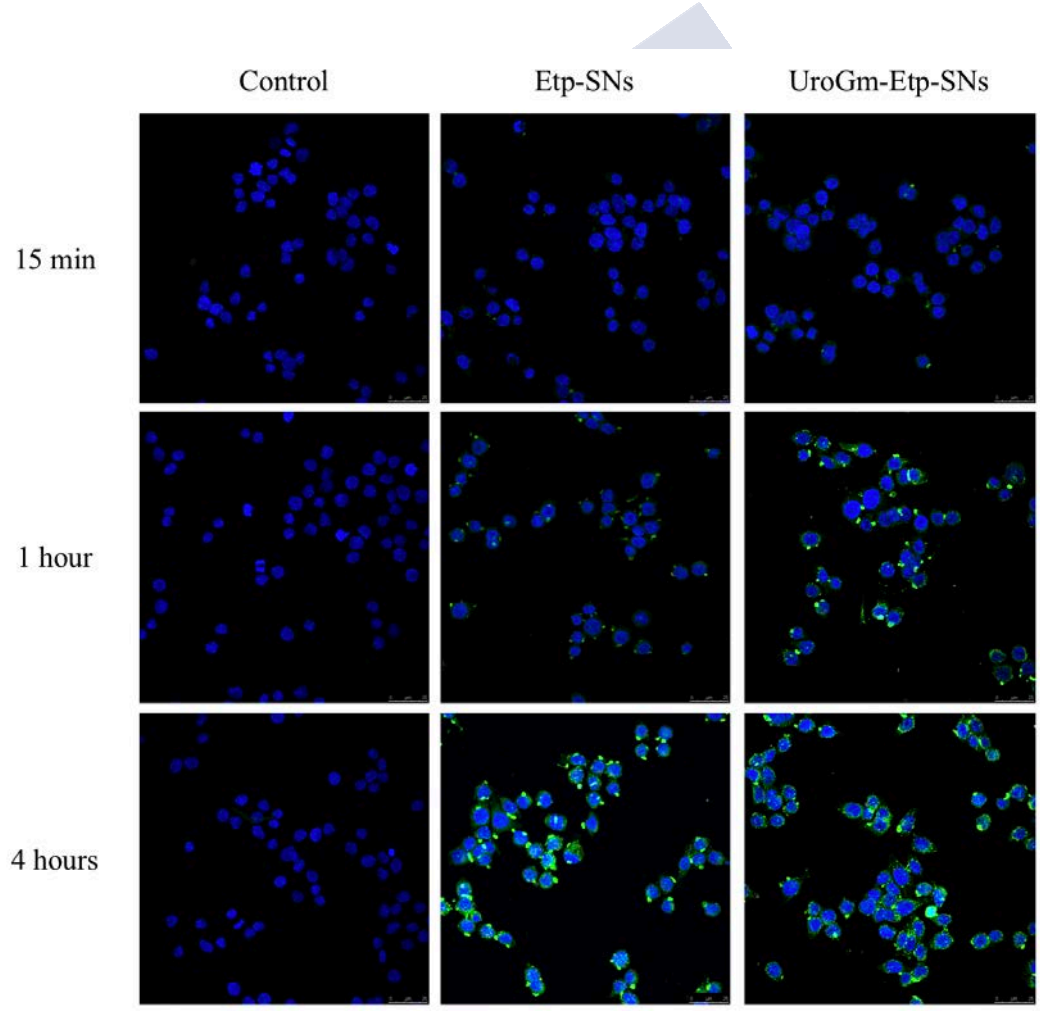

Figure S5. Confocal microscopy images showing the internalization of Etp-SNs and UroGm-Etp-SNs in SW620 colon cancer cells after 15 minutes, 1 hour and 4 hours of incubation. Green channel: TopFluor®-sphingomyelin (TopFluor®-SM) labelled nanoemulsions. Blue channel: nuclei staining with Hoechst.

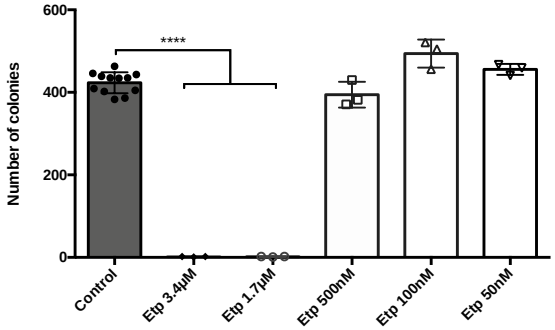

Figure S6. Evaluation of cell proliferation activity by colony forming assay of SW620 cells treated with increasing amounts of the anticancer drug etoposide. *P value **** p < 0.0001*

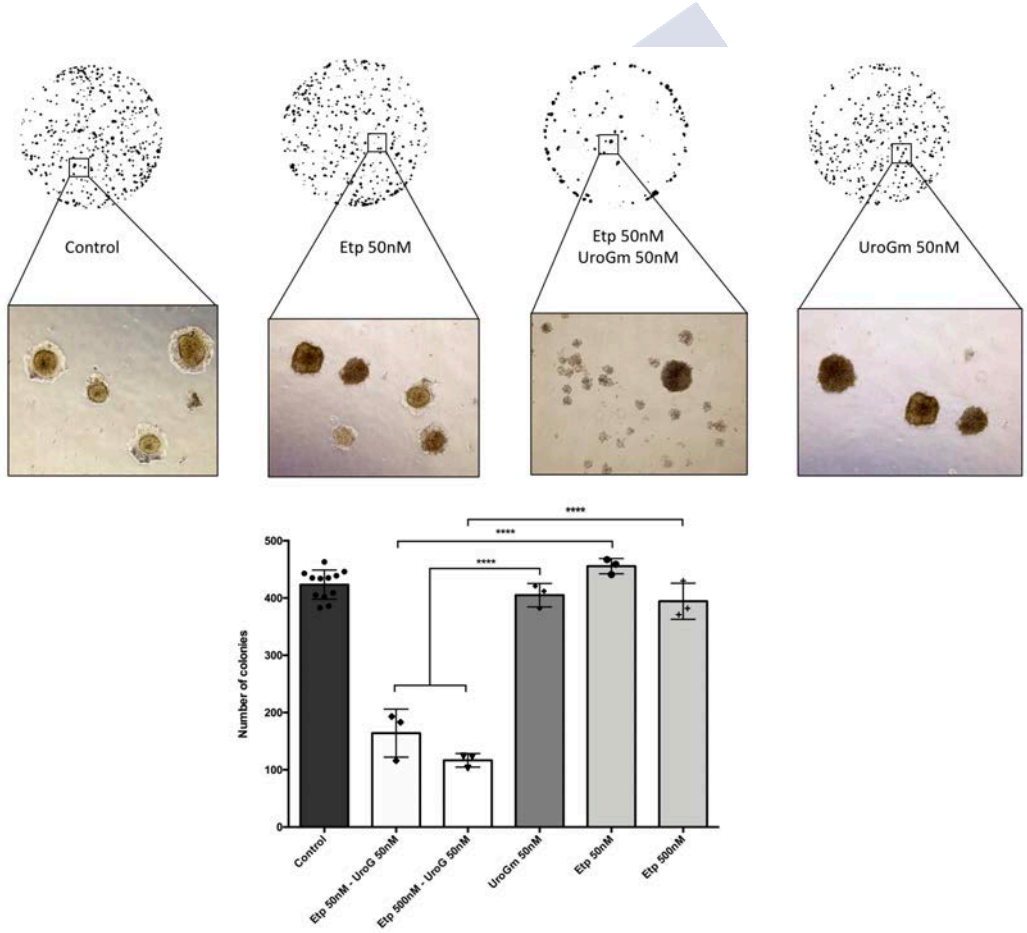

Figure S7. Evaluation of cell proliferation activity by colony forming assay. **(A)** Image of macroscopic colonies photographed from P12 well plates and cellular detail of each condition. **(B)** Graph showing the successful combinatorial effect between UroGm and Etp at two doses without apparent toxicity of isolated drugs alone. *P value **** p < 0.0001.*

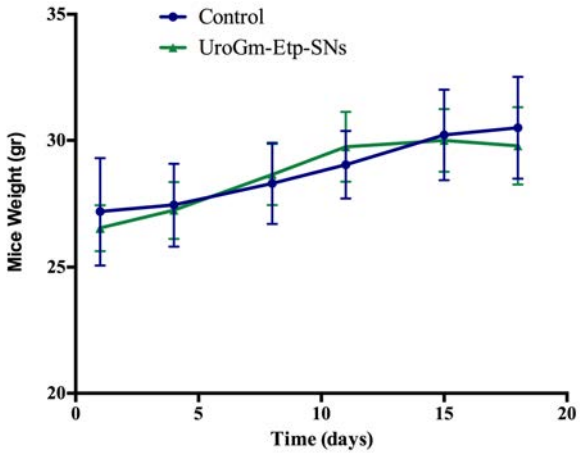

Figure S8. Evaluation of mice bodyweight during the efficacy experiment.

USC
UNIVERSIDADE
DE SANTIAGO
DE COMPOSTELA

OVERALL DISCUSSION

USC
UNIVERSIDADE
DE SANTIAGO
DE COMPOSTELA

Commercialization of nanopharmaceuticals represents nowadays a costly, long and risky enterprise with series of steps ranging from laboratory development through preclinical and clinical phases to the marketplace[1,2]. Development of nanotechnology in biomedicine has led to significant advances in the last decades with several nanoformulations already presented in the clinics and many others currently undergoing clinical trials[3–5]. Although nanotechnology has shown a significant impact in biomedical research, measured by exponential increase of published articles per year since 1990, the number of marketed products is still limited[6–10]. Therefore, a rational design of nanopharmaceuticals is required from the initial development phases[11,12]. The adequate selection of the carrier components followed by a subsequent screening phase to determine the best combination between them[13,14] is thought to be necessary from a translational perspective[5,15]. Potential application of nanotechnology in cancer therapy profiting its capacity to modulate the biodistribution profile and decrease toxicity associated with chemotherapy is already a reality with more than 30% of commercialized nanoproducts indicated for this condition[5]. Nevertheless, the high incidence and mortality of cancer makes actual treatments insufficient highlighting the need to find new, more effective and powerful treatments.

Within this frame, the aim of the work carried out in this PhD thesis has been the development of a versatile biodegradable nanosystem platform with the capacity to entrap and deliver different types of drugs (classic chemotherapy and biomolecules) and, ultimately, to enhance their pharmacological activity. The experimental workflow started by the investigation of the key parameters affecting the nanosystem formation from an formulation standpoint (i.e. molecular composition, concentration and ratio of the forming components).

Additionally, *in silico* molecular modelling techniques were applied to simulate the formation of the experimentally selected nanosystems as well as to predict interaction of six particular

drugs with this model nanosystems of interest and determine whether the drug - nanosystem interaction was or was not favorable. Furthermore, *in vitro* and *in vivo* testing was done to demonstrate safety, stability and biocompatibility of the developed nanosystems (Chapter 1). Subsequently, we have investigated the potential of the nanosystem platform for its application as oncological treatments. First, we have explored the ability of neutral and non-toxic nanosystems to associate and effectively deliver hydrophobically modified oligonucleotides (Rlas-CH) (Chapter 2). Second, we evaluated the decoration of the nanosystems with a dual-acting paracrine hormone (targeting ligand and therapeutic compound), Uroguanylin (UroG). For this, we chemically modify UroG with a PEGylated carbon chain (UroG-PEG_6-C_{18}, UroGm) in order to favor its assembling to the surface of the nanosystems. Then, we have encapsulated the cytostatic drug, etoposide (Etp), with the final purpose of achieving a synergistic effect of both molecules. *In vitro* and *in vivo* studies were performed in order to determine the potential of this strategy (Chapter 3).

1. Nanosystems rational design.

The possibility of engineering different nanotechnological platforms with a great variety of nanomaterials has led to a massive development in the last decades[16]. However, there are still some challenges concerning the so-called "design process" to achieve a reliable and consistent nanopharmaceutical products[17]. This idea goes in line with the "Quality by Design" principle adopted by the ICH (International Council for Harmonization) and successively by the FDA for the discovery, development and manufacturing of nanomedicines[18]. Following these currents, one of the main goals of this work has been the design of a biocompatible and biodegradable nanosystem with adequate physicochemical properties and safety profile by controlling the experimental design from the initial point.

Taking this in consideration, we have selected as an interesting alternative the GRAS-listed fat soluble vitamin naturally transported from the diet by lipoproteins, vitamin E (V) as the main core component[19]. Additionally we have chosen to stabilize this oil with one of the most representative lipids presented in the lipoprotein monolayer, coinciding as well with the third main representative lipids in the outer cell membrane leaflet sphingomyelin (SM)[20–25]. Nanosystems were produced using a very mild and simple technique named ethanol injection method, an optimized low energy manufacturing technique traditionally used for liposome preparation[26–29]. A first screening, using the afford mentioned compounds was performed in order to identify the adequate combination oil-surfactant to obtain the best physicochemical properties (**Table 1**). All the results obtained from this systematic study brought to light the importance of carefully selection of the forming components in order to obtain appropriate characteristics. Physicochemical characterization of the developed formulations was first assessed by Dynamic Light Scattering (DLS) and Laser Doppler Anemometry (LDA) to perform the preliminary screening (**Table 1**), methods of reference in nanosystem characterization[30–32].Thereafter, complementary characterization of the selected nanosystems was performed by Nanoparticle Tracking Analysis (NTA), innovative technique design for the direct visualization and recording of nanosystems in solution[33]. Example of the measurement information obtained from the formulation composed by a V nuclei and SM as surfactant at w/w ratio 1:0.1 is presented in **Figure 1A**. Moreover, morphological examination of the nanosystems were performed by Transmission Electron Microscopy techniques, i.e. TEM, STEM and/or Cryo-TEM (**Figure 1B**) showing, as expected, spheroidal shape and confirming the size distribution obtained in the previous techniques.

Table 1: Initial screening conditions of nanosystems consisting in vitamin E (V) core and sphingomyelin (SM) as a stabilizing surfactant. Nanosystem physicochemical characterization by Dynamic Light Scattering (DLS) and Laser Doppler Anemometry (LDA).

	Total amount of Vitamin E (mg)								
	2			**5**			**10**		
Mass Ratio (V:SM)	**Size (nm)**	**PdI**	**ZP (mV)**	**Size (nm)**	**PdI**	**ZP (mV)**	**Size (nm)**	**PdI**	**ZP (mV)**
1:1	119 ± 20	0.3	0 ± 1	187 ± 16	0.2	-2 ± 3	Aggregated		
1:0.5	72 ±12	0.3	-1 ± 2	101 ± 10	0.2	-3 ± 2	254 ± 33	0.3	-9 ± 0
1:0.2	58 ± 18	0.2	-2 ± 0	123 ± 14	0.2	-4 ± 4	239 ± 18	0.2	-4 ± 0
1:0.1	63 ± 7	0.1	-5 ± 2	85 ± 7	0.1	-3 ± 1	169 ± 5	0.2	-1 ± 0
1:0.05	64 ± 7	0.2	-4 ± 1	97 ± 6	0.2	-2 ± 0	162 ± 2	0.2	-3 ± 2

V: vitamin E; SM: sphingomyelin; nm: nanometer; PdI: Polydispersity index; ZP: surface charge; mV: millivolts. Total volume of the nanoparticle suspension: 1 mL Ethanol to water ratio: 1:10 v/v . Results presented in mean ± SD, n=3.

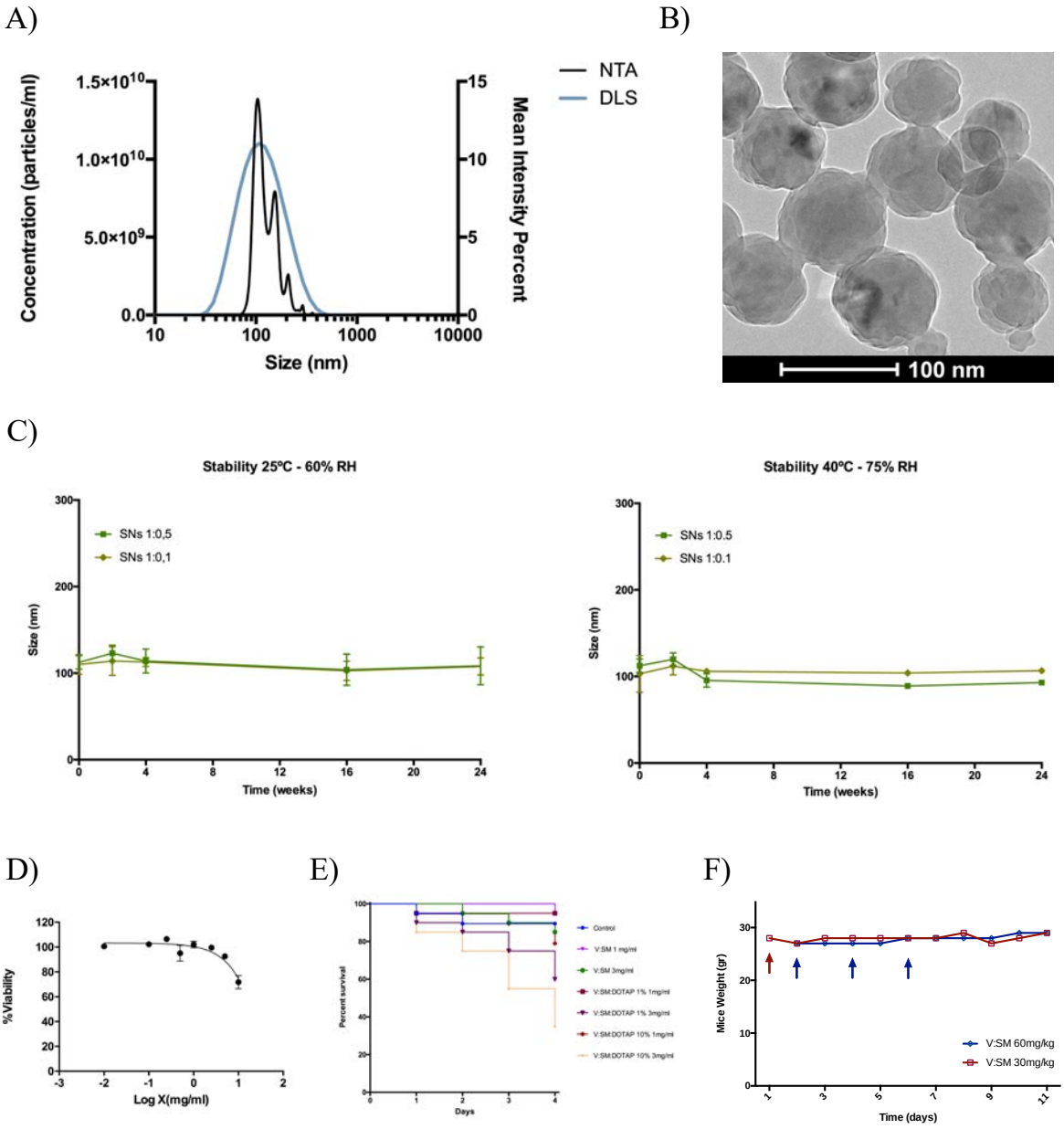

Figure 1: Characterization of several developed sphingomyelin nanosystems (SNs). **(A)** Complementary physicochemical characterization by Dynamic Light Scattering (DLS) and Nanoparticle Tracking Analysis (NTA). **(B)** Morphological examination by Cryogenic Transmission Electron Microscopy (Cryo-TEM). **(C)** Accelerated stability following International Council for Harmonization (ICH) guidelines[34] at controlled room temperature (right panel, 40ºC 75%RH) and storage conditions (left panel, 25ºC 60%RH). **(D)** Cellular cytotoxicity evaluated in SW480 colon cancer cells for SNs (V:SM 1:0.1) after 24h incubation with a maximum concentration tested 10mg/ml. **(E)** Toxicity comparison between neutral SNs (V:SM) and cationic SNs (V:SM:DOTAP) evaluated in zebrafish embryo model and measured by survival rate. **(F)** Toxicity data evaluated in healthy mice and measured in terms of body weight loss. *Figures A, B, D and F correspond to SNs V:SM at 1:0.1 w/w mass ratio.*

The main purpose of stability testing is to provide evidence on how the quality of drugs or pharmaceutical products may vary within time under the influence of various factors such as temperature, humidity, and light[35]. Stability of nanosystems remain a challenging issue during product development which directly conditions dosage form, delivery route and even nature of the possible associated drug[36]. Hence, it should be noted that the homogeneity of the administration depends on the homogeneity of the initial product[37].

In order to explore stability of our nanosystem we have performed accelerated colloidal stability studies following the guideline "Stability testing of new drug substances and products Q1A(R2)" from the ICH (International Conference on Harmonization)[38]. We have evaluated accelerated stability for drug substances or products intended for storage in a refrigerator (25ºC ± 2ºC; 60%RH ± 5%RH) and at controlled room temperature (40ºC ± 2ºC; 75%RH ± 5%RH) with a test frequency of 5 time points (recommended minimum of 3 points) in a 6 months period (**Figure 1C**). Stability of two SNs ratios namely V:SM ratio w/w 1:0.5 and 1:0.1 were assessed. Results showed outstanding stability profile in both conditions obtaining a two years equivalence stability in colloidal solution. This physicochemical stability results are directly related to the screening composition showing the importance of the initial choice of components and their chemical structure.

One of the main goals of nanotechnology is to exploit the advantages of nanometric scale to achieve the maximum clinical benefit with the minimum side effects[1]. Toxicology of nanomaterials is becoming an important issue nowadays, especially with regard to nanomaterials intended for medical use[39]. Therefore, a better understanding of the risk factors associated to nanomaterials in biomedicine applications will aid future nanopharmaceuticals development[40]. Nanotoxicology was proposed as a new branch of toxicology to address the gaps in knowledge of the adverse health effects caused by nanomaterials[41,42]. It is considered

of great importance for many authors that possible toxicological effects and doses calculation could be obtained out of *in vitro* studies reducing greatly subsequent *in vivo* ones. In line with this, several reference studies were conducted in order to evaluate and compare the potential toxicity of two formulations with opposite charge. Neutral SNs (V:SM) and cationic SNs (V:SM:DOTAP) were subsequently tested. MTT studies were performed at 4 and 24h contact periods in colorectal cancer cells (SW480). Neutral SNs reveal slight dose-dependent toxicity, but not enough to calculate IC50 value which being above the maximum dose tested (10mg/ml) (**Figure 1D**), which represents at least 5 to 100 times less toxic concentration in comparison with the one obtained by the cationic SNs (0.1mg/ml to 2mg/ml range). This results goes in line with current literature were cationic compounds are known to exhibit a more toxic behaviour[43]. Remarkably, oxidative stress and ROS production seams currently the most appealing methods to evaluate nanoparticle toxicity and stress at cellular level but colorimetric methods based on tetrazolium salts (MTT and MTS) remains the references methods to evaluate toxicity associated with nanocarriers[39,44].

Subsequent, we evaluate *in vitro* hemolysis activity to assess the biocompatibility of nanosystems and the impact of its physicochemical characteristics on human red blood cells[40,45]. Results showed less than 20% haemolytic activity in neutral SNs while cationic SNs obtain a 20% of hemolytic activity from the first concentration tested (0.1mg/ml). Concentrations up to 10mg/ml SNs were tested to evaluate a supersaturated condition and less than 40% hemolytic capacity was obtained for neutral SNs while cationic SNs presented more than 60% of hemolytic effect (see Chapter 2).

However, it is well known that *in vitro* models do not experience the same range of toxic effects that are likely to be observed *in vivo*. So, in order to complete the toxicological characterization we have evaluated the previous nanosystems both in zebrafish model and healthy mice.

Zebrafish embryo (*Danio rerio*) have become a prominent animal model in a variety of disciplines due to several inherent advantages such as small size, inexpensive to maintain and easily bred in large numbers[46,47]. Taking into account that zebrafish embryo are able to absorb small molecules presented in the surrounding water through their skin and gills this animal has been increasingly used as predictive drug-induced toxicity model[48]. The effective use of zebrafish as toxicological model is achievable mainly by four factors, i.e. possibility of larvae to live in a 96 or 384 well plate for one week, simple administration in less than 200µl well volume, transparent embryo body and statistically significative testing at small amounts[46,48]. Guidelines for zebrafish embryo use as a toxicological model have already been developed[47,49]. Evaluation of the previous tested neutral and cationic nanosystems was done in zebrafish embryo evaluating the possible alterations in zebrafish embryo during 96h period. As showed in **Figure 1E**, no relevant toxicity was found for neutral SNs at the concentration range tested (1mg/ml to 3mg/ml) while cationic SNs presented 40 to 60% of zebrafish death in the same concentration.

In order to confirm the apparent non-toxic behavior exhibited by our SNs both *in vitro* and in zebrafish embryo model, complementary *in vivo* studies were conducted in Swiss female mice. Following the principle of a Maximum Tolerated Dose (MTD) study, mice were injected with one dose (30mg/kg) or repeated doses (three consecutive doses of 60mg/kg) (**Figure 1F**). Sacrifice of animals would have been considered if they lose more than 20% of their body weight or if they presented other signs of significant toxicity[50]. However, after a cumulative dose of 180mg/kg, no apparent toxicity was founded affecting on mice behavior (food and water consumption) or body weight.

Understanding how nanosystems behave at a molecular level is of great importance for potential biomedical applications[51–53]. Linked to the advance in computer technology and particularly of computational simulation methods, we decided to make use of the generated knowledge to obtain data covering time and dimensions scales that otherwise would be technically unreachable[54]. Combining experimental and computational studies resulted in a synergy that allows a deep understanding of the internal structure of drug developed nanosystems alone or in combination with specific drugs.

In this PhD work we aimed to explore the capacity of Multiscale Molecular Dynamic (MD) Simulations to predict the formation of the nanosystems. Replacing the atomistic detail level by beads, Coarse Grained (CG) simulation method has opened a new horizon to simulate large-scale biomolecular processes on time scales inaccessible to all-atom (AT) models[55–57]. Using an experimentally characterized nanosystem platform (SNs) we intended to investigate its formation using an *in silico* method. As a first step, three w/w ratios previously described in the screening phase (**Table 1**) were chosen, namely, 1:0.1, 1:0.5 and 1:1 (**Figure 2A**). Interestingly, only by applying CG simulations we were able to locate a so-called "pocket" of water at the nanosystem core, which has been also confirmed by Nuclear Magnetic Resonance (NMR).

Based on both experimental and CG simulation data, V:SM 1:0.1 w/w ratio was selected for subsequent modelling with six physiochemically different drugs. Schematic representation of both CG and AT simulation of the components of the nanosystem and the selected drugs are presented in **Figure 2B**. Results presented in **Figure 2C** showed the structural and dynamic characteristics of the nanosystems loading the six drug molecules. MD simulations allowed us to study drug loading capacity, drug distribution/localization and dominant drug-nanosystem interactions and being validated by experimental characterization.

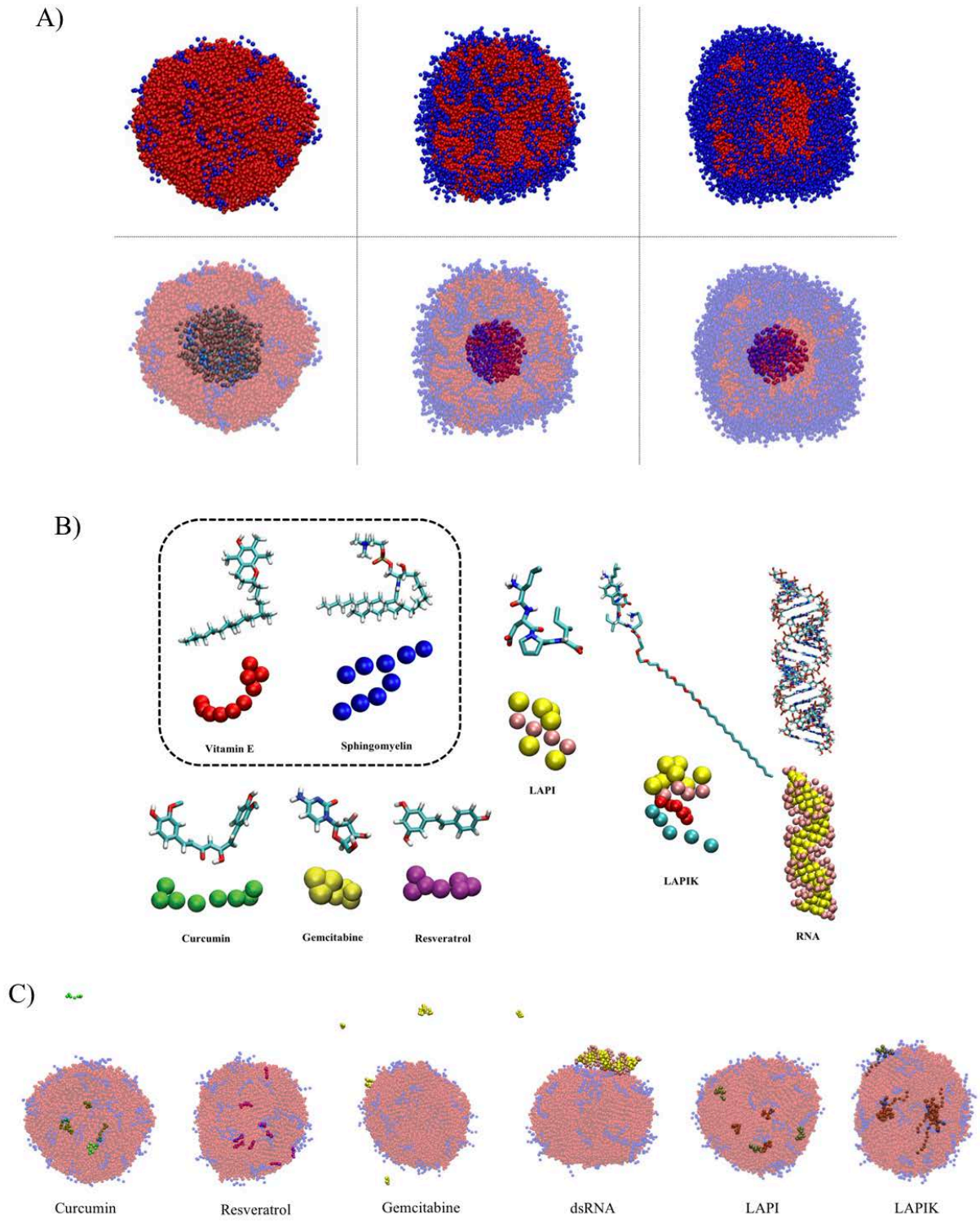

Figure 2: Molecular Dynamic Coarse-Grained (CG) Simulation of Vitamin E and sphingomyelin nanosystems at different oil:surfactant w/w ratio (from left to right 1:0.1, 1:0.5 and 1:1) **(A)**. Atomistic (AT) and GC representation of the nanosystems forming components plus the evaluated drugs **(B)**. Molecular representation of nanosystems 1:0.1 w/w ratio loading the six selected molecules **(C)**.

These results suggest that quantitative measurements at molecular level could be applied to design, optimize and perform a virtual screening of nanosystem platforms. MD simulations have advanced to such a level that nowadays it is possible to talk about 'computational microscopy' as an added tool to experimental methods[55].

There have been many computational works reported in literature on cell-nanosystems interactions, especially focused on the role of physicochemical properties of nanoparticles or their chemical surface modifications to generate membrane contact and insertion[52,54,58]. Nonetheless the possibility of applying GC simulation as a screening tool for nanopharmaceuticals development have been little explored so far[12]. Even though there may exist a gap between the computational results and the real process, these simulations represent a very promising tool that will permit testing an extensive conditions range during nanosystem development which otherwise would be much difficult or impossible to obtain experimentally.

Overall, the rapid expansion of nanotechnology has resulted in a vast collection of nanosystems that vary in a myriad of characteristics such as size, shape, charge, chemical composition, coating and solubility among others[40,44]. Considering this first part of the PhD thesis work, we propose a strategy to be followed for nanosystems production and physicochemical characterization, strategy that could benefit a wide range of nanosystems that are currently being produced or that will someday be produced[32]. Therefore, in our opinion, ideally rational design should include a complete physicochemical characterization of new developed nanocarriers with extensive analysis of chemical and biomolecular structure by combining *in silico*, *in vitro* and *in vivo* techniques to ensure that the quality and safety profile of the investigational product would be satisfactory throughout the preclinical and subsequent clinical periods.

2. Applications of nanosystems in colorectal cancer therapy.

Colorectal cancer (CRC) is the third most frequently diagnosed cancer malignancy and the fourth leading cause of cancer-related deaths in the world[59,60]. Even after surgical resection and aggressive chemotherapy, 50% of colorectal carcinoma patients develop recurrent disease[61]. This fact highlight the need for development of novel therapeutic approaches to improve the current chemotherapeutic treatment[62]. In this thesis we have proposed the development and characterization of a sphingomyelin nanosystem platform (SNs) based on a dual component strategy, one oil nuclei and one surfactant stabilizing layer. Once the nanosystem platform was optimized, two applications were explored, i.e. SNs in colorectal cancer gene therapy and SNs as vehicles for a combinatory therapy in metastatic colorectal cancer.

2.1. SNs in colorectal cancer gene therapy

Gene therapy has emerged as a promising strategy for the modification of genetic material of living cells for therapeutic purposes. This new therapy involves the introduction of functional nucleic acid that replace, amplify, suppress or correct a defective gene[63]. In this regard, nanosystems have proven to serve as an attractive vehicle for the delivery not only of poor-soluble drugs but also for biomolecules such as oncotherapeutic nucleic acids (e.g. plasmid DNA (pDNA), small-interfering RNA (siRNA) and microRNA (miRNA)) widely reported for cancer managing[64–66]. Gene delivery became a complex process that needs an efficient carrier to go through each cellular step involved. Despite the intensive research in the field some limitations in gene therapy such as improvement in their cellular uptake, bioavailability, and half-life in blood circulation needs to be overcome to ensure the translation of gene-based therapies. Therefore, a successful formulation will be the one that can find the equilibrium among acceptable toxicity, transfection efficiency and stability[63,65,67,68].

The design of nanosystems with both, appropriate physicochemical and biological characteristics represents a critical parameter in order to assure their correct interactions with biological systems[69]. DNA complexation with cationic compounds has been the most explored strategy to overcome enzymatic degradation of the genetic material and to promote their capability to cross biological membranes[63]. In order to achieve substantial cationic charge lipids such as DOTAP (1,2-diolyoxy-3-(trimethylammonium)propane), DOTMA (N-[1-(2,3-Dioleoyloxy)propyl]-N,N,N-trimethyl-ammonium methyl sulphate), ST (Stearylamine), DC-CH (3β-[N-(N',N'-dimethylaminoethane)-carbamoyl] cholesterol) and CTAB (cetyltrimethylammonium bromide) have been commonly incorporated to the nanosystems[65,68]. Cationic nanosystems, while efficiently taking up nucleic acids, have had limited success for *in vivo* gene delivery mainly by their toxicity. In addition, cationic components are known to be predisposed to interact with serum proteins, lipoproteins, and the extracellular matrix, leading to aggregation or release of oligonucleotides before reaching the target cells[70].

On the other side, negatively charged nanosystems (usually avidly taken up by phagocytic cells) might not represent an attractive alternative since they may not result in optimal loading efficiency due to charge repulsion between the nanostructure and the highly negative charged oligonucleotides. Therefore, neutral nanosystems could represent a good alternative to avoid toxicity due to positive charges and the repulsion generated by negative charges (**Table 2**).

Chemical modifications of naked oligonucleotides have been used to generate nuclease-resistant nucleic acids to avoid degradation, enhance their stability, and improve circulation time as well as tumor uptake *in vivo*[70]. Replacement of the phosphodiester group with phosphorothioate group was the first chemical modification applied to antisense oligonucleotide modification[71,72]. Although it improve oligonucleotide stability,

phosphorothioate alone do not fully protect strategy, so the subsequent modification with several hydrophobic moieties (such as cholesterol) have been explored in this work.

Table 2: Physicochemical characterization and association efficiency of SNs composed of vitamin E (V) and sphingomyelin (SM) formulated with a decrescent amount of surfactant and 0.5% constant loading of the modified oligonucleotide (Rlas-CH).

Nanosystem components		**Physicochemical Characterization**			
Ratio V:SM	**Rlas Type**	**Size (nm)**	**PdI**	**ZP (mV)**	**AE%**
1:0.1	-	125 ± 15	0.1	-6 ± 3	-
1:0.1	**Rlas-CH**	100 ± 8	0.2	-16 ± 2	19 ± 3
1:0.05		88 ± 2	0.2	-23 ± 1	17 ± 2
1:0.01		88 ± 1	0.2	-23 ± 1	19 ± 0
1:0		102 ± 12	0.2	-34 ± 3	21 ± 3

V: Vitamin E; SM: Sphingomyelin; nm: nanometer; PdI: Polydispersity index; ZP: surface charge; mV: millivolts; AE%: association efficiency represented in percentage.

As shown in **Table 2**, nanosystems with a charge close to neutral values (-6 ± 3 mV) were used to associate cholesterol-modified oligonucleotides (Rlas-CH). The inclusion of a hydrophobically modified component imply the addition of a new surfactant to the developed nanosystem. This new surfactant performs a dual function, initially it makes possible for the Rlas to be anchored into the surfactant layer and on the other hand it increases in the compaction of the nanostructure. Since one of the hypothesis was that the cholesterol (CH) residue could favor the disposition of the oligonucleotides at the interface due to its ability to act as a surfactant and a potential interaction with the sphingomyelin (SM)[73]. Following experiments were aimed to determine if decreasing the amount of SM maintaining the same concentration of Rlas-CH could have a positive effect. Interestingly, we observed that cholesterol modified

oligonucleotides (Rlas-CH) were able to stabilize nanosystem in absence of SM, acting that way as the only surfactant of the formulation. This strategy lead us to the engineering of nanosystems containing minimum surfactant presence or even surfactant-free nanosystems (**Table 2**). However, stability studies regarding this formulation have not been done. To confirm the effective encapsulation and delivery of Rlas to cells the oligonucleotide was covalently linked to a fluorescent molecule (Cy3) prior to its incorporation to nanosystems. As observed in **Figure 3**, effective internalization in colorectal cancer cell line SW480 was achieved.

In summary, even being a neutral charged formulation, this nanosystem have showed a good ability to associate hydrophobically modified oligonucleotides and effectively deliver them to cancer cells rendering this as a promising alternative to cancer gene therapy.

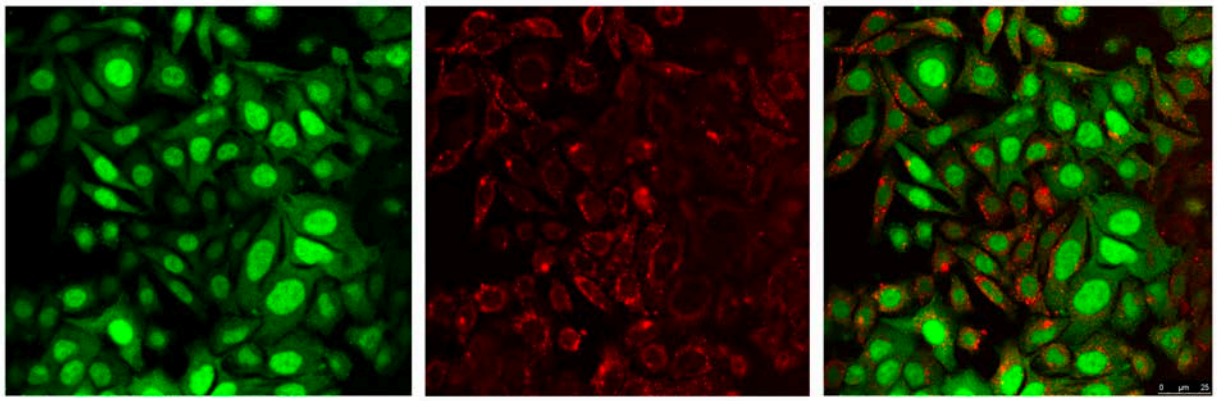

Figure 3: Uptake studies showing 500ng/well of Cy3-DNA-CH loaded nanosystem (red signal) efficiently internalized in SW480 colorectal cancer cells expressing GFP (green signal).

2.2. SNs as vehicles for a combinatorial therapy in metastatic colorectal cancer

Nanosystems intended for cancer treatment have been mostly designed relying on the capacity of nanoscale particles to enhance circulation times and eventually undergo passive accumulation into the tumour tissues due to the Enhanced Permeability and Retention effect (EPR effect) promoted by tumour-associated leaky vasculatures and poor lymphatic drainage[74]. Recent studies highlighted the need to still reach improved accumulation of nanoparticles in the tumour[75,76]. By means of active targeting, nanoparticles can theoretically achieve higher levels of drug concentration in tumour tissues via receptor-mediated endocytosis[77–79]. Indeed, the use of targeting ligands has demonstrated to improve the targeting efficiency and reduced side effects by recognizing and binding to specific receptors unique to tumour cells, thus increasing the therapeutic output[80–82]. Typically, well-known receptors involved in tumour progression, such as HER2, folate receptor, CD44, and EGFR, have been exploited for that purpose[83]. One of the main problems is that most of these receptors are non-specific for cancer cells but ubiquitously expressed in the body, and in many occasions competition with endogenous ligands hamper the potential of this approach. Therefore, it is critical to seek for unique or great overexpressed marker on tumor cells but not on normal cells to enable selectivity for tumor tissue over normal cells[61].

Guanylyl Cyclase C receptor (GCC) is only expressed at the apical membrane of enterocytes and also by primary and metastatic colorectal cancer cells, but not by healthy extraintestinal tissue where colorectal cancer cells usually metastasize[84–88]. GCC is activated upon binding to the paracrine hormones Guanylin (Gn) and Uroguanylin (UroG), as well as with the enterotoxigenic *Escherichia coli* heat stable enterotoxin (ST)[89]. Based on this previous knowledge, several publications have exploited the ability to target GCC for PET and SPECT

molecular diagnosis, based on the chemical modification of the endogenous agonists (UroG, Gn and ST)[90–93]. Recently it has become clear that activation of GCC receptor also plays a protective role against colorectal cancer mainly because endogenous GCC-agonist hormones disappear early on colorectal cancer tumorigenesis[94,95]. Thus, a strategy based on chemoprevention by hormone replacement have come to scene. In this work we have proposed the synthesis of a derivative from the paracrine hormone Uroguanylin with a PEGylated carbon chain (UroGm, **Figure 4**) to maximize hydrophobically interactions with nanosystems and exploit the targeting and therapeutic capacity of this natural occurring hormone.

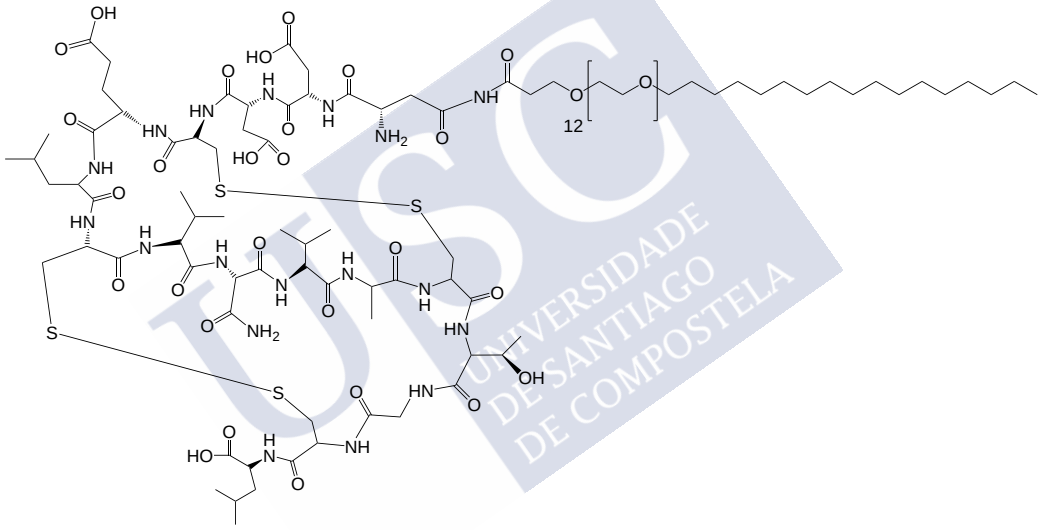

Figure 4. Hydrophobically modified Uroguanylin (UroG-PEG$_{12}$-C$_{18}$, UroGm).

It is proven that using only a single drug to treat cancer may not produce complete remissions or a better therapeutic effect. Thereby, a combined therapy with several anticancer agents into a nanosystem may provide a more effective cure and overcome the drug-resistance as different drugs may attack cancer cells at varying stages of their growth cycles[96]. Convincing arguments about the encapsulation of multiple drugs in a single nanosystem have been proposed for the development of colorectal anticancer applications[61]. However, one of the key parameters to control in detail is the unification of both therapeutic agents pharmacokinetics and cellular

uptake, which will allow the precise control of the dosage and scheduling of the multiple drugs[96]. Considering this factors, combinatorial nanomedicine should be designed in such a way so that it should target multiple signaling pathways with limited toxicity[61]. Nanosystem decoration with the Uroguanylin hydrophobic derivative (UroGm) combined with the encapsulation of a poorly soluble anticancer drug (etoposide) has been evaluated.

A)

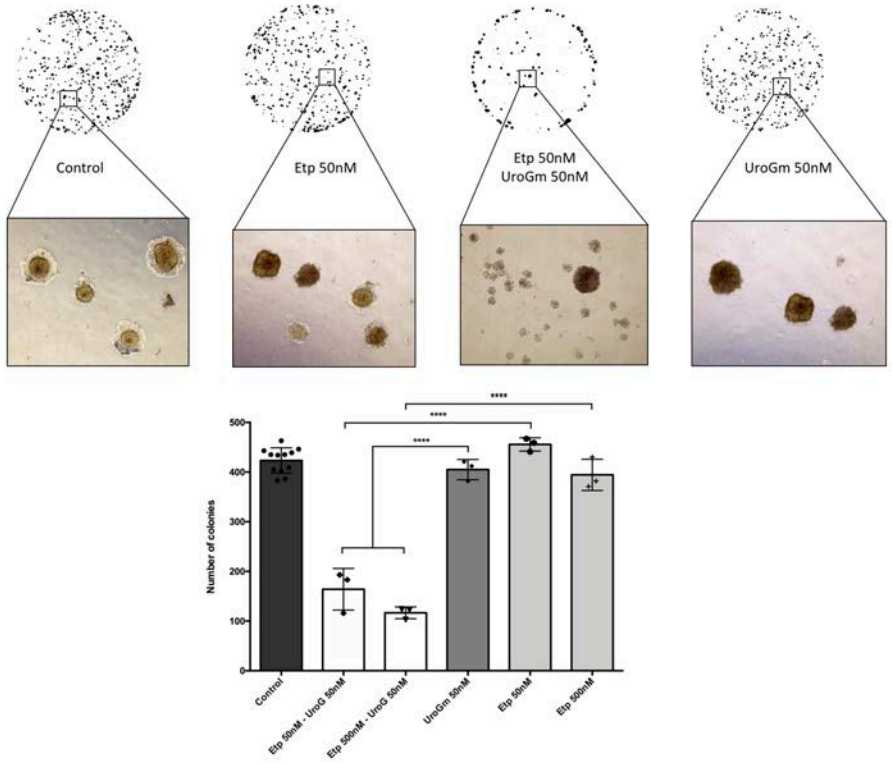

B)

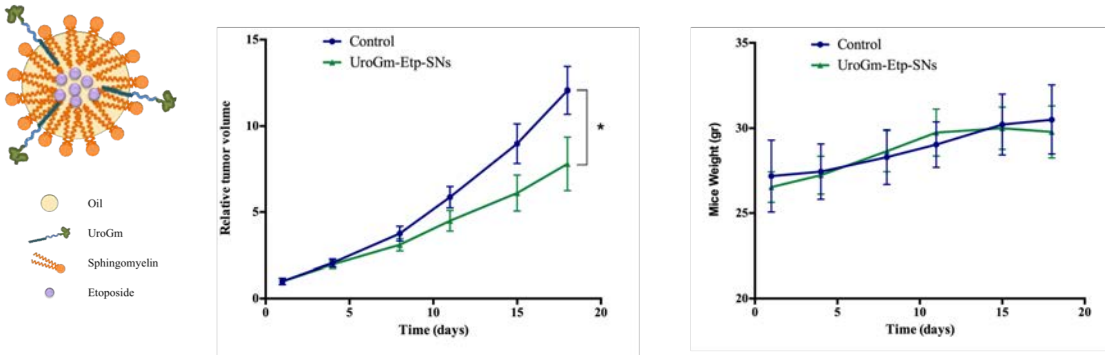

Figure 5: **(A)** Colony Forming Assay determining the concentration range in which a synergistic effect between UroGm and Etp is observed **(B)** Schematic representation of the developed nanosystems loaded with the modified peptide (UroGm) and the chemotherapeutic drug etoposide. Antitumor efficacy in terms of relative tumor volume and mice body weight.

In vitro experiments aimed to confirm the effectiveness of the drugs against metastatic colorectal cancer cell SW620 (ATCC® CCL-227™) has been done (Chapter 3). Colony Forming Assay was performed to evaluate the exact concentration range when a combinatorial effect of both drugs is obtained. As shown in **Figure 5A,** a concentration of 50nM of both UroGm and Etp is able to produce the reduction of colony formation up to 4 times. Moreover, *in vivo* efficacy study was performed in xenograft mice to evaluate the potential of this dual nanosystem therapy (UroGm + Etp). As shown in **Figure 5B**, significative reduction of the tumor volume have been observed for the mice treated with the combination nanosystem (UroGm-Etp-SNs) while mice body weight was not significatively altered.

In conclusion, our results expose the great potential of this targeting and therapeutic alternative for metastatic colorectal cancer treatment.

REFERENCES

(1) Farjadian, F.; Ghasemi, A.; Gohari, O.; Roointan, A.; Karimi, M.; Hamblin, M. R. Nanopharmaceuticals and Nanomedicines Currently on the Market: Challenges and Opportunities. *Nanomedicine* **2019**, *14*, 93–126.

(2) Ferrari, M. Cancer Nanotechnology: Opportunities and Challenges. *Nat. Rev. Cancer* **2005**, *5*, 161–171.

(3) Wagner, V.; Dullaart, A.; Bock, A. K.; Zweck, A. The Emerging Nanomedicine Landscape. *Nat. Biotechnol.* **2006**, *24*, 1211–1217.

(4) Ventola, C. L. Progress in Nanomedicine: Approved and Investigational Nanodrugs. *P T* **2017**, *42*, 742–755.

(5) Wicki, A.; Witzigmann, D.; Balasubramanian, V.; Huwyler, J. Nanomedicine in Cancer Therapy: Challenges, Opportunities, and Clinical Applications. *J. Control. Release* **2015**, *200*, 138–157.

(6) Venditto, V. J.; Szoka, F. C. Cancer Nanomedicines: So Many Papers and so Few Drugs! *Adv. Drug Deliv. Rev.* **2013**, *65*, 80–88.

(7) Hua, S.; de Matos, M. B. C.; Metselaar, J. M.; Storm, G. Current Trends and Challenges in the Clinical Translation of Nanoparticulate Nanomedicines: Pathways for Translational Development and Commercialization. *Front. Pharmacol.* **2018**, *9*, 790.

(8) Morigi, V.; Tocchio, A.; Bellavite Pellegrini, C.; Sakamoto, J. H.; Arnone, M.; Tasciotti, E. Nanotechnology in Medicine: From Inception to Market Domination. *J. Drug Deliv.* **2012**, *2012*, 1–7.

(9) Bobo, D.; Robinson, K. J.; Islam, J.; Thurecht, K. J.; Corrie, S. R. Nanoparticle-Based Medicines: A Review of FDA-Approved Materials and Clinical Trials to Date. *Pharm. Res.* **2016**, *33*, 2373–2387.

(10) Date, A. A.; Patil, R. R.; Panicucci, R.; Souto, E. B.; Lee, R. W. Translating Nanotechnology from Bench to Pharmaceutical Market: Barriers, Success, and Promises. *J. Drug Deliv.* **2012**, *2012*, 1–2.

(11) Hall, J. B.; Dobrovolskaia, M. A.; Patri, A. K.; McNeil, S. E. Characterization of Nanoparticles for Therapeutics. *Nanomedicine* **2007**, *2*, 789–803.

(12) Huynh, L.; Neale, C.; Pomès, R.; Allen, C. Computational Approaches to the Rational Design of Nanosystems, Polymeric Micelles, and Dendrimers for Drug Delivery. *Nanomedicine Nanotechnology, Biol. Med.* **2012**, *8*, 20–36.

(13) FDA. *Drug Products, Including Biological Products, That Contain Nanomaterials - Guidance for Industry*; 2017.

(14) Niu, Z.; Conejos-Sánchez, I.; Griffin, B. T.; O'Driscoll, C. M.; Alonso, M. J. Lipid-Based Nanocarriers for Oral Peptide Delivery. *Adv. Drug Deliv. Rev.* **2016**, *106*, 337–354.

(15) Duncan, R.; Gaspar, R. Nanomedicine(s) under the Microscope. *Mol. Pharm.* **2011**, *8*, 2101–2141.

(16) Patra, J. K.; Das, G.; Fraceto, L. F.; Campos, E. V. R.; Rodriguez-Torres, M. del P.; Acosta-Torres, L. S.; Diaz-Torres, L. A.; Grillo, R.; Swamy, M. K.; Sharma, S.; *et al.* Nano Based Drug Delivery Systems: Recent Developments and Future Prospects. *J. Nanobiotechnology* **2018**, *16*, 71.

(17) Eaton, M. A. W.; Levy, L.; Fontaine, O. M. A. Delivering Nanomedicines to Patients: A Practical Guide. *Nanomedicine Nanotechnology, Biol. Med.* **2015**, *11*, 983–992.

(18) Havel, H.; Finch, G.; Strode, P.; Wolfgang, M.; Zale, S.; Bobe, I.; Youssoufian, H.; Peterson, M.; Liu, M. Nanomedicines: From Bench to Bedside and Beyond. *AAPS J.* **2016**, *18*, 1373–1378.

(19) Rowe, R. C.; Sheskey, P.; Quinn, M. E. *Handbook of Pharmaceutical Excipients – 7th Edition*; Pharmaceutical Press, 2013; Vol. 18.

(20) Ingólfsson, H. I.; Melo, M. N.; van Eerden, F. J.; Arnarez, C.; Lopez, C. A.; Wassenaar, T. A.; Periole, X.; de Vries, A. H.; Tieleman, D. P.; Marrink, S. J. Lipid Organization of the Plasma Membrane. *J. Am. Chem. Soc.* **2014**, *136*, 14554–14559.

(21) Sezgin, E.; Levental, I.; Mayor, S.; Eggeling, C. The Mystery of Membrane Organization: Composition, Regulation

and Roles of Lipid Rafts. *Nat. Rev. Mol. Cell Biol.* **2017**, *18*, 361–374.

(22) Rauschert, S.; Gázquez, A.; Uhl, O.; Kirchberg, F. F.; Demmelmair, H.; Ruíz-Palacios, M.; Prieto-Sánchez, M. T.; Blanco-Carnero, J. E.; Nieto, A.; Larqué, E.; *et al.* Phospholipids in Lipoproteins: Compositional Differences across VLDL, LDL, and HDL in Pregnant Women. *Lipids Health Dis.* **2019**, *18*, 20.

(23) Dashti, M.; Kulik, W.; Hoek, F.; Veerman, E. C.; Peppelenbosch, M. P.; Rezaee, F. A Phospholipidomic Analysis of All Defined Human Plasma Lipoproteins. *Sci. Rep.* **2011**, *1*, 139.

(24) Skipski, V.; Barclay, M.; Barclay, R.; Fetzer, V.; Good, J.; Archibald, F. Lipid Composition of Human Serum Lipoproteins. *Biochem. J.* **1967**, *104*, 340–352.

(25) Hidaka, H.; Hanyu, N.; Sugano, M.; Kawasaki, K.; Yamauchi, K.; Katsuyama, T. Analysis of Human Serum Lipoprotein Lipid Composition Using MALDI-TOF Mass Spectrometry. *Ann. Clin. Lab. Sci.* **2007**, *37*, 213–221.

(26) Pons, M.; Foradada, M.; Estelrich, J. Liposomes Obtained by the Ethanol Injection Method. *Int. J. Pharm.* **1993**, *95*, 51–56.

(27) Maitani, Y.; Soeda, H.; Junping, W.; Takayama, K. Modified Ethanol Injection Method For Liposomes Containing β-Sitosterol β-D-Glucoside. *J. Liposome Res.* **2001**, *11*, 115–125.

(28) Jaafar-Maalej, C.; Diab, R.; Andrieu, V.; Elaissari, A.; Fessi, H. Ethanol Injection Method for Hydrophilic and Lipophilic Drug-Loaded Liposome Preparation. *J. Liposome Res.* **2010**, *20*, 228–243.

(29) Batzri, S.; Korn, E. D. Single Bilayer Liposomes Prepared without Sonication. *Biochim. Biophys. Acta - Biomembr.* **1973**, *298*, 1015–1019.

(30) Filipe, V.; Hawe, A.; Jiskoot, W. Critical Evaluation of Nanoparticle Tracking Analysis (NTA) by NanoSight for the Measurement of Nanoparticles and Protein Aggregates. *Pharm. Res.* **2010**, *27*, 796–810.

(31) Hou, J.; Ci, H.; Wang, P.; Wang, C.; Lv, B.; Miao, L.; You, G. Nanoparticle Tracking Analysis versus Dynamic Light Scattering: Case Study on the Effect of Ca2+and Alginate on the Aggregation of Cerium Oxide Nanoparticles. *J. Hazard. Mater.* **2018**, *360*, 319–328.

(32) Gao, X.; Lowry, G. V. Progress towards Standardized and Validated Characterizations for Measuring Physicochemical Properties of Manufactured Nanomaterials Relevant to Nano Health and Safety Risks. *NanoImpact* **2018**, *9*, 14–30.

(33) Nanosight. *Applications of Nanoparticle Tracking Analysis (NTA) in Nanoparticle Research*; 2009.

(34) ICH. Stability Testing of New Drug Substances and Products International Conference on Harmonization of Technical Requirements for Registration of Pharmaceuticals for Human Use. **2003**.

(35) Khan, M. S.; Akhtar, N. Regulation of Stability Studies to Enhance the Efficiency of Drug Registrations to Regulatory Authorities. *Arch. Pharm. Pract.* **2015**, *6*, 48.

(36) Wu, L.; Zhang, J.; Watanabe, W. Physical and Chemical Stability of Drug Nanoparticles. *Adv. Drug Deliv. Rev.* **2011**, *63*, 456–469.

(37) Heurtault, B.; Saulnier, P.; Pech, B.; Proust, J.-E.; Benoit, J.-P. Physico-Chemical Stability of Colloidal Lipid Particles. *Biomaterials* **2003**, *24*, 4283–4300.

(38) ICH. *Stability Testing of New Drug Substances and Products International Conference on Harmonization of Technical Requirements for Registration of Pharmaceuticals for Human Use*; 2003.

(39) Doktorovova, S.; Souto, E. B.; Silva, A. M. Nanotoxicology Applied to Solid Lipid Nanoparticles and Nanostructured Lipid Carriers - A Systematic Review of in Vitro Data. *Eur. J. Pharm. Biopharm.* **2014**, *87*, 1–18.

(40) Arora, S.; Rajwade, J. M.; Paknikar, K. M. Nanotoxicology and in Vitro Studies: The Need of the Hour. *Toxicol. Appl. Pharmacol.* **2012**, *258*, 151–165.

(41) Donaldson, K.; Stone, V.; Tran, C. L.; Kreyling, W.; Borm, P. J. a. Nanotoxicology : A New Frontier in Particle Toxicology Relevant to Both the Workplace and General Environment and to Consumer Safety. *Occup. Environ. Med.*

2004, *61*, 727–728.

(42) Oberdörster, G. Safety Assessment for Nanotechnology and Nanomedicine: Concepts of Nanotoxicology. *J. Intern. Med.* **2010**, *267*, 89–105.

(43) Lv, H.; Zhang, S.; Wang, B.; Cui, S.; Yan, J. Toxicity of Cationic Lipids and Cationic Polymers in Gene Delivery. *J. Control. Release* **2006**, *114*, 100–109.

(44) Stone, V.; Donaldson, K. Nanotoxicology: Signs of Stress. *Nat. Nanotechnol.* **2006**, *1*, 23–24.

(45) Yu, T.; Malugin, A.; Ghandehari, H. Impact of Silica Nanoparticle Design on Cellular Toxicity and Hemolytic Activity. *ACS Nano* **2011**, *5*, 5717–5728.

(46) Hill, A. J.; Teraoka, H.; Heideman, W.; Peterson, R. E. Zebrafish as a Model Vertebrate for Investigating Chemical Toxicity. *Toxicol. Sci.* **2005**, *86*, 6–19.

(47) Gutiérrez-Lovera, C.; Vázquez-Ríos, A.; Guerra-Varela, J.; Sánchez, L.; de la Fuente, M. The Potential of Zebrafish as a Model Organism for Improving the Translation of Genetic Anticancer Nanomedicines. *Genes (Basel).* **2017**, *8*, 349.

(48) McGrath, P.; Li, C.-Q. Zebrafish: A Predictive Model for Assessing Drug-Induced Toxicity. *Drug Discov. Today* **2008**, *13*, 394–401.

(49) OECD. *Guidelines for the Testing of Chemicals, Fish Embryo Acute Toxicity (FET) Test, Test No. 236.*; OECD, 2013.

(50) Chapman, K. L.; Holzgrefe, H.; Black, L. E.; Brown, M.; Chellman, G.; Copeman, C.; Couch, J.; Creton, S.; Gehen, S.; Hoberman, A.; *et al.* Pharmaceutical Toxicology: Designing Studies to Reduce Animal Use, While Maximizing Human Translation. *Regul. Toxicol. Pharmacol.* **2013**, *66*, 88–103.

(51) Yang, K.; Ma, Y.-Q. Computer Simulation of the Translocation of Nanoparticles with Different Shapes across a Lipid Bilayer. *Nat. Nanotechnol.* **2010**, *5*, 579–583.

(52) Ding, H. ming; Ma, Y. qiang. Computer Simulation of the Role of Protein Corona in Cellular Delivery of Nanoparticles. *Biomaterials* **2014**, *35*, 8703–8710.

(53) Ding, H. M.; Tian, W. De; Ma, Y. Q. Designing Nanoparticle Translocation through Membranes by Computer Simulations. *ACS Nano* **2012**, *6*, 1230–1238.

(54) Ding, H. M.; Ma, Y. Q. Design Strategy of Surface Decoration for Efficient Delivery of Nanoparticles by Computer Simulation. *Sci. Rep.* **2016**, *6*, 1–10.

(55) Ingólfsson, H. I.; Lopez, C. A.; Uusitalo, J. J.; de Jong, D. H.; Gopal, S. M.; Periole, X.; Marrink, S. J. The Power of Coarse Graining in Biomolecular Simulations. *Wiley Interdiscip. Rev. Comput. Mol. Sci.* **2014**, *4*, 225–248.

(56) Marrink, S. J.; Risselada, H. J.; Yefimov, S.; Tieleman, D. P.; De Vries, A. H. The MARTINI Force Field: Coarse Grained Model for Biomolecular Simulations. *J. Phys. Chem. B* **2007**, *111*, 7812–7824.

(57) Marrink, S. J.; de Vries, A. H.; Mark, A. E. Coarse Grained Model for Semiquantitative Lipid Simulations. *J. Phys. Chem. B* **2004**, *108*, 750–760.

(58) Nielsen, S. O.; Lopez, C. F.; Srinivas, G.; Klein, M. L. Coarse Grain Models and the Computer Simulation of Soft Materials. *J. Phys. Condens. Matter* **2004**, *16*, R481–R512.

(59) Ferlay, J.; Soerjomataram, I.; Dikshit, R.; Eser, S.; Mathers, C.; Rebelo, M.; Parkin, D. M.; Forman, D.; Bray, F. Cancer Incidence and Mortality Worldwide: Sources, Methods and Major Patterns in GLOBOCAN 2012. *Int. J. Cancer* **2015**, *136*, E359–E386.

(60) Arnold M, Sierra MS, Laversanne M, et al. Global Patterns and Trends in Colorectal Cancer Incidence and Mortality. *Gut* **2016**, *66*, 683–691.

(61) Anitha, A.; Maya, S.; Sivaram, A. J.; Mony, U.; Jayakumar, R. Combinatorial Nanomedicines for Colon Cancer Therapy. *Wiley Interdiscip. Rev. Nanomedicine Nanobiotechnology* **2016**, *8*, 151–159.

(62) Shi, J.; Kantoff, P. W.; Wooster, R.; Farokhzad, O. C. Cancer Nanomedicine: Progress, Challenges and Opportunities.

Nat. Rev. Cancer **2017**, *17*, 20–37.

(63) Verissimo, L. M.; Agnez Lima, L. F.; Monte Egito, L. C.; De Oliveira, A. G.; Do Egito, E. S. T. Pharmaceutical Emulsions: A New Approach for Gene Therapy. *J. Drug Target.* **2010**, *18*, 333–342.

(64) Teixeira, H.; Dubernet, C.; Puisieux, F.; Benita, S.; Couvreur, P. Submicron Cationic Emulsions as a New Delivery System for Oligonucleotides. *Pharm. Res.* **1999**, *16*, 30–36.

(65) Teixeira, H. F.; Bruxel, F.; Fraga, M.; Schuh, R. S.; Zorzi, G. K.; Matte, U.; Fattal, E. Cationic Nanosystems as Nucleic Acids Delivery Systems. *Int. J. Pharm.* **2017**, *534*, 356–367.

(66) Yin, H.; Kanasty, R. L.; Eltoukhy, A. A.; Vegas, A. J.; Dorkin, J. R.; Anderson, D. G. Non-Viral Vectors for Gene-Based Therapy. *Nat. Rev. Genet.* **2014**, *15*, 541–555.

(67) Mazza, M.; Alonso-Sande, M.; Jones, M.-C.; de la Fuente, M. The Potential of Nanosystems in Biomedicine. In *Fundamentals of Pharmaceutical Nanoscience*; Springer New York: New York, NY, 2013; pp. 117–158.

(68) Tamilvanan, S. Formulation of Multifunctional Oil-in-Water Nanosized Emulsions for Active and Passive Targeting of Drugs to Otherwise Inaccessible Internal Organs of the Human Body. *Int. J. Pharm.* **2009**, *381*, 62–76.

(69) Fischer, H. C.; Chan, W. C. Nanotoxicity: The Growing Need for in Vivo Study. *Curr. Opin. Biotechnol.* **2007**, *18*, 565–571.

(70) Ozpolat, B.; Sood, A. K.; Lopez-Berestein, G. Nanomedicine Based Approaches for the Delivery of SiRNA in Cancer. *J. Intern. Med.* **2010**, *267*, 44–53.

(71) Manoharan, M.; Johnson, L. K.; McGee, D. P. C.; Guinosso, C. J.; Ramasamy, K.; Springer, R. H.; Bennett, C. F.; Ecker, D. J.; Vickers, T.; Cowsert, L.; *et al.* Chemical Modifications to Improve Uptake and Bioavailability of Antisense Oligonucleotides. *Ann. N. Y. Acad. Sci.* **1992**, *660*, 306–309.

(72) Khvorova, A.; Watts, J. K. The Chemical Evolution of Oligonucleotide Therapies of Clinical Utility. *Nat. Biotechnol.* **2017**, *35*, 238–248.

(73) Barenholz, Y. Sphingomyelin and Cholesterol:From Membrane Biophysics and Rafts to Potential Medical Applications. In *Subcellular Biochemistry*; Springer, Boston, MA, 2004; Vol. 37, pp. 167–215.

(74) Maeda, H.; Greish, K.; Fang, J. The EPR Effect and Polymeric Drugs: A Paradigm Shift for Cancer Chemotherapy in the 21st Century. *Advances in Polymer Science*, 2006, *193*, 103–121.

(75) Teijeiro-Valiño, C.; Novoa-Carballal, R.; Borrajo, E.; Vidal, A.; Alonso-Nocelo, M.; Freire, M. D. L. F.; Lopez-Casas, P. P.; Hidalgo, M.; Csaba, N.; Alonso, M. J. A Multifunctional Drug Nanocarrier for Efficient Anticancer Therapy. *J. Control. Release* **2019**, *294*, 154–164.

(76) Wilhelm, S.; Tavares, A. J.; Dai, Q.; Ohta, S.; Audet, J.; Dvorak, H. F.; Chan, W. C. W. Analysis of Nanoparticle Delivery to Tumours. *Nat. Rev. Mater.* **2016**, *1*, 16014.

(77) Danhier, F.; Feron, O.; Préat, V. To Exploit the Tumor Microenvironment: Passive and Active Tumor Targeting of Nanocarriers for Anti-Cancer Drug Delivery. *Journal of Controlled Release*, 2010, *148*, 135–146.

(78) Byrne, J. D.; Betancourt, T.; Brannon-Peppas, L. Active Targeting Schemes for Nanoparticle Systems in Cancer Therapeutics. *Adv. Drug Deliv. Rev.* **2008**, *60*, 1615–1626.

(79) Ganta, S.; Talekar, M.; Singh, A.; Coleman, T. P.; Amiji, M. M. Nanosystems in Translational Research—Opportunities and Challenges in Targeted Cancer Therapy. *AAPS PharmSciTech* **2014**, *15*, 694–708.

(80) Hak, S.; Helgesen, E.; Hektoen, H. H.; Huuse, E. M.; Jarzyna, P. A.; Mulder, W. J. M.; Haraldseth, O.; Davies, C. de L. The Effect of Nanoparticle Polyethylene Glycol Surface Density on Ligand-Directed Tumor Targeting Studied in Vivo by Dual Modality Imaging. *ACS Nano* **2012**, *6*, 5648–5658.

(81) Béduneau, A.; Saulnier, P.; Hindré, F.; Clavreul, A.; Leroux, J. C.; Benoit, J. P. Design of Targeted Lipid Nanocapsules by Conjugation of Whole Antibodies and Antibody Fab' Fragments. *Biomaterials* **2007**, *28*, 4978–4990.

(82) Loureiro, A.; Nogueira, E.; Azoia, N. G.; Sárria, M. P.; Abreu, A. S.; Shimanovich, U.; Rollett, A.; Härmark, J.; Hebert, H.; Guebitz, G.; *et al.* Size Controlled Protein Nanosystems for Active Targeting of Folate Receptor Positive Cells. *Colloids Surfaces B Biointerfaces* **2015**, *135*, 90–98.

(83) Shi, J.; Kantoff, P. W.; Wooster, R.; Farokhzad, O. C. Cancer Nanomedicine: Progress, Challenges and Opportunities. *Nat. Rev. Cancer* **2017**, *17*, 20–37.

(84) Potter, L. R. Regulation and Therapeutic Targeting of Peptide-Activated Receptor Guanylyl Cyclases. *Pharmacol. Ther.* **2011**, *130*, 71–82.

(85) Forte, L. R. Uroguanylin and Guanylin Peptides: Pharmacology and Experimental Therapeutics. *Pharmacol. Ther.* **2004**, *104*, 137–162.

(86) Pitari, G. M.; Li, P.; Lin, J. E.; Zuzga, D.; Gibbons, A. V.; Snook, A. E.; Schulz, S.; Waldman, S. A. The Paracrine Hormone Hypothesis of Colorectal Cancer. *Clin. Pharmacol. Ther.* **2007**, *82*, 441–447.

(87) Camici, M. Guanylin Peptides and Colorectal Cancer (CRC). *Biomed. Pharmacother.* **2008**, *62*, 70–76.

(88) Buc, E.; Der Vartanian, M.; Darcha, C.; Déchelotte, P.; Pezet, D. Guanylyl Cyclase C as a Reliable Immunohistochemical Marker and Its Ligand Escherichia Coli Heat-Stable Enterotoxin as a Potential Protein-Delivering Vehicle for Colorectal Cancer Cells. *Eur. J. Cancer* **2005**, *41*, 1618–1627.

(89) Yarla, N. S.; Gali, H.; Pathuri, G.; Smriti, S.; Farooqui, M.; Panneerselvam, J.; Kumar, G.; Madka, V.; Rao, C. V. Targeting the Paracrine Hormone-Dependent Guanylate Cyclase/CGMP/Phosphodiesterases Signaling Pathway for Colorectal Cancer Prevention. *Semin. Cancer Biol.* **2018**.

(90) Giblin, M. F.; Sieckman, G. L.; Watkinson, L. D.; Daibes-Figueroa, S.; Hoffman, T. J.; Forte, L. R.; Volkert, W. A. Selective Targeting of E. Coli Heat-Stable Enterotoxin Analogs to Human Colon Cancer Cells. *Anticancer Res* **2006**, *26*, 3243–3251.

(91) Tian, X.; Michal, A. M.; Li, P.; Wolfe, H. R.; Waldman, S. A.; Wickstrom, E. STa Peptide Analogs for Probing Guanylyl Cyclase C. *Biopolym. - Pept. Sci. Sect.* **2008**, *90*, 713–723.

(92) Liu, D.; Overbey, D.; Watkinson, L. D.; Daibes-Figueroa, S.; Hoffman, T. J.; Forte, L. R.; Volkert, W. A.; Giblin, M. F. In Vivo Imaging of Human Colorectal Cancer Using Radiolabeled Analogs of the Uroguanylin Peptide Hormone. *Anticancer Res.* **2009**, *29*, 3777–3783.

(93) Liu, D.; Overbey, D.; Watkinson, L. D.; Smith, C. J.; Daibes-Figueroa, S.; Hoffman, T. J.; Forte, L. R.; Volkert, W. A.; Giblin, M. F. Comparative Evaluation of Three Cu-64-Labeled E-Coli Heat-Stable Enterotoxin Analogues for PET Imaging of Colorectal Cancer. *Bioconjug. Chem.* **2010**, *21*, 1171–1176.

(94) Brierley, S. M. Guanylate Cyclase-C Receptor Activation: Unexpected Biology. *Curr. Opin. Pharmacol.* **2012**, *12*, 632–640.

(95) Waldman, S. A.; Camilleri, M. Guanylate Cyclase-C as a Therapeutic Target in Gastrointestinal Disorders. *Gut* **2018**, *67*, 1543–1552.

(96) Aryal, S.; Hu, C. M. J.; Zhang, L. Combinatorial Drug Conjugation Enables Nanoparticle Dual-Drug Delivery. *Small* **2010**, *6*, 1442–1448.

CONCLUSIONS

USC
UNIVERSIDADE
DE SANTIAGO
DE COMPOSTELA

The work described in this thesis was intended to the rational design of a new type of nanotechnological platform, consisting of Sphingomyelin Nanosystems (SNs), for the delivery of oncological drugs. Data obtained from the experimental work led us to withdraw the following conclusions:

1. We have developed nanosystems made out of sphingomyelin as stabilizing surfactant and one oil in the core (SNs), using a simple and very mild methodology, the ethanol injection method. The nanosystems showed a good colloidal stability during storage and, also, upon incubation in biologically relevant media.
2. Making use of *in silico* computational strategies (Molecular Dynamic Simulations), we studied the fundamental interactions governing the assembly, structural and dynamical characteristics of SNs. Moreover, we evaluated their drug loading capacity and gathered information about the drug distribution/localization within the nanosystem and the drug–nanosystem interactions.
3. SNs showed a moderate capacity to load oligonucleotides. SNs showed a very low cytotoxicity while they preserve the capacity to promote the intracellular delivery of the associated biomolecules.
4. SNs were found to be useful for the development of targeted anticancer therapies. A natural hormone (Uroguanylin, UroG), able to target the Guanylyl Cyclase C (GCC) receptor and act in an agonist manner towards it, was efficiently associated to SNs after the preparation of a hydrophobized derivative (UroGm). The combination of this targeted formulation with the anticancer drug etoposide resulted in a synergistic effect *in vitro* and a moderate, but significant response in a xenograft model of metastatic colorectal cancer.

Overall, this work highlights the importance of rational design in order to obtain nanosystems with appropriate physicochemical and morphological characteristics, colloidal and toxicological profiles to maximize the prospects of clinical translation. Besides, it provides the bases for the development of multiple applications.

LIST OF ABBREVIATIONS

USC
UNIVERSIDADE
DE SANTIAGO
DE COMPOSTELA

API	Active pharmaceutical ingredient
AT	All-atoms
BCS	Biopharmaceutics Classification System
CaCo-2	ATCC® HTB-37™ Colon epithelial cell
CG	Coarse-Grained
cGMP	Cyclic guanosine monophosphate
CH	Cholesterol
CMC	Critical micelle concentration
CNS	Central Nervous System
CPI	Catastrophic Phase Inversion
CRC	Colorectal Cancer
CryoTEM	Cryogenic Transmission Electronic Microscopy
CTAB	Cetyltrimethylammonium Bromide
Cy3	Cyanine Dye
d	Diameter
D	Diffusion coefficient
D_2O	Deuterated water
DAPI	Nuclear Fluorescent Marker
DLS	Dynamic light Scattering
DMEM	Dulbecco's Modified Eagle Medium
DMTMM	4-(4,6-dimethoxy-1,3,5-triazin-2-yl)-4-methyl-morpholinium chloride
DOSY	Diffusion-ordered spectroscopy
DOTAP	1,2-dioleoyl-3-trimethylammonium-propane
dsRNA	double stranded RNA
EE%	Encapsulation efficiency in percentage
EMA	European Medicines Agency
EPR	Enhanced permeability and retention effect
Etp	Etoposide
EU	European Union
FBS	Fetal Bovine Serum
FDA	Food and Drugs Administration
FESEM	Field Emission Scanning Electron Microscopy
GCC	Guanylyl Cyclase C
GFP	Green fluorescent protein
Gn	Guanylin
GRAS	General Recognized as Safe
HA	Hyaluronic acid
HEPES	4-(2-hydroxyethyl)-1-piperazineethanesulfonic acid

HPLC	High Performance Liquid Chromatography
hpf	Hours Post-fertilization
HT29	ATCC® HTB-38™ Colon epithelial cell
IC50	Half maximal inhibitory concentration
ICH	International Congress of Harmonization
IUPAC	International Union of Pure and Applied Chemistry
LAPI	LDFI, Leu-Asp-Phe-Ile
LAPIK	LDFIK, Leu-Asp-Phe-Ile-Lys-PEG6-C18
LDA	Laser Doppler Anemometry
LogP	Partition coefficient
MALDITOF	Matrix-Assisted Laser Desorption/Ionization Time-Of-Flight
MD	Molecular Dynamic
MiaPaCa 2	ATCC® CRL-1420™ Pancreatic epithelial cell
miRNA	micro-RNA
MTD	Maximum Tolerated Dose
MTT	3-(4,5-dimethylthiazol-2-yl)-2,5-diphenyltetrazolium
MW	Molecular weight
MWCO	Molecular weight cut off
NCI	National Cancer Institute
NMR	Nuclear Magnetic Resonance
NTA	Nanoparticle Tracking Analysis
O/W	Oil-in-water
O/W/O	Oil-in-water-in-oil
PBS	Phosphate Buffer Saline
PC3	ATCC® CRL-1435™ Prostate-derived bone metastasis
PdI	Polydispersity Index
pDNA	Plasmid DNA
PEG	Polyethylene glycol
RBCs	Red Blood Cells
RCF	Relative Centrifuge Force
RDF	Radial Distribution Function
RES	Reticuloendothelial System
RH	Relative Humidity
RT	Room Temperature
SD	Standard Deviation
siRNA	Small interfering RNA
SM	Sphingomyelin
SNs	Sphingomyelin Nanosystems

SPIONs	Superparamagnetic Iron Oxide Nanoparticles
ST	Stearylamine
STEM	Scanning Transmission Electronic Microscopy
SW480	ATCC® CCL-228™ Primary colon adenocarcinoma
SW620	ATCC® CCL-227™ Metastatic colorectal adenocarcinoma
T84	ATCC® CCL-248™ Colon-derived lung metastasis
TEM	Transmission Electronic Microscopy
TFA	Trifluoroacetic acid
TOCSY	Totally Correlated Spectroscopy
TSP	Trimethylsilyl propanoic acid
UK	United Kingdom
UroG	Uroguanylin
UroGm	Uroguanylin hydrophobic derivative
US	United States
USA	United States of America
USP	US Pharmacopeia
UV-Vis	Ultraviolet-Visible Spectrum
V	Vitamin E
v/v	Volume/Volume
W/O	Water-in-oil
W/O/W	Water-in-oil-in-water
w/w	Weight/Weight
WHO	World Health Organization
WT	Wildtype
ZP	Zeta Potential

USC
UNIVERSIDADE
DE SANTIAGO
DE COMPOSTELA

ETHICAL CONSIDERATIONS

USC
UNIVERSIDADE
DE SANTIAGO
DE COMPOSTELA

Cell culture

All cancer cell lines used in this work were acquired from commercially available resources (American Tissue Culture Collection, ATCC), i.e. **HT29** (ATCC® HTB-38™) Colon epithelial cell line; **MiaPaCa-2** (ATCC® CRL-1420™, Pancreatic epithelial cell line); **PC3** (ATCC® CRL-1435™, Prostate-derived bone metastasis cell line); **SW480** (ATCC® CCL-228™, Primary colon adenocarcinoma cell line) and **SW620** (ATCC® CCL-227™, Metastatic colorectal adenocarcinoma cell line). Cells were cultured in the conditions recommended by the manufacturers and only used for the research purposes specifically described in this thesis.

***In vivo* Studies**

Zebrafish related studies (Chapter 2) were done in Lugo in the animal facilities AE-LU-003 following European and National regulations. The procedures were approved by the ethical committee of the USC and Xunta de Galicia (MR110250)

Toxicity and efficacy studies (Chapter 2 and 3) were done in Santiago de Compostela by the group of Dr. Anxo Vidal (USC). All animal experiments were reviewed and approved by the ethics committee (ID: 15010/14/001, "Avaliación biolóxica de nanosistemas") and were executed in accordance with governing Spanish law and European Directives and Guidelines for the use of animals. Studies were performed therefore in compliance with the Directive 2010/63/EU of the European Parliament and Council of 22nd September 2010 on the protection of animals used for scientific purposes and under the Spanish Royal Decree 53/2013 February 1st on the protection of animals used for experimental and other scientific purposes.

USC
UNIVERSIDADE
DE SANTIAGO
DE COMPOSTELA